LEABHARLANN CHOLÁISTE NA TRÍONÓIDE, BAILE ÁTHA CLIATH | TRINITY COLLEGE LIBRARY DUBLIN
Ollscoil Átha Cliath | The University of Dublin

Terms and Conditions of Use of Digitised Theses from Trinity College Library Dublin

Copyright statement

All material supplied by Trinity College Library is protected by copyright (under the Copyright and Related Rights Act, 2000 as amended) and other relevant Intellectual Property Rights. By accessing and using a Digitised Thesis from Trinity College Library you acknowledge that all Intellectual Property Rights in any Works supplied are the sole and exclusive property of the copyright and/or other IPR holder. Specific copyright holders may not be explicitly identified. Use of materials from other sources within a thesis should not be construed as a claim over them.

A non-exclusive, non-transferable licence is hereby granted to those using or reproducing, in whole or in part, the material for valid purposes, providing the copyright owners are acknowledged using the normal conventions. Where specific permission to use material is required, this is identified and such permission must be sought from the copyright holder or agency cited.

Liability statement

By using a Digitised Thesis, I accept that Trinity College Dublin bears no legal responsibility for the accuracy, legality or comprehensiveness of materials contained within the thesis, and that Trinity College Dublin accepts no liability for indirect, consequential, or incidental, damages or losses arising from use of the thesis for whatever reason. Information located in a thesis may be subject to specific use constraints, details of which may not be explicitly described. It is the responsibility of potential and actual users to be aware of such constraints and to abide by them. By making use of material from a digitised thesis, you accept these copyright and disclaimer provisions. Where it is brought to the attention of Trinity College Library that there may be a breach of copyright or other restraint, it is the policy to withdraw or take down access to a thesis while the issue is being resolved.

Access Agreement

By using a Digitised Thesis from Trinity College Library you are bound by the following Terms & Conditions. Please read them carefully.

I have read and I understand the following statement: All material supplied via a Digitised Thesis from Trinity College Library is protected by copyright and other intellectual property rights, and duplication or sale of all or part of any of a thesis is not permitted, except that material may be duplicated by you for your research use or for educational purposes in electronic or print form providing the copyright owners are acknowledged using the normal conventions. You must obtain permission for any other use. Electronic or print copies may not be offered, whether for sale or otherwise to anyone. This copy has been supplied on the understanding that it is copyright material and that no quotation from the thesis may be published without proper acknowledgement.

Functional analyses of a novel transmembrane protein, Plxdc2, in the developing nervous system of the chick and mouse

A thesis submitted to the University of Dublin for the degree of Doctor of Philosophy.

2009

Suzanne F. C. Miller B.A.

Smurfit Institute of Genetics,
University of Dublin,
Trinity College

TRINITY COLLEGE
10 AUG 2009
LIBRARY DUBLIN
THESIS
8823

Declaration

I declare that I am the sole author of this thesis and that the work presented in it, unless otherwise referenced, is entirely my own. I also declare that the work has not been submitted, in whole or in part, to any other university as an exercise for a degree or other qualification.

I agree that the library of Trinity College Dublin may lend or copy this thesis upon request.

Summary

Studies utilising the PLAP secretory trap method isolated a gene trap insertion in a novel gene (mouse line KST37) (Leighton *et al.*, 2001) which has since been named *Plexin domain containing 2 (Plxdc2)*. *Plxdc2* encodes a novel transmembrane protein with an expression pattern and architecture suggestive of a role in axon guidance and development of the brain. In addition to a region of nidogen homology, the Plxdc2 protein contains a plexin repeat, a domain found in known axon guidance molecules such as Semaphorins and Plexins. A comprehensive description of Plxdc2 expression in the developing mouse was established, with particular emphasis on the developing brain, and was compared and contrasted with that of the related gene, *Plxdc1*. This description was achieved using the PLAP secretory trap lines, KST37 (Leighton *et al.*, 2001) and TEM7 (Friedel *et al.*, 2005) and the *in situ* transgenic reporters included in the PLAP Secretory Trap vector (β-geo and PLAP). A combination of light microscopy and optical projection tomography (OPT) were employed to achieve a comprehensive 3D description of expression. At early embryonic stages, Plxdc2 expression was highlighted in a number of important patterning centres of the developing mouse brain including the cortical hem, floorplate and midbrain-hindbrain boundary (MHB) (Miller *et al.*, 2007). In later development, Plxdc2 is expressed in a discrete subset of nuclei and tracts in the brain including the Purkinje cells of the cerebellum, the fimbria, cerebellar peduncle, posterior commissure, and mammillotegmental tract (Miller *et al.*, 2007).

Homozygous *Plxdc2* gene trap mice did not survive to birth, with lethality occurring at a stage precluding analysis of the role of *Plxdc2* in brain development and axon guidance. Preliminary analysis of the effect of loss of *Plxdc2* was carried out in a viable *Plxdc2* mouse line, Plxdc2GFP. The Plxdc2GFP mouse line was made available late in the time span of this project and therefore, limited analyses of the brain at embryonic day (E) 15.5 were carried out. An investigation of *Plxdc2* transcript levels in the cerebella of Plxdc2GFP homozygotes illustrated approximately a ten fold decrease in *Plxdc2* transcript when compared to wildtype controls. Loss of *Plxdc2* during early brain development did not result in major defects in the E15.5 brain. The gross morphology of the brain of homozygous Plxdc2GFP mice appeared normal and no guidance defects were evident in axons of the cerebellar peduncle, posterior commissure and mammillotegmental tract.

The Plxdc2 protein is highly conserved across species, and analysis of *Plxdc2* expression in the chick confirmed similar expression to that documented in the mouse in many areas of the developing brain including the MHB, floor of the midbrain and cortical hem. Functional analyses of Plxdc2 were therefore carried out in the chick both by misexpression of the protein and by knockdown of endogenous gene function. Examination of gene function was facilitated by the construction of a full-length *Plxdc2* expression plasmid and by the design of several short hairpin forming RNAs (shRNAs) against the gene. Ectopic/overexpression of Plxdc2 was carried out by *in ovo* electroporation of the full-length *Plxdc2* plasmid into the Hamburger-Hamilton (HH) stage 10-11 neural tube. Misexpression of Plxdc2 in the developing brain resulted in thickening of the neural tube 24 hours after electroporation. Neural tube thickening was significant, robust and reproducible. Electroporation of a plasmid encoding a secreted form of the mouse extracellular Plxdc2 protein resulted in a similar thickening effect indicating that Plxdc2 functions in a cell non-autonomous manner and most likely acts as a ligand. The biochemical function of the protein also appears to be conserved between species: in the chick, the extracellular portion of the mouse Plxdc2 protein can bind a receptor and activate the same pathways as the endogenous chick Plxdc2 protein.

Plxdc2-induced neural tube thickening in the chick was accompanied by an increase in proliferation on the electroporated side. In addition, *Plxdc2* misexpression in the mesencephalon and dorsal diencephalon of the chick induced increased expression of a proneural gene, *Cash1*. Examination of *Plxdc2* expression in culture illustrated approximately a nine fold increase in transcript levels in neural stem cells derived from embryonic stem cells. *Plxdc2* may therefore play an important role in proliferation and differentiation in the developing neural tube.

Acknowledgements

There are so many people who have supported me over the last few years and I would like to thank each of them personally.

Firstly, I would like to thank, Dr. Kevin Mitchell, whose expertise and endless enthusiasm for developmental neurobiology has spurred me forward throughout this research. Thank you for not letting go of the KST37 dream! I would also like to thank all the members of the Mitchell lab who have given me so much time and advice: Graham, Annette, Tatsuya, Jackie, Karen, Hiroshi and Francesc, thank you for helping in every way.

I would like to give a special mention to Dr. Paula Murphy, without whom, much of my project would not have been possible. Her guidance throughout my undergraduate and postgraduate training has been invaluable, and her expertise has inspired a true love of developmental biology. I would also like to thank the members of her group, particularly Kristen, Karen and Niamh, whose help and advice eased the transition of my research from mouse to chick.

I would particularly like to mention my parents and siblings; Stan, Ken and Louise. Thank you for your endless words of encouragement and support.

And finally, I would like to dedicate this thesis to Tim. Thank you for every hug, every encouraging word and for believing in me.

Table of Contents

List of Figures 5
List of Tables 8
List of Abbreviations 9

1. Introduction 12
1.1 An introduction to early development of the brain 12
1.1.1. Patterning of the brain along the AP axis 13
1.1.2. Patterning of the brain along the DV axis 14
1.1.3. Secondary organising centres of the developing brain 16
1.1.4. Proliferation and differentiation in early brain development 18
1.1.5. Apoptosis in brain development 21
1.2 Axon guidance 23
1.3 Screens for novel transmembrane proteins – the PLAP secretory trap method. 25
1.4 *Plexin domain containing 2* (*Plxdc2*) 27
1.5 A role for *Plxdc1* in tumour angiogenesis 30
1.6 Potential binding partners of Plxdc1 and Plxdc2 33
1.7 Objectives of this thesis 34

2. Chapter 2 – *Plxdc2* and *Plxdc1* in the developing nervous system of the mouse 36
2.1 Aims of this chapter 36
2.2 Introduction 36
2.3 Analysis of *Plxdc2* expression, in a gene trap mouse line 38
2.3.1. Characterisation of a PLAP secretory trap insertion in *Plxdc2* 38
2.3.2. Genotyping of *Plxdc2* genetrap mice 39
2.3.3. Plxdc2-βgeo expression in the embryo 39
2.3.4. Comparative definition of Plxdc-βgeo expression within the cortical hem and MHB 42
2.3.5. Plxdc2 expression in the E15.5 brain 47
2.3.6. Plxdc2-PLAP expression in the eye and ear at E15.5 49
2.3.7. Plxdc2 expression in the newborn brain 51
2.3.8. Lethality of homozygous *Plxdc2* gene trap mutants 52
2.4 Analysis of *Plxdc1* expression in a gene trap mouse line 54

2.4.1. Genotyping of *Plxdc1* genetrap mice 54
2.4.2. Plxdc1 expression in the developing nervous system 55
2.5 Phenotypic analysis of a viable *Plxdc2* mouse line, Plxdc2GFP 59
2.5.1. Genotyping of Plxdc2GFP mice 59
2.5.2. Confirmation of knockdown of *Plxdc2* expression in the Plxdc2GFP mouse line 59
2.5.3. Phenotypic analysis in the E15.5 brain 61
2.6 Plxdc2-AP *in situ* hybridisation 65
2.7 Discussion 67
2.8 Materials and Methods 71
2.8.1. Animal Husbandry 71
2.8.2. Genotyping of mice - PCR 71
2.8.3. Visualisation of reporter genes 71
2.8.4. *In situ* hybridisation 72
2.8.5. Immunohistochemistry 74
2.8.6. Optical Projection Tomography 74
2.8.7. Real time PCR 75
2.8.8. Cresyl Violet Staining 77
2.8.9. Production of Plxdc2-AP proteins 77
2.8.10. AP *in situ* hybridisation 77

3. Chapter 3 – Functional Analyses of *Plxdc2* in the chick 79
3.1 Aims of this chapter 79
3.2 Introduction 79
3.2.1. The use of the chick as an experimental model 79
3.2.2. *In ovo* electroporation. 80
3.2.3. Gene silencing in the chick embryo 81
3.3 *Plxdc2* expression in the developing nervous system of the chick 83
3.3.1. Production of chick *Plxdc2* probes for in situ hybridisation: 83
3.3.2. *Plxdc2* expression in the chick 83
3.4 Misexpression of *Plxdc2* in the chick brain 88
3.4.1. Prediction of the complete transcript of the chick *Plxdc2* gene 88
3.4.2. PCR amplification of the Chick *Plxdc2* transcript and ligation into the pcDNA3.1myc-His(B) plasmid. 88
3.4.3. In ovo electroporation of chPlxdc2-Myc plasmid DNA 90

3.4.4. Analysis of chPlxdc2-Myc induced thickening of the neural tube 94
3.4.5. Injection and electroporation of a secreted form of Plxdc2 97
3.4.6. Effect of chPlxdc2-Myc expression on cell proliferation 99
3.4.7. Effect of chPlxdc2-Myc expression on neurogenesis 103
3.4.8. Effect of chPlxdc2-Myc misexpression in later development 103
3.4.9. Expression profile of *Plxdc2* in embryonic stem cells, neural stem cells and neurons. 105
3.5 Knockdown of *Plxdc2* at the midbrain-hindbrain boundary 106
3.5.1. Design of shRNA constructs against the chPlxdc2 gene 106
3.5.2. Examination of *in vitro* shRNA efficiency 109
3.5.3. *In ovo* electroporation of shRNA1&3 112
3.6 Summary statistics 113
3.7 Discussion 118
3.7.1. *Plxdc2* expression in the chick and mouse 118
3.7.2. Thickening of the neural tube following Plxdc2 misexpression 120
3.7.3. Increased proliferation and differentiation following misexpression of Plxdc2 121
3.7.4. Older chick brains lack gross morphological defects 123
3.7.5. *Plxdc2* expression is upregulated in NSCs and neurons derived from ESCs in culture 124
3.7.6. Knockdown of endogenous *Plxdc2* 124
3.8 Materials and Methods 126
3.8.1. Chicken husbandry 126
3.8.2. *In situ* hybridisation 126
3.8.3. Extraction of RNA from chick embryos and reverse transcription 126
3.8.4. PCR amplification of the Chick *Plxdc2* transcript 127
3.8.5. Ligation of the chick *Plxdc2* transcript into pcDNA3.1 myc-His (B) 128
3.8.6. Design of shRNA constructs 129
3.8.7. Ligation of annealed oligonucleotides in the pCA-β-EGFPm5-U6 plasmid. 131
3.8.8. HEK 293T Cell culture 132
3.8.9. Immunocytochemistry 132
3.8.10. Collection of protein and Western Blot Analysis 132
3.8.11. *In ovo* electroporation 133
3.8.12. Immunohistochemistry 133
3.8.13. Incorporation of BrdU 135

3.8.14. Statistical Analysis 135
3.8.15. Real time PCR 135

4. Conclusions and future directions 137
4.1 A potential role for *Plxdc2* in proliferation 137
4.2 *Plxdc2* in apoptosis? 138
4.3 A potential role for *Plxdc2* in neural differentiation and determination of cell fate 138
4.4 Knockdown of endogenous *Plxdc2* expression and analysis of endogenous gene function 140
4.5 Final conclusion 141

5. Appendix 143
5.1 Alignment of the murine Plxdc2 and Plxdc1 proteins 143
5.2 Alignment of Plxdc2 protein across species 144
5.3 Plxdc2GFP mouse line design 146
5.4 Predicted *Plxdc2* Full Length Transcript showing sites of primer design 147
5.5 Alignment of the EST predicted chick Plxdc2 protein against mouse Plxdc2 148
5.6 Alignment of the PCR amplified *Plxdc2* transcript (clone 7) against the EST predicted transcript 149
5.7 Alignment of translated *Plxdc2* cDNA against the EST predicted Plxdc2 protein sequence 151
5.8 Antibodies 152
5.9 Western Blot Analysis 153
5.10 Summary Data 155
5.11 Control Images 160

6. References 162

List of Figures

Figure 1.1 Representation of the PLAP Secretory Trap Vector. 27
Figure 1.2 Analysis of Plxdc2 expression in the *Plxdc2* PLAP secretory gene trap mouse line (KST37) 28
Figure 1.3 The architecture of Plxdc2 & Plxdc1. 30
Figure 2.1 The site of the PLAP secretory trap insertion in the KST37 mouse line in intron 3 of the *Plxdc2* gene 38
Figure 2.2 PCR genotyping of *Plxdc2* gene trap mice 39
Figure 2.3 Plxdc2-βgeo expression in the E9.5 mouse 40
Figure 2.4 Plxdc2-βgeo expression in the E11.5 mouse revealed by OPT analysis of X-gal stained heterozygous *Plxdc2* gene trap embryos 43
Figure 2.5 *In situ* hybridisation confirms the Plxdc2-βgeo expression pattern 44
Figure 2.6 Definition of Plxdc2-βgeo expression within the cortical hem and MHB at E11.5 by comparison to *Wnt1, Wnt3a, Wnt5a* and *Wnt8b* 46
Figure 2.7 Plxdc2-βgeo expression in the E15.5 brain 47
Figure 2.8 Neuronal Plxdc2 (PLAP) expression in the E15.5 brain. 50
Figure 2.9 Plxdc2 (PLAP) expression in the eye and ear at E15.5 51
Figure 2.10 Plxdc2 expression in the P0 Brain 53
Figure 2.11 PCR genotyping of *Plxdc1* gene trap mice 54
Figure 2.12 Plxdc1-βgeo expression in the E16.5 brain 55
Figure 2.13 Plxdc1-βgeo expression in the P0 brain 56
Figure 2.14 Comparison of PLAP expression in *Plxdc1* and *Plxdc2* gene trap mice 58
Figure 2.15 PCR genotyping of Plxdc2GFP mice 60
Figure 2.16 Examination of Plxdc2 transcript levels in Plxdc2GFP mice by realtime PCR 60
Figure 2.17 Plxdc2 expression in the E15.5 Plxdc2GFP mouse brain 61
Figure 2.18 Cresyl violet staining of coronal sections through the brain of E15.5 Plxdc2GFP mice 63
Figure 2.19 Phenotypic analysis of the axon tracts of the E15.5 brain which normally express Plxdc2 64
Figure 2.20 Extracellular Plxdc2-AP(CT) *in situ* hybridisation 67
Figure 3.1 Production of probes for use in *in situ* hybridisation experiments in the chick 84

Figure 3.2 *Plxdc2* expression in the chick at Hamburger Hamilton stages 17, 20 and 21.... 85
Figure 3.3 Comparison of *Plxdc2* expression in the HH stage 20 and stage 21 chick head. 86
Figure 3.4 Comparison of *Plxdc2* expression in the hind brain of the chick and mouse....87
Figure 3.5 Amplification of the full length *Plxdc2* transcript from chick cDNA 89
Figure 3.6 Confirmation of size of insert and orientation within the pcDNA3.1myc-His(B) plasmid 89
Figure 3.7 Electroporation of *Plxdc2* into the HH stage 10-11 chick brain results in thickening of the neural tube on the experimental side 92
Figure 3.8 OPT analysis of a HH16 embryo electroporated with chPlxdc2-Myc 24 hours earlier 93
Figure 3.9 Summary of results from OPT analysis of chPlxdc2-Myc expression and neural tube thickening in seven embryos (A-G), 24 hours post electroporation.....95
Figure 3.10 Analysis of chPlxdc2-Myc-induced thickening of the neural tube 96
Figure 3.11 Expression of Plxdc2-AP(CT) in the chick brain causes thickening of the neural tube on the experimental side 98
Figure 3.12 Analysis of Plxdc2-AP-induced thickening of the neural tube 99
Figure 3.13 Examination of BrdU-positive cells in the neural tube of a HH stage 18 chick ectopically expressing chPlxdc2-myc. 100
Figure 3.14 Difference in BrdU-positive cell number plotted against thickening ratio of each section 101
Figure 3.15 *Cash1* expression in the region of the neural tube, 24 hours following electroporation with chPlxdc2-Myc. 104
Figure 3.16 The effect of chPlxdc2-Myc misexpression at HH stage 10-11 on the brain at later stages of development 105
Figure 3.17 Relative expression of *Plxdc2* in embryonic stem cells (ESCs), and in neural stem cells (NSCs) and neurons derived from ESCs *in vitro* 107
Figure 3.18 Confirmation of successful ligation of annealed oligonucleotides into the pCA-β-EGFPm5-U6 plasmid by digestion with *Hind*III 108
Figure 3.19 Immunocytochemistry of transfected HEK293T cells showing knockdown of chPlxdc2-Myc by shRNAs 110
Figure 3.20 Western blot analysis of chPlxdc2-Myc knockdown by shRNA 111
Figure 3.21 EGFP expression in the neural tube of a HH stage 18 embryo, 24 hours following electroporation with shRNA1&3 114

Figure 3.22 Apparent increase in *Plxdc2* transcript following expression of shRNAs against the gene 115
Figure 3.23 Maximum thickening ratios of individuals across *in ovo* electroporation experiments 116
Figure 3.24 Complete set of thickening ratios from multiple sections of individuals across *in ovo* electroporation experiments 117
Figure 3.25 The pcDNA 3.1 myc-His (B) Plasmid (Invitrogen). 129
Figure 3.26 The pCA-β-EGFPm5-U6 plasmid 130
Figure 5.1 Alignment of the murine Plxdc2 and Plxdc1 proteins 143
Figure 5.2 Plxdc2 is highly conserved in the human, mouse, chicken, fly and worm 145
Figure 5.3 Cartoon of design strategy for the creation of the Plxdc2GFP mouse line 146
Figure 5.4 The chick *Plxdc2* transcript 147
Figure 5.5 Alignment of the predicted chick Plxdc2 protein sequence against mouse Plxdc2 148
Figure 5.6 Alignment of the PCR amplified chPlxdc2 transcript (Clone 7) against the EST predicted transcript 150
Figure 5.7 Alignment of the translated Plxdc2 cDNA clone (Clone 7) against the EST predicted protein sequence 151
Figure 5.8 Representative images of controls for *in situ* hybridisation experiments 161

List of Tables

Table 2.1 Description of primers used in genotyping PCR reactions. 73
Table 2.2 Description of genotyping PCR program 74
Table 2.3 Primers used in real time PCR experiments 76
Table 2.4 Real time PCR program 76
Table 3.1 BrdU-positive cell counts on either side of the neural tube of three experimental embryos expressing chPlxdc2-Myc, and the corresponding thickening ratio for each section 102
Table 3.2 Primers used for the amplification of the *Plxdc2* transcript and the predicted size of the PCR product 127
Table 3.3 PCR program used for the amplification of the full length *Plxdc2* transcript ... 128
Table 3.4 ShRNA sequences targetted to *Plxdc2*, location of the target sites and corresponding SFOLD scores. 130
Table 3.5 Design of shRNA template oligonucleotides 131
Table 3.6 Concentration of plasmids used in *in ovo* electroporation experiments 134
Table 3.7 Primers used in real time PCR experiments 136
Table 5.1 List of primary and secondary antibodies used in immunocytochemistry (ICC), immunohistochemistry (IHC) and western blot (WB) analysis 152

List of Abbreviations

AER Apical Ectodermal Ridge

amy amygdala

ANR Anterior Neural Ridge

AP Alkaline Phosphatase

β-gal β- galactosidase

β-geo A fusion of β-gal to neomycin phosphotransferase

BrdU Bromodeoxyuridine

Cash1 Chicken achaete-scute homolog-like 1

ChP Choroid Plexus

CNS Central Nervous System

cb cerebellum

cp cerebellar peduncle

CP Caudate Putamen

CPe Choroid Plexus Epithelium

CR Cajal-Retzius Cells

cx cortex

DG Dentate Gyrus

DRG Dorsal Root Ganglia

E Embryonic day

EP Entopeduncular nucleus

ESCs embryonic stem cells

fim fimbria

GW Glial Wedge

hab habenula

HH Hamburger-Hamilton (1951)

hip hippocampus

hy hypothalamus

ic inferior colliculus

IC Internal Capsule

mb mammillary bodies

mc motor column

MDB Mesencephalon-Diencephalon Boundary

med medulla oblongata

mes mesonephros

MHB Midbrain-Hindbrain Boundary

MRF Midbrain Reticular Formation

mtg mammillotegmental tract

N5n trigeminal motor nucleus

NPCs Neural Projenitor Cells

NSCs Neural Stem Cells

ob olfactory bulb

OGS Osteogenic Sarcoma

OPT Optical Projection Tomography

ot otic vesicle

PCL Purkinje Cell Layer

pco posterior commissure

PLAP Placental Alkaline Phosphatase

Plxdc2 Plexin domain containing 2

Plxdc1 Plexin domain containing 1

Pr5 principle sensory trigeminal nucleus

PRF Pontine Reticular Formation

pt pretectum

pvn paraventricular nucleus

sc superior colliculus

shRNAs short hairpin ribonucleic acids

TEM7 Tumour Endothelial Marker 7

TEM7R Tumour Endothelial Marker 7-related

teg tegmentum

th thalamus

V trigeminal ganglion

vn vestibular nuclei

VSC Ventral Spinal Cord

ZLI Zona Limitans Intrathalamica

1. Introduction

The vertebrate brain is a highly complex organ made up of many intricate networks of neurons. During neurodevelopment, patterning of the neuroepithelium, establishment of cell fate along the anteroposterior (AP) and dorsoventral (DV) axes, and the control of proliferation, apoptosis and differentiation are followed by (or sometimes linked with) migration of cells to appropriate positions and guidance of growing axons along stereotyped pathways to appropriate targets. Cell-cell communication, mediated by secreted and cell surface proteins (including transmembrane proteins), is vital for the coordination of these processes. In many cases, these distinct processes are controlled by the same molecules and signaling pathways, acting in different contexts throughout many aspects of brain development.

1.1 An introduction to early development of the brain

The central nervous system (CNS) arises from the neural plate, a sheet of epithelial cells that forms the dorsal surface of the gastrula stage embryo. During neurulation, the edges of the neural plate thicken and subsequently roll up, forming the primitive neural tube along the AP axis. Expansion of the anterior end of this tube results in the partition of vesicles which represent the primitive forebrain, midbrain and hindbrain structures (Echevarria *et al.*, 2003, Lumsden and Krumlauf, 1996). Work carried out in the amphibian demonstrated that the dorsal lip of the blastopore confers polarity on the neuroaxis (Spemann's organiser) (Spemann, 1938; reviewed in (Lumsden and Krumlauf, 1996). The inductive interaction of cells during gastrulation movements confer crude positional information that is later refined. In addition to patterning of the whole AP neuroaxis, there are also head-specific induction pathways. A posterior to anterior gradient of Wnt signaling results in posterior to anterior allocation of cell fate in the neural plate. Wnts are more highly expressed posteriorly and Wnt inhibitors, such as secreted Frizzled Related Proteins (sFRPs), Cerberus and Dickkopf1 (Dkk1), are more highly expressed anteriorly (Chapman *et al.*, 2004, Mukhopadhyay *et al.*, 2001, Piccolo *et al.*, 1999, Zhu *et al.*, 1999, Glinka *et al.*, 1998, Leyns *et al.*, 1997, Wang *et al.*, 1997, Bouwmeester *et al.*, 1996). Overexpression of Wnt inhibitors leads to enlarged forebrain and head structures, whereas inhibition of these molecules results in loss of forebrain and head structures with posteriorization of the remaining tissue (Houart *et al.*, 2002, Mukhopadhyay *et al.*, 2001,

Glinka *et al.*, 1998, Glinka *et al.*, 1997). Other important molecules in the determination of head specific cell fate include *Lim1* and *Orthodenticle homeobox 2* (*Otx2*). *Lim1* and *Otx2* are expressed in the head organiser region (Henson's node of amniotic embryos) and deletion of these genes in the mouse results in the absence of all head structures including the prosencephalon, mesencephalon and anterior hindbrain (Acampora *et al.*, 1995, Ang *et al.*, 1996, Shawlot and Behringer, 1995). Soon after neural induction, neural cells acquire distinct characteristics and fates according to their position along the AP or DV axes of the neural tube (Guillemot, 2007).

1.1.1. Patterning of the brain along the AP axis

The coordinated expression of transcription factors early in development of the nervous system subdivides the neural primordium into distinct domains, providing progenitor cells in these domains with distinct positional identities (Guillemot, 2007). Patterning proteins that provide positional identity along the AP axis include homeodomain proteins of the Otx, Gbx, Engrailed (En) and homeobox (Hox) families. More specifically, *Hox* genes have been shown to encode positional identity along the AP axis of the hindbrain (Kiecker and Lumsden, 2005, Lumsden and Krumlauf, 1996). The segmented nature of the primitive hindbrain emerges upon neural tube closure, as a series of seven or eight rhombomeres. This segmentation bares a striking resemblance to the bauplan of the Drosophila embryo. *Hox* genes in the hindbrain are expressed in a nested fashion and expression boundaries coincide with the interface between rhombomeres (Wilkinson *et al.*, 1989). *Hox* gene regulation of rhombomere identity has been demonstrated by several gain and loss of function experiments. Loss of *Hoxa1* function leads to the complete deletion of rhombomere 5, reduction of rhombomere 4 and loss of specific neuronal nuclei (Krumlauf, 1994, Lumsden and Krumlauf, 1996). Ectopic expression of *Hoxa1* results in the transformation of rhombomere 2 to rhombomere 4 identity (Alexandre *et al.*, 1996, Zhang *et al.*, 1994). *Hoxb1* is uniquely expressed in rhombomere 4(Murphy *et al.*, 1989). In *Hoxb1* knockout mice, facial motor neurons born in rhombomere 4 fail to migrate caudally into rhombomere 6 and vestibuloacoustic neurons fail to migrate to the contralateral side of rhombomere 4. Instead, both types of neuron migrate dorsolaterally, adopting the rhombomere 2 like path of trigeminal motor neurons (Studer *et al.*, 1996). Ectopic expression of *Hoxb1* in rhombomere 2 of the chick hind brain leads trigeminal motor

neurons to adopt rhombomere 4 like characteristics (Bell *et al.*, 1999). The important role of Hox genes in the regulation of rhombomere identity can not be disputed.

Efforts have been made to find and define similar segmental identity genes in the forebrain and midbrain regions. *Hox* genes are not expressed anterior to rhombomere 2, however, other transcription factor-encoding genes, many of which are orthologues of genes regulating anterior development in *Drosophila melanogaster*, exhibit highly localised expression patterns in forebrain and midbrain. These include members of the *distalless* (*Dlx*), *empty spiracles* (*Emx*), *forkhead* (*Fox*), *Otx*, *paired* (*Pax*) and *sine oculis* (*Six*) families (Reichert, 2002, Simeone *et al.*, 1992). The prosomeric model of segmentation identity was proposed based on the differential expression of these marker genes combined with morphological considerations (Rubenstein *et al.*, 1994). Initally, six transverse subdivisions (prosomeres) were proposed, three in the diencephalon and three in the prosencephalon. However, studies have highlighted the highly dynamic expression domains of various forebrain markers (Bell *et al.*, 2001). Paired with this finding was the discovery of widespread migration of cells across prosomeric boundaries (Larsen *et al.*, 2001). Therefore, a revised prosomeric model of segmentation has been proposed in which the diencephalon is composed of three neuromeres and the telencephalon remains unsegmented (Puelles and Rubenstein, 2003).

1.1.2. Patterning of the brain along the DV axis

In additional to AP patterning, establishment of cell fate must also be determined along the DV axis. DV patterning of the brain is primarily governed by two structures; the floor plate, which expresses ventralising factors including *sonic hedgehog* (*Shh*) and *nodal* (Placzek and Briscoe, 2005) and the roof plate at the dorsal midline, which expresses members of the BMP and Wnt families (Furuta *et al.*, 1997, Lee and Jessell, 1999). Genes involved in DV patterning of the neural tube are not restricted to the Hh, Wnt, and BMP families. Homeodomain factors of the *Pax*, *Nkx* and *Irx* families as well as the basic helix-loop-helix (bHLH) protein *Olig2* have also been shown to provide possitional identity to cells along the DV axis of the brain and spinal cord (Guillemot, 2007).

Shh is an important ventralising factor of the developing neural tube and is expressed in the notochord and specifies the floor plate (Echevarria *et al.*, 2003, Ishibashi *et al.*, 2005,

Yamada *et al.*, 1991). The floorplate also secretes Shh, and the identity of several types of neurons in the ventral neural tube are determined according to concentrations of secreted Shh (Briscoe and Ericson, 1999). In mice, removal of *Shh* results in failure of ventral neural tube formation (Chiang *et al.*, 1996). However, the complex nature of dorsalising and ventralising factor interaction is highlighted in *Shh* mutants. Proliferation and cell survival in these animals is also decreased in dorsal regions of the mesencephalon and diencephalon (Ishibashi and McMahon, 2002, Litingtung and Chiang, 2000).

Recently, it has been proposed that dorsal and ventral growth of the brain are co-ordinated via a signalling cascade of *Shh*, *FGF* and *Wnt* activity (Ishibashi *et al.*, 2005). *Shh* signalling directly induces expression of *FGF15* in the diencephalon and mesencephalon (Ishibashi and McMahon, 2002, Saitsu *et al.*, 2005). *FGF15* has been shown to upregulate *TCF4* expression in the dorsal diencephalon and *TCF4* expressing cells can respond to *Wnt* signals from the roofplate and are prompted to proliferate (Ishibashi *et al.*, 2005). *BMP4* expression in the roof plate has been shown to be involved in cell death in the developing brain (Golden *et al.*, 1999). In *Shh* mutants, *BMP4* expression in the roof plate of the diencephalon and mesencephalon in upregulated, leading to increased cell death (Ishibashi *et al.*, 2005). The DV coordination of neural tube growth is therefore mediated by the complex interaction of several proteins expressed along the DV axis.

The roofplate represents the major dorsalising centre of the developing neural tube. It has been proprosed that *BMP* and *Wnt* expression in the roof plate perform separate dorsalising functions. The blocking of *BMP* and *TFGβ* function in the chick using *Noggin*, a *BMP* antagonist, has shown that *BMP* expression is necessary for dorsal patterning of the neural tube and regulation of the domains of *Wnt* ligand, receptor and antagonist expression (Chesnutt *et al.*, 2004). On the other hand, *Wnts* in the roof plate are thought to act as mitogenic factors regulating proliferation in the dorsal neural tube (Chesnutt *et al.*, 2004, Dickinson *et al.*, 1994, Megason and McMahon, 2002). Double knockout of *Wnt1* and *Wnt3a* in the roof plate results in the reduction and loss of the same cell types that are lost in roofplate ablation studies (Lee *et al.*, 2000, Muroyama *et al.*, 2004).

1.1.3. Secondary organising centres of the developing brain

At neural plate and tube stages, local signalling centres in the neuroepithelium including the anterior neural ridge (ANR), the *zona limitans intrathalamica* (ZLI) and the midbrain-hindbrain boundary (MHB) refine AP specification of the three main brain domains (Echevarria *et al.*, 2003). An additional signalling centre, the cortical hem, patterns the dorsal telencephalon. The ANR is a secondary organiser of the anterior prosencephalon, involved in the maintenance and refinement of regionally restricted identities (Echevarria *et al.*, 2003). Removal of the ANR in explant cultures eliminates expression of *Bf1*, a transcription factor later expressed in most of the telencephalon (Tao and Lai, 1992). Transplantation of the ANR into more posterior regions induces the expression of *Nkx2.1*, a homeobox gene required for normal development of the hypothalamus and ventral forebrain, and *Emx* and *Dlx* which are normally expressed in the telencephalon (Houart *et al.*, 1998, Pera and Kessel, 1997, Price *et al.*, 1992). Members of the fibroblast growth factor (FGF) family, *FGF8* and *FGF15* are expressed in the ANR. In fact, *FGF8* has been shown to be crucial for the specification of the anterior forebrain and for telencephalic polarity (Meyers *et al.*, 1998, Vasiliauskas and Stern, 2001). *FGF8* beads can rescue *BF1* epxression following ANR elimination and the knockdown of *FGF8* expression in the most rostral domain of the ANR reduces *BF1* expression in the neural plate (Shimamura *et al.*, 1995). *Shh* is also expressed in close relation to the ANR, later in development, and has been shown to be involved in the regulatory activity of Nkx2.1, suggesting a role in regionalisation and cellular specification in the ventral telencephalon (Shimamura *et al.*, 1995, Brand *et al.*, 1996, Ericson *et al.*, 1995).

The ZLI constitutes the central boundary in the diencephalon, separating the posterior diencephalon (prosomere 1 and 2) from the anterior diencephalon (prosomere 3) (Echevarria *et al.*, 2003). The ZLI and surrounding regions express many proteins indicative of a secondary organising centre and the ZLI controls proliferation, regionalisation and polarity in diencephalic segments. *Shh* is expressed along the entire organiser, and at the dorsal end, the ZLI is flanked by *Wnt* expression caudally and *Fgf* expression rostrally (Echevarria *et al.*, 2003). *Wnt8b* is expressed and maintained in the ZLI until late embryonic stages (Garda *et al.*, 2002). The release of *Shh* from the ZLI is an essential step in the establishment of a functional thalamus (Scholpp *et al.*, 2007). *Shh* expression is necessary and sufficient to induce characteristic pro-neural transcription

factors within the mid-diencephalon (Hashimoto-Torii *et al.*, 2003, Kiecker and Lumsden, 2005, Scholpp *et al.*, 2006). The ZLI is induced within the area established by preceding *Otx1l* and *Otx2* expression. Knockdown of *Otx1l* and *Otx2* in the zebrafish (*Danio rerio*) results in the failure of ZLI and thalamus formation (Scholpp *et al.*, 2007).

The MHB forms at the boundary of the mesencephalon and metencephalon, within the anatomical restriction known as the isthmus at the border of *Otx2* and *Gbx2* expression (Millet *et al.*, 1999, Broccoli *et al.*, 1999, Brodski *et al.*, 2003, Waters and Lewandoski, 2006). The organiser capabilities of the boundary have been demonstrated by classic transplantation studies in the chick and quail. Isthmic grafts induce ectopic midbrain structures in the anterior brain and ectopic cerebellar structures in the posterior hindbrain (Gardner and Barald, 1991, Martinez *et al.*, 1991, Marin and Puelles, 1995). *Wnt1* and *FGF8* are expressed within the MHB, and loss of either gene function leads to failure of midbrain and anterior hindbrain formation (Chi *et al.*, 2003, McMahon and Bradley, 1990, Megason and McMahon, 2002, Meyers *et al.*, 1998, Thomas and Capecchi, 1990). When ectopically expressed, FGF8 but not Wnt1 is sufficient to mimic the organiser activity first detected in heterotopic grafts of the MHB itself (Chi *et al.*, 2003, Crossley *et al.*, 1996, Liu and Joyner, 2001, Martinez *et al.*, 1999, Meyers *et al.*, 1998, Irving and Mason, 1999, Liu *et al.*, 1999, Reifers *et al.*, 1998, Lee *et al.*, 1997). Implantation of a FGF8 soaked bead into the diencephalon leads to the transformation of surrounding tissues into tectum (Crossley *et al.*, 1996, Martinez *et al.*, 1999). Wnt signaling is required to maintain the correct expression of *FGF8* at the isthmus (Canning *et al.*, 2007). A cascade of transcription factors in the MHB is also necessary for *FGF8* expression, including *Pax2*, *Pax5*, *En1*, and *En2* (Liu and Joyner, 2001, Okafuji *et al.*, 1999). *Pax2* plays a crucial role in tectal development and ectopic expression of the gene in the chick mesencephalon and diencephalon transforms the diencephalon into a tectum-like structure (Okafuji *et al.*, 1999).

In addition to the ANR, which patterns the developing telencephalon along the AP axis, a second signalling centre, the cortical hem, patterns the dorsal telencephalon. Situated at the dorsomedial edge of the cerebral cortical hemisphere, the cortical hem expresses proteins of the BMP and Wnt families (including BMP2, BMP4, BMP5, BMP7, Wnt3a, Wnt5a and Wnt2b) (Furuta *et al.*, 1997, Grove *et al.*, 1998, Lee *et al.*, 2000, Shimogori et

al., 2004). The cortical hem forms the boundary between the developing hippocampus, the most medial part of the cerebral cortex, and the telencephalic choroid plexus (O'Leary *et al.*, 2007). Wnt3a is crucial for hippocampal development and removal of the canonical Wnt signal from the hem leads to failure of hippocampus formation (Lee *et al.*, 2000, Galceran *et al.*, 2000). BMP signalling seems to be responsible for generation of the choroid plexus epithelium (CPe). The conditional knockdown of the BMP receptor, BMPr1a, in the cortex leads to failure of choroid plexus differentiation (Hebert *et al.*, 2002, O'Leary *et al.*, 2007). Continuous activation of BMP in the hem transforms the entire cortical primordium into CPe (Panchision *et al.*, 2001). It has been suggested that telencephalic signalling centres interact during cortical development (Grove *et al.*, 1998, O'Leary *et al.*, 2007). Ectopic expression of FGF8 and Shh inhibits the expression of BMPs and Wnts (Huang *et al.*, 2007, Shimogori *et al.*, 2004). In fact, reduction of FGF8 expression in the ANR leads to anterior expansion of the Wnt8b expression domain (Storm *et al.*, 2006). Reduction of BMP signalling by the ectopic expression of Noggin leads to expansion of the anterior FGF8 expression domain (Ohkubo *et al.*, 2002). It is therefore most likely that signals from the ANR and the cortical hem interact intimately to pattern the dorsal telencephalon.

1.1.4. Proliferation and differentiation in early brain development

In early development of the vertebrate brain, neural progenitor cells (NPCs) proliferate in the neuroepithelium of the cephalic vesicle. Differentiating cells migrate out of the ventricular zone to the mantle zone, whereas precursor cells remain in the ventricular zone, where they continue to proliferate (Ishibashi *et al.*, 2005). *Notch* signalling and *Hes1/5* expression are intimately involved in the expansion of brain size and determination of the timing of neuronal differentiation (Ishibashi *et al.*, 2005, Kageyama *et al.*, 2005, Sasai *et al.*, 1992, Bai *et al.*, 2008). One of several *notch* ligands, *Delta-like 1*, is expressed on differentiating neurons and signals to surrounding precursor cells to remain in a proliferative state (Campos *et al.*, 2001). The onset of neural differentiation is induced by the expression of several proneural genes.

The proneural family of genes are a group of bHLH transcription factors which initiate programs of neurogenesis in NPCs (Bai *et al.*, 2008, Guillemot, 2007, Holmberg *et al.*, 2008). In the mouse and chick, the main proneural proteins include achaete-scute homolog-like 1 (Mash1 and Cash1 in mouse and chick respectively), Neurogenin 1 to 3

(Ngn1-3) and homologues of the drosophila gene, atonal (Math and Cath in mouse and chick respectively) (Bai *et al.*, 2008, Guillemot, 2007). Following extensive self renewal to enlarge their cell population, NPCs initiate the expression of proneural genes in response to region-specific neurogenic signals (Lillien, 1998, Guillemot, 2007). With this progression, cells in the neural tube become heterogeneous, including progenitors which do not express proneural genes and those which do (Bertrand *et al.*, 2002). The progression of neural differentiation within a NPC has been suggested to be determined by proneural gene expression or activity levels (Bertrand *et al.*, 2002). Progenitors may remain in a self-renewing state when low levels of proneural genes are expressed, but high levels of proneural gene expression committ NPCs to differentiation. The spatial regulation of proneural gene expression is controlled by patterning proteins and by cross-repression by other proneural genes (Scardigli *et al.*, 2003, Zhou and Anderson, 2002).

Proneural protein-mediated influence on neurogenesis is achieved by several cellular mechanisms. Firstly, proneural proteins suppress the self-renewal and multipotency qualities of NPCs by blocking the expression of the SoxB1 transcription factors (Sox1, Sox2 and Sox3)(Bylund *et al.*, 2003, Guillemot, 2007). This is partially achieved by the actitivation of an antagonistic Sox gene, Sox21 (Sandberg *et al.*, 2005). Secondly, proneural proteins influence the regional specification of neural identities by regulation of homeodomain proteins. Mutations in distal-less homeobox 1 and 2 (*Dlx1* and *Dlx2*), two genes directly induced by *Mash1*, result in a block in the differentiation of striatal neurons (Poitras *et al.*, 2007, Yun *et al.*, 2002, Anderson *et al.*, 1997, Guillemot, 2007). Proneural proteins can specify different neuronal fates in different regions of the CNS, depending on the differential expression of interacting transcription factors (Lee and Pfaff, 2003). Thirdly, proneural proteins can indirectly influence the fate of progenitor cells by determining the time of cell cycle exit and thus, the nature of the inductive signals the cells are exposed to. Repression of proneural gene expression mainly occurs through the Notch signalling pathway (Bai *et al.*, 2008, Holmberg *et al.*, 2008, Kageyama *et al.*, 2005). Activation of proneural gene expression seems to be more complex, and patterning molecules including members of the Wnt family have been implicated in the process (Yu *et al.*, 2006).

Notch is a transmembrane protein which is activated upon binding of its ligands, Delta and Jagged (Jarriault *et al.*, 1995, Kageyama *et al.*, 2005, Ohtsuka *et al.*, 1999). Upon activation of Notch, the intracellular domain of the protein is transported to the nucleus, where it forms a complex with the DNA-binding protein RBP-J, releasing transcriptional repression of Hes1 and Hes5 by RBP-J (Honjo, 1996, Ohtsuka *et al.*, 1999, Selkoe and Kopan, 2003). *Hes1* is expressed highly in NPCs, repressing proneural gene expression and maintaining cells in a self renewing state (Kageyama *et al.*, 2005, Sasai *et al.*, 1992). Onset of proneural gene expression in subsets of progenitor cells coincides with a decrease in Hes1 expression (Bai *et al.*, 2008, Kageyama *et al.*, 2005). *Hes1* expression represses Mash1 expression both at the transcriptional level, by binding to the promoter, and at the level of protein-protein interaction, by forming a non-functioning heterodimer with E47, thus inhibiting formation of the Mash1-E47 functional heterodimer (Chen *et al.*, 1997, Kageyama *et al.*, 2005, Sasai *et al.*, 1992). Disruption of Hes1 expression in *Hes1* mutant mice leads to increased expression of proneural genes including *Mash1*, premature neurogenesis and severe neural tube defects leading to death (Hatakeyama *et al.*, 2004, Ishibashi *et al.*, 1995). In fact, depletion of Hes expression (Hes1,3 and 5) in transgenic mice does not simply lead to premature neurogenesis, but to the differentiation of virtually all progenitors into neurons at the expense of later-born cell types (Hatakeyama *et al.*, 2004).

Members of the Wnt family have been implicated in the maintanance of progenitor pools in the developing neural tube and the suppression of neural differentiation (Chenn and Walsh, 2002, Dickinson *et al.*, 1994, Megason and McMahon, 2002). As was briefly mentioned earlier, ectopic expression of Wnt1 or stabilized β-catenin in the early stages of chick spinal cord or mouse forebrain development, respectively, has been shown to result in an increased number of NPCs and suppression of neuronal differentiation (Chenn and Walsh, 2002, Megason and McMahon, 2002, Matsunaga *et al.*, 2002). Retroviral expression of Wnt7a in mouse forebrain explants also promoted proliferation, suppressing neuronal differentiation (Viti *et al.*, 2003).

Wnt involvement in proneural gene expression seems to be more complicated than initially thought, and members of the Wnt family have recently been implicated in the activation of neuronal differentiation in a stage-related manner. Wnt7a promotes neuronal differentiation in the developing mouse neocortex, at the expense of NPCs, at later stages

of cortical development (Embryonic day (E)13.5), through the activiation of the canonical pathway (Hirabayashi *et al.*, 2004). This effect appears to be mediated at least in part by direct regulation of Ngn1 promoter by the β-catenin-TCF complex. However, activation of the canonical pathway by stabilised β-catenin in NPCs dissociated from the neocortex at earlier stage of development (E10.5) does not promote neural differentiation (Hirabayashi *et al.*, 2004, Chenn and Walsh, 2002).

It is important to note that members of the Wnt family do not always affect proliferation at the expense of differentiation and vice versa. The expression of Wnt3a and/or Wnt5a in postnatal or adult NPCs in culture results in increased proliferation and neuronal differentiation (Yu *et al.*, 2006). The stage-dependent effect of Wnt expression on cell proliferation has also been illustrated by Wnt3a. Although Wnt3a has been shown to increase proliferation at postnatal or adult stages (Yu *et al.*, 2006), expression of the protein inhibits proliferation of NSCs isolated from E11.5 mice (Muroyama *et al.*, 2004). In postnatal and adult neural progenitor cells, Wnt3a and Wnt5a expression does not result in increased glial differentiation and therefore, induced neuronal differentiation is owing to an increase in neuronal fate choice of neural progenitor cells. In general, it is thought that the expression of proneural proteins reinforces the process of neuronal fate specification by inhibiting the alternative fate (Kageyama *et al.*, 2005). In *Mash1;Math3* double knock-out or *Mash1;Ngn2* double knock-out mice, the cells that should normally become neurons adopt the glial fate instead (Nieto *et al.*, 2001, Tomita *et al.*, 2000). Thus, there is a fate switch from neurons to glia in the absence of proneural gene expression, indicating that *Mash1*, *Math* and *Ngn* regulate neuronal versus glial cell fate determination (Nieto *et al.*, 2001, Tomita *et al.*, 2000, Kageyama *et al.*, 2005).

1.1.5. Apoptosis in brain development

Controlled cell death (apoptosis) plays a major role in normal brain development by the control of progenitor and neuronal cell number (Ahlgren *et al.*, 2003, Oppenheim, 1991) . Absence of apoptosis leads to neural tube overgrowth phenotypes in a number of mouse models. Key apoptopic effectors in early development of the nervous system are members of the cysteine-containing, aspartate-specific family of proteases, the *caspases* (Nicholson and Thornberry, 1997, Alnemri *et al.*, 1996). Several *caspase* knockout mice lines exhibit malformations due to brain overgrowth. Mice lacking *Caspase9* display greatly enlarged telencephalon and expanded midbrain, but no expansion of posterior neural tissues (Kuida

et al., 1998, Hakem *et al.*, 1998). *Caspase3* null mice exhibit abnormal growths in the cranial neural tube including ectopic cell masses and abnormal protrusions of neuroepithelium (Kuida *et al.*, 1996). Knockdown of a gene involved in regulation of caspase activity, *APAF-1*, results in hyperplasia in the diencephalon and mesencephalon but not in the rhombencephalon (Cecconi *et al.*, 1998, Yoshida *et al.*, 1998).

Several other familys have been implicated in the control of programmed cell death within the developing nervous system. *Winged helix* (*Forkhead*) transcription factors have been implicated in a wide variety of developmental events including patterning, differentiation, proliferation, cell-cycle control, signalling and apoptosis. Retroviral over-expression of *FoxG1* in the neural tube of the chick results in overgrowth of the telencephalon and mesencephalon but not of more posterior regions (Ahlgren *et al.*, 2003). This phenotype is not a result of increased proliferation, but rather of decreased apoptosis in the neuroepithelium. Members of the FGF family have also been implicated in control of apoptosis in the developing brain. *FGF receptor 3* (*FGFr3*) controls development of the cortex by regulating proliferation and apoptosis of progenitor cells (Inglis-Broadgate *et al.*, 2005). Overexpresssion of *FGFr3* in the mouse brain results in enlargement of the brain and an increase in cortical thickness. In fact, ventricular zone volume is doubled by E14.5, due to a mild increase in proliferation and a profound decrease in apoptosis (Inglis-Broadgate *et al.*, 2005).

Programmed cell death also plays an essential role in later brain development. The nervous system is initially generated with an excess number of neurons. Over-production of neurons is followed by extensive apoptosis during the period of connectivity with target tissue (this is sometimes referred to as nervous system 'pruning'). Some studies have suggested that as many as half of the originally produced cells are pruned at this stage in development (Oppenheim, 1991). Evidence from *in vitro* and *in vivo* experiments suggests that neuronal apoptosis of this kind is partially controlled by the *c-Jun N-terminal kinase* (*JNK*) signalling pathway (Becker and Bonni, 2005, Harper and LoGrasso, 2001, Mielke *et al.*, 2000, Yang *et al.*, 1997, Kuan *et al.*, 1999). *JNK* signalling stimulates expression of pro-apoptotis genes through the activation of the transcription factor, *c-jun*, and activates members of the cell-intrinsic death machinery in neurons (Becker *et al.*, 2004, Donovan *et al.*, 2002, Ham *et al.*, 2000, Putcha *et al.*, 2003).

1.2 Axon guidance

The mature mammalian brain is a complex organ made up of many intricate networks of neurons. During development, axons are guided to their final destination and through a series of choice points by extracellular guidance cues in their environment (Dickson, 2002, Yu and Bargmann, 2001, TessierLavigne and Goodman, 1996). An axon's response to a particular guidance cue is dependent on the repertoire of receptors that are expressed on the cell surface of the axon. Individual guidance cues may have a positive (attractive) or negative (repulsive) effect on an axon depending on the receptors present. There is, however, only a rudimentary understanding of the necessary factors involved in the coordination of axon guidance during mammalian brain development and the genetic programming that governs its intricacy. A number of conserved families of molecules involved in axon guidance have been identified in several species, including the mouse. These include the netrins, semaphorins, slits and ephrins (Dickson, 2002, Yu and Bargmann, 2001). Netrins, slits and some semaphorins are secreted molecules, whereas ephrins and other semaphorins are transmembrane or GPI-linked proteins, expressed on the cell surface. For each of the axon guidance molecules of these families, one or more families of transmembrane receptors have been identified; for example, UNC-40 (DCC) and UNC-5 receptors for the netrins, roundabout (Robo) for the slit proteins, neuropilin and plexin receptors for the semaphorins, and Eph receptors for the ephrins (Dickson, 2002, Yu and Bargmann, 2001). The complex nature and versatility of the system can be illustrated by the fact that each of the guidance cues mentioned has been implicated in numerous axon guidance events.

In addition to these conserved families of axon guidance molecules, a number of families of classically defined morphogens, including Wnt, BMP and Hh have also been found to act in axon guidance (Charron and Tessier-Lavigne, 2005). These molecules and their receptors are characterised by a variety of extracellular motifs involved in cell-cell interactions, dimerisation or autoregulation. During spinal cord development, the axons of dorsally differentiated commissural neurons project towards, and eventually cross the floor plate, forming axon commissures (Charron and Tessier-Lavigne, 2005). Initially, studies of the process of commissural axon migration, floor plate crossing and post-crossing guidance in the fly, chick and mouse provided much evidence for a role for classically defined morphogens in axon guidance.

Netrin 1 (Ntn1), a long-range chemoattractant which is secreted by the floorplate of the spinal cord during development, attracts axons of commissural neurons into ventral regions (Charron and Tessier-Lavigne, 2005). In *Ntn1* knockout mouse, many commissural axon trajectories are halted, and misguided axons fail to invade the ventral spinal cord. However, a subset of commissural axons continues in a 'normal' trajectory towards the midline, indicating the existence of an alternative attractive molecule. Shh has been shown to function as an axonal chemoattractant that can mimic the Ntn1-independent chemoattractant activity of the floor plate *in vitro* (Charron and Tessier-Lavigne, 2005, Charron *et al.*, 2003). In *Ntn1* mutant mice, commissural axons initally project ventrally before becoming misrouted, suggesting the presence of an additional chemorepellent in the roof plate. BMP6 and BMP7 *have* been shown to contribute to the chemorepellent activity of the roof plate. In fact, BMP7 induces the collapse of commissural axon growth cones, eliciting a rapid change in cytoskeletal organization (Augsburger *et al.*, 1999, Butler and Dodd, 2003).

In the chick spinal cord, Shh has also been shown to guide commissural axons in the rostral direction along the longitudinal axis (Bourikas *et al.*, 2005). Silencing of *Shh* using RNAi or a hybridoma producing a function-blocking Shh antibody, resulted in the stalling of axons at the contralateral floor plate border and random turning of axons caudally or rostrally (Bourikas *et al.*, 2005). In the fly, loss of *Wnt5* function results in the mis-projection of axons which normally project into the anterior commissure, into the posterior commissure (Yoshikawa *et al.*, 2003). In fact, ectopic expression of *Wnt5* through the midline of the CNS prevented formation of the anterior commissure. In the rat, a second family member, *Wnt 4,* is expressed in an increased gradient along the posterior to anterior axis of the spinal cord, and is essential for normal guidance of post-crossing commissural axons, acting as an instructive post-crossing attractant (Lyuksyutova *et al.*, 2003, Charron and Tessier-Lavigne, 2005). *In vitro*, the posterior placement of an ectopic Wnt4 source causes redirection of post-crossing axons posteriorly (Lyuksyutova *et al.*, 2003). The addition of the wnt inhibitors *sFRP1* (secreted frizzled-related protein 1),sFRP2 and sFRP3 *in vitro* caused axons which had crossed the midline to stop and turn randomly along the AP axis. Mice lacking the wnt receptor Frizzled 3 (Fz3) also have defects in AP guidance of commissural axons after midline crossing (Lyuksyutova *et al.*, 2003).

However, roles for classical morphogens in axon guidance have not only been demonstrated in commissural axons. *In vitro*, Wnt5a has been shown to increase olfactory sensory neuron axon outgrowth and to alter growth cone morphology (Rodriguez-Gil and Greer, 2008). The loss of a BMP receptor, BMPr1b, leads to abnormal ventral ganglion cell axon guidance to the optic nerve head (Liu *et al.*, 2003). In mice lacking *BMPr1b*, many axons arising from the ventrally located ganglion cells fail to enter the optic nerve head, and instead, make abrupt turns in this region. Retinal ganglion cell axons growing towards the ventral midline of the diencephalon project either contralaterally or ipsilaterally in response to specific guidance cues at the optic chiasm. Pax2 is essential for the development of the normal trajectory of retinal ganglion cells, and in *Pax2* mutant mice, axons fail to cross the midline (Torres *et al.*, 1996). *Shh* is normally down regulated at the optic chiasm during the guidance of retinal ganglion axons to the region, however, in *Pax2* mutant mice, mistargetting of retinal ganglion axons is accompanied by maintained Shh expression. In fact, ectopic expression of Shh at the midline has been shown to interfere with retinal ganglion cell axon growth, preventing axons from successfully crossing the midline (Trousse *et al.*, 2001). *In vitro*, the addition of Shh to retinal explants causes rapid growth cone arrest and subsequent retraction of retinal ganglion cell axons (Trousse *et al.*, 2001). These examples highlight the varying roles classic morphogens such as Shh, Wnt and BMP play in axon guidance throughout the developing nervous system.

1.3 Screens for novel transmembrane proteins – the PLAP secretory trap method.

In addition to conserved families of axon guidance molecules and classically defined morphogens, a large number of novel transmembrane protein-encoding genes containing axon guidance motifs are predicted in mammalian genomes, many of which are expressed in the developing brain and are good candidates to be involved in axon guidance or other aspects of nervous system development. In recent years, annotation of the mouse genome and improved bioinformatic techniques have led to whole genome studies of conserved proteins that may have roles in axon guidance and development of the nervous system (Dolan *et al.*, 2007). In addition to bioinformatic screens for novel genes, phenotypic based screens involving random insertional mutation of genes encoding cell surface proteins have been carried out in mice with much success (Mitchell *et al.*, 2001).

The PLAP secretory trap method was designed and developed to screen for novel axon guidance receptors in the mouse by simultaneous mutation of the trapped gene and transgenic labelling of neurons that normally express it and their axons (Leighton *et al.*, 2001). Mutagenesis is carried out in embryonic stem cells by the insertion of a vector at random into the mouse genome and the characterisation of insertional mutations by 5' RACE (Rapid amplification of cDNA ends). Successful insertion of the vector into a gene induces null or severely hypomorphic mutations (Leighton *et al.*, 2001, Mitchell *et al.*, 2001). The endogenous promoter of the trapped gene drives production of a bicistronic transcript that encodes two proteins, a fusion of the endogenous protein to β-geo (a fusion of β-gal to neomycin phosphotransferase) and placental alkaline phosphatase (PLAP), which is translated independently using an internal ribosome entry site (Figure 1.1). It is important to note that both markers report gene expression and not necessarily endogenous protein localisation; PLAP labels axons of neurons expressing the trapped gene, whereas the β-geo fusion protein remains membrane bound inside cell bodies. Comparisons of corresponding X-gal and PLAP stainings confirm that PLAP reliably labels the axons of neurons stained with X-gal (Leighton *et al.*, 2001). Studies of previously trapped genes have shown that both the PLAP and β-gal markers faithfully reflect reported expression patterns (Leighton *et al.*, 2001), although perdurance of the β-geo fusion protein may be an issue in comparing the dynamics of expression to results from *in situ* hybridisation techniques (Miller *et al.*, 2007). In recent years the PLAP secretory trap method has been modified further by the addition of homology arms to the vector construct, allowing targeted gene trapping. Homology arms can be designed to a specific gene of interest, directing the recombination event and ensuring that the correct gene is isolated (Friedel *et al.*, 2005).

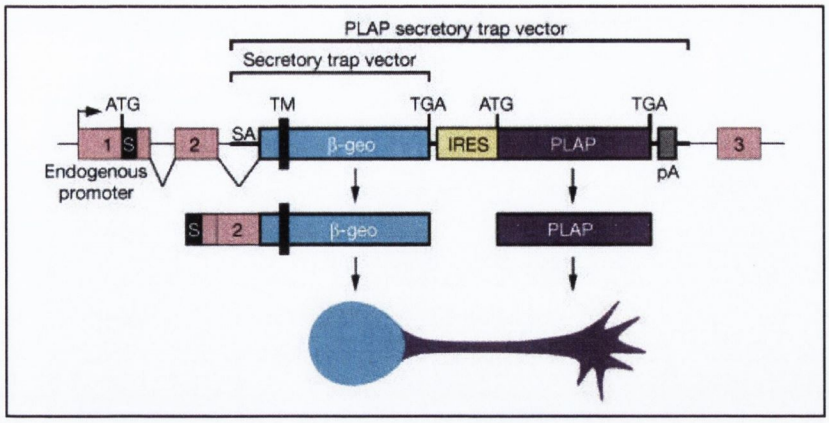

Figure 1.1 Representation of the PLAP Secretory Trap Vector. S, signal peptide; SA, splice acceptor; β-geo, fusion of β-galactosidase and neomycin phosphotransferase; IRES, internal ribosome entry site; PLAP, placental alkaline phosphatase; TM, transmembrane region. Figure adapted from (Leighton *et al.*, 2001).

1.4 *Plexin domain containing 2 (Plxdc2)*

Studies utilising the PLAP secretory trap method isolated a gene trap insertion in a novel gene (mouse line KST37) (Leighton *et al.*, 2001) which has since been named *Plexin domain containing 2 (Plxdc2)*. In the mouse, the *Plxdc2* gene encodes a type I transmembrane protein of 530 amino acids, characterised by an extracellular region of weak nidogen homology and a plexin repeat or PSI domain, a domain found in known axon guidance molecules such as semaphorins and plexins as well as integrins and a small number of other molecules (Bork *et al.*, 1999). The PSI domain is a cysteine rich repeat, usually containing 6 to 8 cysteine residues, which has been shown to be involved in autoregulatory intramolecular contacts in a number of cases (Zang and Springer, 2001, Bunch *et al.*, 2006, Mould *et al.*, 2005). In Plxdc2, the PSI domain is missing the 7th cysteine residue but is otherwise highly conserved.

Prior to this study, limited analysis of the KST37 line had been carried out. Plxdc2-βgeo expression was documented in the floorplate, dorsal root ganglia, sympathetic preganglionic neurons and motorneurons of the E12.5 spinal cord, with PLAP reliably labelling the axons of Plxdc2-βgeo expressing neurons (Figure 1.2, a and b) (Leighton *et al.*, 2001). In the newborn brain, Plxdc2 (PLAP) expression was noted in the fimbria, hippocampus and in stripes of Purkinje cells in the cerebellum (Figure 1.2, c and d) (Leighton *et al.*, 2001).

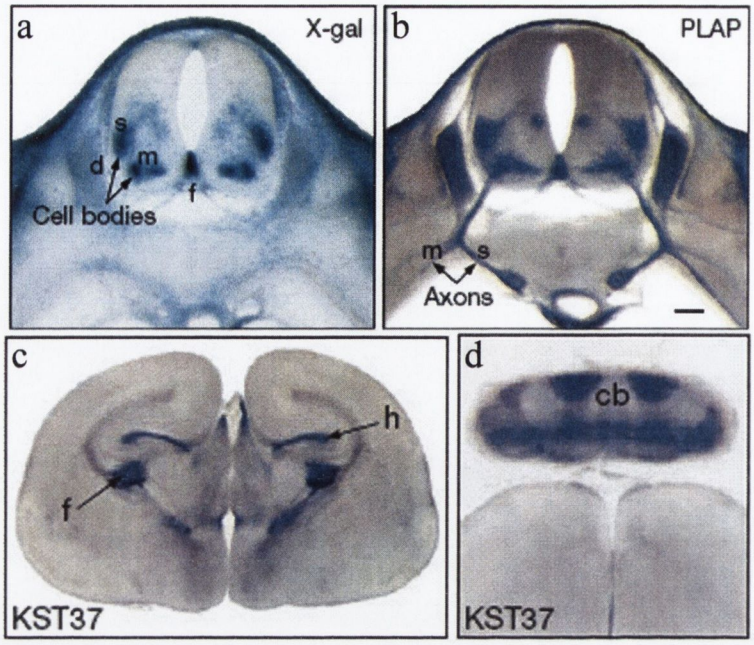

Figure 1.2 Analysis of Plxdc2 expression in the *Plxdc2* PLAP secretory gene trap mouse line (KST37). a and b, transverse sections through a *Plxdc2* heterozygote at E12.5 illustrating Plxdc2 expression in the spinal cord and peripherally projecting axons. c and d, coronal sections through the brain of a newborn *Plxdc2* gene trap heterozygote. a, X-gal staining; b, c and d, PLAP staining. cb, cerebellum; f, fimbria; h, hippocampus; d, dorsal root ganglia; f, floor plate; m, motorneurons; s, sympathetic preganglionic neurons. Scale bar: a and b, 100μm; c, 205μm; d, 700μm. Figure adapted from (Leighton *et al.*, 2001).

A related gene (now called *Plxdc1*) was isolated in a screen for genes upregulated in human tumour endothelium and named *tumour endothelial marker 7* (*TEM7*) (St Croix *et al.*, 2000, Carson-Walter *et al.*, 2001). *Plxdc2* is thus also referred to as *TEM7-related* (*TEM7R*). The TEM family is a large group of unrelated proteins whose expression is upregulated in tumour endothelium (Carson-Walter *et al.*, 2001). In recent years, there has been growing interest in TEMs owing to their potential use in anti-angiogenic therapies for the treatment of cancerous growths. The grouping of TEMs has been based solely on their over-expression in tumour endothelium and not on any structural or genomic homologies. Therefore, members of the TEM family have contrasting architectures and are probably involved in a wide range of pathways and functions. In one study, an unbiased gene expression analysis of endothelial cells from normal human colonic tissue versus cancerous colonic tissue isolated forty-six TEMs, four of which were transmembrane bound and structurally conserved in mouse and human (Carson-Walter *et al.*, 2001).

Plxdc1 (*TEM7*) encodes a protein of 500 amino acids and shares all the architectural domains of Plxdc2 (TEM7R) (Figure 1.3, Appendix 5.1). Alignment of mouse Plxdc2 and Plxdc1 illustrates 47% similarity across the protein sequences (Appendix 5.1). The Plxdc2 and Plxdc1 proteins share a conserved cytoplasmic region which is unrelated to other known proteins (Carson-Walter *et al.*, 2001) (Appendix 5.1).

Plxdc2 is highly conserved across vertebrate species. Human, murine and avian proteins display striking conservation in protein architecture, particularly in the region of nidogen homology, the PSI domain and the transmembrane domain (Appendix 5.2). The human and mouse Plxdc2 proteins are 91% identical, and the mouse and chicken proteins are 81% identical (Appendix 5.2). The cytoplasmic tail of human, mouse and chick Plxdc2 is highly conserved. A related gene, *CG2221*, has also been identified in the fly (*Drosphila melanogaster*). *CG2221* is the only member of the plexin domain containing family in the fly, and the protein exhibits similar levels of homology to mouse Plxdc2 and Plxdc1 proteins (26% and 29% identical respectively). Deletion of *CG2221* causes a lethal phenotype (www.flybase.org). The fact that CG2221 is expressed in neuroblasts and the mRNA is asymmetrically localised in neuroblasts (Lecuyer *et al.*, 2007) is consistent with a possible role in control of proliferation or neurogenesis in the fly. A member of the plexin domain containing family, *Pxd-1*, has been identified in the worm (*Caenorhabditis elegans*)(Appendix 5.2). Deletion of *Pxd1* does not cause a lethal phenotype (www.wormbase.org). The cytoplasmic domains of the fly and worm proteins show more similarity to each other than to chick, mouse or human proteins. There is, however, a single region of conserved sequence in the cytoplasmic domain of all five plexin domain containing proteins (Appendix 5.2).

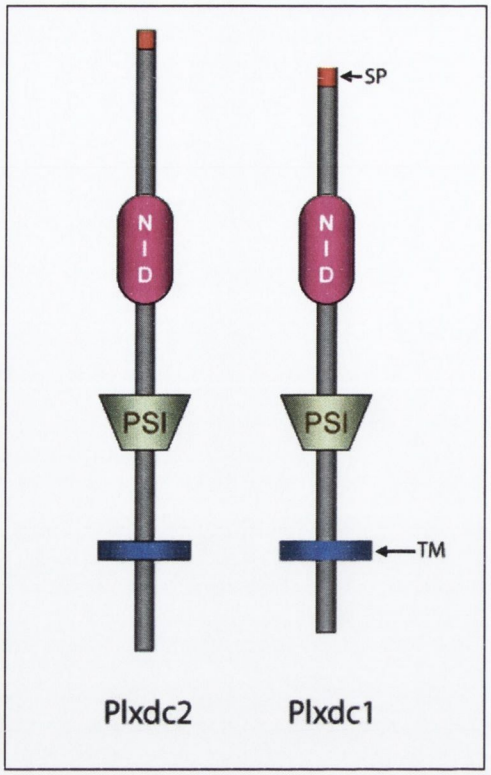

Figure 1.3 The architecture of Plxdc2 & Plxdc1. *Plxdc2*: 530 amino acids. *Plxdc1*: 500 amino acids. NID, area of weak nidogen homology; PSI, plexin repeat; SP, signal peptide; TM, transmembrane domain.

1.5 A role for *Plxdc1* in tumour angiogenesis

To date, much of the functional analyses of the Plexin domain containing family of proteins has concentrated on *Plxdc1* (*TEM7*) and its implication in cancer, more specifically in the formation of new blood vessels from pre-existing capillaries (angiogenesis). The principal cell type involved in angiogenesis is the epithelial cell, which must undergo proliferation, migration and differentiation for angiogenesis to occur (this is termed endothelial cell capillary morphogenesis). The initial finding that both *Plxdc1* and *Plxdc2* are upregulated in human colorectal cancers (Carson-Walter *et al.*, 2001) has spurred further research which has advanced our understanding of the role of *Plxdc1* in this field. *Plxdc1* has since been shown to be upregulated & essential during endothelial cell capillary morphogenesis (Wang *et al.*, 2005). The expression of several TEMs was investigated in primary aortic endothelial cells during capillary morphogenesis and compared to normal culture levels of the genes. Of the markers tested, only *Plxdc1* (*TEM7*) expression was up-regulated upon endothelial cell capillary morphogenesis (Wang

et al., 2005). Primary cultured mouse aortic endothelial cells expressed all of the TEMs examined except *Plxdc1 (TEM7)*, whose expression was relatively low in normal culture. Stimulation of endothelial cell capillary morphogenesis dramatically enhanced *Plxdc1* expression whereas inhibition of capillary morphogenesis by serum stimulation completely blocked *Plxdc1* expression. In contrast, *Plxdc2* was expressed at relatively high levels within cultured endothelial cells and its expression was not affected during capillary morphogenesis. Investigation of *Plxdc1* and *Plxdc2* expression in a mouse endothelial cell line derived from mouse axillary lymph node vessels showed similar results (Wang *et al.*, 2005).

Plxdc1 research has not been limited to *in vitro* assays of expression. *Plxdc1* has also been shown to be upregulated in human glioblastoma endothelium (Beaty *et al.*, 2007). This result adds credence to the *in vitro* study of Wang *et al.*, as glioblastomas are a highly aggressive brain tumor, with one of the highest rates of new blood vessel formation. Immunohistochemistry with an antibody for Plxdc1 illustrated protein expression in glioblastoma microvasculature, but not in normal brain endothelium (Beaty *et al.*, 2007).

High expression of *Plxdc1* has also been associated with metastasis and poor survival of patients with osteogenic sarcoma (OGS)(Fuchs *et al.*, 2007). A database of differentially expressed genes was created from human tissue samples of six low-grade and six high-grade OGS tumours and results compared with those from a normal immortalized osteoblast cell line (FOB) and four commercially available OGS-derived cell lines. *Plxdc1* mRNA was abundantly expressed in SAOS cells (derived from high-grade OGS), but not in FOB or MG63 cells (derived from low-grade OGS)(Fuchs *et al.*, 2007). Furthermore, immunostaining of 50 high-grade and 42 lowgrade human OGS specimens with an antibody for Plxdc1 illustrated that 97% of high-grade OGS specimens with metastasis had high Plxdc1 staining and elevated expression of Plxdc1 was found to correlate with poor survival of affected patients. Importantly, inhibiting *Plxdc1* function by siRNA inhibited invasion and migration of OGS cells with metastatic potential.

The parallels between angiogenesis and nerve growth have been noted previously and several molecules originally identified in axon guidance have been directly implicated in angiogenesis (Carmeliet and Tessier-Lavigne, 2005, Basile *et al.*, 2006, Freitas *et al.*, 2008,

Lu *et al.*, 2004). These include *Sema4D*, an established regulator of axonal growth cone guidance. *Sema4D* is highly expressed in head and neck squamous cell carcinomas (HNSCCs) and stimulates endothelial cell migration when the protein is shed from HNSCCs *in vitro* (Basile *et al.*, 2006). Short hairpin RNA (ShRNA) mediated gene silencing of *Sema4D* in HNSCC cells before grafting into nude mice results in a dramatic reduction in tumour vascularity and tumour growth (Basile *et al.*, 2006). Other members of the semaphorin family, *Sema3B* and *Sema3F* have been shown to be negative regulators of tumour growth and can act as tumour suppressors, inhibiting tumour cell proliferation, colony formation, and growth *in vivo* ((Neufeld and Kessler, 2008, Bielenberg and Klagsbrun, 2007, Futamura *et al.*, 2007, Kusy *et al.*, 2005, Xiang *et al.*, 2002, Tse *et al.*, 2002, Tomizawa *et al.*, 2001). *Netrin1* and *Unc5b* have been shown to regulate normal blood vessel guidance (Carmeliet and Tessier-Lavigne, 2005, Lu *et al.*, 2004). Unc5b is expressed in endothelial tip cells and loss of the protein in mice results in aberrant extension of tip cell filopodia and excessive branching of many vessels. Treatment of cultured endothelial cells or growing vessels *in vivo* with Netrin1 induces filopodial retraction (Lu *et al.*, 2004).

Several classically defined morphogens have also been implicated in angiogenesis. Expression of exogenous *Wnt5a* in human primary endothelial cells promotes angiogenesis, inducing endothelial cell proliferation, migration and the formation of capillary like networks (Masckauchan *et al.*, 2006, Masckauchan and Kitajewski, 2006). Several members of the Wnt family have been implicated in normal development of the vasculature, including Wnt2, Wnt4 and Wnt7b, along with several Wnt receptors (Zerlin *et al.*, 2008). In mice, targeted disruption of *Wnt2* or *Frizzled5* leads to defects in placental vasculature (Ishikawa *et al.*, 2001, Monkley *et al.*, 1996), whereas disruption of the *Wnt7b* gene results in severe defects in the smooth muscle component of the major pulmonary vessels causing rupture of major vessels which leads to perinatal death (Shu *et al.*, 2002).

1.6 Potential binding partners of Plxdc1 and Plxdc2

In vitro studies have suggested Cortactin as a putative binding protein of both Plxdc2 and Plxdc1 (Nanda *et al.*, 2004), however, this interaction has not been demonstrated *in vivo.* Cortactin is an intracellular protein, activated via phosphorylation to promote rearrangement of the actin cytoskeleton (Campbell *et al.*, 1999, Huang *et al.*, 1998). Binding of cortactin and the extracellular domain of Plxdc1 and Plxdc2 was demonstrated by biochemical techniques including immunoprecipitation of cortactin from mouse brain extract, and subsequent probing of blots with extracellular Plxdc1 and Plxdc2 protein. However, Plxdc2 and Plxdc1 are putative cell surface proteins and interaction of their exracellular domains with an intracellular protein such as Cortactin seems unlikely. The development of Plxdc1 antibodies confirmed protein expression at the cell surface of endothelial cells in human tumour endothelium (Nanda *et al.*, 2004). Characterisation of *Plxdc1* gene products in human tumour endothelium isolated an alternative transcript of *Plxdc1* which lacks a signal peptide, PSI domain and transmembrane domain (Nanda *et al.*, 2004). This transcript could potentially interact with cortactin intracellularly, but it is important to note that no evidence of this interaction has been demonstrated *in vivo*. Mouse *Plxdc2* has three possible annotated transcripts, all of which encode proteins containing PSI domains, regions of nidogen homology and transmembrane domains (ENSMUST00000028081, ENSMUST00000114702 and ENSMUST00000114703, Ensembl release 50). It therefore, seems very unlikely that Plxdc2 could interact with cortactin, *in vivo*.

Although no definitive binding partner for Plxdc2 has been identified, several studies have isolated nidogen as a binding partner for Plxdc1 (Lee *et al.*, 2006b, Lee *et al.*, 2007). Using a recombinant ectodomain of Plxdc1 as a probe, an interaction between nidogen and Plxdc1 was identified *in vitro* (Lee *et al.*, 2006b). Furthermore, a cell overlay binding assay demonstrated that nidogen interacted with full length Plxdc1 on the cell surface, enhancing cell spreading in *Plxdc1* transfected cells (Lee *et al.*, 2006b). Additional studies involving a model of sciatic nerve injury have also supported Nidogen as a binding partner of Plxdc1 (Lee *et al.*, 2007). Nidogens are routinely upregulated in the sciatic nerve following transection and recombinant Nidogen-1 increases the process formation of Schwann cells cultured from adult rat sciatic nerves. Nidogen-1 induced process formation of Schwann cells is completely inhibited by the addition of extracellular Plxdc1, indicating the strong interaction capability of the proteins *in vivo* (Lee *et al.*, 2007).

1.7 Objectives of this thesis

The primary aim of this work is the examination of *Plxdc2* expression *in vivo* and the investigation of potential roles of the protein in embryonic axon guidance and general development of the vertebrate nervous system. The overall aim of the work can be divided into two objectives:

i. To establish a comprehensive description of *Plxdc2* expression in the developing mouse, with particular emphasis on the developing brain.

Prior to this study, no detailed description of *Plxdc2* expression in the developing nervous system had been published. A comprehensive description of *Plxdc2* expression was documented through the use of the *Plxdc2* PLAP secretory trap line, KST37 and the *in situ* transgenic reporters included in the PLAP Secretory Trap vector (β-geo and PLAP) (Miller *et al.*, 2007). This work is presented in Chapter 2.

ii. To investigate endogenous *Plxdc2* function by establishing an experimental model in which an examination of *Plxdc2* function can be explored, both by the knockdown of endogenous gene function and by misexpression of the Plxdc2 protein.

The phenotypic analysis of loss of *Plxdc2* expression in embryonic development and axon guidance events was investigated in mutant mouse lines. Homozygous *Plxdc2* gene trap mutants did not survive to birth and lethality occurred at a stage precluding analysis of the protein in axon guidance events. Preliminary analyses of the effect of loss of Plxdc2 were subsequently carried out on homozygous mutants of a viable Plxdc2 line, Plxdc2GFP. This work is presented in Chapter 2.

Investigation of the effects of *Plxdc2* misexpression in the developing vertebrate nervous system was carried out in the chick. Following the confirmation of a similar *Plxdc2* expression pattern in the chick and mouse, manipulation of *Plxdc2* expression was achieved by *in ovo* electroporation. Examination of gene function in the chick was facilitated by the construction of a full-length *Plxdc2* expression plasmid to effect ectopic

expression, and by the design of several short hairpin forming RNAs (shRNAs) against *Plxdc2* to knockdown gene expression. This work is presented in Chapter 3.

These analyses revealed dynamic Plxdc2 expression in several signalling centres of the early embryonic brain including the floorplate, dorsal midline, midbrain-hindbrain boundary and the cortical hem. At later stages of development, Plxdc2 expression was revealed in a discrete subset of nuclei and tracts in the brain including the mammillotegmental tract, cerebellar peduncle, posterior commissure and a subset of hypothalamic nuclei. Functional assays in the chick led to the surprising findings of a Plxdc2 effect on proliferation and differentiation within the developing neural tube.

2. Chapter 2 – *Plxdc2* and *Plxdc1* in the developing nervous system of the mouse

2.1 Aims of this chapter

The principle aim of the work in this chapter was to establish a comprehensive description of *Plxdc2* expression in the developing mouse, with particular emphasis on the developing brain, and to compare and contrast this expression with that of the related gene, *Plxdc1*. This description was achieved using the PLAP secretory trap lines, KST37 (Leighton *et al.*, 2001) and TEM7 (Friedel *et al.*, 2005) and the *in situ* transgenic reporters included in the PLAP Secretory Trap vector (β-geo and PLAP). A combination of light microscopy and OPT were employed to achieve a comprehensive 3D description of expression. The major findings of this study were published in Gene Expression Patterns (Miller *et al.*, 2007). Functional analysis was not carried out in the KST37 line as homozygous gene trap mice did not survive to birth, with lethality occurring at a stage precluding analysis of the role of *Plxdc2* in brain development and axon guidance. Following confirmation of knockdown of *Plxdc2* transcript, preliminary analysis of the effect of loss of *Plxdc2* was carried out on homozygous mutants of a viable *Plxdc2* line, Plxdc2GFP. In addition to these analyses, an alkaline phosphatase (AP) tagged form of mouse Plxdc2 was produced in culture and was used as a probe on wildtype brains in order to investigate extracellular Plxdc2 binding *in vivo*.

2.2 Introduction

One of the preliminary steps in deciding whether a novel gene may be of interest for further study is the investigation of its expression pattern *in vivo*. This can provide tantalising insights in to the potential function of the gene by highlighting its discrete expression in regions of interest to the investigator. The comparison of a novel gene expression pattern with those of established genes can provide clues to the molecules and pathways that it may interact with. As was discussed in chapter one, the *in situ* transgenic reporters included in the PLAP Secretory Trap vector (β-geo and PLAP) provide invaluable aids in the process of documenting the expression of the trapped gene. The 3D representation of expression data from *in situ* transgenic reporter approaches, or other techniques, such as *in situ* hybridization and immunohistochemistry, can be limited by the

imaging methods used to document expression. Analysis of serial sections through a specimen can provide detailed information on gene expression within each section. 3D digital reconstruction of serial sections can sometimes result in significant gaps in data and the distortion of 3D shape, owing to missing sections and physical stress on tissues during sectioning. Techniques such as confocal microscopy provide beautiful 3D reconstructions of optical sections, but are limited by sample size constraints and to the use of fluorescent markers.

Optical Projection Tomography (OPT) has overcome many of the limitations of other microscopy techniques and produces high-resolution 3D images of both fluorescent and nonfluorescent whole biological specimens (Sharpe *et al.*, 2002). OPT successfully documents the spatial distribution of expression in all dimensions in the context of the morphology of the embryo. Expression can then be visualised across various developmental stages, and the dynamism of the expression pattern studied in detail. Rather than scanning through different depths of focus in the specimen to reconstruct the 3D object (as in confocal microscopy), OPT maximises the depth of focus, capturing projected optical density images of the whole specimen (Sharpe *et al.*, 2002). Computer software then reconstructs the original 3D information from 400 images taken through one complete 360 degree revolution. The 3D computer object can then be viewed as a series of virtual sections in any orientation or can be viewed from "external" view-points (when volume rendered). However, virtual sectioning through OPT 3D reconstructions does not produce images of equal resolution to those produced by the microscopic imaging of serial sections through a specimen. OPT visualisation of gene expression is therefore best used in collaboration with microscopic imaging of expression on serial sections.

Several studies have demonstrated OPT's invaluable contribution to the comparison of specific gene expression patterns (Fisher *et al.*, 2008, Summerhurst *et al.*, 2008, Miller *et al.*, 2007). The value of 3D expression databases for the comparison of expression patterns of several genes and for the comparative definition of 3D structures within the developing embryo has been recognised (Fisher *et al.*, 2008, Venkataraman *et al.*, 2008). 3D mapping of OPT expression data from several sources into a common database is a challenge but is now being adopted (Fisher *et al.*, 2008). OPT has also been used to great effect to document the normal anatomy of organs and systems of the developing embryo. Abnormal liver morphogenesis in the absence of Wnt1 (Ijpenberg *et al.*, 2007) and

abnormal spleen and pancreatic morphology in the absense of Bapx1 (Asayesh *et al.*, 2006) have been documented using the technique. More recently, OPT has been used to create a high resolution, three-dimensional atlas of mouse vascular development between E8 and E10 (Walls *et al.*, 2008).

2.3 Analysis of *Plxdc2* expression, in a gene trap mouse line

2.3.1. Characterisation of a PLAP secretory trap insertion in Plxdc2

Previous studies utilising the PLAP secretory trap method isolated a gene trap insertion in a novel gene (mouse line KST37) (Leighton *et al.*, 2001). Using a candidate primer approach, the exact site of the PLAP secretory trap insertion in the KST37 mouse line was characterised to intron 3 of the Plxdc2 gene (Figure 2.1, Ensembl: ENSMUST00000028081, work carried out by Dr. Roland Friedel, Stanford University). Insertion of the PLAP secretory trap vector into an intron, results in the creation of a fusion transcript through the splicing of the 'trapped' gene's upstream regions to vector sequences (See section 1.3 and Figure 1.1 for PLAP secretory trap vector details).

Figure 2.1 The site of the PLAP secretory trap insertion in the KST37 mouse line in intron 3 of the *Plxdc2* gene (Ensembl: ENSMUST00000028081, release 50). Black font, wildtype sequence; blue font, vector sequence; underlined font, site of primer design; Black arrowhead, exact location of a PLAP secretory trap insertion in the Plxdc2 gene.

2.3.2. Genotyping of Plxdc2 genetrap mice

Plxdc2 gene trap mice were genotyped by polymerase chain reaction (PCR) as outlined in section 2.8.2 using the primers detailed in table 2.1. PCR of genomic DNA from a wildtype animal resulted in amplification of a single band of 436 basepairs (bp, Lane A, figure 2.2). In a heterozygous animal, an additional mutant band of 246 bp was amplified (Lane B, figure 2.2)

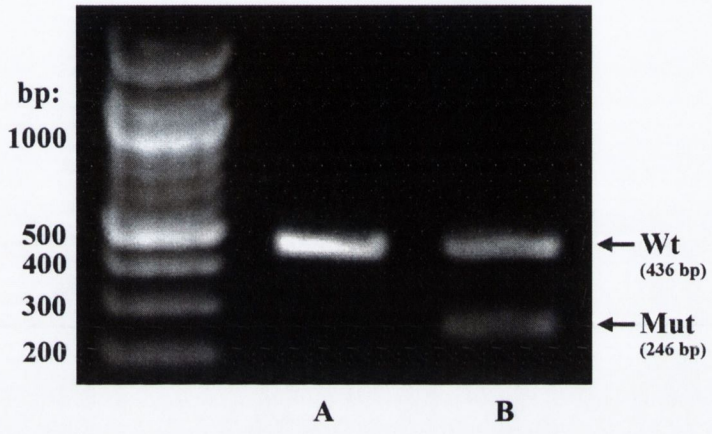

Figure 2.2 PCR genotyping of *Plxdc2* gene trap mice. Lane A, wildtype *Plxdc2* animal; Lane B, heterozygous *Plxdc2* gene trap mutant. Size of bands compared against 100 bp DNA ladder (New England Biolabs) with sizes in bps indicated.

2.3.3. Plxdc2-βgeo expression in the embryo

Expression of Plxdc2-βgeo in the embryo was investigated by whole mount X-gal staining of heterozygous gene trap mice at embryonic day (E) 9.5, E11.5 and in the brain of E15.5 embryos. At E9.5, Plxdc2-βgeo expression was observed in the floor of the midbrain and in an anterior and medial area of the telencephalon that included the choroid plexus epithelium and presumptive cortical hem (Figure 2.3). Expression of Plxdc2-βgeo was also evident in the midbrain-hindbrain boundary (MHB), a major organising centre of the developing brain (Raible and Brand, 2004). Within the trunk region, Plxdc2-βgeo expression occurred in a segmented pattern. At later stages of development, Plxdc2-βgeo expression was found in the dorsal root ganglia (DRG, see below) and expression at E9.5 was thus most likely to include the neural crest-derived spinal primordia which give rise to the sensory cells of the DRG. Plxdc2-βgeo expression was also evident in the limb buds,

the lung buds and in the otic vesicle (Figure 2.3). In the most caudal region of the embryo, expression was seen in the lateral edges of the neuroepithelium in the region of the still open posterior neuropore (future dorsal midline) and in the extreme distal tip of the tail bud (Figure 2.3).

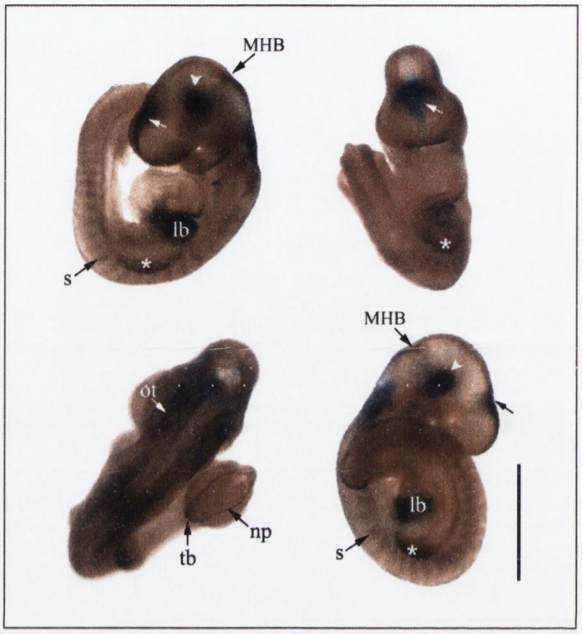

Figure 2.3 Plxdc2-βgeo expression in the E9.5 mouse. X-gal staining of heterozygous gene trap mice illustrated cellular Plxdc2-βgeo expression in discrete regions of the developing embryo. Arrow, anteromedial region of the telencephalon that includes the choroid plexus epithelium and presumptive cortical hem; arrowhead, floor of midbrain; asterisk, limb-bud; lb, lung bud; MHB, midbrain–hindbrain boundary; ot, otic vesicle; np, lip of neuropore; tb, tail bud; s, Plxdc2-βgeo expression within the somites. Scale bar 1.25 mm.

By E11.5, Plxdc2-βgeo expression was more complex and widespread, and its intricate expression pattern became increasingly difficult to document using classical microscopy and photography techniques. OPT was therefore utilised to visualise Plxdc2-βgeo expression in the E11.5 mouse (Figure 2.4; Supplementary video 1). OPT highlighted Plxdc2-βgeo expression in restricted domains in a number of areas of the E11.5 embryo (Figure 2.4; Supplementary video 1) including the brain, limb bud, sensory ganglia, branchial arches, heart, lung buds (Figures 2.4 and 2.5) and urogenital tract (data not

shown). In the eye, cellular Plxdc2-βgeo expression was restricted to a region of localised expression in the centre of the lens (Figure 2.4 a and b).

In both hind and fore limb buds, Plxdc2-βgeo was expressed in broad domains of distal mesenchyme, extending more proximally on the posterior side (Figure 2.4 a and d) with a reduced level at the extreme distal tip (Figure 2.4 f and h). Expression was also seen in the apical ectodermal ridge, a major signalling centre involved in the proximal-distal patterning of the developing vertebrate limb (Figure 2.4 f and inset in h). Continued Plxdc2-βgeo expression was also evident in regions of the developing otic vesicle (Figure 2.4 b). Plxdc2-βgeo expression within the trunk at E11.5 had resolved to a clear restriction within the developing DRG (Figure 2.4 f). This pattern of expression agrees with previously published data at E12.5, which showed Plxdc2-βgeo expression in the DRG and PLAP expression in the corresponding axons (Leighton *et al.*, 2001). These data also showed reporter gene expression in motor and sympathetic preganglionic axons and the floorplate of the spinal cord (Leighton *et al.*, 2001). In the present study, Plxdc2-βgeo expression is evident in the ventral spinal cord, including the floorplate from an anterior limit at the midbrain, and the motor column of the neural tube from an anterior limit at the level of prevertebrae C2/C3 (Figure 2.4 f and h). A broad band of expression is also evident in the lateral plate mesoderm.

In the E11.5 brain, Plxdc2-βgeo expression was observed in a number of discrete areas, including important patterning centres. The broad expression seen in the medial telencephalon at E9.5 had evolved to a clearly defined domain (Figure 2.4 i and j; Supplemental Movie 1). By this stage of development the telencephalic vesicles have expanded and are separated by a medial invagination of the dorsal midline due to low levels of proliferation combined with high levels of apoptosis (Furuta *et al.*, 1997). Plxdc2-βgeo expression was observed throughout the medial invagination encompassing the cortical hem and choroid plexus epithelium (CPe) and extending slightly caudal in the medial diencephalon (Figure 2.4 i and j, arrow). The cortical hem is crucial for normal cortical development and disruption of the area can lead to severe hippocampal abnormalities (Shimogori *et al.*, 2004). At E11.5, a complete ring of Plxdc2-βgeo expression was evident at the MHB (Figure 2.4 I; Supplemental Movie 1) with significantly more intense expression both dorsally and ventrally. Elsewhere in the brain,

Plxdc2-βgal continues to be expressed in the floor of the midbrain although this expression now extends into the hindbrain. Two clusters of cellular Plxdc2-βgeo expression were also evident in the ventral midbrain, lateral to and distinct from the floor plate expression (Figure 2.4 b, c, d and h).

The specificity of the reporter gene expression was confirmed by whole-mount *in situ* hybridisation with a *Plxdc2* antisense riboprobe (Figure 2.5). At E11.5, *in situ* hybridisation showed the same overall pattern of expression as the Plxdc2-βgeo reporter gene, although there was a reduction in the relative intensity in certain areas, particularly in the cortical hem and the limbs (Figure 2.5 a, d and e). These areas gave a stronger *in situ* hybridisation signal at E10.5 (Figure 2.5 b and c). This modest disparity could be due to technical differences in the protocols used for *in situ* hybridisation on E10.5 and E11.5 embryos (the former being freshly prepared and the latter having been frozen), or possibly to perdurance of the Plxdc2-βgeo fusion protein. Despite this difference, *in situ* hybridisation confirmed *Plxdc2* expression in the cortical hem, the MHB, the floor of the midbrain and in all of the areas highlighted by X-gal staining of heterozygous gene trap embryos. Later expression in specific brain areas was also confirmed by *in situ* hybridisation (data not shown). A control sense probe for *Plxdc2* was routinely employed in *in situ* hybridisation experiments a showed a very low level of non-specific background staining. Representative images of *in situ* hybridisation using the sense probe for *Plxdc2* are shown in appendix 5.11.

2.3.4. Comparative definition of Plxdc-βgeo expression within the cortical hem and MHB

We noted remarkable similarities between the expression of Plxdc2-βgeo and that of a number of members of the Wnt family, several of which are expressed in the cortical hem and MHB, for example. *Wnt1* is essential for the development of the posterior midbrain and anterior hindbrain and is expressed in a thin ring at the MHB as early as E9.5 (Panhuysen *et al.*, 2004). *Wnt3a* expression can be used to distinguish the structure of the cortical hem as early as E10.5 (Grove *et al.*, 1998). By E11.5, *Wnt5a* and *Wnt8b* are also expressed in the cortical hem (Grove *et al.*, 1998, Shimogori *et al.*, 2004, Tole *et al.*, 2000).

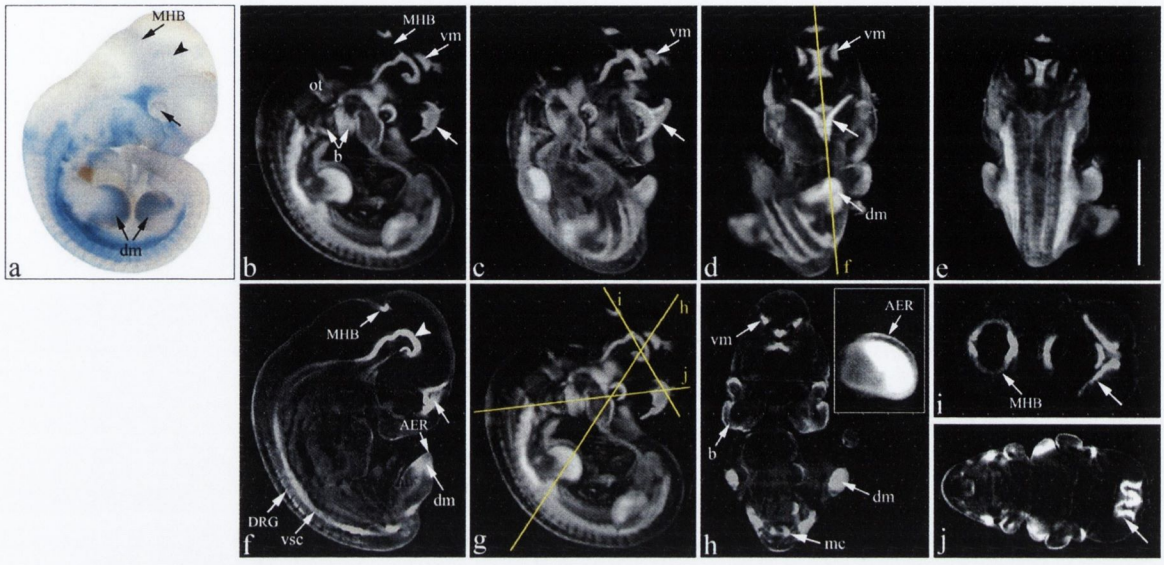

Figure 2.4 Plxdc2-βgeo expression in the E11.5 mouse revealed by OPT analysis of X-gal stained heterozygous *Plxdc2* gene trap embryos. a, whole mount image of an X-gal stained E11.5 embryo. b–e and g, still images from different external viewing angles of a volume rendered specimen (Supplemental data, movie 1). f and h–j, virtual sections through the specimen with section planes illustrated in g. Insert in h, sagittal section through the forelimb showing Plxdc2-βgeo expression in the AER. Panels i and j, anterior to the right. Apparent optic cup staining is owing to pigmentation of this area in C57Bl6 mice. a: arrow, Plxdc2-βgeo expression in the lens of the eye. b–j; arrow, cortical hem and developing choroid plexus. Arrowhead, floor of midbrain; AER, apical ectodermal ridge; b, branchial arches; dm, distal mesenchyme of the limb; DRG, dorsal root ganglia; mc, motor column; MHB, midbrain–hindbrain boundary; ot, otic vesicle; vm, clusters of Plxdc2-βgeo expression in the ventral midbrain; vsc, ventral spinal cord, including floorplate and motor column. Scale bar: a–g and j, 2.9 mm; h, 2.6 mm; i, 2 mm.

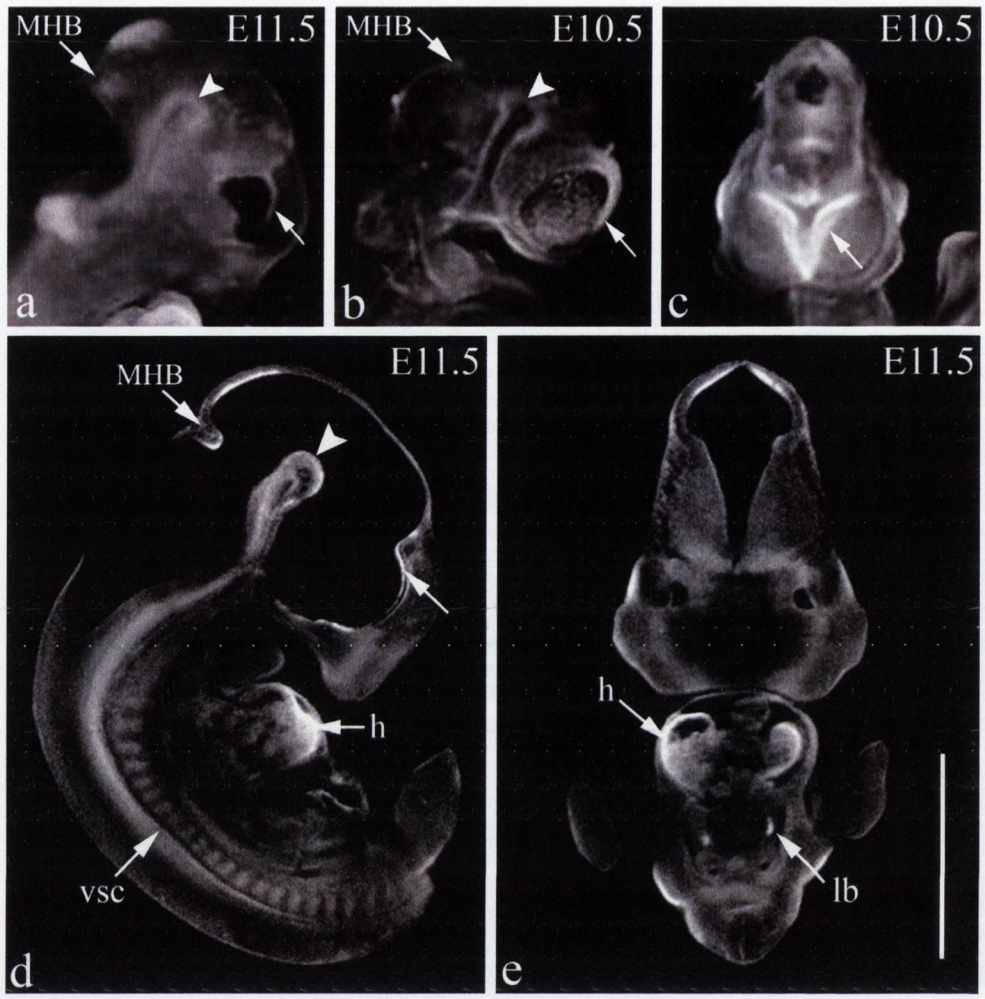

Figure 2.5 *In situ* hybridisation confirms the Plxdc2-βgeo expression pattern. Whole-mount Plxdc2 *in situ* hybridisation on E10.5 (b,c) and E11.5 (a,d,e) wildtype embryos analysed by OPT. a–c, still images from different external viewing angles of volume rendered specimens. d and e, virtual sections through an E11.5 embryo showing reduced Plxdc2 expression in the cortical hem and MHB. Arrow, cortical hem and choroid plexus; arrowhead, floor of midbrain; h, heart; lb, lung bud; MHB, midbrain–hindbrain boundary; vsc, ventral spinal cord, including floorplate and motor column. Scale bar: a, d and e 2.7 mm; b and c 1.9 mm.

In order to more closely define the domains of Plxdc2-βgeo expression within brain structures, its expression at E11.5 was compared to that of *Wnt1*, *Wnt3a*, *Wnt5a* and *Wnt8b*, examined and viewed with the same OPT methodology (Figure 2.6). Comparison with *Wnt1* and *Wnt5a* confirms co-expression with Plxdc2-βgeo at the MHB and in the floor of the midbrain (Figure 2.6 a, b and c), but unlike *Wnt1*, Plxdc2-βgeo is not detected in the dorsal midline of the midbrain. In the floorplate, Plxdc2-βgeo expression is more extensive rostrocaudally than either of the Wnt genes and is not restricted to the ventricular aspect. *Wnt5a* expression also shows striking similarities with that of *Plxdc2* in the limb (Figure 2.4, h) (Yamaguchi *et al.*, 1999) and in the glial wedge (see below and (Keeble *et al.*, 2006).

The extent of the expression domain in the medial cerebral cortex was more closely defined by comparison with domains of *Wnt3a*, *Wnt8b* (Figure 2.6 d-p) and *Wnt5a* expression (data not shown). Figure 2.6 d-f show dorsal external views of the midbrain-forebrain regions of 3D reconstructed (volume rendered) specimens. Figure 2.6 h-j represents the overall shape and size of the domains by showing them in isolation at a constant viewing angle, whereas Figure 2.6 k-p shows comparable virtual sections. As previously described (Grove *et al.*, 1998), *Wnt3a* is expressed precisely within the cortical hem (Figure 2.6 i and l) as well as the dorsal midline of the more caudal brain. *Wnt8b* is expressed in a broader domain encompassing the cortical hem but extending also into the choroid plexus medially, and more laterally along the walls of the telencephalic vesicles including the region of the prospective hippocampus (Figure 2.6 j and m). The domain of Plxdc2-βgeo expression is less broad than *Wnt8b* but also includes the choroid plexus and the prospective hippocampus (Figure 2.6 h and k). Rostrocaudally, the midline expression of Plxdc2-βgeo is more extensive than either Wnt gene; as mentioned earlier, it extends caudally into the dorsal midline of the diencephalon and Figure 2.6 n-p shows that rostrally, Plxdc2-βgeo is expressed at a level where *Wnt3a* is no longer expressed and *Wnt8b* is localised more laterally.

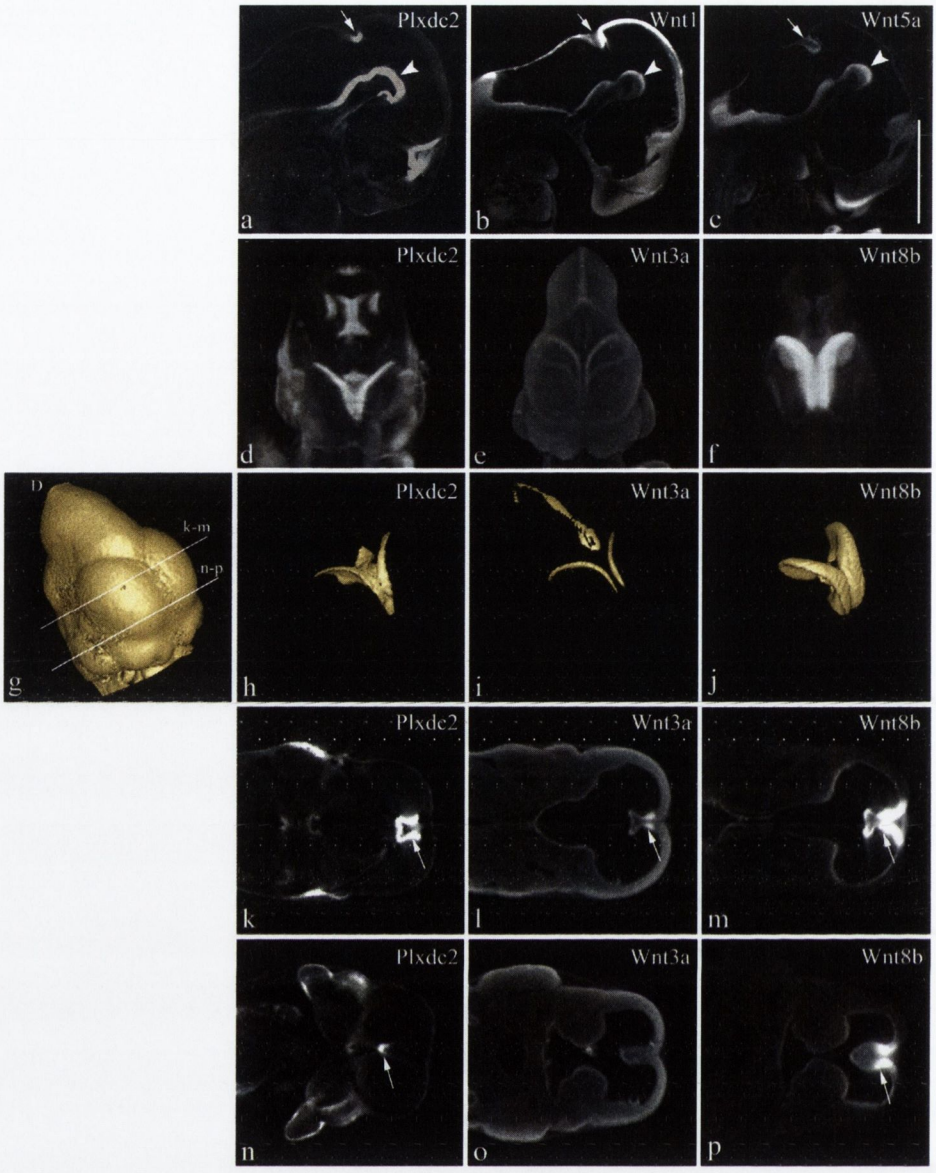

Figure 2.6 Definition of Plxdc2-βgeo expression within the cortical hem and MHB at E11.5 by comparison to *Wnt1, Wnt3a, Wnt5a* and *Wnt8b*. a–c and k–p, virtual sections and d–f, frontal external views of heads of volume rendered specimens. g–j, surface rendered views of whole head (g) and stained region of anteromedial telencephalon (h–j). Lines in g indicate plane of sections in k–m and n–p. a–c: arrow, MHB; arrowhead, floor of midbrain. k–m: arrow indicates position of cortical hem, the extent of which is shown by Wnt3a expression in l. n–p: arrows indicate differential staining at rostral levels, as described in the text. Scale bar: a–j, 1.45 mm; k–p, 2.2 mm.

2.3.5. Plxdc2 expression in the E15.5 brain

Expression of Plxdc2-βgeo in the E15.5 brain was investigated by X-gal staining of 100μm sections from heterozygous *Plxdc2* gene trap mice (Figure 2.7). An intricate pattern of Plxdc2-βgeo expression was observed in a number of nuclei throughout the brain as well as in the neuroepithelium. In the forebrain, regions of cellular Plxdc2-βgeo expression include the glial wedge and the developing medial septum (Figure 2.7 a-c). Expression is evident in the choroid plexus (derived from the CPe) and derivatives of the cortical hem, namely the fimbria and the dentate gyrus of the developing hippocampus as well as Cajal-Retzius cells in the marginal zone of the developing cortex (Figure 2.7 d-f). Plxdc2-βgeo expression is also observed in discrete nuclei within the hypothalamus, habenula, pretectum and amygdala (Figure 2.7 f-k). In more caudal regions, Plxdc2-βgeo is also expressed within the tegmentum and pons in the midbrain reticular formation and pontine reticular formation (Figure 2.7 n-s). Plxdc2-βgeo expression was notable at the border region of the superior colliculus and the pons (Figure 2.7 q) and within the principal sensory trigeminal nucleus and trigeminal motor nucleus (Figure 2.7 r and s). In the hindbrain, extensive Plxdc2-βgeo expression was evident in the floorplate and in distinct compartments of the developing Purkinje cell layer of the cerebellum as well as many nuclei of the medulla oblongata, including the vestibular nuclei (Figure 2.7 t – x).

Figure 2.7 Plxdc2-βgeo expression in the E15.5 brain. Cellular Plxdc2-βgeo expression in the E15.5 brain was investigated by X-gal staining of 100 μm coronal sections from heterozygous *Plxdc2* gene trap mice. a-x, serial sections through the brain of a heterozygous *Plxdc2* gene trap mouse from rostral to caudal regions. Arrow in a-c, Plxdc2-βgeo expression at the medial septum. Insert in d shows high magnification view of presumptive Cajal–Retzius cells. Arrowhead in p-s, clusters of Plxdc2-βgeo expression at the border region of the tectum and the pons. amy, amygdala; cb, cerebellum; ChP, choroid plexus; CP, caudate putamen; CR, Cajal–Retzius cells; cx, cortex; DG, dentate gyrus; EP, entopeduncular nucleus; FIM, fimbria; fp, floorplate; GW, glial wedge; hab, habenula; hip, hippocampus; hy, hypothalamus; ic, inferior colliculus; mb, mammillary bodies; med, medulla oblongata; MRF, midbrain reticular formation; N5n, trigeminal motor nucleus; PCL, Purkinje cell layer; PRF, pontine reticular formation; Pr5, principle sensory trigeminal nucleus; pt, pretectum; sc, superior colliculus; sep, septum; teg, tegmentum; th, thalamus; vn, vestibular nuclei. Scale bar 1.5 mm.

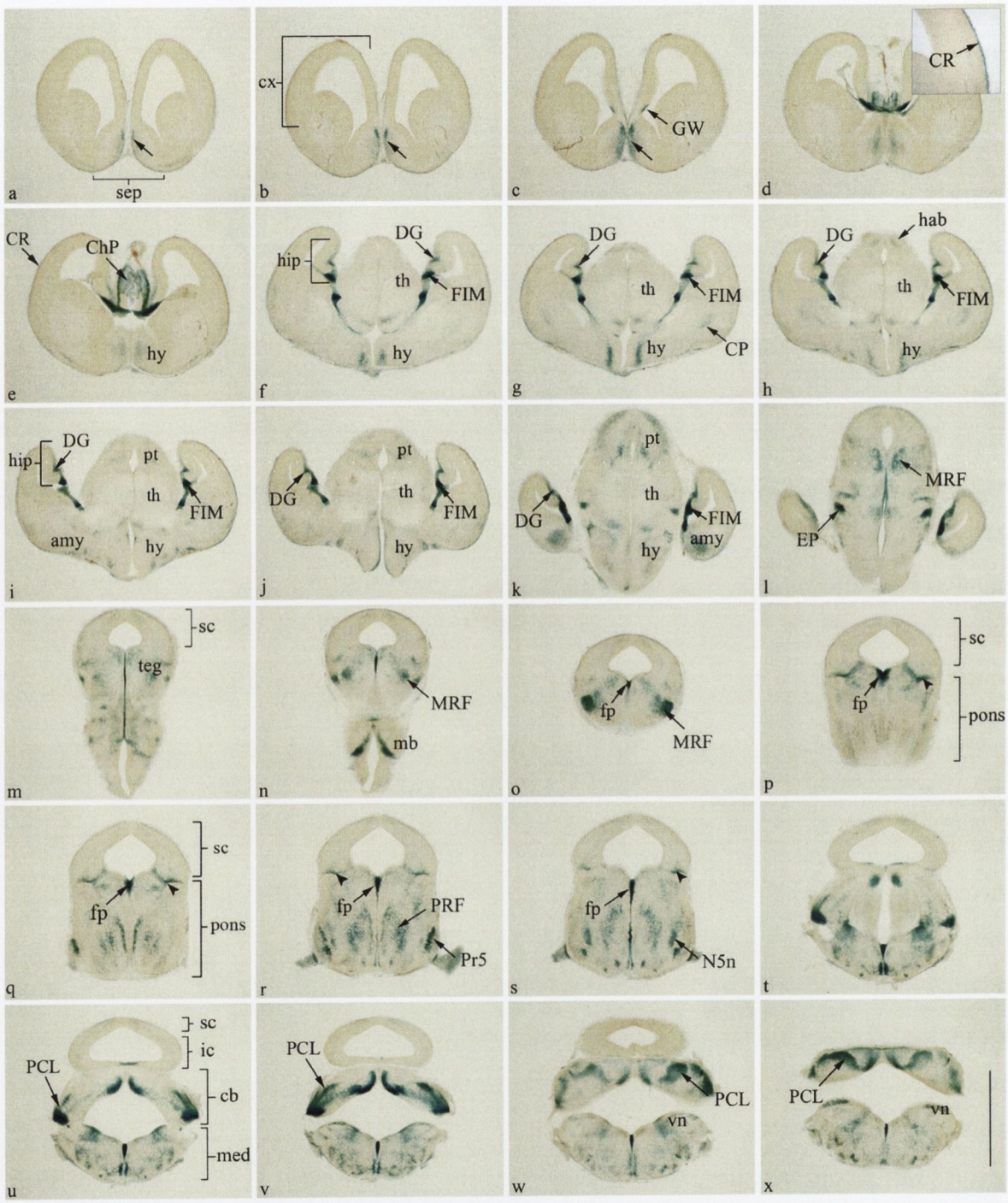
a
sep
b
cx
c
GW
d
CR
e
CR
ChP
hy
f
hip
DG
th
FIM
hy
g
DG
th
FIM
hy
CP
h
DG
hab
th
FIM
hy
i
hip
DG
pt
th
FIM
amy
hy
j
DG
pt
th
FIM
hy
k
DG
pt
th
FIM
amy
hy
l
EP
MRF
m
sc
teg
n
MRF
mb
o
fp
MRF
p
sc
fp
pons
q
sc
fp
pons
r
fp
PRF
Pr5
s
fp
N5n
t
u
sc
ic
PCL
cb
med
v
PCL
w
PCL
vn
x
PCL
vn

Staining in several areas including the glial wedge and fimbria, for example, indicates that Plxdc2-βgeo expression is, at least in part, glial in nature. Neuronal Plxdc2 expression was also confirmed by PLAP staining of several axon tracts in the E15.5 brain (Figure 2.8). PLAP staining was evident in axons of the posterior commissure which crosses the midline at the dorsal midbrain, connecting right and left pretectal areas (Figure 2.8 a-d). PLAP expression also occurred in axons of the mammillotegmental tract which project from the mammillary nuclei to the tegmentum (Figure 2.8 c-d). In the hindbrain, strong PLAP staining was evident in the cerebellar peduncle connecting the cerebellum and the medulla oblongata (Figure 2.8 e-g). The sagittal view also highlights the uneven expression in the developing cerebellum with much greater expression in the caudal half at this mid-sagittal level (Figure 2.8 b and d). Very discrete expression at the border between the inferior colliculus and developing cerebellum is also evident in this view (Figure 2.8 b and d). Widespread vascular Plxdc2 expression in the brain was also apparent by PLAP staining (Figure 2.8).

2.3.6. Plxdc2-PLAP expression in the eye and ear at E15.5

PLAP staining of 100μm sections through the head illustrated continued Plxdc2 expression in the eye and ear at E15.5 (Figure 2.9). PLAP staining within the eye was restricted to the proliferating region of the inner neuroblastic layer and the cuboidal epithelium of the lens (Figure 2.9 a). Sagittal sections through the ear illustrated Plxdc2 expression in the cochlea. PLAP staining was evident in the ventral epithelium and a sharp border existed between ventral and dorsal sides (Figure 2.9 b and c). Neuronal Plxdc2 expression was also illustrated by axonal staining within the trigeminal ganglion (Figure 2.9 c).

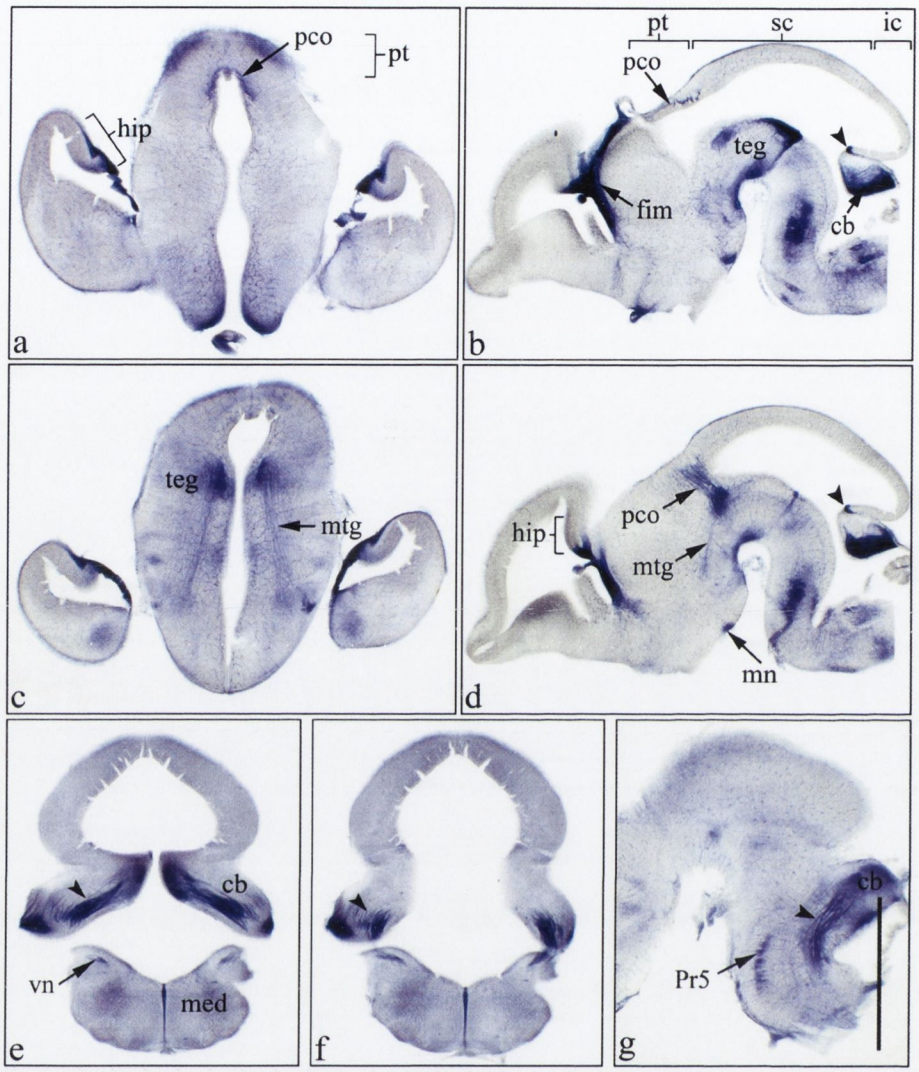

Figure 2.8 Neuronal Plxdc2 (PLAP) expression in the E15.5 brain. a and c, coronal sections through the E15.5 brain illustrating PLAP staining in axons of the posterior commissure and the mammillotegmental tract. b and d, corresponding sagittal sections illustrating the trajectory of these fibre tracts. e and f, coronal sections showing PLAP staining in axons of the cerebellar peduncle projecting between the cerebellum and the medulla oblongata. g, corresponding sagittal section illustrating the trajectory of this tract. b and d: arrowhead, border of inferior colliculus and cerebellum. e–g: arrowhead, cerebellar peduncle. cb, cerebellum; fim, fimbria; hip, hippocampus; ic, inferior colliculus; mn, mammillary nucleus; mtg, mammillotegmental tract; pco, posterior commissure; Pr5, principal sensory trigeminal nucleus; pt, pretectum; sc, superior colliculus; teg, tegmentum; vn, vestibular nuclei. Scale bar: a and c 1.5 mm; b and d–f 1.75 mm; g 1.3 mm.

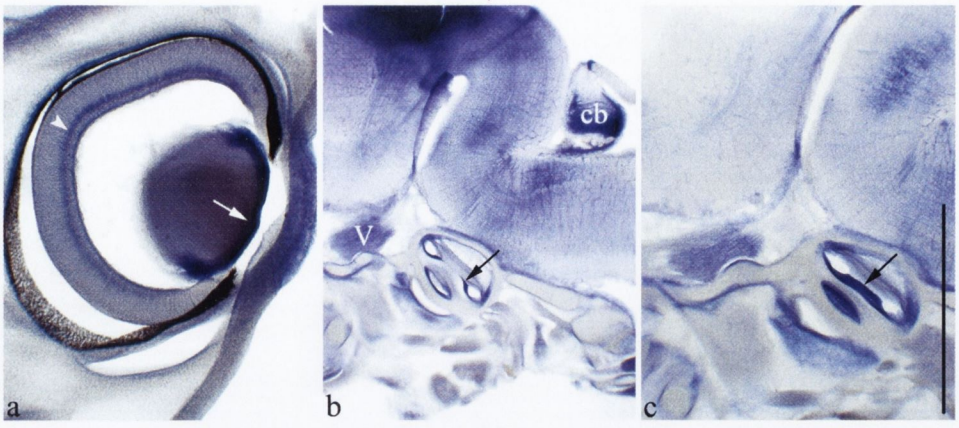

Figure 2.9 Plxdc2 (PLAP) expression in the eye and ear at E15.5. a, coronal section through the eye showing PLAP expression. arrowhead, proliferating region of the inner neuroblastic layer; arrow, cuboidal epithelium of the lens. b and c, sagittal sections through the head illustrating PLAP expression in the ventral epithelium of the cochlea (arrows) and in axons of the trigeminal ganglion (V). cb, cerebellum. Scale bar: a, 0.7 mm; b, 2 mm; c, 1.5 mm.

2.3.7. Plxdc2 expression in the newborn brain

Plxdc2 expression at postnatal day zero (P0) was investigated by PLAP and X-gal staining of sections through the brains of heterozygous *Plxdc2* gene trap mice (Figure 2.10). For the most part, the trend of Plxdc2 expression observed at E15.5 continued in the newborn brain. PLAP staining remained evident in axons of the cerebellar peduncle (Figure 2.10 g) as well as in the posterior commissure and the mammillotegmental tract (data not shown). Plxdc2 expression also persisted in the hippocampus, fimbria and amygdala, with widespread vascular PLAP expression remaining evident (Figure 2.10). By P0, the developing Purkinje cell layer of the cerebellum has become more refined and begins to resemble the single cell layer anatomy which is characteristic of the mature Purkinje cell layer. PLAP and Plxdc2-βgeo expression within the cerebellum demonstrated this change in Purkinje cell layer anatomy (Figure 2.10 f, g, h and i). (Expression in the developing Purkinje cell layer at P0 has previously been described (Leighton *et al.*, 2001). Xgal staining of sagittal sections through the brain highlighted the cellular basis of uneven PLAP expression in the developing cerebellum which had been observed at E15.5, with increased expression in the more caudal Purkinje cell layer (Figure 2.10 h and i, with

reference to Figure 2.8 b-d). Strong cellular Plxdc2-βgeo expression in the neuroepithelium of the lateral ventricle, at the region of the fimbria was also evident in this view (arrow in h). Although largely similar to the expression pattern documented at E15.5, several new regions of Plxdc2 expression were noted in the P0 brain. PLAP expression was observed in a subset of axons of the anterior commissure (Figure 2.10 a and b) and within the internal capsule (figure 2.10 e). Plxdc2–βgeo expression was widespread throughout nuclei of the hypothalamus, tegmentum and medulla oblongata, and was particularly evident in the mammillary bodies (arrowheads, figure 2.10 h). Expression within the superior colliculus had increased greatly from E15.5, with a clear band of expression evident in a region consistent with the border of the superficial and deep layers (Figure 2.10 h and i, with reference to Figure 2.7 m-u).

2.3.8. Lethality of homozygous Plxdc2 gene trap mutants

At an early stage of this study, it became apparent that homozygous *Plxdc2* mice did not survive to birth, with lethality occurring at a stage precluding analysis of the role of *Plxdc2* in brain development and axon guidance. In fact, there was no retrieval of homozygous mutants from E9 onwards. The genomic DNA of four E9 litters from heterozygous *Plxdc2* gene trap crosses was processed for PCR genotyping (as outlined in section 2.8.2). Of a total of forty embryos, thirty were found to be heterozygous for the gene trap insertion and ten were found to have a wildtype genotype. The existence of other viable *Plxdc2* mouse lines suggests that lethality in the KST37 line is not owing to the absence of *Plxdc2* but is possibly owing to some additional linked disruption brought about by the insertion of the PLAP secretory trap vector. The Plxdc2-βgeo expression pattern was confirmed by *in situ* hybridisation using an antisense RNA probe, and the KST37 line could therefore be used confidently for expression analysis.

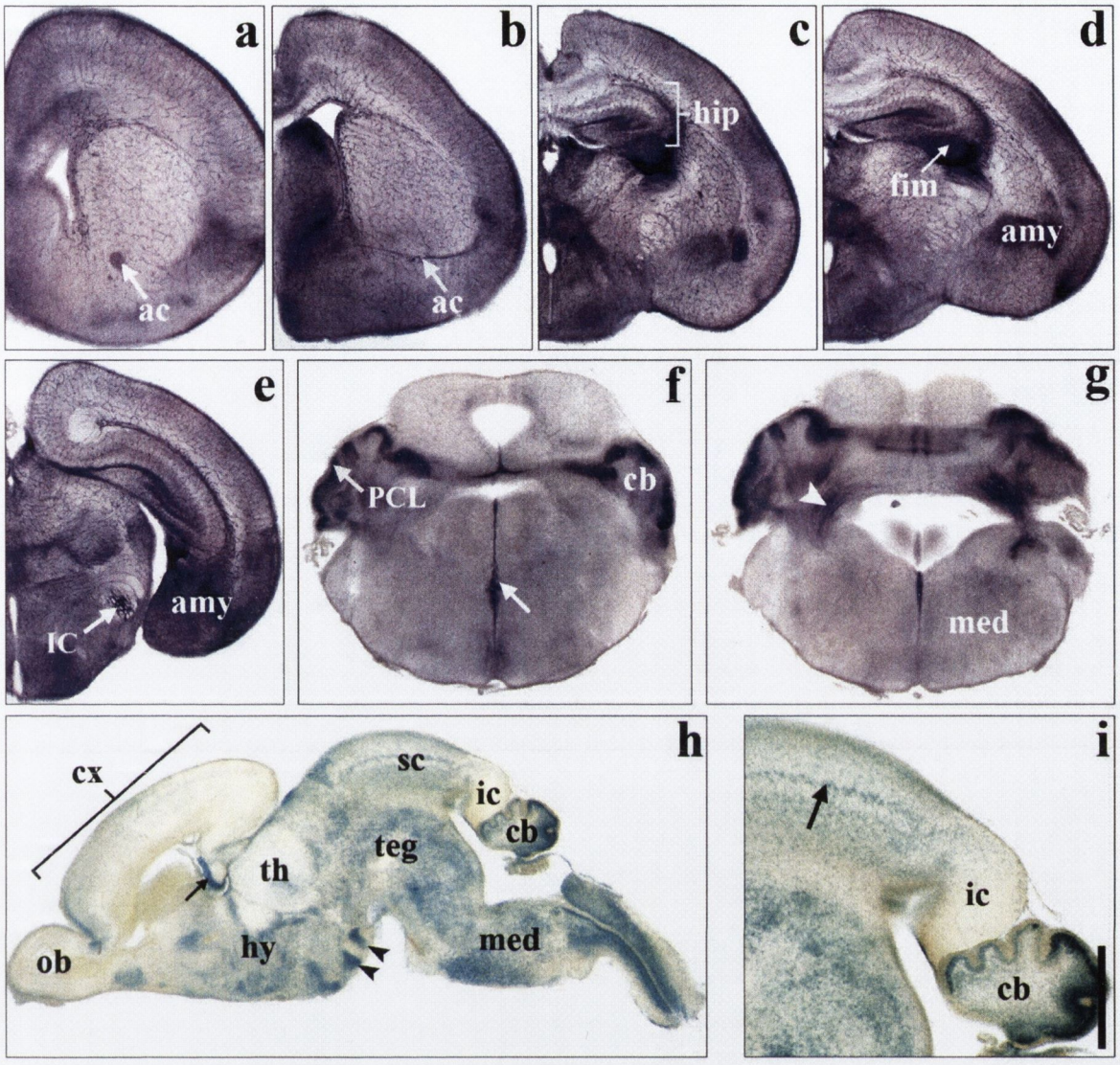

Figure 2.10 Plxdc2 expression in the P0 Brain. a-g, PLAP staining of coronal sections through the brain of a heterozygous Plxdc2 gene trap mouse. h, sagittal section through the brain, illustrating Plxdc2-βgeo expression. i, higher magnification of hindbrain region of h illustrating Plxdc2-βgeo expression in a band of cells marking the border of the superficial and deep layers of the superior colliculus (arrow). Arrow in f, PLAP staining in the neuroepithelium of the fourth ventricle. Arrowhead in g, PLAP staining in the cerebellar peduncle. Arrow in h, the neuroepithelium of the lateral ventricle in the region of the fimbria; arrowheads in h, mammillary bodies. ac, anterior commissure; amy, amygdala; cb, cerebellum; cx, cortex; fim, fimbria; hip, hippocampus; hy, hypothalamus; IC, internal capsule; ic, inferior colliculus; med, medulla oblongata; ob, olfactory bulb; PCL, Purkinje cell layer; sc, superior colliculus; teg, tegmentum; th, thalamus. Scale bar: a, 0.83mm; b-g, 1mm; h, 1.5mm; i, 0.7mm.

2.4 Analysis of *Plxdc1* expression in a gene trap mouse line

An investigation of *Plxdc1* expression in the brain was facilitated by the creation of a *Plxdc1* "targeted trap" mouse line (Friedel *et al.*, 2005). In this case, the PLAP secretory trap vector was fused to gene-specific homology arms, thus utilizing homologous recombination to insert the vector into the intron between exons 11 and 12 of the Plxdc1 gene.

2.4.1. Genotyping of Plxdc1 genetrap mice

Plxdc1 gene trap mice were genotyped by PCR as outlined in section 2.6.2 using the primers detailed in table 2.1. PCR of genomic DNA from a homozygous mutant resulted in amplification of a single band of 370bp (Lane A, figure 2.11). In a heterozygous animal, an additional wildtype band of 600bp was amplified (Lane B, figure 2.11)

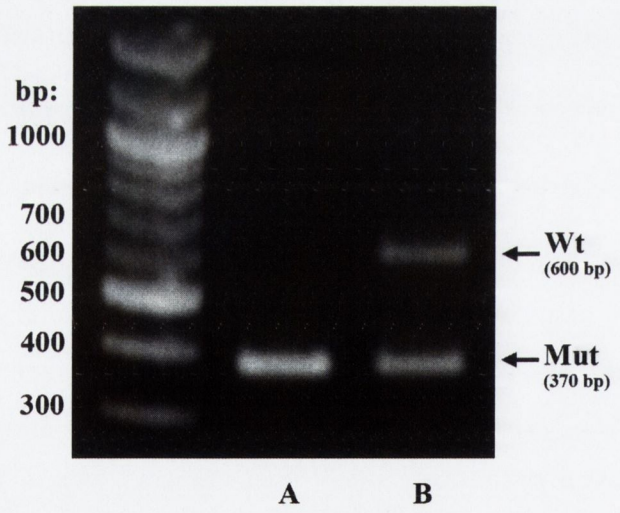

Figure 2.11 PCR genotyping of *Plxdc1* gene trap mice. A, Homozygous *Plxdc1* genetrap mutant; B, heterozygous *Plxdc1* gene trap mutant. Size of bands compared against 100 bp DNA ladder (New England Biolabs) with sizes in bps indicated.

2.4.2. Plxdc1 expression in the developing nervous system

At E10.5, whole mount X-gal staining of homozygous gene trap mice illustrated no Plxdc1-βgeo expression. Expression of Plxdc1-βgeo in the E16.5 brain was investigated by X-gal staining of 100μm sections from homozygous *Plxdc1* targeted trap mice (Figure 2.12). Homozygous mutants appeared phenotypically normal and were examined as they produced more intense βgal staining. Plxdc1-βgeo expression in the brain differed greatly to that of Plxdc2-βgeo. At E16.5, Plxdc1-βgeo expression was restricted to a single paired midbrain nucleus lying ventral to the tectum (Figure 2.12a), in a location consistent with the pedunculopontine tegmental nucleus. Neuroepithelial expression was also evident at the fourth ventricle (Figure 2.12 b).

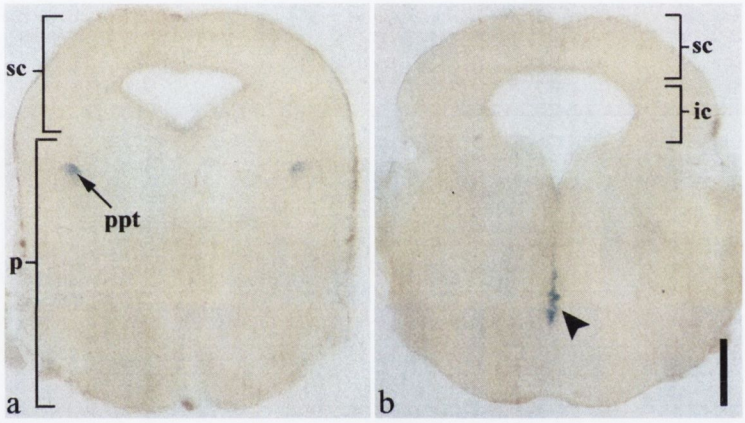

Figure 2.12 Plxdc1-βgeo expression in the E16.5 brain. a, Plxdc1-βgeo expression is restricted to a single paired midbrain nucleus in a position consistent with the pedunculopontine tegmental nucleus (ppt). b, neuroepithelial Plxdc1-βgeo expression is evident at the fourth ventricle (arrowhead). ic, inferior colliculus; p, pons; sc, superior colliculus. Scale bar 0.5 mm.

More widespread expression of Plxdc1 was observed in neonatal and postnatal brain sections (figure 2.13 and 2.14), in accord with *in situ* hybridisation and immunohistochemistry results in the rat (Lee *et al.*, 2005, Lee *et al.*, 2006a). At P0, Plxdc1-βgeo expression persisted in the pedunculopontine tegmental nucleus and in the neuroepithelium of the fourth ventricle (Figure 2.13 a, b and e). Plxdc1-βgeo expression was also apparent in the paraventricular nucleus of the hypothalamus (Figure 2.13 c and d), the choroid plexus epithelium and the neuroepithelium of the lateral ventricle at the fimbria (figure 2.13 a).

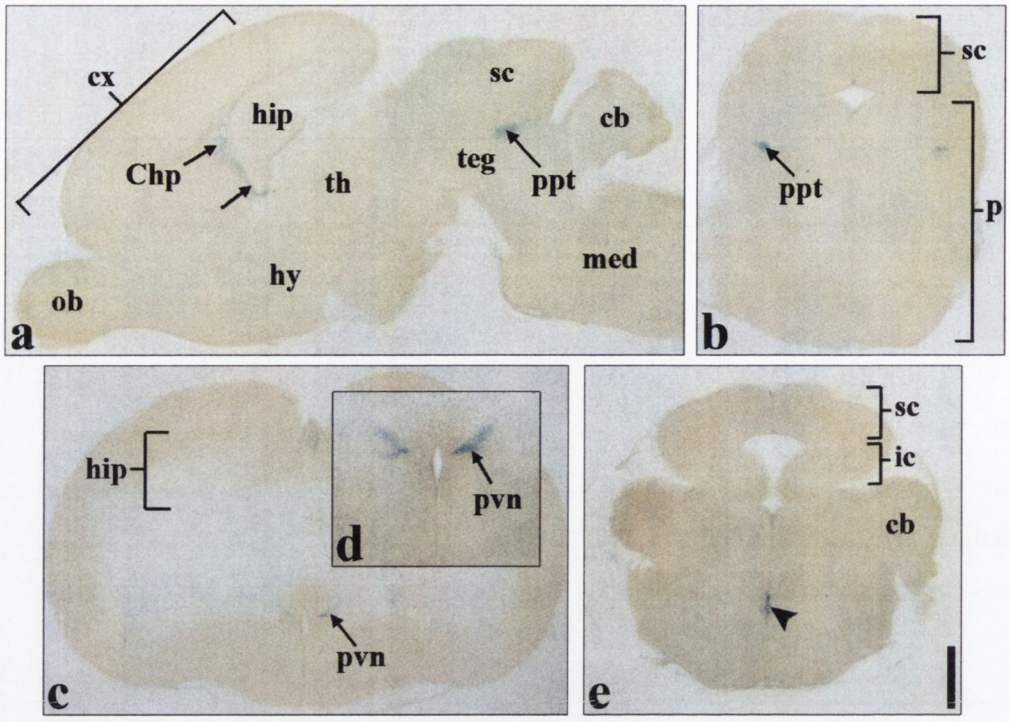

Figure 2.13 Plxdc1-βgeo expression in the P0 brain. a and b, sagittal and coronal sections through *Plxdc1* gene trap homozygote brains illustrating Plxdc1-βgeo expression in the choroid plexus epithelium (Chp), the epithelium of the lateral ventricle at the fimbria (arrow) and in the pedunculopontine tegmental nucleus (ppt). c and d, coronal section through a *Plxdc1* gene trap homozygote brain illustrating Plxdc1-βgeo expression in the paraventricular nucleus of the hypothalamus (pvn) and at higher magnification in d. e, coronal section through the hindbrain illustrating Plxdc1-βgeo expression in the neuroepithelium of the fourth ventricle (arrowhead). cb, cerebellum; cx, cortex; hip, hippocampus; hy, hypothalamus; ic, inferior colliculus; sc, superior colliculus; teg, tegmentum; th, thalamus; med, medulla oblongata; ob, olfactory bulb; p, pons. Scale bar: 0.5mm.

Both of the brain nuclei which were shown to express *Plxdc1* have been extensively studied and their functions well described. The pedunculopontine tegmental nucleus is a rostral brainstem structure that acts as an interface for the basal ganglia and plays a crucial role in the generation and maintenance of the rapid rhythms in the cortex that are associated with wakefulness and REM sleep (Juan Mena-Segovia *et al.*, 2004). In fact, the basal ganglia are more interconnected with the pedunculopontine tegmental nucleus than with any other brain region. The pedunculopontine tegmental nucleus is also involved in control of movement and is thought to make up the central part of the mesencephalic locomotor region (Juan Mena-Segovia *et al.*, 2004).

In the rat, the the paraventricular nucleus receives catecholaminergic (norepinephrinergic, dopaminergic and epinephrinergic) innervation from the caudal brain and has been implicated in the stress response (Mravec & Kiss, 2004). In particular, the Parvocellular neurons of the the paraventricular nucleus have been shown to control the secretion of corticotropin and corticosterone by the synthesis and release of corticotropin-releasing hormone and vasopressin (Engelmann *et al.,* 2004). The magnocellular neurones of the the paraventricular nucleus, which play a crucial role in the hypothalamic-neurohypophysial system, project to the posterior pituitary, where they terminate at capillaries, secreting vasopressin and oxytocin into the blood upon appropriate stimulation (Engelmann *et al.,* 2004). In the rat, *Plxdc1* expression has also been documented in the supraoptic nucleus, whose magnocellular neurones act similarly to those of the the paraventricular nucleus (Lee *et al.*, 2005). No evidence of *Plxdc1* expression was documented in the supraoptic nucleus of the *Plxdc1* gene trap mouse.

Plxdc1 expression was also compared and contrasted with that of Plxdc2 in the adult brain. As was illustrated at E16.5 and P0, Plxdc1 expression was extremely restricted in the adult brain. Widespread vascular PLAP expression was evident, with staining persisting in the neuroepithelium of the fourth ventricle. At this stage, PLAP expression was also evident in Purkinje cell dendrites located in the molecular layer of the cerebellum (Figure 2.14 a and b). Plxdc1 expression in the Purkinje cells of the cerebellum has previously been noted in the rat (Lee *et al.*, 2005). No specific PLAP labelling of axon tracts was observed. In complete contrast, widescale PLAP staining of myelinated axon tracts was observed in heterozygous Plxdc2 gene trap mutants (Figure 2.14 c and d). Similar PLAP staining to that observed in Plxdc1 gene trap mutants was evident in the molecular layer of the cerebellum of heterozygous Plxdc2 gene trap mice (Figure 2.14 d). Xgal staining of sagittal slices through the hindbrain confirmed Plxdc2- βgeo staining in mature Purkinje cells of the cerebellum (Figure 2.14 e).

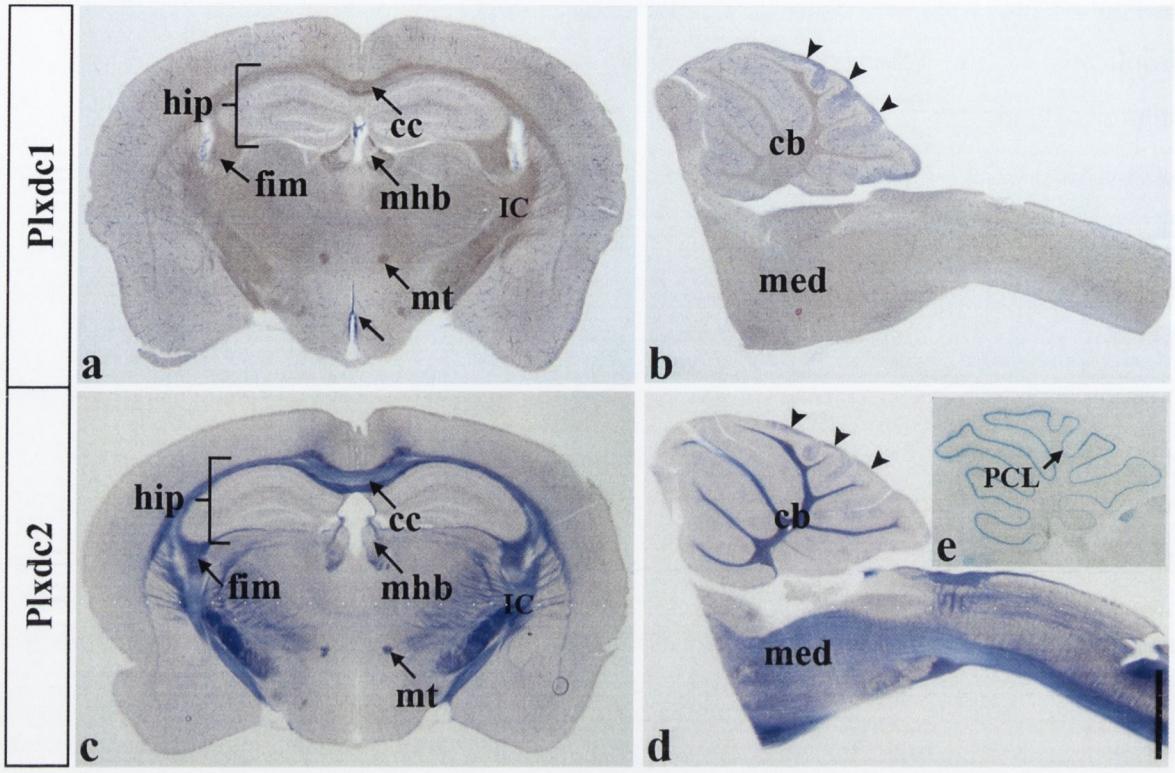

Figure 2.14 Comparison of PLAP expression in *Plxdc1* and *Plxdc2* gene trap mice. a, coronal section through the forebrain of a homozgygous *Plxdc1* gene trap adult brain showing neuroepithelial PLAP expression at the fourth ventricle (arrow) and widespread vascular PLAP expression. b, sagittal section through the hindbrain of the same individual illustrating PLAP expression in the molecular layer of the cerebellum (arrowheads). c, coronal section through a heterozygous *Plxdc2* gene trap adult brain illustrating widespread PLAP expression in myelinated axon tracts of the brain. d, sagittal section through the hindbrain of the same individual illustrating PLAP expression in Purkinje cell dendrites located in the molecular layer of the cerebellum, similar to that observed in *Plxdc1* gene trap mice (arrowheads). e, alternative sagittal slice through the same individual showing Plxdc2-βgeo expression in the mature Purkinje cells of the cerebellum. cb, cerebellum; cc, corpus callosum; fim, fimbria; hip, hippocampus; IC, internal capsule; med, medulla oblongata; mhb, medial habenular nucleus; mt, medial terminal nucleus of accessory optic tract; PCL, Purkinje cell layer. Scale bar: a and c, 1.5mm; b and d, 1mm; e, 1.25mm.

2.5 Phenotypic analysis of a viable *Plxdc2* mouse line, Plxdc2GFP.

Another line of mice was sought for the functional analyses of loss of *Plxdc2* as homozygous *Plxdc2* gene trap mutants were found to be embryonic lethal. Several viable *Plxdc2* mutant mice lines have been recently developed. One such line is the Plxdc2GFP line in which the *Plxdc2* start codon & leader peptide is replaced by a 5S-EGFP-pA cassette (See Appendix 5.3; line used with the kind permission of T. Jessell, Colombia University). In total contrast to the Plxdc2 PLAP secretory trap line, Plxdc2GFP homozygous mutants survived to adulthood. Confirmation of the *Plxdc2* expression pattern documented in the PLAP secretory trap mouse line was achieved by comparison to GFP expression in Plxdc2-GFP mice. Preliminary investigation of the effect of loss of *Plxdc2* on general brain morphology and axon guidance was carried out in Plxdc2GFP homozygous mutants at E15.5.

2.5.1. Genotyping of Plxdc2GFP mice

Plxdc2GFP mice were genotyped by PCR as outlined in section 2.8.2, using the primers detailed in table 2.1. PCR of wildtype DNA resulted in amplification of a single band of 461 basepairs (Figure 2.15). In mutant animals, an additional band of 363 bp was amplified from the inserted vector sequence (Figure 2.15).

2.5.2. Confirmation of knockdown of Plxdc2 expression in the Plxdc2GFP mouse line

Relative levels of *Plxdc2* expression in wildtype, heterozygous and homozygous Plxdc2GFP mice were examined by realtime PCR. RNA was extracted from the cerebella of adult brains and reverse transcribed as detailed in Section 2.8.7. Samples for real time PCR were normalised to the mouse ribosomal phosphoprotein (RPO) gene and negative controls were routinely employed (see section 2.8.7 for details). Primers for amplication of the *Plxdc2* transcript were designed to exon 7 of *Plxdc2*, downstream of the targetted insertion of the 5S-EGFP-pA cassette in exon 1 of *Plxdc2*. Triplicates of each PCR reaction were carried out. *Plxdc2* transcript levels were significantly reduced in heterozygous Plxdc2GFP mice when compare to wildtype animals, and in homozygous Plxdc2GFP mice when compared to heterozygous animals (Independent T-test, $p \leq 0.0001$ in both cases). *Plxdc2* expression in heterozygous mutants was approximately half that evident in wildtype animals. There was approximately a ten fold decrease in *Plxdc2*

transcript levels in the cerebella of Plxdc2GFP homozygous mutants, when compared to wildtype animals (Figure 2.16).

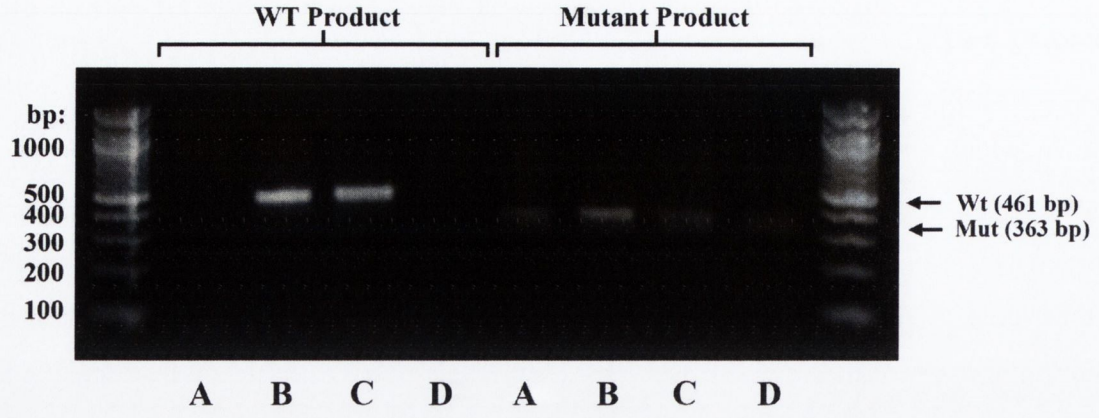

Figure 2.15 PCR genotyping of Plxdc2GFP mice. A, Homozygous Plxdc2GFP mutant; B, heterozygous Plxdc2GFP mutant; C, heterozygous Plxdc2GFP mutant; D, homozygous Plxdc2GFP mutant. Size of bands compared against 100 bp DNA ladder (New England Biolabs) with sizes in bps indicated to the right.

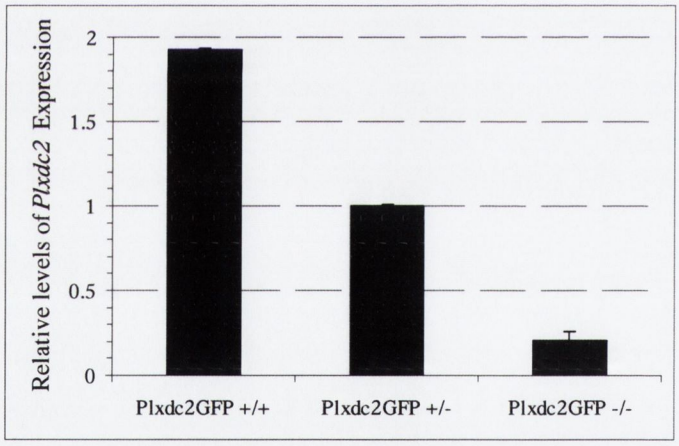

Figure 2.16 Examination of Plxdc2 transcript levels in Plxdc2GFP mice by realtime PCR. Samples for real time PCR were normalised to the mouse RPO gene. *Plxdc2* transcript levels were significantly reduced in heterozygous Plxdc2GFP mice when compared to wildtype animals (Independent T-test, $p \leq 0.0001$). *Plxdc2* expression in heterozygous mutants was approximately half that evident in wildtype mice. *Plxdc2* transcript levels were significantly reduced in homozygous Plxdc2GFP mice when compared to those in heterozygous animals (Independent T-test, $p \leq 0.0001$). There was approximately a ten fold decrease in *Plxdc2* transcript levels in the cerebella of Plxdc2GFP homozygous mutants, when compared to wildtype animals.

2.5.3. Phenotypic analysis in the E15.5 brain

Plxdc2 expression in the brain of E15.5 Plxdc2GFP mice was investigated by immunohistochemistry using an antibody against GFP (Invitrogen). GFP expression in heterozygous animals was compared to that of Plxdc2-βgeo in heterozygous PLAP secretory trap mice at the same stage of development. *Plxdc2* expression in the Plxdc2GFP mouse line mirrored that in the PLAP secretory trap line in all areas of the E15.5 brain including the glial wedge, fimbria, dentate gyrus, caudate putamen, midbrain reticular formation, principle sensory trigeminal nucleus, Purkinje cell layer and vestibular nuclei (Figure 2.17). The documentation of similar patterns of *Plxdc2* expression in the brain of E15.5 mice of both transgenic lines, validates the *Plxdc2* expression pattern documented in the PLAP secretory trap mouse line.

The brains of heterozygous and homozygous Plxdc2GFP mutants were compared at E15.5. In the first instance, cresyl violet staining of nissl bodies was carried out on 50μm vibratome sections (Section 2.8.8). No gross morphological defect was evident in the Plxdc2GFP homozygous brain (Figure 2.18). Overall brain size and organisation was normal when compared to heterozygous animals. In addition, areas which normally express Plxdc2, including the hippocampus, hypothalamus, pretectum, cerebellum and medulla oblongata appeared morphologically normal (Figure 2.18).

Figure 2.17 Plxdc2 expression in the E15.5 Plxdc2GFP mouse brain. GFP expression was compared to that of Plxdc2-βgeo in heterozygous PLAP secretory trap mice at the same stage of development. *Plxdc2* expression in the Plxdc2GFP mouse line mirrored that in the PLAP secretory trap line in all areas of the E15.5 brain. Representative images through the brain are shown illustrating GFP expression in many regions of the E15.5 brain including the glial wedge (GW), fimbria (fim), dentate gyrus (DG), caudate putamen (CP), midbrain reticular formation (MRF), floor plate (fp), principle sensory trigeminal nucleus (Pr5), Purkinje cell layer (PCL) and vestibular nuclei (vn). a,c,e,g and i: coronal sections through the brain of a heterozygous Plxdc2 gene trap mouse illustrating Plxdc2-βgeo expression. b,d,f,h and j: corresponding coronal sections through the brain of a heterozygous Plxdc2GFP mouse illustrating GFP expression. arrow in a and b, Plxdc2 expression at the medial septum; arrowhead in g and h, clusters of Plxdc2 expression at the border region of the tectum and the pons; cb, cerebellum; cx, cortex; hip, hippocampus; hy, hypothalamus; ic, inferior colliculus; med, medulla oblongata; sc, superior colliculus; sep; septum; teg, tegmentum; th, thalamus. Scale bar:1mm.

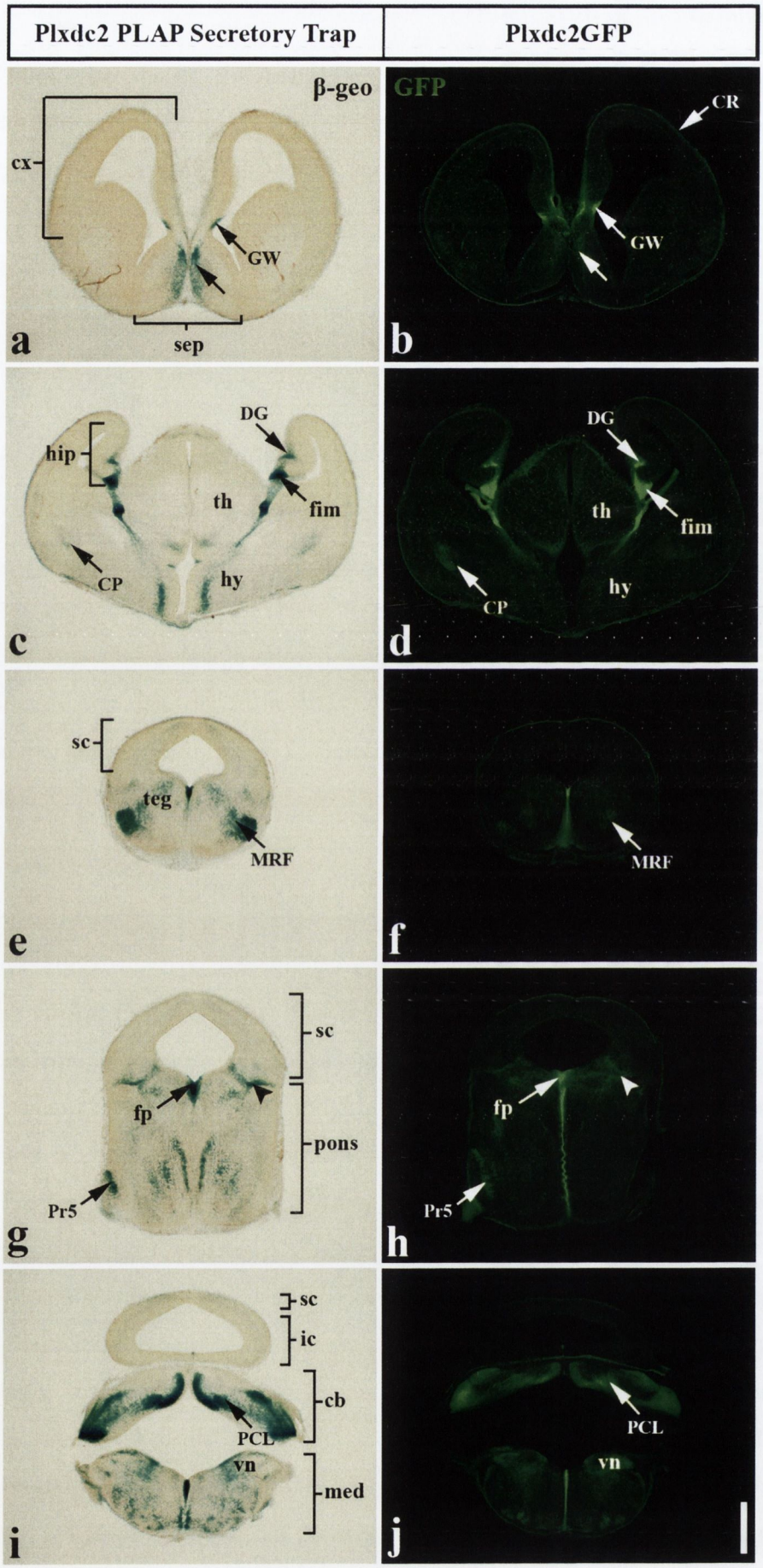
Plxdc2 PLAP Secretory Trap
Plxdc2GFP
β-geo
GFP
cx
GW
sep
a
CR
GW
b
DG
hip
th
fim
CP
hy
c
DG
th
fim
CP
hy
d
sc
teg
MRF
e
MRF
f
sc
fp
pons
Pr5
g
fp
Pr5
h
sc
ic
cb
PCL
vn
med
i
PCL
vn
j

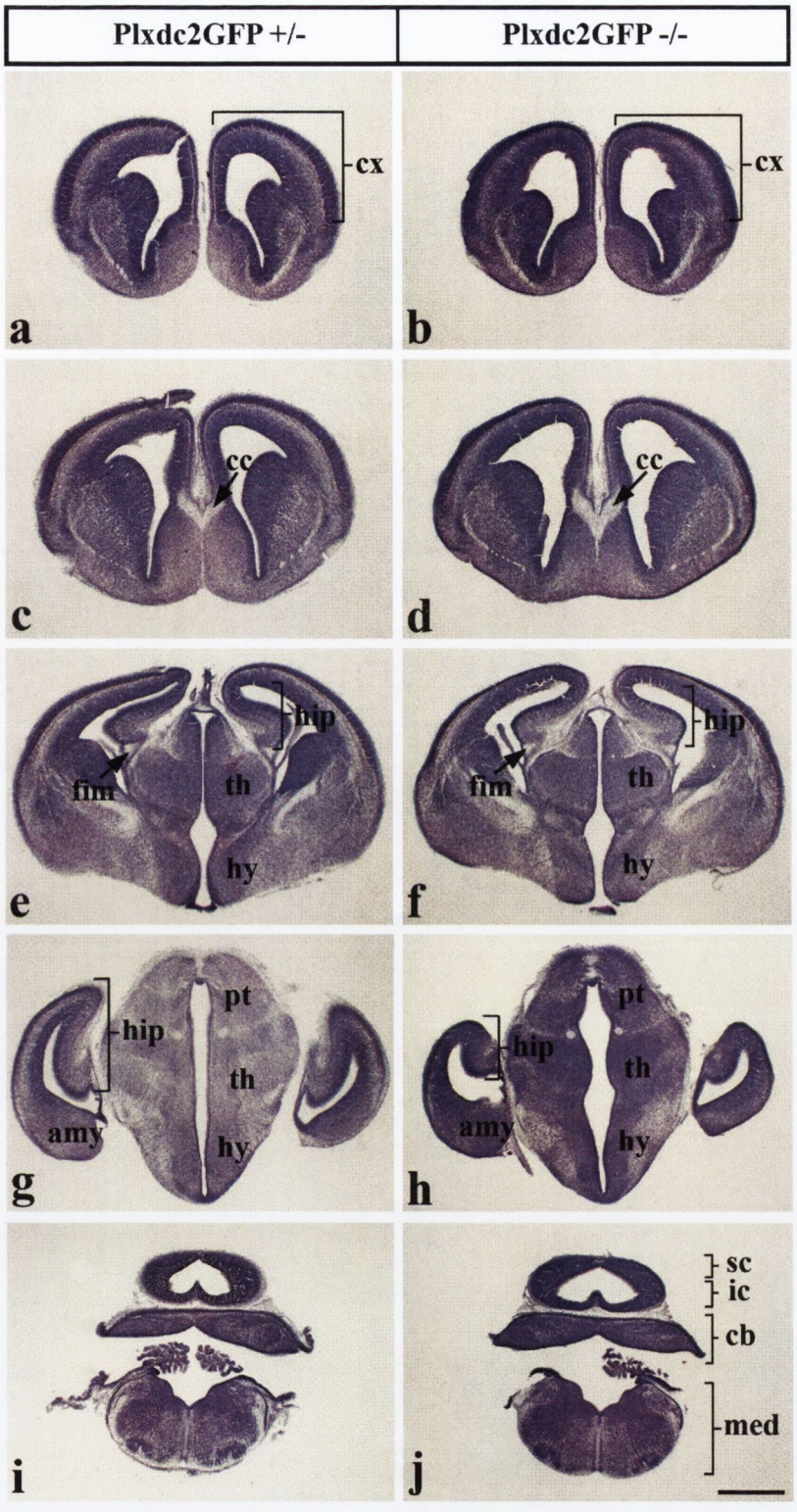

Figure 2.18 Cresyl violet staining of coronal sections through the brain of E15.5 Plxdc2GFP mice. No gross morphological phenotype was evident in Plxdc2GFP homozygous mutants. amy, amydala; cb, cerebellum; cc, corpus callosum; cx, cortex; fim, fimbria; hip, hippocampus; hy, hypothalamus; ic, inferior colliculus; med, medulla oblongata; pt, pretectum; sc, superior colliculus; th, thalamus. Scale bar: 500μm.

Neuronal *Plxdc2* expression had previously been documented in the *Plxdc2* gene trap mouse at E15.5 (Figure 2.8). GFP expression in neurons of the posterior commissure (PCO), cerebellar peduncle (cp) and mammillotegmental tract (mtg) was confirmed at E15.5 by immunohistochemistry using a GFP antibody (Figure 2.19 b, f and j). Examination of these tracts using an antibody against neurofilament (NF) highlighted no axon guidance defects in Plxdc2GFP homozygous mutants (Figure 2.19 d, h and l).

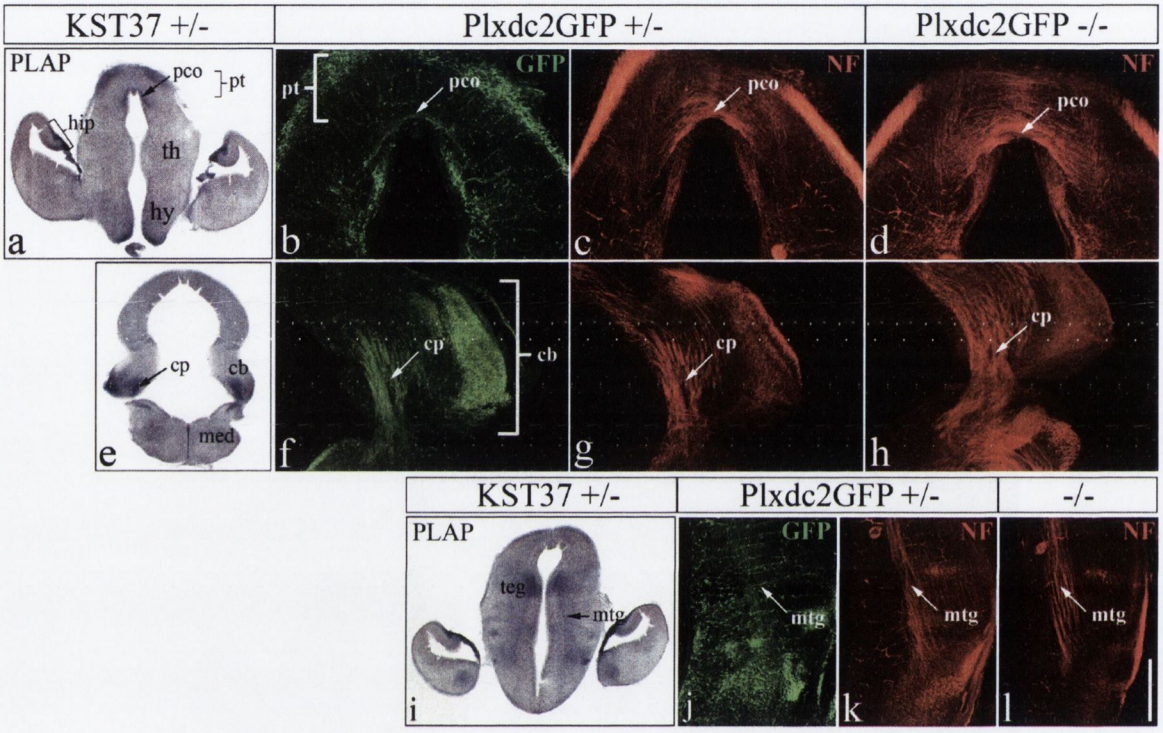

Figure 2.19 Phenotypic analysis of the axon tracts of the E15.5 brain which normally express Plxdc2. a, e and i: 50μm coronal sections through the brain of a *Plxdc2* gene trap heterozygous mutant, stained for PLAP. b-d, f-h and j-l: higher magnification images through coronal sections of Plxdc2GFP heterozygous and homozygous mutants, illustrating GFP and neurofilament (NF) expression in the posterior commissure (PCO), cerebellar peduncle (cp) and mammillotegmental tract (mtg). cb, cerebellum; hip, hippocampus; hy, hypothalamus; med, medulla oblongata; pt, pretectum; teg, tegmentum; th, thalamus. Scale bar: a and i, 1mm; b-d, 280μm; e, 830μm; f-h, 240μm; j-l, 350μm.

2.6 Plxdc2-AP *in situ* hybridisation

An investigation into extracellular *Plxdc2* binding *in vivo* was facilitated by the production of extracellular Plxdc2-Alkaline Phosphatase (AP) plasmids (Work carried out by Géraldine Kerjan, see section 2.8.9). C-terminal (CT) and N-terminal (NT) AP tagged *Plxdc2* proteins were produced in HEK293T cells and hybridised to wildtype brain sections (Figure 2.20). AP *in situ* hybridisation was carried out as detailed in section 2.8.10 and AP produced by pAPtag-5 plasmid (Genhunter) was used routinely as a negative control (for AP control images, see Appendix 5.11).

Extracellular Plxdc2-AP(CT) bound to wildtype brain sections in a widespread, but specific pattern. At P0, the mitral cell layer of the olfactory bulb, which was free of PLAP staining in the Plxdc2 gene trap line, bound Plxdc2-AP(CT) strongly (Figure 2.20 a and b). Conversely, axons of the anterior commissure which had been shown to express PLAP in the Plxdc2 gene trap mutant, did not bind Plxdc2-AP(CT) (Figure 2.20 c and d). In several other regions, cells which had been shown to express Plxdc2 (Xgal and PLAP) were also shown to bind Plxdc2-AP(CT). Widespread binding was evident in the hippocampus, a structure which has been shown to express *Plxdc2* strongly at P0 (Figure 2.20 e). A detailed analysis of the hippocampus at later stages illustrates that this binding persists into adult stages (Figure 2.20 f and g). At P0, extensive Plxdc2-AP(CT) binding was also evident in the developing Purkinje cell layer of the cerebellum (Figure 2.20 h). In the adult brain, mature Purkinje cells which have been shown to express Plxdc2, were also shown to bind the AP-tagged extracellular portion of Plxdc2 (Figure 2.20 i). Plxdc2-AP(NT) plasmids did not bind specifically to wildtype brain sections.

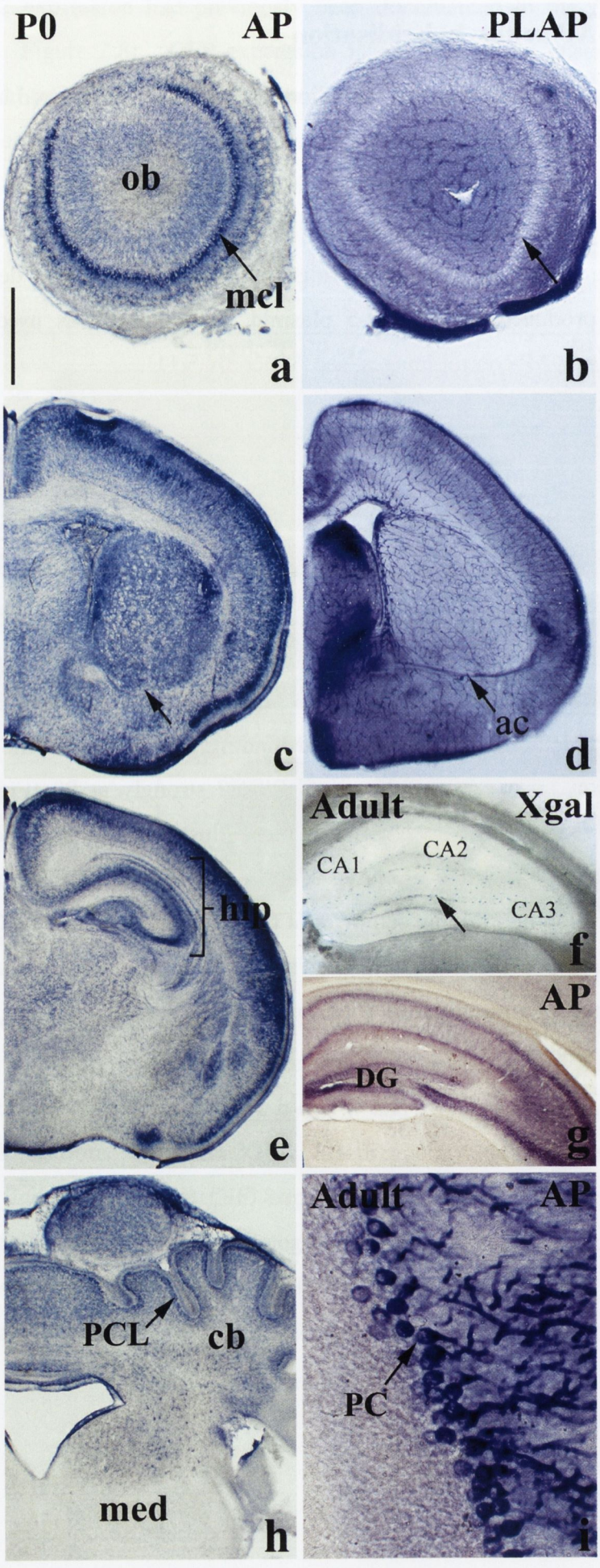
P0
AP
ob
mcl
a
PLAP
b
c
ac
d
hip
e
Adult
Xgal
CA1
CA2
CA3
f
AP
DG
g
PCL
cb
med
h
Adult
AP
PC
i

Figure 2.20 Extracellular Plxdc2-AP(CT) *in situ* hybridisation. Plxdc2-AP(CT) bound to wildtype brain sections in a widespread, but specific, pattern. a,c,e and h, coronal sections through the brain at P0 showing Plxdc2-AP(CT) binding. b and d, PLAP staining of coronal sections through a heterozygous *Plxdc2* gene trap brain at P0. f, cells scattered throughout the hippocampus of an adult *Plxdc2* gene trap heterozygote express Plxdc2-βgeo (arrow). g, coronal section thorough the hippocampus of a wildtype brain showing Plxdc2-AP(CT) binding in CA1, CA2, CA3 and dentate gyrus (DG). i, high magnification image of the Purkinje cells (PC) of the cerebellum in an adult wildtype brain, illustrating extensive binding of Plxdc2-AP(CT). ac, anterior commissure; cb, cerebellum; hip; hippocampus; mcl, mitral cell layer; med, medulla oblongata; ob, olfactory bulb; PCL, Purkinje cell layer. Scale bar: a and b, 250μm; c-e, 750μm; f and g, 1mm; h, 500μm; i, 40μm

---

2.7 Discussion

The *Plxdc2* PLAP secretory gene trap mouse line (KST37) provided an invaluable tool for the documentation of *Plxdc2* expression in the developing embryo (Miller *et al.*, 2007). At mid-embryonic stages (E9.5–E11.5), OPT highlighted Plxdc2-βgeo expression in a number of patterning centres of the brain, including the cortical hem, midbrain–hindbrain boundary and the midbrain floorplate. Remarkable similarities between the expression of Plxdc2-βgeo and that of a number of members of the Wnt family were noted, particularly in the regions of the cortical hem and midbrain-hindbrain boundary. In order to more closely define the 3D domains of Plxdc2-βgeo expression within these brain structures, expression at E11.5 was compared to that of *Wnt1*, *Wnt3a*, *Wnt5a* and *Wnt8b* using OPT. *Plxdc2* was expressed in other tissues, most notably the limbs, lung buds and developing heart, as well as the spinal cord and dorsal root ganglia. By E15.5, expression was apparent in a large number of discrete nuclei and structures throughout the brain, including the glial wedge and derivatives of the cortical hem. Plxdc2-βgeo expression was found to be particularly strong in the developing Purkinje cell layer, especially in the posterior half of the cerebellum and the PLAP marker was expressed in a number of axonal tracts, including the posterior commissure, mammillotegmental tract and cerebellar peduncle. At P0, PLAP expression persisted in these tracts and in addition, was described in the internal capsule and in a subset of axons of the anterior commissure.

In total contrast to *Plxdc2* findings, *Plxdc1* expression was found to be extremely limited within the developing mouse. *Plxdc1* homozygous gene trap mice survived to adulthood and their brains appeared phenotypically normal. No evidence of Plxdc1-βgeo expression was found in the E10.5 embryo. At E16.5, Plxdc1-βgeo expression within the brain was restricted to a single paired nucleus in a location consistent with the pedunculopontine tegmental nucleus, and to the neuroepithelium of the fourth ventricle. By P0, Plxdc1-βgeo expression was also evident in the paraventricular nucleus, in the choroid plexus epithelium and in the neuroepithelium of the lateral ventricle, at the fimbria. At adult stages, PLAP expression is widespread in the *Plxdc2* gene trap brain, marking most of the myelinated axon tracts. In contrast, in the *Plxdc1* mutant brain, widespread vascular PLAP expression was evident with weak staining of the neuroepithelium and molecular layer of the cerebellum. Specific expression in the Purkinje cells and paraventricular nucleus at P0 and adult stages, however, matches observations in the rat precisely (Lee *et al.*, 2005), confirming the specificity and sensitivity of the reporter genes.

The contrast noted in the expression patterns of *Plxdc1* and *Plxdc2*, suggests divergent functions within the developing embryo. As was discussed in Chapter 1, *Plxdc1* has recently been shown to play a vital role in endothelial cell capillary morphogenesis, a function not shared by *Plxdc2* (Wang *et al.*, 2005). The upregulation of *Plxdc1* in human glioblastoma endothelium (Beaty *et al.*, 2007) and its association with metastasis and poor survival of patients with osteogenic sarcoma (OGS) (Fuchs *et al.*, 2007), implicate *Plxdc1* in cancer and, more specifically, in angiogenesis within growing tumours. Such roles have not been described for *Plxdc2*.

Preliminary analysis of the effect of loss of *Plxdc2* was carried out in a second Plxdc2 mouse line, Plxdc2GFP. In total contrast to the *Plxdc2* PLAP secretory trap line, Plxdc2GFP mutants survived to adulthood. GFP expression in the brain of Plxdc2GFP mice mirrored that previously documented in the *Plxdc2* PLAP secretory trap mouse at E15.5 thus confirming the validity of the expression pattern documented using the PLAP secretory trap line. An investigation of *Plxdc2* transcript levels in the cerebella of homozygous Plxdc2GFP mutants illustrated approximately a ten fold decrease in *Plxdc2* transcript when compared to wildtype controls. The Plxdc2GFP mouse line was made available late in the time span of this project and therefore, limited analyses of the brain at E15.5 were carried out. Nevertheless, several conclusions can be drawn from analysis of

homozygous mutants at this stage of development. Loss of *Plxdc2* during early brain development did not result in major defects in the E15.5 brain. The gross morphology of the brain of homozygous Plxdc2GFP mice appeared normal. No guidance defects were evident in axons of the cerebellar peduncle, posterior commissure and mammillotegmental tract in homozygous Plxdc2GFP mice. Plxdc2 may therefore be redundant in early brain development or alternatively, loss of Plxdc2 expression may be compensated for by another protein. However, a role in later brain development and axon guidance should not be dismissed and should be investigated fully in future experiments. The key to establishing endogenous *Plxdc2* function may, however, be in ectopic/overexpression of the gene and not in endogenous gene silencing. This possibility will be investigated further in chapter 3, through the use of the chick as a experimental model.

In retrospect, one of the first objectives of the work undertaken should have been the generation of an antibody against Plxdc2. Analysis of *Plxdc2* expression in the mouse was carried out at the transcript level, either by *in situ* hybridisation or using the transgenic markers present in the PLAP secretory trap and Plxdc2GFP mouse lines. The existance of an antibody against Plxdc2 would have added greatly to Plxdc2 expression analysis, enabling additional documentation of Plxdc2 expression at the protein level. In addition to the benefits of using a Plxdc2 antibody in expression analysis *in vivo*, an antibody against the protein would allow for the confirmation of Plxdc2 expression on the cell surface. Cell surface expression of Plxdc1 has previously been confirmed using an antibody against the protein (Nanda *et al.*, 2004) but Plxdc2 is described as a putative cell-surface protein. Considering the similarities of the Plxdc1 and Plxdc2 protein structures and the prediction of five N-linked glycosylation sites of the Plxdc2 protein (prediction of N-linked glycosylation sites carried out using NetNGlyc 1.0), Plxdc2 does appear to be expressed on the cell surface. However, the existance of an antibody against the protein would allow for the confirmation of Plxdc2 expression at the cell surface. A Plxdc2 antibody could also have been used to investigate binding partners of the protein by various biochemical means.

An investigation of Plxdc2 binding *in vivo* was carried out by AP *in situ* hybridisation of wildtype brain sections using an extracellular form of the mouse Plxdc2 protein as a probe. Plxdc2-AP(CT) protein bound to wildtype P0 brain slices in a widespread, but specific pattern. Plxdc2-AP(NT) did not bind to any regions of the brain, suggesting that in this

case, the AP tag inhibited the binding of interacting molecules, possible by altering protein structure at the N-terminal and/or blocking binding sites. Plxdc1 has been previously shown to bind to Nidogen, *in vitro* and *in vivo* (Lee *et al.*, 2006b). Nidogen is expressed widely in the brain, acting as a bridge between the extracellular matrix molecules laminin-1 and type IV collagen, and thus participating in the assembly of basement membranes (Erickson and Couchman, 2000, Poschl *et al.*, 2004). Although purely speculative, binding of Plxdc2 with Nidogen could explain the widespread staining pattern observed following AP *in situ* hybridisation with the Plxdc2-AP(CT) probe, and may mask binding of Plxdc2 to other proteins.

2.8 Materials and Methods

2.8.1. Animal Husbandry

Mice were maintained and bred in a 12hr light/ 12hr dark cycle, in a specific pathogen free animal unit. All procedures involving mice were performed in accordance with Statutory Instrument No. 566 of 2002 (Amendment of Cruelty to Animals Act, 1876). Mice strains: E10.5, C57BL/6JOlaHsd (Harlan); E11.5, CD1.

2.8.2. Genotyping of mice - PCR

Genotyping of mice was carried out by PCR. For gene trap lines, forward and reverse primers were designed to wildtype genomic sequence close to the site of vector insertion. An additional reverse primer was designed to the vector sequence in order to amplify mutant fragments. For Plxdc2GFP mice, vector sequence was amplified in a separate PCR reaction using a separate primer pair. At late embryonic (E15 onwards), P0 and adult stages, genomic DNA was extracted from small tail sections by digestion in Boston Buffer (50mM Tris pH 8.0, 50mM KCl, 2.5mM EDTA, 0.45% NP40, 0.45% Tween 20, Proteinase K) overnight at 56°C and used as template for the PCR reaction. At E9, whole embryos were carefully dissected out in sterile PBS, with extra care taken to avoid contamination by maternal tissues. All membranes were removed and genomic DNA extracted from embryos using the Qiagen Micro DNA kit (as per kit instructions). In all genotyping PCRs, Taq DNA Polymerase (Invitrogen) and corresponding buffers were used. Primers were produced by Sigma-Genosys.

2.8.3. Visualisation of reporter genes

Whole embryos were fixed in 0.2% glutaraldehyde (0.1M phosphate buffer, 2mM MgCl2, 5mM EGTA) for 30 mins. Following fixation, three washes were carried out at room temperature in washing buffer (0.1M phosphate buffer, 2mM MgCl2, 0.02% NP40, 0.1% sodium deoxycholate). Embryos were transferred to X-gal staining solution (1mg ml-1 X-gal, 5mM K4Fe(CN)6, 5mM K3Fe(CN)6 in embryo washing buffer) and incubated at 37°C until colour developed. Stained embryos were post-fixed in 4% paraformaldehyde (PFA)/ phosphate buffered saline (PBS) at 4°C overnight in order to preserve staining patterns and stored in PBS.

Embryonic and P0 brains for X-gal staining were fixed in 1% glutaraldehyde for 5 hours. Adult mice were deeply anaesthetised by injection with sodium pentabarbital (2µl/g body weight), perfused with 2% PFA in PBS for strictly ten minutes only (Xgal staining is PFA sensitive), and their brains dissected out in sterile PBS. 100µm sections were collected using a vibrating microtome (Leica, model VT1000S) and free floating sections were stained for βgal activity (as previously described). Following staining, sections were post-fixed in 4% PFA/PBS, air dried onto glass slides and mounted in Aqua Polymount (Polysciences Inc.).

E15 and P0 brains for PLAP staining were fixed overnight in 4% PFA/PBS at 4°C. Adult mice were deeply anaesthetised by injection with sodium pentabarbital (2µl/g body weight), perfused with 4% PFA in PBS, and their brains dissected out in sterile PBS. Fixed tissues were embedded in 6% agar and 100 µm sections collected using a vibrating microtome. Sections were air dried onto glass slides. Following incubation in PBS for 45mins at 65°C to inactivate endogenous phosphatases, PLAP activity was detected with AP staining buffer (0.1 mg ml-1 5-bromo-4-chloro-3-indolyl phosphate, 1 mg ml-1 nitroblue tetrazolium in 100mM Tris-HCL pH 9.5, 100mM NaCl, 5 mM MgCl2). Sections were dehydrated in increasing concentrations of methanol and cleared in benzyl benzoate: benzyl alcohol (BB:BA, 2:1). Following rehydration, cleared sections were mounted in Aqua Polymount.

2.8.4. In situ hybridisation

Whole mount *in situ* hybridisation was carried out largely according to (Wilkinson, 1992)) with minor adjustments. Hybridisation times were extended to 2-3 days at 65°C. Final post-hybridisation washes were in 0.2%SSC/0.1%CHAPS, 3 times for 20 mins at 65°C. Mouse antisense probes used are represented by the following Genbank sequences: *Plxdc2*; nucleotides 1524-2188 on NM_026162. Wnt1; nucleotides 138-2345 on BC005449. Wnt3a; nucleotides 2310-2676 on NM_009522. Wnt5a; nucleotides 193-2324 on BC018425. Wnt8b; nucleotides 942-1634 on NM_011720. Sense control probes were routinely employed in each experiment. Mice strains: E10.5, C57BL/6JOlaHsd (Harlan); E11.5, CD1.

Mouse line	Primer type	Primer Sequence (5' – 3')	Product Size (bp)
Plxdc2 PLAP secretory trap	Wildtype Forward	GAGAGCTACTTAGGCTGATTCTGT	
	Wildtype Reverse	CCTCGACAGTAATTCAACCTGCTG	436
	Vector Reverse	GCTACCGGCTAAAACTTGAGACCT	246
Plxdc1 PLAP secretory trap	Wildtype Forward	TCTCTCTACATAGCTCTGGCTGTC	
	Wildtype Reverse	AGTCAGGTCTGAGGTCAGCTGTCT	600
	Vector Reverse	ACTTCCGGAGCGGATCTCAAACTC	370
Plxdc2 GFP Mouse line	Wildtype Forward	TCTCTCCTTCACTTCTGTTACCCG	
	Wildtype Reverse	AAGCAAACCTCTTTCCCCATTC	461
	Vector Forward	CCCAAGACTCACCAGCAGAGC	
	Vector Reverse	GGAGAGAAAGGCAAAGTGGATGTC	363

Table 2.1 Description of primers used in genotyping PCR reactions. All primers were produced by Sigma Genosys.

Plxdc1 or Plxdc2 PLAP secretory trap	Plxdc2 GFP
95°C for 2.5 min	95°C for 2 min
32 cycles of: Denaturing: 95°C for 15 sec Annealing: 65°C for 30 sec Extension: 72°C for 1 min	35 cycles of: Denaturing: 94°C for 30 sec Annealing: 60°C for 1 min Extension: 72°C for 1 min
72°C for 10 min	72°C for 10 min

Table 2.2 Description of genotyping PCR program. PCR Programs were varied according to varying annealing temperature of primers and expected product length (1min extension time was used per kb of expected product).

2.8.5. Immunohistochemistry

Immunohistochemistry was carried out on free floating vibratome sections. E15 brains were embedded in 4% agar/PBS and 50µm free floating sections collected using a vibrating microtome (Leica, model VT1000S). Following three, fifteen minute washes in PBS, sections were blocked in 5% normal goat serum (NGS) for one hour at room temperature, with gentle agitation. Incubation in primary antibody was carried out in PBS, overnight at 4°C (a complete list of antibodies used is available in Appendix 5.8). Sections were washed as before and incubated in secondary antibody for one hour at room temperature, in the dark. Sections were briefly air-dried onto glass slides and mounted in Aqua Polymount (Polysciences Inc.).

2.8.6. Optical Projection Tomography

In situ hybridised or X-gal stained embryos were rinsed briefly in water, and embedded in 1% low melting point agarose. Once set, the block of agarose was cut in the desired orientation and affixed to a metal mount. Specimens were then dehydrated overnight in 100% methanol and cleared in BB:BA (2:1). OPT was carried out as described (Sharpe *et*

al., 2002) on a prototype scanner built at the MRC Human Genetics Unit Edinburgh (now commercially available from BioOptonics).

Volume renditions of the data allow 3D representation of the full data set, resulting in a 3D representation of the expression domain in the context of the morphology of the embryo (Figure 2.4, b-e). Software for 3D reconstruction, volume rendering and analysis was kindly provided by James Sharpe and the Edinburgh Mouse Atlas Project (EMAP) (MA3Dview and MAPaint downloadable from EMAGE). For surface rendering, thresholds on the data are set that eliminate data below a particular intensity so that a particular structure or expression domain can be viewed. The isolated structure or expression domain is then represented as a solid surface by joining the datapoints above that threshold level (see Figure 2.6, g-j). Scripts provided by the EMAP set the thresholds on the data and the surface representations were generated using software from the Visualisation Tool Kit (vtk) suite (vtkDecimate).

2.8.7. Real time PCR

RNA was extracted from the cerebella of adult wildtype, heterozygous and homozygous Plxdc2GFP mice using TRI Reagent (Sigma, as per protocol). Purified RNA was treated with DNAse (Promega) in order to remove contaminating DNA. Reverse transcription of RNA was carried out using Superscript II reverse transcriptase (Invitrogen) and Oligo d(T) primer (New England Biolabs, as per protocol). Negative controls were routinely employed. These included a dH_20 control in which no RNA template was included in the reaction and reverse transcription (-RT) controls for each of the RNA samples, in which no Superscript II reverse transcriptase was added. Three primer pairs for the amplification of *Plxdc2* were designed using the Primer Express 2.0 program (Applied Biosystems), each of which were tested in real time PCR reactions. These primer pairs were designed to regions within exon 7 and exon 14 of the Plxdc2 transcript (downstream of the targeted insertion of the 5S-EGFP-pA cassette in exon 1 of Plxdc2). The most sensitive of these primer pairs amplified a product of 61bp from exon 7 of the *Plxdc2* transcript and was subsequently used for calculation of Plxdc2 transcript levels in Plxdc2GFP heterozygous and homozygous mice (Primers listed in Table 2.3). Samples for real time PCR were normalised using the mouse ribosomal phosphoprotein (RPO) gene (Primers designed and routinely used by members of the Kristian Helin lab, University of Copenhagen). Triplicates of each PCR reaction were carried out and negative controls were routinely

employed. Negative controls included the use of dH_20 in place of template in order to rule out cross contamination between wells. In addition, the -RT controls for each of the RNA samples were used as template for the real time PCR reaction. Real time PCR on negative controls did not result in any amplification of the Plxdc2 transcript. The real time PCR reaction was carried out using SYBR green PCR master mix (Applied Biosystems, as per protocol) and the 7500 Fast Real Time PCR System (Applied Biosystems). The PCR program is outlined in Table 2.4. A dissociation step was included at the end of every PCR program to identify if more than one PCR product was produced in the reaction. This step involves a gradual increase in temperature from the primer annealing temperature (60 °C) to the melting temperature (95 °C) over a period of 22 minutes.

Gene	Primer Type	Primer Sequence (5'-3')
Plxdc2	Forward	CCAGTGAAAGTCGGGTTGTCTG
Plxdc2	Reverse	TGGGTATTTGCTGGATCCTGTG
RPO	Forward	TTCATTGTGGGAGCAGAC
RPO	Reverse	CAGCAGTTTCTCCAGAGC

Table 2.3 Primers used in real time PCR experiments

50°C for 2 mins
95°C for 10 mins
40 cycles of : 95°C for 15 secs 60°C for 1 min
Dissociation step

Table 2.4 Real time PCR program.

2.8.8. Cresyl Violet Staining

50μm sections of E15.5 brain tissue were collected by vibrating microtome (Leica, model VT1000S) and briefly air-dried onto glass slides. Sections were washed for two minutes in sterile water (Sigma) and stained in cresyl violet (0.2% cresyl violet in 100mM Acetate Buffer, pH4.5) at room temperature for 30 minutes or until dark. Following a 2 minute wash in sterile water, sections were dehydrated in ascending percentage of ethanol (70% for 1 min, 80% for 2 mins, 96% for 5 mins, 100% for 5 mins). A second 5 minute wash in 100% ethanol was carried out prior to two, 5 minute washes in Xylene (Fisher Scientific). Sections were mounted in Depex (BDH).

2.8.9. Production of Plxdc2-AP proteins

Plxdc2-AP plasmids were prepared by Géraldine Kerjan (Lab of Alain Chédotal, Université de Paris 6, France) using the pAPtag-5 plasmid (Genhunter). The extracellular region of the mouse *Plxdc2* transcript was amplified by PCR and ligated into pAPtag5 using a combination of either the Xho I and Xba I restriction enzyme sites (N-terminal AP tagging of extracellular Plxdc2) or the Nhe I and Bgl II restriction enzyme sites (C-terminal AP tagging of extracellular Plxdc2).

AP proteins were produced in HEK 293T cells, cultured in DMEM high glucose growth medium (10% FBS, 25 mM HEPES, 1x glutamine, 1x penstrep). HEK293T cells were cultured to approximately 60% competency and transfected with plasmids using Fugene 6 Transfection Reagent (Roche, as per protocol). Three to four days following transfection, growth medium (containing the secreted AP fusion proteins) was collected, centrifuged and sterile filtered to remove debris. 0.05% NaN_3 was added for long term storage. AP produced by pAPtag-5 plasmid was collected for control experiments.

2.8.10. AP in situ hybridisation

Brains were removed from newborn C57black6 mice and fixed overnight in 4% PFA. Adult mice were deeply anaesthetised by injection with sodium pentabarbital (2μl/g body weight), perfused with 4% PFA in PBS, and their brains dissected out in sterile PBS. Free-floating 100μm vibrating microtome sections (Leica, model VT1000S) were collected in PBS and washed twice in HBAH (HBSS, 0.5mg/ml BSA, 0.05% NaN3, 10mM HEPES pH

7.4). Brain sections were then incubated in Plxdc2-AP fusion protein overnight at 4ºC. AP produced by pAPtag-5 plasmid was routinely used as a control. Following six washes in cold HBAH, the sections were placed in formalin for 15 sec and washed twice in HBS (150mM NaCl, 20mM HEPES pH 7.4). Heat inactivation of endogenous phosphatases was carried out in HBS at 65ºC for one hour. Sections were incubated in AP staining buffer at 37ºC in the dark until colour developed.

3. Chapter 3 – Functional Analyses of *Plxdc2* in the chick

3.1 Aims of this chapter

The principle aim of this work was to establish an experimental model in which an examination of *Plxdc2* function could be explored, both by misexpression of the protein and by knockdown of endogenous gene function. A preliminary investigation in the chick confirmed conserved *Plxdc2* expression in several regions of the developing embryo and *in ovo* electroporation was therefore employed to manipulate *Plxdc2* expression *in vivo*. The lack of an obvious phenotype in Plxdc2GFP homozygous mice indicated that the key to establishing *Plxdc2* function could be in ectopic/overexpression (misexpression) of the gene. Examination of gene function in the chick was facilitated by the construction of a full-length *Plxdc2* expression plasmid and by the design of several short hairpin forming RNAs (shRNAs) against the gene. In parallel to this work, *Plxdc2* expression was examined in neural stem cells in culture.

3.2 Introduction

3.2.1. The use of the chick as an experimental model

Throughout scientific history, the embryo of the domestic chicken (*Gallus gallus*) has featured strongly as a popular model for biological investigation. The first documentation of its use was by the ancient Egyptians who opened hen's eggs to observe the embryos inside at various stages of development (Needham, 1934; reviewed in Stern, 2004, Stern, 2005, Wolpert, 2004). In fact, it was Aristotle who undertook the first truly scientific approach, when he documented the morphological development of the embryo (approximately 300BC). By the late sixteenth and early seventeenth century, the preformation/epigenesis debate was at its height and examinations of the developing chick embryo were used to fuel arguments on either side. Observations during this period led to an understanding of blood circulation and the roles of veins and arteries within the developing embryo (Stern, 2004, Stern, 2005, Wolpert, 2004). The development of a simple microscope at this time aided in the discovery of the neural groove (neural tube) and the somites, as well as the observation that the developing heart began beating before blood was formed (Malpighi, 1672, 1675; reviewed in Stern, 2005, Wolpert, 2004). Even

during this early era in developmental biological research, the embryological basis behind important biological concepts were being founded in the chick.

During the modern era of embryological research, many major biological principles have been established and defined within the chick owing to ease of physical and genetic manipulation of the developing embryo. Physical perturbation of the embryo began in the early 1900s, and in 1930, Waddington showed that the endoderm (now called the hypoblast) influenced the direction of the primitive streak, and that its reversal caused the development of an additional primitive streak above its posterior end (Waddington, 1940; reviewed in Stern, 2004, Stern, 2005, Wolpert, 2004). In the later half of the twentieth century, the development of transplantation studies led to the discovery of several important signalling centres within the developing chick embryo. In the limb, these included the zone of polarising activity (ZPA) and the apical ectodermal ridge (AER), the former being responsible for patterning along the anterior-posterior axis and the latter for proximal-distal outgrowth (Saunders, 1948, Tickle, 2004, Zwilling and Hansborough, 1956). In the developing brain, transplantation of midbrain-hindbrain tissue in the chick results in the development of ectopic midbrain or cerebellum structures, illustrating the organizer potential of the region (Puelles and Martinez, 1996, Raible and Brand, 2004). In the 1970s, development of chick-quail chimera techniques enabled the documentation of migration and differentiation of cell populations in whole embryos (Douarin, 1973). This allowed further definition of the origin and fate of the neural crest, and led to an understanding of many patterning processes within the developing neural tube (Le Douarin, 2004). The chick model has since been successfully used to investigate many principles of embryonic development and has helped establish the modern field of developmental biology.

3.2.2. In ovo electroporation.

Recent use of the chick as an experimental model has been influenced by the development of *in ovo* electroporation techniques. The successful electroporation of plasmid DNA into chick retinal explants was first carried out by Pu and Young (1990). Electroporation of the embryo *in ovo* was initially investigated by Muramatsu *et al.* (1997) and since then, the technique has been further developed to improve embryonic survival and transfection efficiency (Funahashi *et al.*, 1999, Katahira and Nakamura, 2003, Krull, 2004, Nakamura *et al.*, 2004, Nakamura *et al.*, 2000, Okafuji *et al.*, 1999). *In ovo* electroporation is now

routinely used in the targetted misexpression or silencing of a gene of interest in the chick embryo.

Many different vectors can be used for the misexpression of a gene by *in ovo* electroporation. For long-term misexpression, retroviral vectors such as the replication-competent ASLV long terminal repeat with a splice acceptor (RCAS) provirus vector are routinely used (Havens *et al.*, 2008, Wu *et al.*, 2008, Mina *et al.*, 2007). Misexpression is restricted to the descendents of the transfected cells and detailed cell lineages can be traced (Bell and Brickell, 1997, Krull, 2004, Nakamura *et al.*, 2000, Sugiyama and Nakamura, 2003). There are, however, limitations on the size of inserts that can be expressed by several retroviral vectors (Bell and Brickell, 1997, Krull, 2004). Transient expression of an ectopic protein is often driven by the chick β-actin promoter in combination with a Rous sarcoma virus (RSV) or cytomegalovirus (CMV) enhancer. Vectors using these promoters have consistently been shown to drive expression of an ectopic protein for 72 hours *in ovo* (Nakamura *et al.*, 2004).

3.2.3. Gene silencing in the chick embryo

RNA mediated interference (RNAi) was first discovered in the nematode *Caenorhabditis elegans (C. elegans)* (Fire *et al.*, 1998). When double stranded RNA (dsRNA) is introduced into a cell it is cleaved by the type III endonuclease, Dicer, into small interfering RNAs (siRNAs). These associate with the RNA-induced silencing complex (RISC), guiding it to target specific mRNAs which are cleaved by RISC enzymatic activity (Maine, 2008).

Although homologous gene silencing by RNAi using long dsRNA is routinely successful in *C. elegans* and *Drosophila*, the introduction of long dsRNA into higher vertebrates triggers a strong cytotoxic response (Baglioni and Nilsen, 1983, Williams, 1999). The use of shorter dsRNA vectors circumvented the problem of toxicity in higher vertebrates. ShRNA vectors have been shown to exert RNAi effects in cultured mammalian cells (Brummelkamp *et al.*, 2002, Paddison *et al.*, 2002, Paul *et al.*, 2002, Sui *et al.*, 2002, Yu *et al.*, 2002, Svoboda *et al.*, 2001). These vectors are comprised of short synthetic oligonucleotides (40-50mer), encorporating a short hairpin sequence and are processed into dsRNA by cell machinery to exert RNAi effects. In recent years they have been shown to

be very effective for the targetted knockdown of genes through *in ovo* electroporation (Bron *et al.*, 2004, Chesnutt and Niswander, 2004, Das *et al.*, 2006, Harpavat and Cepko, 2006, Katahira and Nakamura, 2003, Nakamura *et al.*, 2004, Okamoto *et al.*, 2008). ShRNA vectors used in the chick incorporate a RNA polymerase promoter (routinely the U6 or HI promoter) (Bron *et al.*, 2004, Brummelkamp *et al.*, 2002, Das *et al.*, 2006, Paddison *et al.*, 2002, Paul *et al.*, 2002, Sui *et al.*, 2002, Svoboda *et al.*, 2001, Yu *et al.*, 2002). Analysis of *in vivo* shRNA silencing activity, driven by the mouse U6 promoter, has demonstrated shRNA expression 6 hours following electroporation. Significant gene silencing was detectable 12 hours following transfection, and persisted 36 hours later (Katahira and Nakamura, 2003). Retroviral vectors such as the RCAS provirus vector can be used to drive persistant shRNA expression, but slow onset of expression has been noted (Bron *et al.*, 2004, Harpavat and Cepko, 2006).

Gene silencing has also been demonstrated in the chick by the electroporation of morpholino antisense oligonucleotides (Kos *et al.*, 2001, Kos *et al.*, 2003, Sugiyama and Nakamura, 2003, Mende *et al.*, 2008). Morpholino antisense oligonucleotides are non-degradable antisense nucleotides in which the ribose or deoxyribose rings characteristic of RNA and DNA oligoucleotides are replaced by a morpholine ring structure. Initial difficulties in morpholino electroporation have been overcome by the conjugation of flourescein isothiocyanate (FITC) to the molecules in order to increase their charge. As morpholinos interfere with gene function at the level of protein translation, it is imperative that a functioning antibody against the gene of interest exists in order to evaluate experimental results. Morpholino antisense oligonucleotides have been used most successfully in the chick at early stages of development, before or at the stage of primitive streak development (Mende *et al.*, 2008).

In this study, *Plxdc2* function was investigated in the chick by misexpression of the protein and by knockdown of endogenous gene function, using appropriate plasmids and *in ovo* electroporation techniques. A full length *Plxdc2* expression plasmid was constructed. In addition, several shRNAs were designed against the gene and shRNA efficiency was examined in cell culture prior to use *in vivo*. However, before initiating functional analyses in the chick nervous system, it was of upmost importance to examine normal *Plxdc2* expression in this animal model.

3.3 *Plxdc2* expression in the developing nervous system of the chick

3.3.1. Production of chick Plxdc2 probes for in situ hybridisation:

Investigation of *Plxdc2* expression in the chick was carried out by *in situ* hybridisation using an antisense DIG-labelled probe. DIG-labelled RNA probes for chick *Plxdc2* were produced using a EST from the BBSRC chick EST database, ChEST 853h24, as a template (Geneservice, as outlined in section 3.8.2). An antisense probe and sense probe of approximately 1.1kb were successfully produced for use in *in situ* hybridisation experiments in the chick (Figure 3.1). Sense controls were routinely employed in *in situ* hybridisation experiments and resulted in no staining of chick tissue (Representative images are shown in Appendix 5.11).

3.3.2. Plxdc2 expression in the chick

Plxdc2 expression in the chick was examined from Hamburger Hamilton (HH)(1951) stage 16 to 21, and in several regions of the developing embryo was found to be similar to that previously documented in the mouse (Figure 3.2, 3.3 and 3.4). *Plxdc2* expression in the developing embryo was mainly consistent between HH stage 16 and 17, and HH stage 17 is shown here for clarity. *Plxdc2* was expressed in the dorsal midline of the telencephalon at HH stage 17 but not at HH stage 16. This was the only region where expression differed between the two ages. Embryos were imaged and analysed in 3D using optical projection tomography (OPT). From HH stage 16 to 21, OPT highlighted a ring of *Plxdc2* expression at the midbrain-hindbrain boundary (MHB) and expression throughout the floor of the midbrain, the eye and the otic vesicle (Supplemental data Movies 2, 3 and 4, HH stages 17, 20 and 21 respectively; Figures 3.2 and 3.3). Although not evident in the mouse at comparable stages, a line of intense *Plxdc2* expression was evident at the dorsal midline of the mesencephalon and diencephalon from HH stage 16 (data not shown) and this expression persisted at HH stage 17 and 20 (Figure 3.2, b, c and i). At HH stage 17, *Plxdc2* expression at the dorsal midline extended into the telencephalon. By HH stage 21, dorsal midline Plxdc2 expression was restricted to the mesencephalon only (Figure 3.3 e, Supplemental Movie 4). In the trunk region, *Plxdc2* expression was evident within the motor column and the somites, as well as in the developing mesonephros from HH stage 16. Expression in these regions persisted at HH stage 17 and 20 (Figure 3.2 e and g).

Although still present in the HH stage 21 embryo, *Plxdc2* expression in the motor column and somites was relatively less intense at this stage (Supplemental Movie 4).

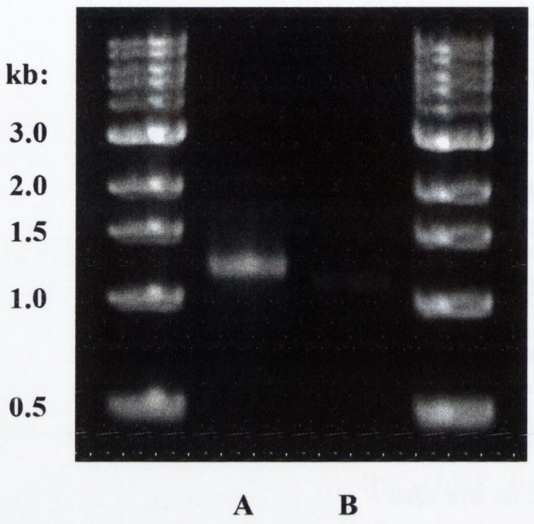

Figure 3.1 Production of probes for use in *in situ* hybridisation experiments in the chick. Lane A, DIG labelled antisense probe; Lane B, DIG labelled sense probe. Gel shows intact RNA product and size is estimated against 1kb DNA ladder (New England Biolabs).

Dynamic changes in *Plxdc2* expression were documented in the chick head between HH stage 20 and stage 21 (Figure 3.3). *Plxdc2* expression at the mesencephalon-diencephalon boundary (MDB) was first noted in the HH stage 20 brain (MDB, Figure 3.3 b) and by HH stage 21, an intense band of expression was evident. *Plxdc2* expression in this region did not occur within the neural tube but rather in the surrounding mesoderm (Figure 3.3 e,f and h). *Plxdc2* expression in the forebrain of the chick at HH stage 20 was found to be almost complementary in pattern to that observed in the mouse (Figure 3.3 b). Expression was extensive throughout the dorsal diencephalon and telencephalon but was absent from the region of the cortical hem (Figure 3.3 b-d). By HH stage 21, widespread Plxdc2 expression was evident throughout the telencephalon and intense expression was obvious at the region of the cortical hem and in the surrounding mesoderm (Figure 3.3 f, g and i). Although still present in the HH stage 21 brain, *Plxdc2* expression at the midbrain-hindbrain boundary and the floor of the midbrain was more discrete in nature (Figure 3.3 g).

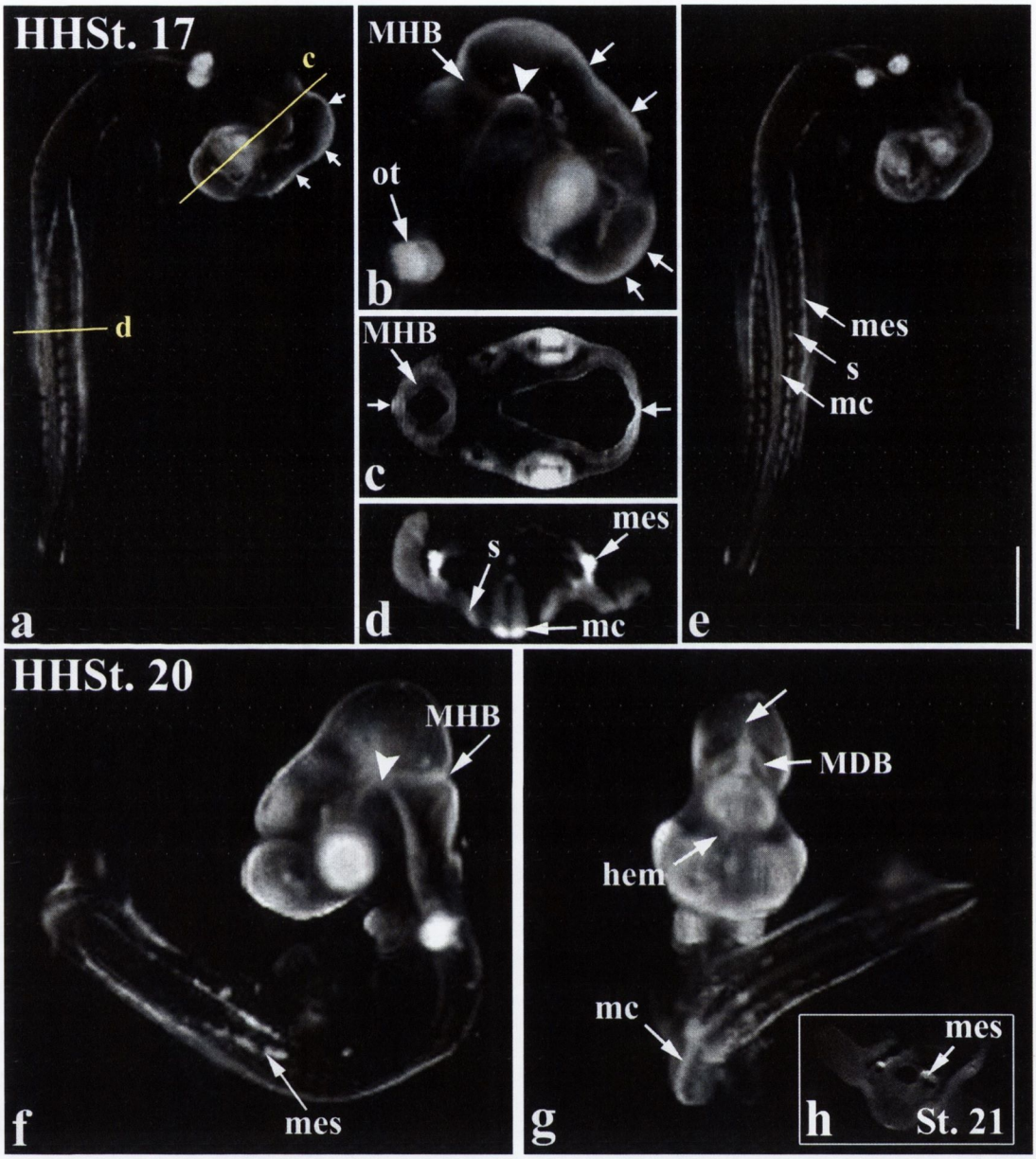

Figure 3.2 *Plxdc2* expression in the chick at Hamburger Hamilton stages 17 (a-e), 20 (f and g) and 21 (h). a, b, e – g, still images from different external viewing angles of volume-rendered representations. c, d and h, virtual sections through the computer reconstruction. hem, cortical hem; mc, motor column; MDB, mesencephalon–diencephalon boundary; mes, mesonephros; MHB, midbrain-hindbrain boundary; ot, otic vesicle; s, somites. Arrowhead, floor of the midbrain; arrow, region of more intense *Plxdc2* expression at the dorsal midline. Scale bar: a, e, and h 1mm; b-d, 0.5mm; f and g, 0.75mm.

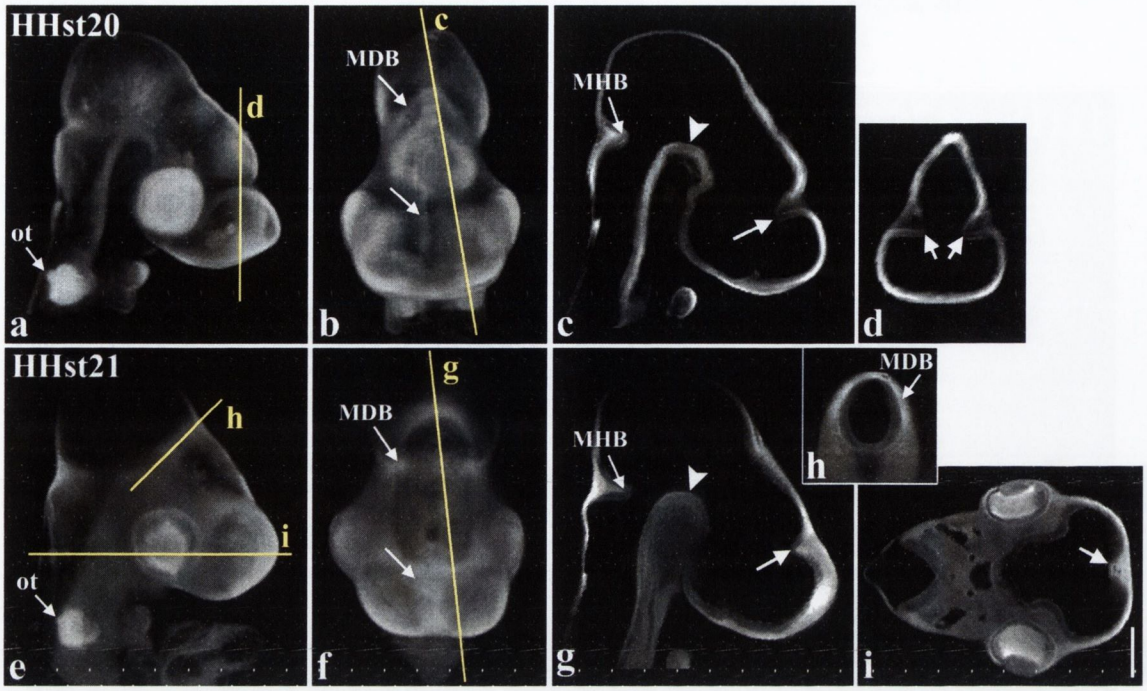

Figure 3.3 Comparison of *Plxdc2* expression in the HH stage 20 and stage 21 chick head. *Plxdc2* expression was absent from the region of the cortical hem at HH stage 20 (arrow: b,c and d). By HH stage 21, *Plxdc2* expression in the cortical hem and surrounding mesoderm was evident (arrow: f, g and i). a, b, e and f, still images from different external viewing angles of volume rendered specimens. c, d and g-i, virtual sections through the embryo arrowhead, floor of midbrain; ot, otic vesicle; MDB, surrounding mesenchyme of the mesencephalon-diencephalon boundary; MHB, midbrain-hindbrain boundary. Scale bar: a-d, 0.4mm; e-i, 0.5mm.

Although the forebrain regions of the mouse and chick are not directly comparable, the cerebellar structure and hindbrain are highly conserved between species. A detailed comparison of *Plxdc2* expression in the mouse and chick was carried out in the hindbrain (Figure 3.4). In the HH stage 36 chick, *Plxdc2* expression was evident in the Purkinje cell layer of the cerebellum and in several distinct nuclei within the medulla oblongata including the trigeminal motor nucleus (N5n) and the principle sensory trigeminal nucleus (Pr5) (Figure 3.4, d-g). Expression in these regions, and at the neuroepithelium, corresponded to the pattern previously noted in the mouse. In the developing chick cerebellum, migration of granule cells from the external granule layer (EGL) to the inner granule layer occurs through parasagittal linear arrays known as granule cell raphes (Lin and Cepko, 1998). Purkinje cells appear to be segregated into discrete parasagittal

domains, interrupted by Purkinje cell-poor regions that correspond to the granule cell raphes. At HH stage 36, Plxdc2 expression was evident in the purkinje cell layer of the cerebellum, with a lack of expression within the granule cell raphes (Figure 3.4 f and g).

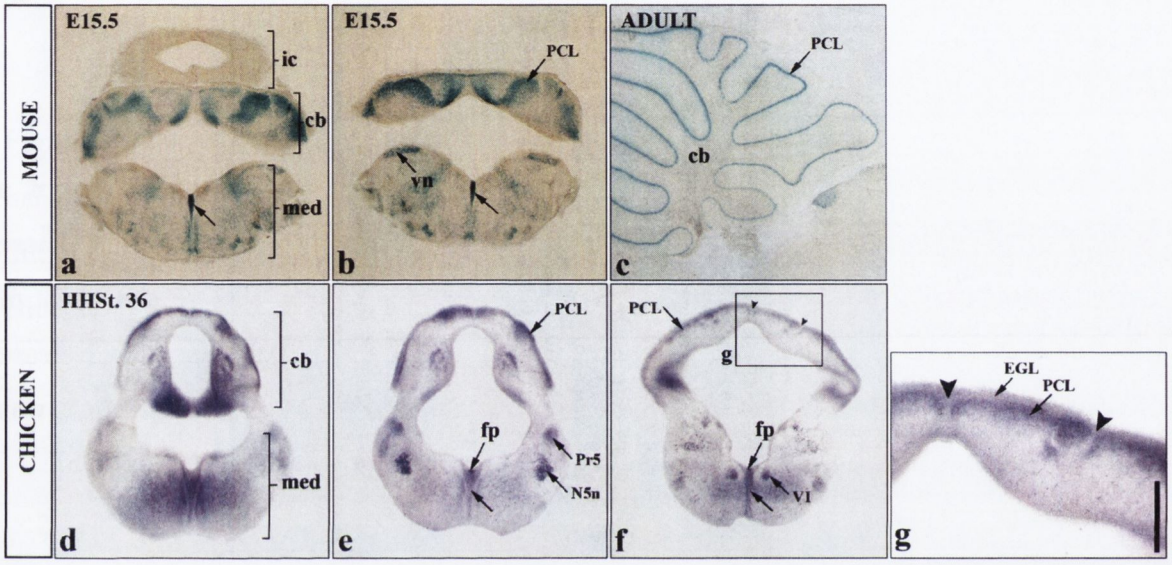

Figure 3.4 Comparison of *Plxdc2* expression in the hind brain of the chick and mouse. a and b, coronal sections through the brain of a heteozygous E15.5 *Plxdc2* gene trap mouse, stained for βgal activity. c, sagittal section through the brain of a heterozygous adult *Plxdc2* gene trap mouse showing Plxdc2-βgeo expression in the mature Purkinje cell layer of the cerebellum. d-f, Plxdc2 *in situ* hybridisation of coronal sections through the brain of a HH stage 36 chick brain. g, higher magnification image of indicated region of f showing Plxdc2 expression in the Purkinje cell layer and a lack of Plxdc2 expression in granule cell raphes (arrowheads). Arrow, *Plxdc2* expression in the neuroepithelium; cb, cerebellum; ic, inferior colliculus; fp, floor plate; med, medulla oblongata; N5n, trigeminal motor nucleus; PCL, Purkinje Cell Layer; Pr5, principle sensory trigeminal nucleus; VI, abducens nucleus; vn, vestibular nuclei. (For *in situ* hybridisation of chick brain using the sense *Plxdc2* probe, see Appendix 5.11). Scale bar: a-c, 0.8mm; d-f, 1mm; e, 250μm.

3.4 Misexpression of *Plxdc2* in the chick brain

3.4.1. Prediction of the complete transcript of the chick Plxdc2 gene

At the time of experimental design, NCBI and ENSEMBL differed in the predicted sequence for the chick *Plxdc2* transcript with neither version including sequence encoding the signal peptide of the protein. The full coding region of the gene was therefore predicted by compilation of Expressed Sequence Tags (ESTs) from the BBSRC chick EST database (www.chick.manchester.ac.uk) and alignment against the mouse *Plxdc2* protein.

Two overlapping ESTs, ChEST 636b10 and ChEST 853h24, were retrieved from a BLAST search of the BBSRC chick EST database using the partial chick transcript. These were used to predict the full length chick *Plxdc2* sequence (Appendix 5.4). Alignment of the predicted protein against mouse Plxdc2 (ENSMUSP00000028081, Ensembl Release 50) supported the validity of the predicted chick transcript. Protein architecture was conserved between species and the Plxdc2 proteins were 81% identical (Appendix 5.5).

3.4.2. PCR amplification of the Chick Plxdc2 transcript and ligation into the pcDNA3.1myc-His(B) plasmid.

RNA was extracted from HH stage 21 embryos and reverse transcribed as outlined in section 3.8.3. The full length *Plxdc2* transcript was amplified by PCR, using the primers and program detailed in section 3.8.4. A product of approximately 1.6 kb, corresponding to the predicted length of the *Plxdc2* transcript (1611bp), was amplified (Figure 3.5). PCR product and pcDNA3.1myc-His(B) plasmid were digested with *Eco*RI and *Xho*I (New England Biolabs, as per protocol), cleaned and ligated as outlined in section 3.8.5. Following transformation into Top 10F' competent cells (Invitrogen), DNA extracted from selected colonies were checked for insert orientation and size by digestion of plasmid DNA with appropriate enzymes prior to sequencing (Figure 3.6).

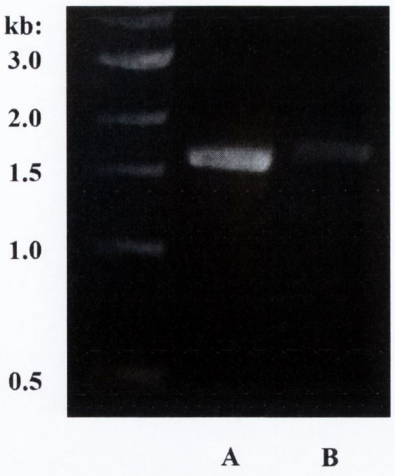

Figure 3.5 Amplification of the full length *Plxdc2* transcript from chick cDNA. Lane A, band amplified from 1µl of template cDNA; Lane B, band amplified from a 1 in 10 dilution of template cDNA. Band size compared to 1kb DNA ladder (New England Biolabs) with fragment sizes indicated on the left.

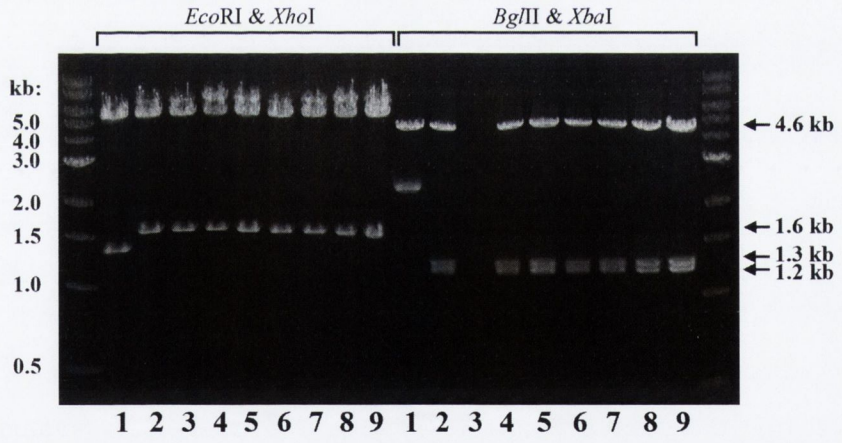

Figure 3.6 Confirmation of size of insert and orientation within the pcDNA3.1myc-His(B) plasmid. DNA from nine single colonies was digested with *Eco*RI and *Xho*I in order to confirm correct insert size. Colonies 2-9 contained an insert of the correct size (1.6kb). Digestion with *Bgl*II and *Xba*I confirmed insert of the *Plxdc2* transcript in the correct orientation for *in vitro* transcription in colonies 2 and 4-9. Size of bands compared to 1kb DNA ladder (New England Biolabs) with fragment sizes indicated on the right.

Of nine colonies tested, seven were found to contain an insert of the correct size and orientation (Figure 3.6). Plasmid DNA from these colonies was sequenced (MWG Biotech) and compared to the predicted *chPlxdc2* EST sequence. Several inserts contained deletions of varying severity, but the *Plxdc2* insert in clone 7 differed to the predicted sequence at two points only, a C/G base change at 1117bp and an A/G base change at 1167bp (Appendix 5.5). Alignment against the EST predicted protein highlighted a single conservative difference in the translated protein at amino acid 373. Translation of the Plxdc2 EST transcript resulted in glutamine at amino acid 373, however translation of clone 7 would lead to glutamic acid at this position. This region was sequenced in four independent clones and in each of these glutamic acid was predicted at amino acid 373. The conservative difference in amino acid translation in clone 7 corresponds to the annotation of glutamic acid at this location in the complete Ensembl and NCBI annotated *Plxdc2* proteins (ENSGALP00000012907, Ensembl Release 50; XP_418613.2, NCBI). Therefore, it would appear that there was a conservative discrepancy at this location in the sequence of the Plxdc2 EST used to predict the full length Plxdc2 transcript. Plasmid DNA from clone 7 was prepared in large quantities and used in subsequent *in ovo* electroporation overexpression/ectopic expression experiments. This plasmid is referred to as chPlxdc2-Myc since it is designed to express a Myc tagged version of chPlxdc2 in eukaryotic cells.

3.4.3. In ovo electroporation of chPlxdc2-Myc plasmid DNA

An investigation of the effects of over/ectopic expression (misexpression) of *Plxdc2* in the chick brain was carried out by means of *in ovo* electroporation of the expression construct, chPlxdc2-Myc (Section 3.8.11). ChPlxdc2-Myc was injected into the lumen of the neural tube at the level of the myelencephalon at HH stage 10-11 and electroporated into cells on one side of the neural tube. Embryos were dissected out 24 hours post electroporation. The pCA-β-EGFPm5-U6 plasmid was routinely co-electroporated with chPlxdc2-Myc, allowing visually assessment of transfection efficiency using the EGFP marker. Controls consisted of the empty pcDNA3.1myc-His(B) plasmid, co-electroporated with pCA-β-EGFPm5-U6. Initially, sections through the embryo were collected by vibrating microtome and the Myc tag and EGFP visualised by immunohistochemical techniques (section 3.8.12). It was immediately evident that, when compared to controls, expression of chPlxdc2-Myc in the neural tube resulted in apparent thickening on the experimental side (Figure 3.7).

A constant plane of sectioning was very difficult to achieve in embryos of this size, and it was feared that inaccuracies in vibratome sectioning could account for the apparent thickening of the neural tube. 3D OPT imaging captures all of the data and allows manipulation of the plane of virtual sectioning in 3D space, so it was employed in order to confirm the validity of the thickening effect. Comprehensive analyses of the region of chPlxdc2-Myc expression and corresponding neural tube thickening were also carried out using OPT.

Wholemount immunohistochemistry with antibodies against Myc and EGFP, and subsequent OPT analysis, confirmed the validity of the thickening phenotype in the chick, 24 hours post electroporation (Figure 3.8). Analysis of several embryos indicated that ChPlxdc2-Myc was expressed throughout the DV axis of the neural tube, from the mesencephalon-diencephalon boundary through to rhombomere 2 (Figure 3.8 and supplemental movie 5). Thickening of the neural tube was evident throughout the region of chPlxdc2-Myc expression (Figure 3.8, c-e).

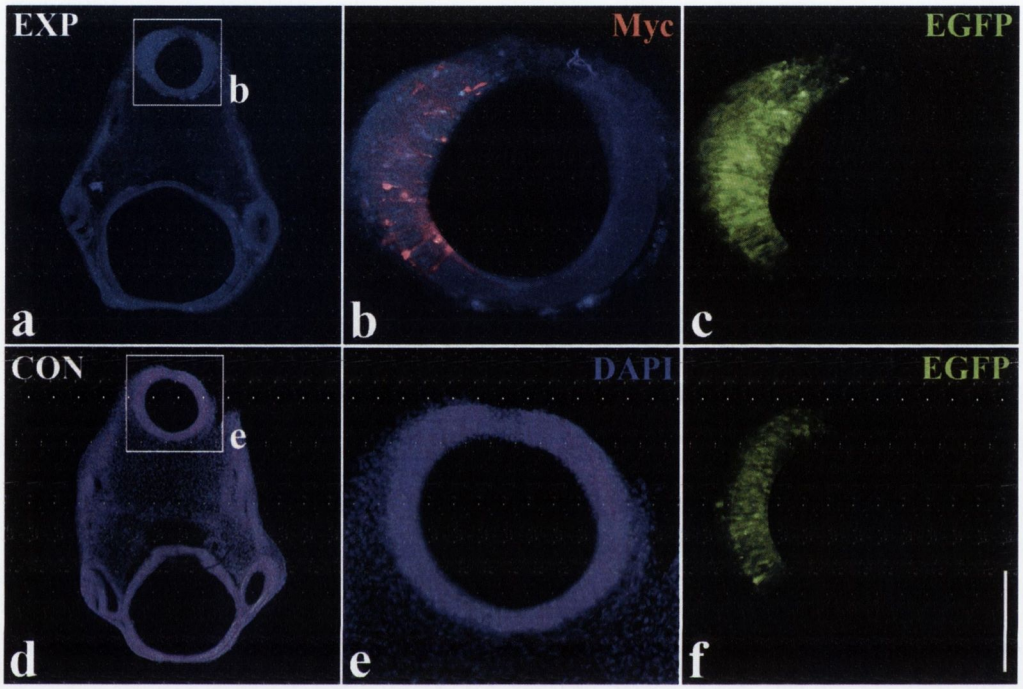

Figure 3.7 Electroporation of *Plxdc2* into the HH stage 10-11 chick brain results in thickening of the neural tube on the experimental side. a-c, 50μm transverse sections through the head of a HH stage 17 embryo, electroporated with chPlxdc2-Myc 24 hours previously. d-f, 50μm horizontal sections through a control embryo, electroporated with pcDNA3.1myc-His(B). Empty pCA-β-EGFPm5-U6 plasmid was routinely co-electroporated (e and f). Scale bar: a and d, 400μm; b,c,e and f, 100μm.

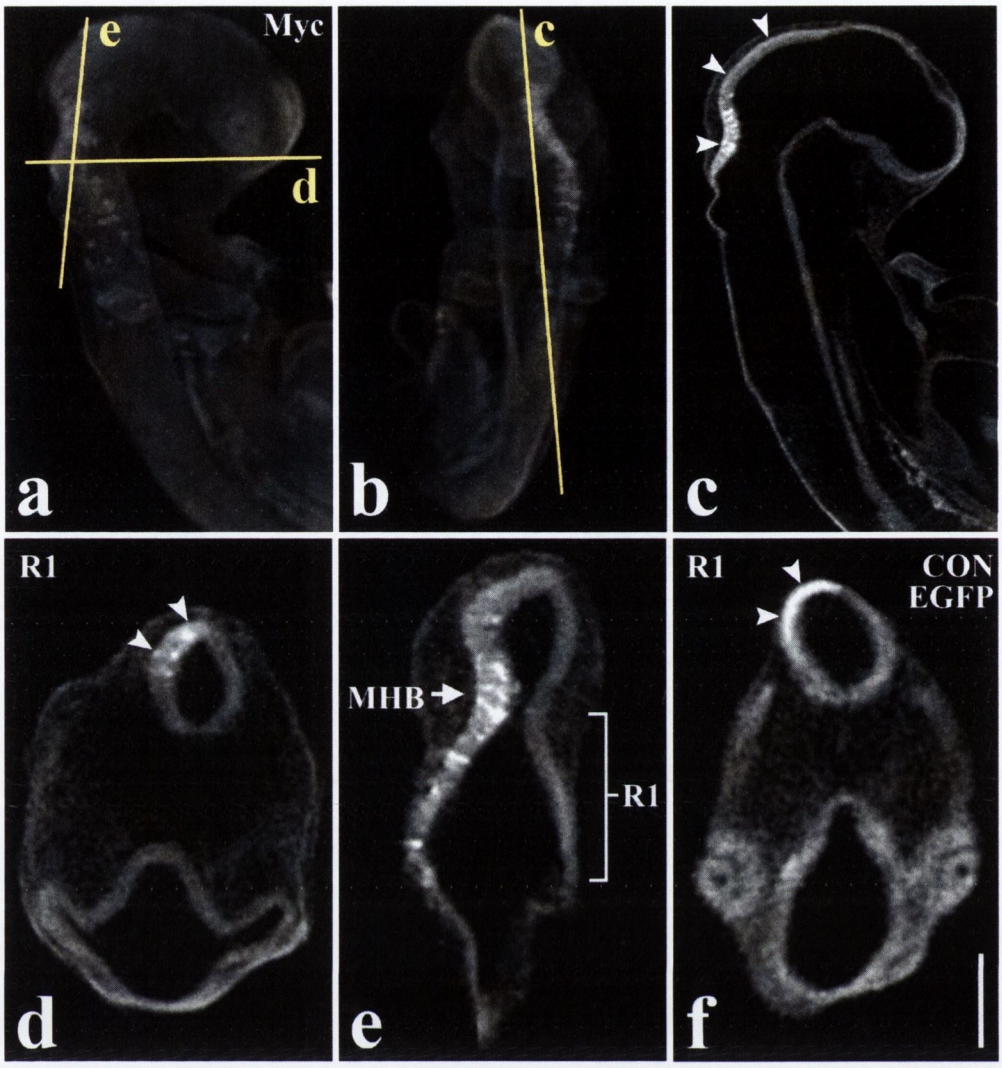

Figure 3.8 OPT analysis of a HH16 embryo electroporated with chPlxdc2-Myc 24 hours earlier. ChPlxdc2-Myc was detected by wholemount immunohistochemistry using a myc antibody (DSHB). a and b, still images from different external viewing angles of a volume rendered reconstruction (Supplemental data, movie 5). c-e, virtual sections through the specimen highlighting thickening of the neural tube on the experimental side (arrowheads). Planes of sectioning are indicated in a and b. f, virtual section through rhombomere 1 of a control specimen electroporated with empty pcDNA3.1myc-His(B) plasmid and pCA-β-EGFPm5-U6 under the same conditions. Thickening of the neural tube is not evident in the electroporated region (arrowheads). In control specimens, wholemount immunohistochemistry was carried out using an EGFP antibody (Invitrogen). MHB, midbrain-hindbrain boundary; R1, rhombomere 1. Scale bar: a-c, 0.4mm; d and e, 0.25mm; e, 0.2mm.

In a study of eight experimental specimens injected and electroporated with chPlxdc2-Myc and analysed by OPT, seven were found to exhibit significant neural tube thickening. No expression of chPlxdc2-Myc was evident in the remaining embryo and this was most likely owing to experimental failure. The spatial domains showing expression of EGFP, chPlxdc2-Myc and corresponding thickening in these embryos were mapped to a representation of the chick neural tube at this stage of development (Figure 3.9). In general, the region of detectable chPlxdc2-Myc expression was more restricted than that of EGFP with the exceptions of specimens C and G, where both markers were expressed to the same extent (Figure 3.9, a and b). Differences in the region of EGFP and chPlxdc2-Myc expression may be real, or may be owing to differences in the efficiency of marker detection. In the midbrain and anterior hindbrain, thickening generally occurred throughout the region of chPlxdc2-Myc expression. However, of five specimens exhibiting chPlxdc2-Myc expression in the region of rhombomere 2 and more posteriorly, only two exhibited clear thickening in this area (Figure 3.9, c and d). Neural tube thickening was observed most commonly in the region surrrounding the MHB and its occurance decreased gradually as one moved through the neural tube in an anterior or posterior direction (Figure 3.9 d).

3.4.4. Analysis of chPlxdc2-Myc induced thickening of the neural tube

In order to measure the extent of thickening and compare it to control specimens in a qualitative and systematic way, ten measurements were taken through either side of the neural tube (Cell A software, Figure 3.10 a). Electroporation affects the rate of normal development in experimental animals and, 24 hours post electroporation, embryos ranged from HH stage 15 to HH stage 20. Therefore, absolute measurements of neural tube width could not be compared across experimental specimens. In order to circumvent this problem and generate a standardised measurement of thickening effect, the average thickness of the experimental side of the neural tube was divided by the average thickness of the control side, resulting in a standardised 'thickening ratio'. Taking the mean of ten measurements throughout one side of the neural tube undoubtedly lessened the observed thickening effect, but was considered a more robust measurement than trying to compare an exact point on the experimental side with the equivalent point on the control side.

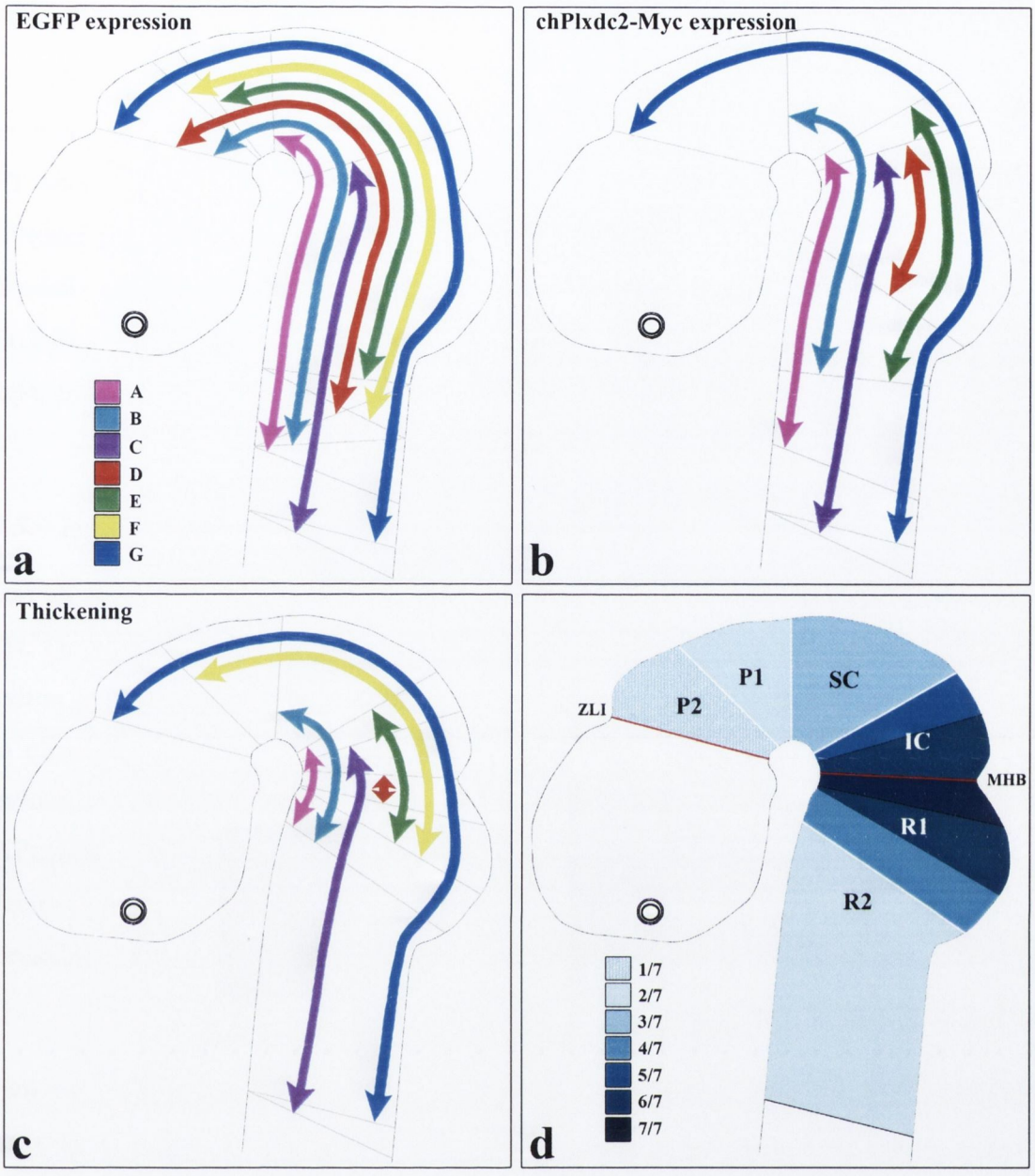

Figure 3.9 Summary of results from OPT analysis of chPlxdc2-Myc expression and neural tube thickening in seven embryos (A-G), 24 hours post electroporation. a, Extent of EGFP expressing cells; b, corresponding extent of chPlxdc2-Myc expression (chPlxdc2-Myc data was not obtained for specimen F); c, extent of neural tube thickening in each of seven specimens; d, occurence of thickening in individual brain regions. Grey lines in a-c represent the limits of expression/thickening. IC, inferior colliculus ; MHB, midbrain-hindbrain boundary; P1, prosomere 1; P2, prosomere 2; R1, rhombomere 1; R2, rhombomere 2; SC, superior colliculus; ZLI, Zona Limitans Intrathalamica.

a.

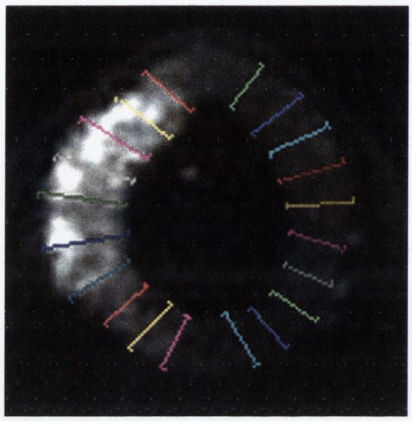

b.

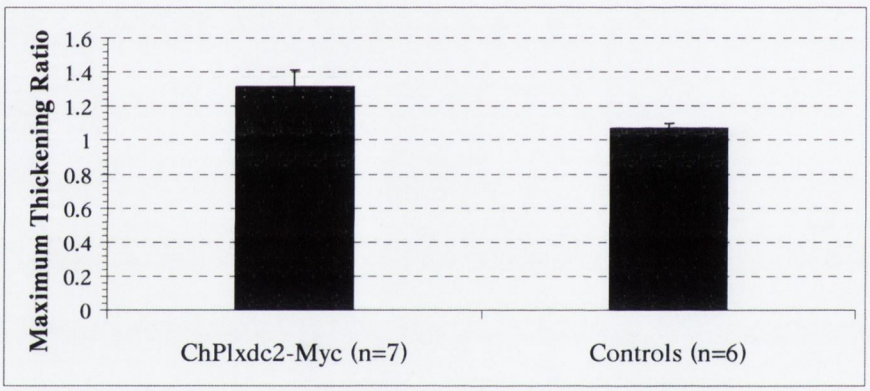

Figure 3.10 Analysis of chPlxdc2-Myc-induced thickening of the neural tube. a, representation of the ten measurements taken through each side of the neural tube in order to calculate the maximum thickening ratio; b, graph displaying the maximum thickening ratio of 7 experimental animals (as in figure 3.8) compared to 6 control animals, electroporated with the empty pcDNA3.1myc-His(B) plasmid. Maximum thickening ratios in embryos electroporated with chPlxdc2-Myc were significantly greater than those in control embryos (independent T-test, $p \leq 0.0001$).

For each specimen, the thickening ratio of several sections was calculated (appendix 5.10). The mean maximum thickening ratio observed in each of the seven embryos examined by OPT was plotted against the mean maximum thickening ratio in control embryos (those electroporated with an equivalent concentration of the empty pcDNA3.1myc-His(B) plasmid). Maximum thickening ratios in embryos electroporated with chPlxdc2-Myc were found to be significantly greater than those in control embryos (Figure 3.10, Independent T-test, $p \leq 0.0001$).

3.4.5. Injection and electroporation of a secreted form of Plxdc2

In order to define the mode of *Plxdc2* action in the neural tube more precisely, Plxdc2-AP(CT), which encodes the extracellular portion of the mouse *Plxdc2* protein, tagged with alkaline phosphatase(AP) at the C-terminal (CT) (plasmid previously used in section 2.19), was electroporated into HH stage 10-11 embryos under the same conditions as used in previous experiments (section 3.8.11). Cryostat sections of experimental and control (pAPtag-5) specimens were collected 24 hours following electroporation and colorimetric detection of the AP tag highlighted a similar phenotype to that observed in chPlxdc2-Myc expressing embryos.

When compared against plasmid controls expressing AP alone (pAPTag5), expression of the secreted form of *Plxdc2* resulted in thickening of the neural tube on the experimental side (Figure 3.11 a, b, d and e). Maximum thickening ratios for each of five experimental embryos were calculated as previously described (Section 3.4.4; Appendix 5.10) and were compared to controls (Figure 3.12). Control results across experiments were later shown to be consistent and pAPtag5 controls are pooled with those from chPlxdc2-Myc experiments in order to increase the power of analysis. Mean maximum thickening ratios in embryos electroporated with Plxdc2-AP were found to be significantly greater than those in control embryos (Independent T-test, $p \leq 0.0001$).

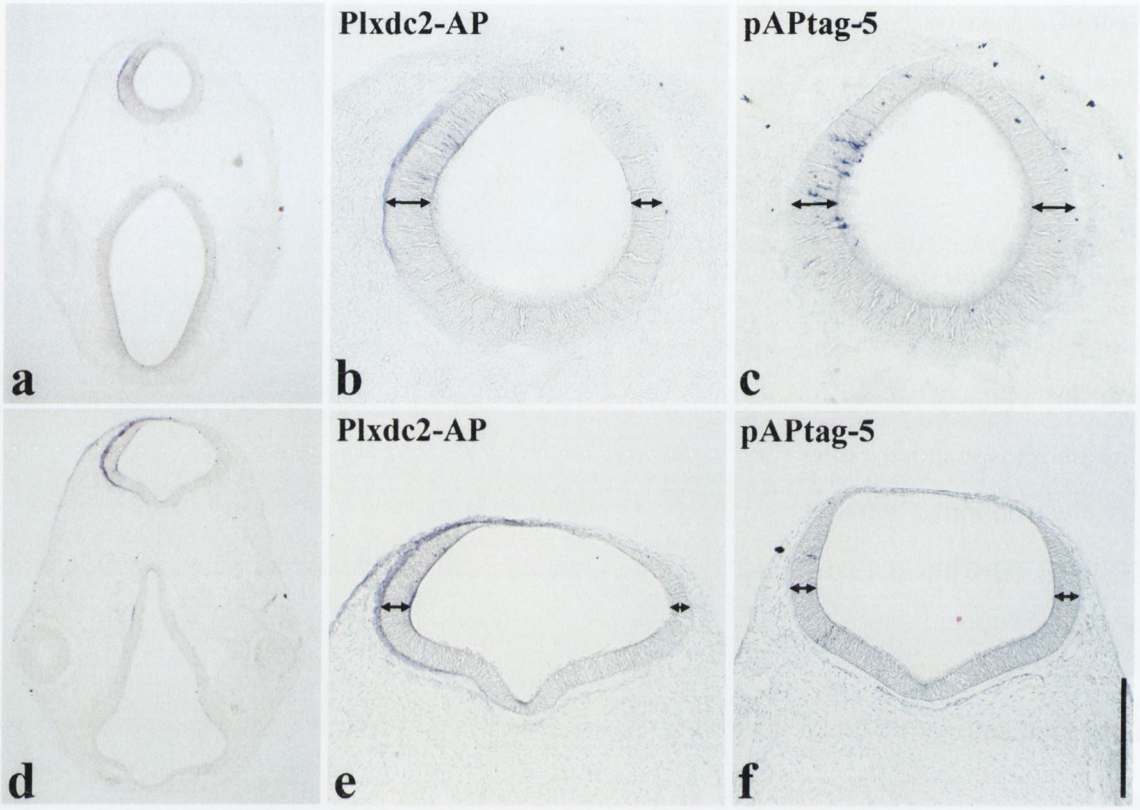

Figure 3.11 Expression of Plxdc2-AP(CT) in the chick brain causes thickening of the neural tube on the experimental side. a and d, 20μm cryostat sections through chick embryos electroporated with Plxdc2-AP, 24 hours previously. b and e, higher magnification images highlighting neural tube thickening on the experimental side. c and f, 30μm cryostat sections through control specimens electroporated with the empty pAPtag5 plasmid. Scale bar: a and d, 400μm; b and c, 100μm; e and f, 200μm.

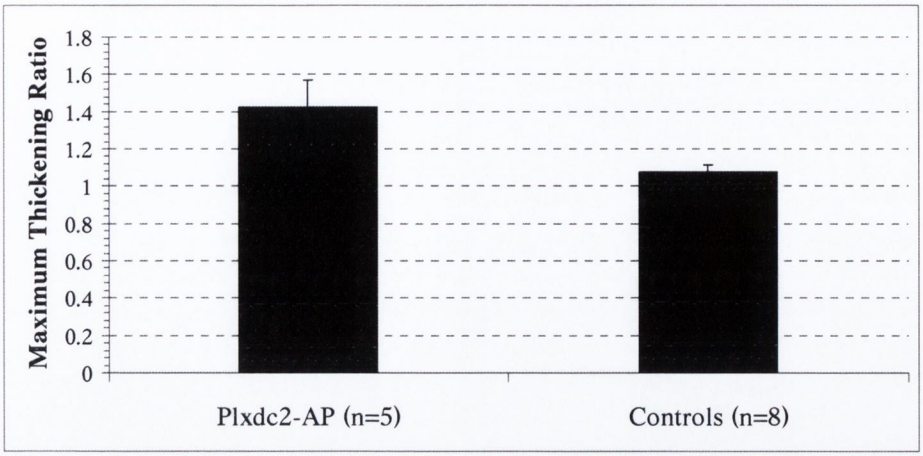

Figure 3.12 Analysis of Plxdc2-AP-induced thickening of the neural tube. The maximum thickening ratios of 5 experimental embryos were compared to those of combined controls from chPlxdc2-Myc and Plxdc2-AP experiments (n=8). Maximum thickening ratios in embryos electroporated with Plxdc2-AP were significantly greater than those in control embryos (independent T-test, $p \leq 0.0001$).

3.4.6. Effect of chPlxdc2-Myc expression on cell proliferation

To investigate whether increase in neural tube width was owing to an increase in cell proliferation at the site of electroporation with chPlxdc2-Myc, Bromodeoxyuridine (BrdU) was injected into the yolk vein 24 hours post electroporation and embryos dissected, half an hour later (section 3.8.13). Embryos were cryoprotected and 20μm sections collected by cryostat sectioning (section 3.8.12). Immunohistochemistry with an antibody against BrdU highlighted an increase in the number of BrdU-positive cells on the experimental side (Figure 3.13). EGFP expression from the co-electroporated reporter plasmid was used to highlight electroporated cells. In some instances EGFP expressing cells were positive for BrdU, although this was not exclusively the case. Many EGFP-positive cells did not incorporate BrdU (Figure 3.13).

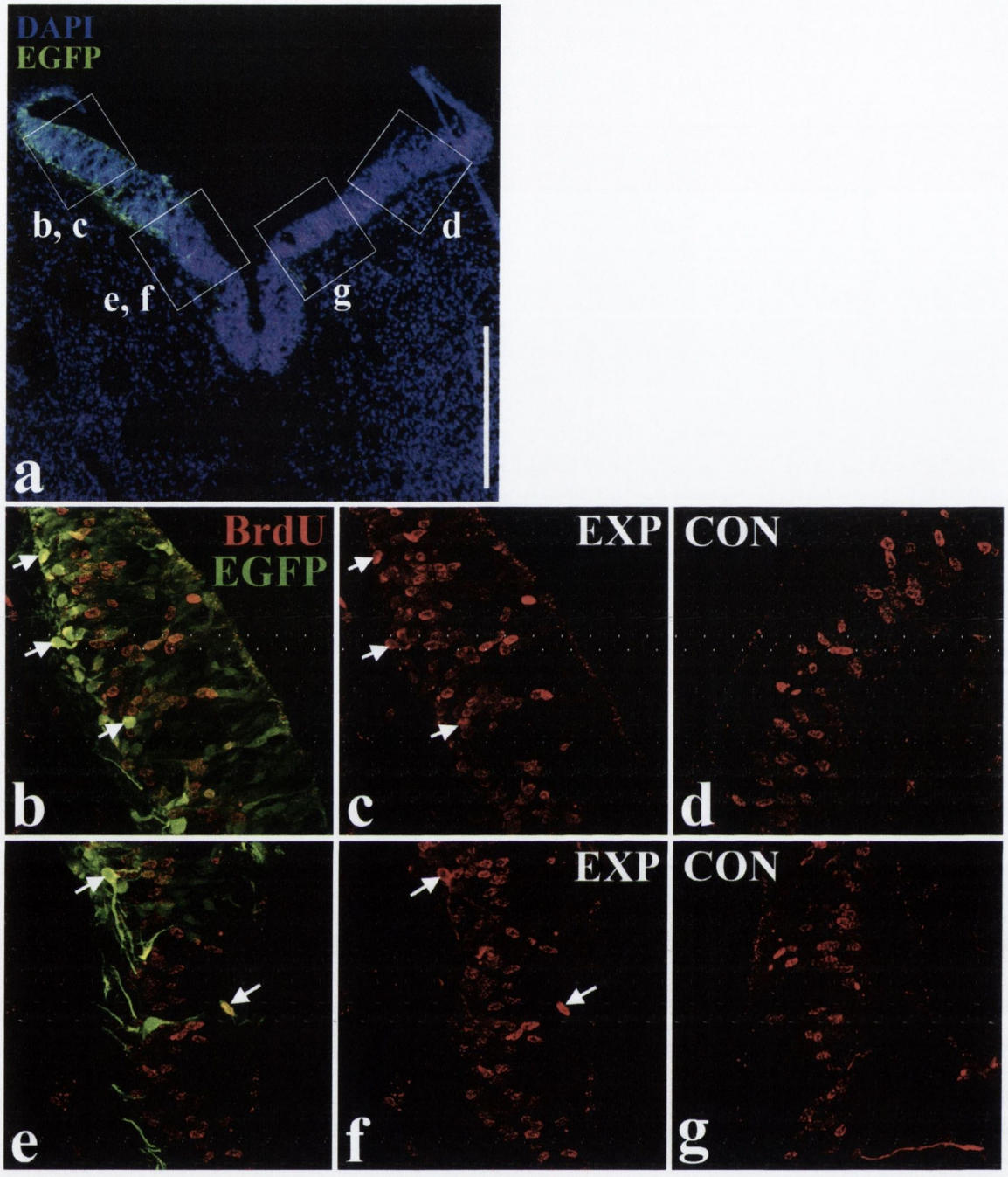

Figure 3.13 Examination of BrdU-positive cells in the neural tube of a HH stage 18 chick ectopically expressing chPlxdc2-myc. a, low magnification image of a transverse section of the neural tube in the region of rhombomere 1/2 highlighting the regions shown in b-g. b-g, compressed confocal z-stack images through the neural tube at higher magnification. b and e, overlay of EGFP expression and BrdU incorporation on the experimental side of the neural tube showing examples of cells co-expressing EGFP and BrdU (arrows). c, d, f and g, examination of BrdU incorporation on either side of the neural tube illustrated an increased number of BrdU positive cells on the electroporated side. Scale bar: a, 200μm; b-g, 50μm .

BrdU-positive cell counts were carried out on a total of sixteen sections from three experimental embryos (8 sections from one specimen and 4 each from two additional specimens). Each side of the neural tube was imaged using an Apotome (Zeiss) and z-stack images were compiled. Cell counts were carried out using compressed Z stack images and ImageJ software (Abramoff *et al.*, 2004). The total number of BrdU-positive cells on the chPlxdc2-Myc-expressing side of the neural tube was compared to the control side (Table3.1). Statistical analysis of BrdU-positive cell counts confirmed a significant increase in BrdU-positive cells on the chPlxdc2-Myc-expressing side of the neural tube (paired T-Test, $p \leq 0.0001$; average increase of 49.3 BrdU-positive cells on the experimental side). For each tissue section, the difference in BrdU-positive cell number was plotted against the thickening ratio. No correlation between thickening ratio and increase in number of BrdU-positive cells was observed (Figure 3.14).

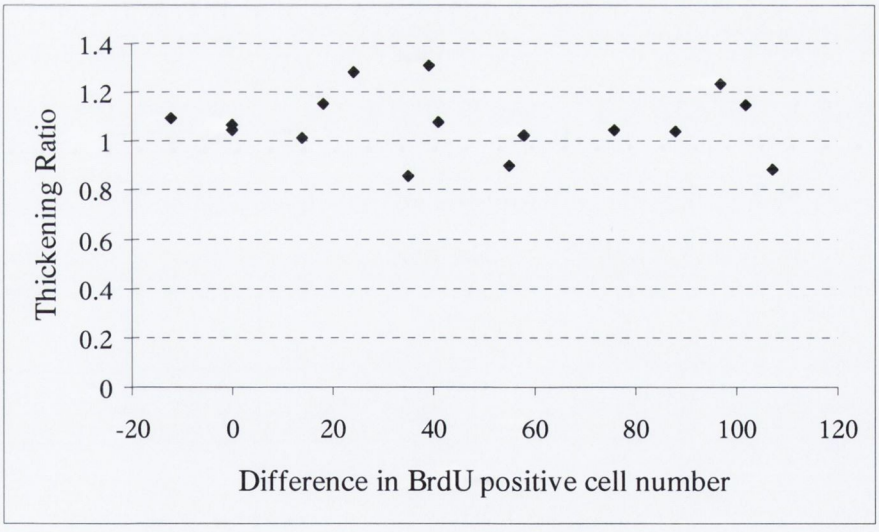

Figure 3.14 Difference in BrdU-positive cell number plotted against thickening ratio of each section. No correlation between thickening ratio and increased number of BrdU cells was found.

Embryo	Section	$BrdU^+$ cells on chPlxdc2-Myc side	$BrdU^+$ cells on control side	Difference	Thickening Ratio
1	A	330	283	47	1.28
	B	235	211	24	1.04
	C	182	182	0	1.07
	D	367	312	55	0.90
2	A	501	394	107	0.88
	B	367	309	58	1.02
	C	346	244	102	1.15
	D	344	305	39	1.30
	E	534	499	35	0.86
	F	585	497	88	1.04
	G	403	306	97	1.23
	H	339	263	76	1.04
3	A	395	354	41	1.08
	B	354	340	14	1.01
	C	392	374	18	1.15
	D	178	190	-12	1.09

Table 3.1 BrdU-positive cell counts on either side of the neural tube of three experimental embryos expressing chPlxdc2-Myc, and the corresponding thickening ratio for each section.

3.4.7. Effect of chPlxdc2-Myc expression on neurogenesis

The effect of chPlxdc2-Myc expression on neurogenesis within the neural tube was investigated by examining the expression of *chicken achaete-scute homolog-like 1* (*Cash1*). Expression was assayed by *in situ* hybridisation using a DIG-labelled antisense riboprobe to *Cash1*. *Cash1* expression forces cells out of a proliferative state and toward differentiation, marking a transient stage of the cell as it differentiates into a neuron (Jasoni *et al.*, 1994).

In a study of seven embryos, chPlxdc2-Myc misexpression in the posterior diencephalon and mesencephalon of four specimens caused a visible increase in *Cash1* expression when compared to the control side (figure 3.15). In one instance, *Cash1* expression was detected in a region of the mesencephalon that normally shows no expression (Figure 3.15, d and e). In the remaining three embryos, and in control embryos (those electroporated with empty pcDNA3.1myc-His(B) plasmid and EGFP) no difference in *Cash1* expression was observed.

3.4.8. Effect of chPlxdc2-Myc misexpression in later development

To examine the effect chPlxdc2-Myc misexpression at HH stage 10-11 has on the brain at later stages of development, embryos were dissected out five and ten days following electroporation (E7 and E12 respectively). Experimental and control embryos were examined for viability one day after electroporation (E3) and of those remaining, only 10% survived to E12. Three experimental embryos were collected at E7 and two at E12.

External examination of experimental specimens (E7) and dissected brains (E12) illustrated no gross morphological effect five or ten days following electroporation (Figure 3.16 a-c). Both sides of the brain appeared to be of the appropriate size and no unusual features were noted at a gross level. Cresyl violet staining of 50μm cryostat sections through the E7 head highlighted no significant abnormalities in brain structure or in organisation of cell layers (data not shown).

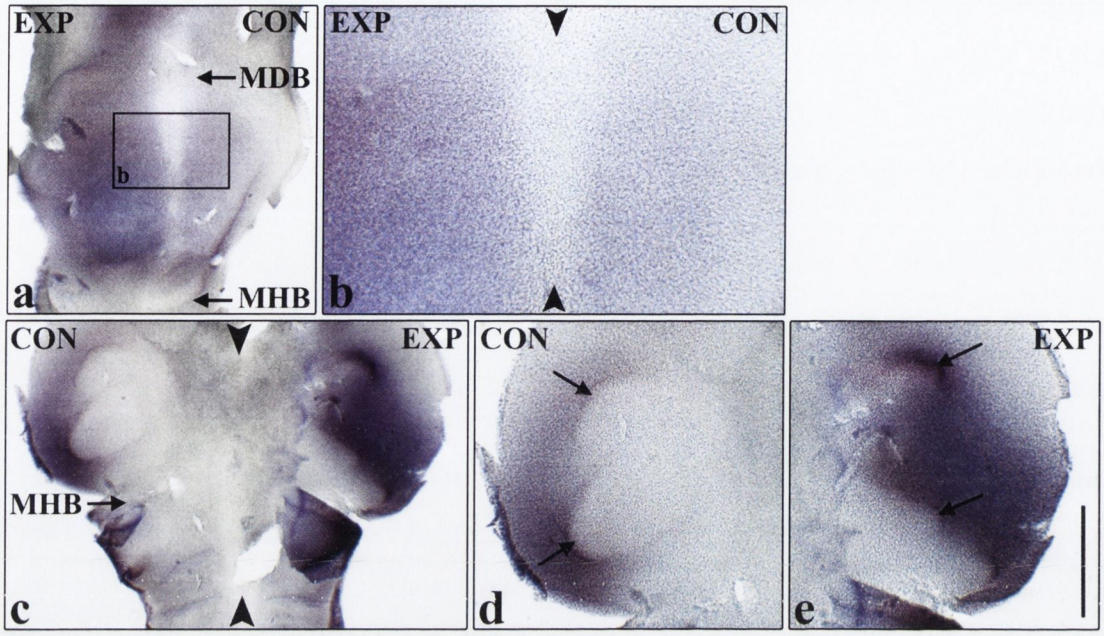

Figure 3.15 *Cash1* expression in the region of the neural tube, 24 hours following electroporation with chPlxdc2-Myc. Embryos were dissected 24 hours post electroporation and *in situ* hybridisation carried out using a DIG-labelled antisense riboprobe to *Cash1*. a, HH stage 20 embryo with the electroporated side to the left. b, higher magnification image showing increased *Cash1* expression on the experimental side of the neural tube. c, HH stage 19 embryo with the electroporated side to the right. d and e, higher magnification images showing increased *Cash1* expression on the experimental side of the neural tube. *Cash1* expression is activated in a territory that normally shows no expression. Note the intense expression at the margin of this territory. Arrows in d, mesencephalic regions lacking *Cash1* expression. Arrows in e, displacement of regions marked in d by expression of chPlxdc2-Myc. Arrowheads in b, dorsal midline; arrowheads in c, ventral midline. MDB, mesencephalon-diencephalon boundary; MHB, midbrain-hindbrain boundary. Scale bar: a and c, 300μm; b, 100μm; d and e, 200μm.

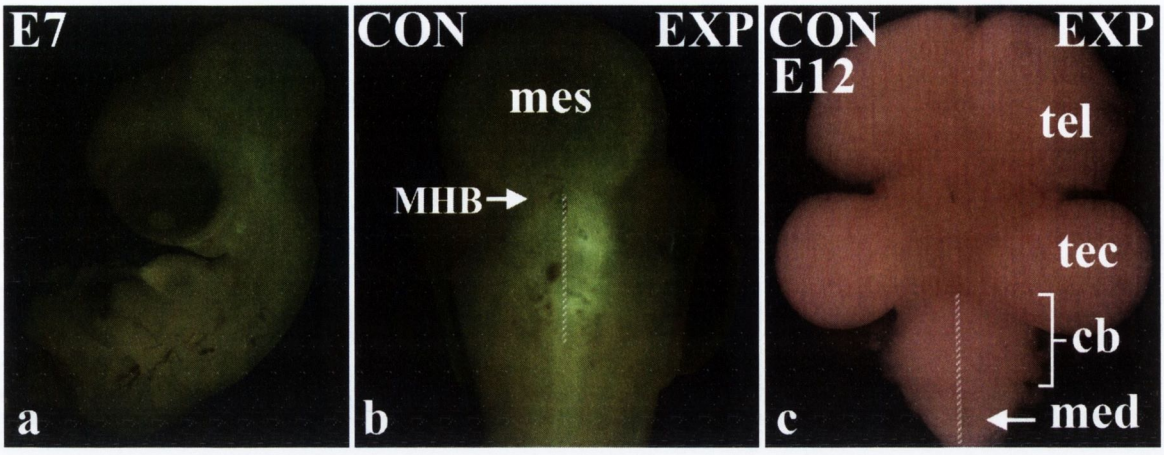

Figure 3.16 The effect of chPlxdc2-Myc misexpression at HH stage 10-11 on the brain at later stages of development. a and b, external wholemount images of an experimental embryo collected 5 days post electroporation (HH stage 29), illustrating no gross morphological defect in brain size or shape. EGFP expression is still clearly visible on the experimental side of the brain (b). c, dorsal view of a HH stage 38 embryo brain, dissected out 10 days post electroporation with chPlxdc2-Myc. cb, cerebellum; med, medulla oblongata; mes, mesencephalon; MHB, midbrain-hindbrain boundary; tec, optic tectum; tel, telencephalon. Scale bar: a, 1mm; b, 0.5mm; c, 2mm.

3.4.9. Expression profile of Plxdc2 in embryonic stem cells, neural stem cells and neurons.

In order to further elucidate the role of *Plxdc2* in neural differentiation, expression of the gene was examined in neural stem cells (NSCs) and neurons derived from the 'E14' embryonic stem cell (ESC) line (Hooper *et al.*, 1987) (Section 3.8.15; cell culture, differentiation and RNA preparation was carried out by Julie Skotte, University of Copenhagen). Transcript levels were assessed quantitatively by real time PCR (Section 3.8.15). Samples were normalised to mouse *ribosomal phosphoprotein* (*RPO*). A significant increase in relative *Plxdc2* expression was evident upon derivation of NSCs from ESCs (Independent T-test, $p \leq 0.0001$; Figure 3.17 A). This increase in *Plxdc2* expression in NSCs corresponded with a significant increase in expression of the NSC marker, *Nestin* and a significant decrease in expression the ESC marker, *Nanog*

(Independent T-test, $p \leq 0.0001$ in both cases; Figure 3.17, B and C). A significant decrease in *Plxdc2* expression was noted when post mitotic neurons were differentiated from NSCs, although *Plxdc2* expression in neurons remained at relatively high levels (Independent T-test, $p \leq 0.0295$; Figure 3.17 A). Neural differentiation was accompanied by a significant decrease in expression of the NSC marker, *Nestin* and a significant increase in expression of the postmitotic neuronal marker, *β3-tubulin* (*βIII*) (Independent T-test, $p \leq 0.0001$ in both cases; Figure 3.17, B and D).

Several protocols exist for the differentiation of NSCs and neurons from ESCs. In this study, relative *Plxdc2* expression was examined using only two of these (Bibel *et al.* 2004; Conti *et al.*, 2005). It is possible that alternative *in vitro* differentiation protocols may result in different levels of relative *Plxdc2* expression. Examination of relative *Plxdc2* expression in differentiating cells in culture should therefore be viewed tentatively and alternative differentiation protocols should be investigated. Nonetheless, the significant increase in relative *Plxdc2* expression evident when NSCs were derived from ESCs in culture is particularly interesting considering the increase in Cash1 expression noted following *Plxdc2* misexpression in the chick neural tube.

3.5 Knockdown of *Plxdc2* at the midbrain-hindbrain boundary

3.5.1. Design of shRNA constructs against the chPlxdc2 gene

No commercial antibody against Plxdc2 was available. Immunohistochemical attempts to detect endogenous Plxdc2 using two antibodies raised against the protein failed (Both antibodies were gifts of T. Jessell, Colombia University, USA). For this reason, shRNA silencing of gene function was favoured over the use of morpholino antisense oligonucleotides. It was proposed that efficiency of shRNA knockdown could be assessed by *in situ* hybridisation using the antisense *chPlxdc2* probe (Section 3.3.1) (Katahira and Nakamura, 2003).

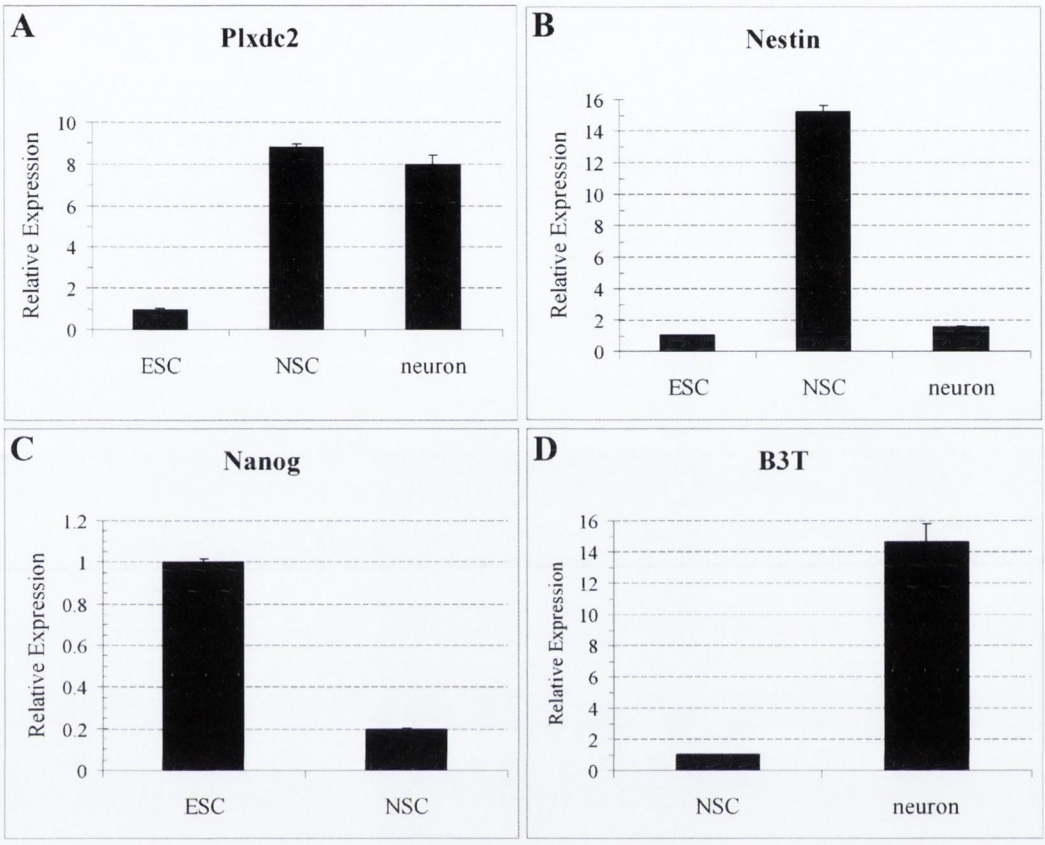

Figure 3.17 Relative expression of *Plxdc2* in embryonic stem cells (ESCs), and in neural stem cells (NSCs) and neurons derived from ESCs *in vitro*. Real time PCR highlighted a significant increase in *Plxdc2* expression when NSCs were derived from mouse ESCs (Independent T-test, $p \leq 0.0001$; A). This increase corresponded with a significant increase in *Nestin* expression and a significant decrease in *Nanog* expression (Independent T-test, $p \leq 0.0001$ in both cases; B and C). A significant decrease in *Plxdc2* expression was noted when neurons were differentiated from NSCs, although *Plxdc2* expression in neurons remained at relatively high levels (Independent T-test, $p \leq 0.0001$; A). Neural differentiation was accompanied by a significant decrease in *Nestin* expression (B) and a significant increase in *β3-tubulin (β3T)* expression (Independent T-test, $p \leq 0.0001$ in both cases; D).

Four target sites for shRNA design were chosen using the SFOLD algorithm (http://sfold.wadsworth.org/index.pl; Table 3.4). Annealed sense and antisense oligonucleotides were ligated into pCA-β-EGFPm5-U6 plasmid as outlined in section 3.8.7. Successful insertion of annealed oligonucleotides was confirmed by restriction digest with *Hind*III (Figure 3.18). Sequencing of the plasmid insert (MWG Biotech) confirmed insertion of correct oligonucleotide sequence in each of the four shRNA constructs.

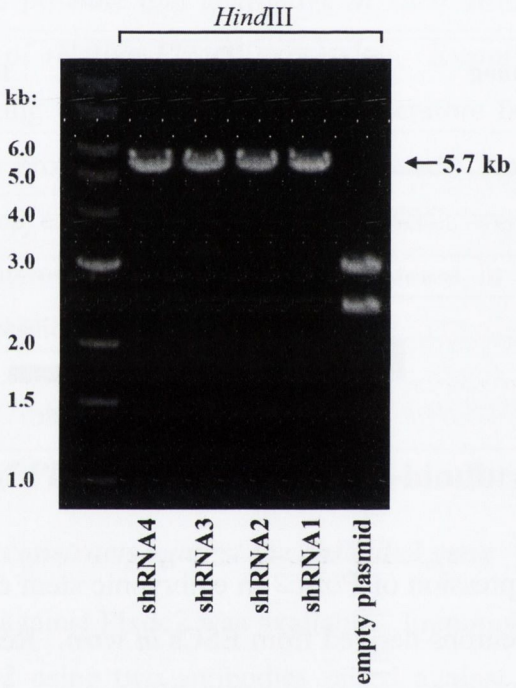

Figure 3.18 Confirmation of successful ligation of annealed oligonucleotides into the pCA-β-EGFPm5-U6 plasmid by digestion with *Hind*III. *Hind*III digestion linearised the plasmid, giving a band of approximately 5.7 kb when annealed oligonucleotides were present and cut twice in the religated empty vector. Size of bands compared to 1kb DNA ladder (New England Biolabs), with sizes in kb indicated on the left.

3.5.2. Examination of in vitro shRNA efficiency

Examination of shRNA efficiency was carried out *in vitro* by co-transfection of shRNAs and chPlxdc2-Myc into HEK293T cells (Section 3.8.8). Immunocytochemistry with antibodies against Myc and EGFP highlighted clear knockdown of chPlxdc2-Myc by shRNA1, 2 and 3, but not by shRNA 4 (data not shown). ShRNAs were then tested in pairs in order to determine the most efficient combination. In the future, if an effect was obvious *in vivo* when using one shRNA pair, other combinations could be used to rule out off-target effects. ShRNA1 and 3, used in combination, were found to cause the most dramatic knockdown of chPlxdc2-Myc (Figure 3.19; g-i). ShRNA pairs were subsequently tested against a FLAG-tagged full length mouse Plxdc2 construct (msPlxdc2-FLAG; gift of T.Jessell) and did not knockdown its expression (Figure 3.19, m-o; shown for shRNA1&3 only). This may indicate specificity of the designed shRNAs to the chick Plxdc2 gene.

Western blot analysis was carried out on total protein collected from lysed cells (as oulined in section 3.8.10). ShRNA1 and 3, used in combination, were found to cause the most dramatic knockdown of chPlxdc2-Myc when compared to controls transfected with chPlxdc2-Myc and the pCA-β-EGFPm5-U6 plasmid (Figure 3.20, b and f). Full length Plxdc2 protein ran as two bands, both of which were significantly larger than the predicted molecular weight of the protein (60kD). This is most likely due to N-glycosylation of the protein.

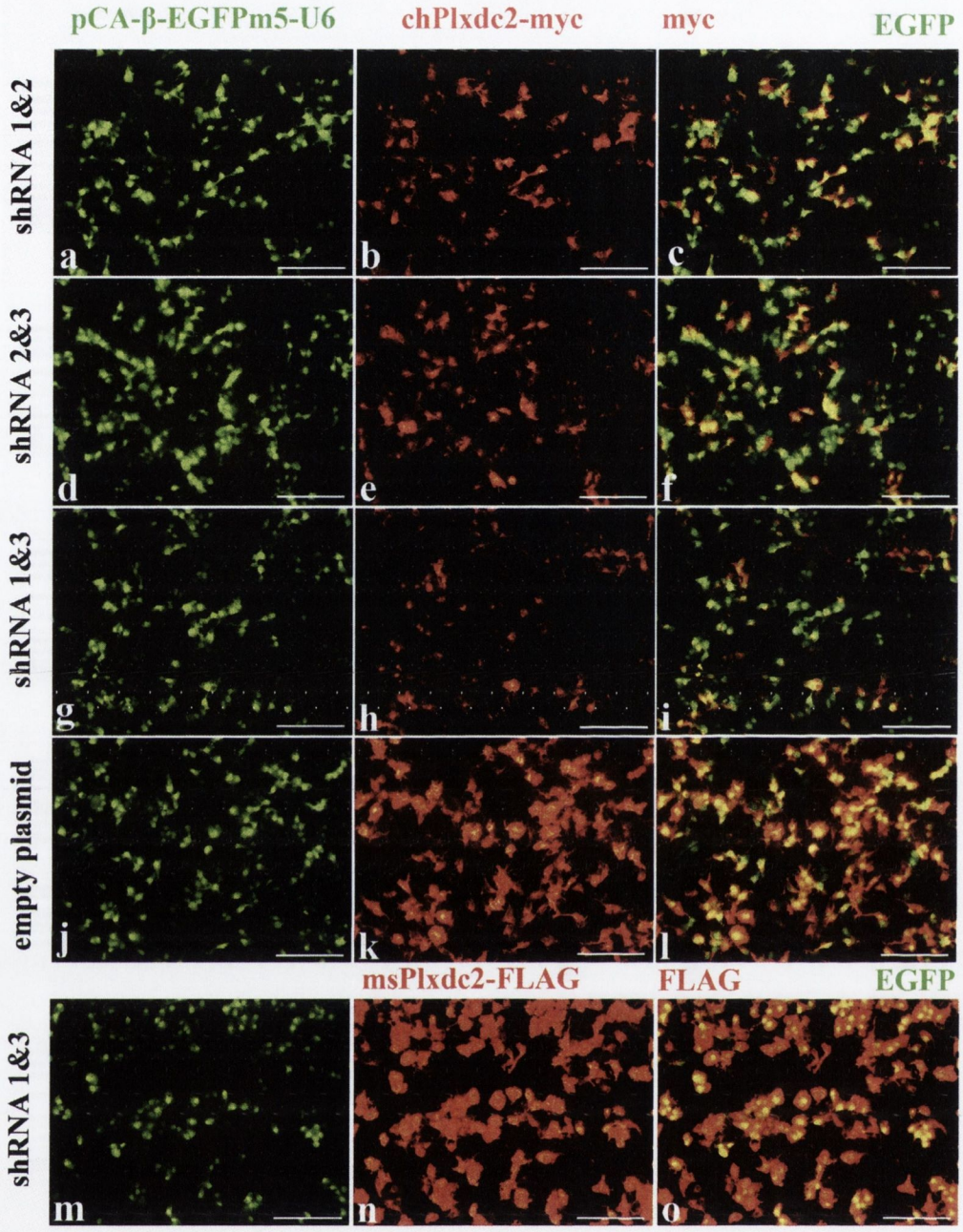

Figure 3.19 Immunocytochemistry of transfected HEK293T cells showing knockdown of chPlxdc2-Myc by shRNAs. Cell were co-transfected with *Plxdc2* constructs (chPlxdc2-Myc or msPlxdc2-FLAG) and the shRNA constructs indicated. Immunocytochemistry was carried out using antibodies against EGFP, Myc or FLAG. The most efficient shRNA combination was found to be ShRNA1&3 (g-i). The empty pCA-β-EGFPm5-U6 plasmid caused no knockdown of chPlxdc2-Myc (j-l). Co-transfection of shRNA1&3 caused no knockdown of msPlxdc2-FLAG. Scale bar, 100μm.

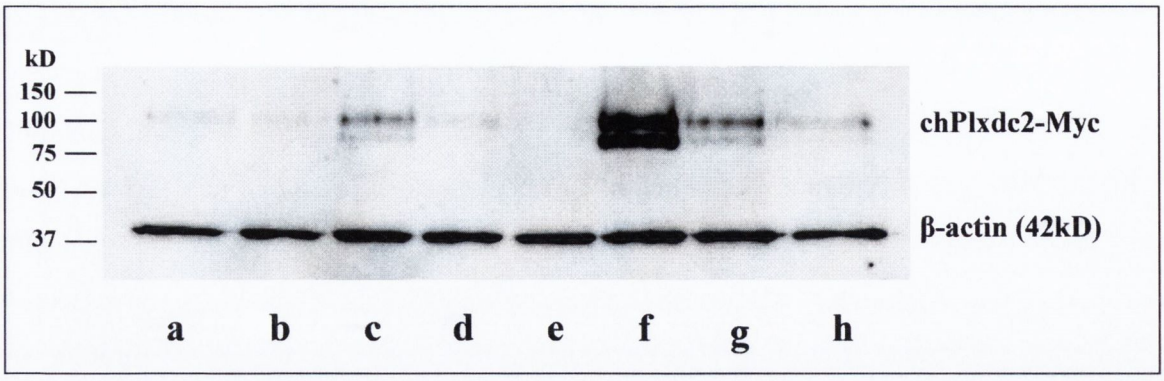

Figure 3.20 Western blot analysis of chPlxdc2-Myc knockdown by shRNA. ShRNA1&3, used in combination, caused the most dramatic knockdown of chPlxdc2-Myc (b). ShRNA pairs including shRNA4 caused the least knockdown of chPlxdc2-Myc (c, g and h). a, shRNA1&2; b, shRNA1&3; c, shRNA1&4; d, shRNA2&3; e, negative control of untransfected cells; f, positive control of cells transfected with chPlxdc2-Myc and the pCA-β-EGFPm5-U6 plasmid; g, shRNA2&4; h, shRNA 3&4.

There were significant weaknesses in the design of experiments examining shRNA efficiency *in vitro*. Firstly, no determination of the level of knockdown of *Plxdc2* transcript was carried out. For shRNA experiments it is typical to demonstrate evidence of knockdown at both the RNA and protein level. Secondly, the design of control experiments was weak. Controls for *in vitro* experiments consisted of the empty pCA-β-EGFPm5-U6 plasmid co-transfected with chPlxdc2-Myc. When two or more plasmids are co-transfected into cells or tissue, competition of some sort may occur between plasmids. In experimental transfections, two shRNA plasmids were co-transfected with chPlxdc2-Myc, whereas in control experiments only one plasmid was co-transfected with chPlxdc2-Myc. A more proper control experiment would have been the transfection of two non-targetting shRNAs with chPlxdc2-Myc. The use of such a control would have ruled out the possibility that the knockdown present in shRNA efficiency experiments was simply owing to less of the target plasmid (chPlxdc2-Myc) being successfully transfected due to competition with shRNA1 and shRNA3 plasmids. In the absense of the proper controls, competition of plasmids cannot be ruled out. In light of this, the demonstration of an absense of knockdown of another target (msPlxdc2-FLAG) by shRNA1&3 must also be viewed tentatively. As control experiments in which two non-targetting shRNAs were co-electroporated with the msPlxdc2-FLAG plasmid were not carried out, this result may also be owing to more of the target plasmid being successfully transfected *in vitro*.

3.5.3. In ovo electroporation of shRNA1&3

Knockdown of *Plxdc2* in the chick was investigated by electroporation of shRNA1&3 into the neural tube of HH stage 10-11 embryos. Direct EGFP flourescence is not compatible with OPT imaging, Wholemount immunohistochemistry using an antibody against EGFP was carried out 24 hours following electroporation and embryos were visualised using OPT. Previous experiments confirmed *Plxdc2* expression at the MHB of the chick (section 3.3.2) and maximum thickening ratios were calculated from virtual sections through this region (Appendix 5.10). No effect on neural tube thickness at the MHB, or in any other region, was observed following electroporation of shRNA1&3 (Figure 3.21 and Figure 3.23).

It was, however, of upmost importance to confirm successful knockdown of endogenous *Plxdc2* by shRNA1&3 *in vivo*. *In situ* hybridisation using an antisense chick *Plxdc2* riboprobe was carried out on vibratome sections of embryos electroporated 24 hours previously with shRNA1&3 (Figure 3.22). Endogenous *Plxdc2* expression in many areas of the developing embryo was detected as expected by *in situ* hybridisation. An apparent increase in *Plxdc2* transcript was evident in regions expressing shRNAs designed against the gene (Figure 3.22 a,b,c-e). Analysis of probe and pCA-β-EGFPm5-U6 sequence yielded no reason for specific binding of the probe to the shRNA constructs. In control embryos, pCA-β-EGFPm5-U6 was electroporated under the same conditions. No apparent increase in *Plxdc2* transcript was evident in these embryos (data not shown). Sense controls were routinely used and did not detect regions of shRNA or endogenous *Plxdc2* expression. *In situ* hybridisation could therefore not be used to confirm successful knockdown of endogenous *Plxdc2* expression by shRNA1&3.

Knockdown of ectopically expressed chPlxdc2-Myc protein was investigated by the co-electroporation of the full length plasmid (chPlxdc2-Myc) and shRNA1&3. Co-electroporation of shRNA1&3 resulted in the apparent rescue of the neural tube thickening phenotype observed when chPlxdc2-Myc was electroporated alone (Figure 3.23). However, controls for this experiment were not sufficient and the result should be viewed tentatively. As was mentioned previously, the co-electroporation of two or more plasmids into cells or tissue may result in competition of some sort between plasmids. It is possible that the apparent rescue of the neural tube thickening phenotype is owing to the successful electroporation of more of the chPlxdc2-Myc plasmid than shRNA1 or 3. Controls in

which two non-targetting shRNA plasmids were co-electroporated with chPlxdc2-Myc should have been included in order to rule out this possibility. In their absence, successful knockdown of ectopically expressed chPlxdc2-Myc by shRNA1&3 cannot be confirmed.

3.6 Summary statistics

A complete table of thickening ratios collected across *in ovo* electroporation experiments is included in Appendix 5.10. The mean maximum thickening ratios of experimental animals were plotted in a single graph and compared to those of controls (Figure 3.23). Controls across experimental parameters were found to provide consistent thickening ratios and were pooled. Mean thickening ratios in control specimens were slightly greater than one. Strong fluorescent signal can create difficulty in determining the outline of particular structures within the embryo, in this case the neural tube. This could account for slightly larger mean thickening measurements on the electroporated side of the neural tube, and therefore maximum thickening ratios slightly greater than one in control specimens. Nonetheless, maximum neural tube thickening ratios of specimens electroporated with plasmids encoding full-length Plxdc2 (chPlxdc2-Myc) or the secreted form of the murine protein (Plxdc2-AP) were significantly greater than those of pooled controls (Independent T-test, $p \leq 0.0001$ in both cases). Thickening ratios calculated at the MHB of six embryos electroporated with shRNA1&3 did not differ significantly from control cases (Independent T-Test). Co-electroporation of the full-length *Plxdc2* plasmid (chPlxdc2-Myc) and shRNA1&3 resulted in apparent rescue of the neural tube thickening phenotype observed when chPlxdc2-Myc was electroporated alone. However, proper controls were not used in this experiment and this result must therefore be viewed tentatively. Maximum thickening ratios in chPlxdc2-Myc and shRNA1&3 co-electroporated specimens did not differ significantly from control cases (Independent T-Test).

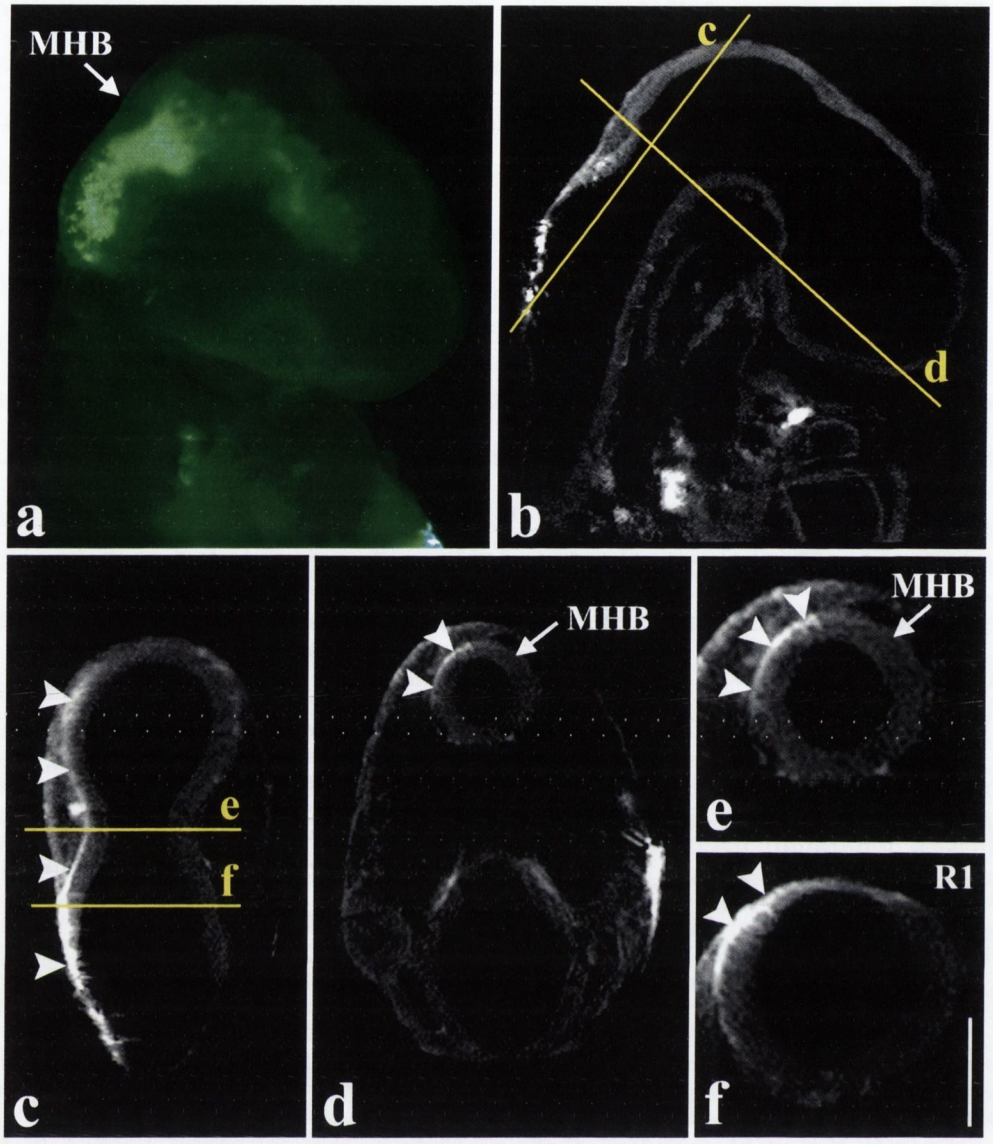

Figure 3.21 EGFP expression in the neural tube of a HH stage 18 embryo, 24 hours following electroporation with shRNA1&3. a, wholemount image of embryo illustrating EGFP expression in the neural tube. b-f, virtual sections through the embryo showing regions of shRNA1&3 expression (arrowheads in c-f). e and f, higher magnification images through the neural tube at the levels indicated in c, showing no effect on neural tube thickness at the Midbrain-hindbrain boundary (MHB) and through rhombomere 1 (R1). Scale bar: a-d, 500μm; e and f, 250μm.

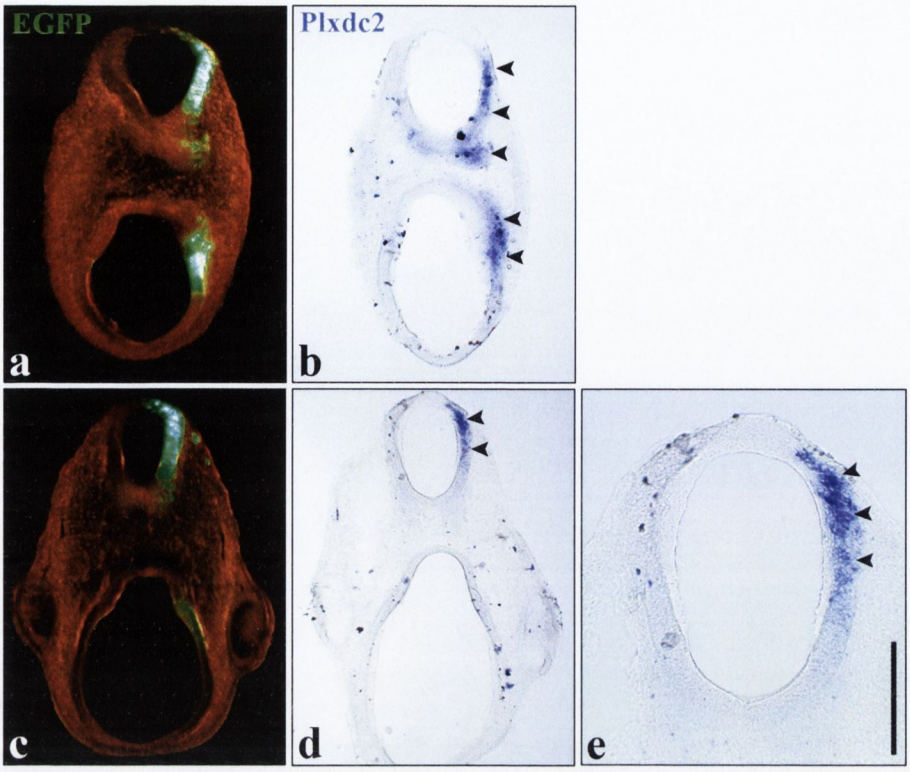

Figure 3.22 Apparent increase in *Plxdc2* transcript following expression of shRNAs against the gene. a-e, 30μm sections through the head of a HH stage 18 embryo, 24 hours following electroporation with shRNA1&3. a and c, Regions of shRNA expression as marked by the reporter gene, EGFP. b and d, *Plxdc2* transcript, as detected by *in situ* hybridisation, is increased in shRNA1&3 expressing regions (arrowheads). e, higher magnification image of d. Scale bar: a,b,d,e, 300μm; c, 60μm; f, 100μm.

The robust nature of these findings was illustrated by statistical analysis of the complete set of thickening ratios from *in ovo* electroporation experiments (in previous experiments only maximum thickening ratios were used). The complete data set was plotted in a single graph and previous statistical findings were reproduced faithfully (Figure 3.24). Mean thickening ratios of specimens electroporated with plasmids encoding full-length Plxdc2 (chPlxdc2-Myc) or the secreted form of the murine protein (Plxdc2-AP) were significantly greater than those of controls (Independent T-test, $p \leq 0.0001$ in both cases). Thickening ratios calculated at the MHB of embryos electroporated with shRNA1&3 did not differ significantly from control cases (Independent T-Test). Thickening ratios in chPlxdc2-Myc and shRNA1&3 co-electroporated specimens did not differ significantly from control cases (Independent T-Test).

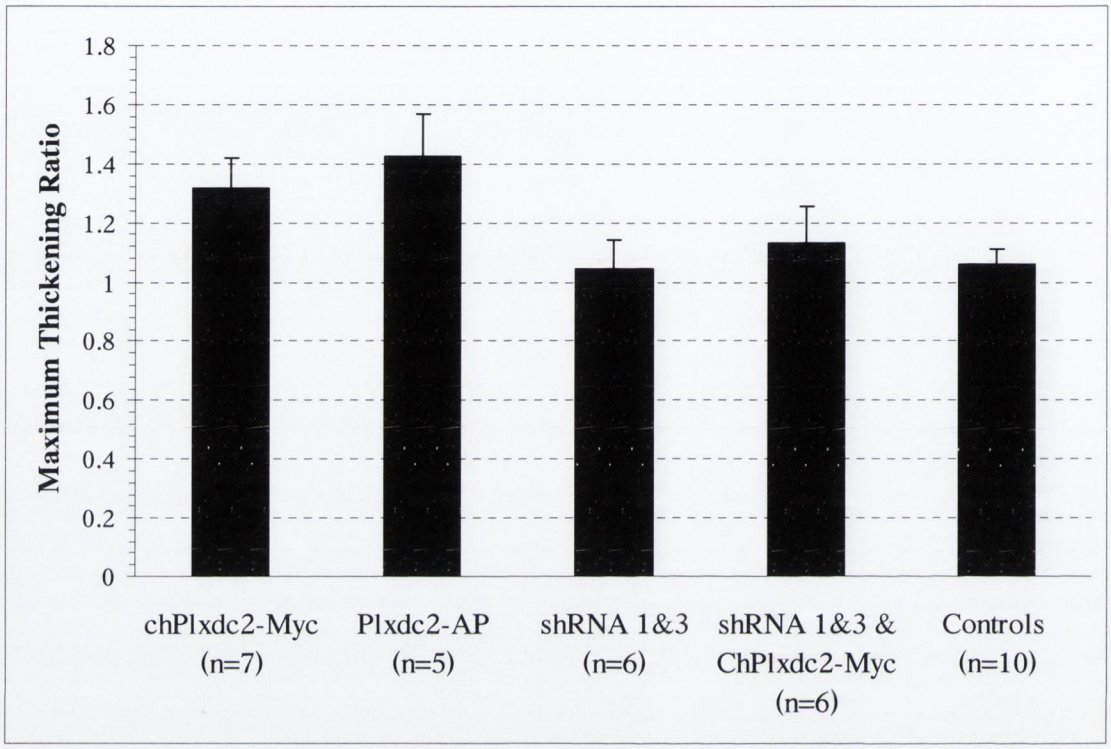

Figure 3.23 Maximum thickening ratios of individuals across *in ovo* electroporation experiments. Maximum thickening ratios of specimens electroporated with chPlxdc2-Myc or Plxdc2-AP were significantly greater than those of control cases ($p \leq 0.0001$ in both cases). No significant effect on thickening ratio was observed following electroporation of shRNA1&3 at the MHB. Maximum thickening ratios in chPlxdc2-Myc and shRNA1&3 co-electroporated specimens did not differ significantly from control cases ($p > 0.05$).

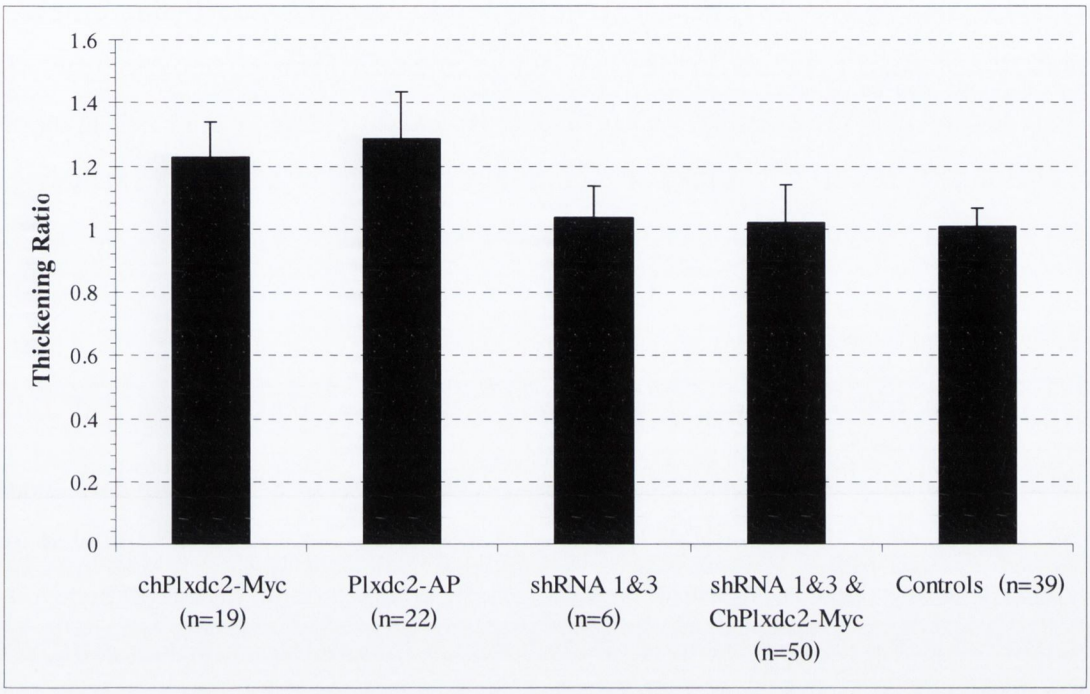

Figure 3.24 Complete set of thickening ratios from multiple sections of individuals across *in ovo* electroporation experiments. Thickening ratios of specimens electroporated with chPlxdc2-Myc or Plxdc2-AP were significantly greater than those of control cases ($p \leq 0.0001$ in both cases). No significant effect on thickening ratio was observed following electroporation of shRNA1&3 at the MHB. Thickening ratios in chPlxdc2-Myc and shRNA1&3 co-electroporated specimens did not differ significantly from control cases ($p > 0.05$).

3.7 Discussion

3.7.1. Plxdc2 expression in the chick and mouse

Plxdc2 expression was examined in the HH stage 16-21 chick by *in situ* hybridisation in order to compare expression with that previously documented in the mouse (Chapter 2). Expression was conserved in many areas of the developing embryo including the eye, otic vesicle, floor of the midbrain, MHB, and motor column (Figure 3.2). Analysis of the chick hindbrain at later stages illustrated *Plxdc2* expression in the Purkinje cell layer of the cerebellum and in several distinct nuclei within the medulla oblongata, including the trigeminal motor nucleus (N5n) and the principle sensory trigeminal nucleus (Pr5) (Figure 3.4). Expression in these regions, and at the neuroepithelium, corresponded to the pattern previously noted in the mouse.

Plxdc2 expression was also evident in the mesonephros of the chick from HH stage 16 through to HH stage 21. Although *Plxdc2* expression was previously documented in the urogenital tract of the E11.5 mouse (Section 2.3.3), an absence of *Plxdc2* expression has been documented in the epithelium of the adult mouse kidney (Carson-Walter *et al.*, 2001). It is possible that *Plxdc2* plays a developmental role in the establishment of the urinary system and its expression is downregulated at adulthood.

A number of differences in *Plxdc2* expression were noted in the chick when compared to the mouse. An intense line of *Plxdc2* expression was evident at the dorsal midline of the chick brain from HH stage 16 to 21. Expression in this region was dynamic over the stages examined. At HH stage 16, expression at the dorsal midline spanned the mesencephalon and diencephalon, but by HH stage 17 it extended into the telencephalon. At HH stage 20, dorsal midline *Plxdc2* expression once again occurred only in the mesencephalon and diencephalon. By HH stage 21, *Plxdc2* expression occurred in the dorsal midline of the diencephalon, but not the mesencephalon, and was widespread in the telencephalon (including the region of the cortical hem). *Plxdc2* expression in the dorsal midline of the brain was not documented in the mouse at E9 or E11.5 in areas other than the cortical hem (Section 2.3.3).

In the mouse, similarities were previously drawn between the expression of *Plxdc2* and *Wnt1* at the MHB, and between *Plxdc2* and *Wnt3a* at the cortical hem (Figure 2.6). The dorsal midline of the neural tube is an important dorsalising centre, expressing both Wnt1 and Wnt3a which are essential for regulating cell fate and proliferation in the dorsal neural tube (Chesnutt *et al.*, 2004, Ikeya *et al.*, 1997, Megason and McMahon, 2002, Muroyama *et al.*, 2004). *Wnt1* and *Wnt3a* expression has been documented in the dorsal midline of the chick (Canning *et al.*, 2007, Hollyday *et al.*, 1995, Matsunaga *et al.*, 2002). The discovery of *Plxdc2* expression in the dorsal midline of the chick brain highlights additional similarities between the expression pattern of *Plxdc2* and that of *Wnt1* and *Wnt3a* in the chick.

Plxdc2 expression was documented in the cortical hem of the chick, although expression in this region was more complex in nature than that documented in the mouse (Chapter 2). Although the three layer structure of the chick cortex is markedly different to that of the six-layered mammalian cortex (Cheung *et al.*, 2007), the major telencephalic signaling centers identified in mouse and chick are strikingly alike, suggesting a consistency between the two species in the basic patterning of the telencephalon (Shimogori *et al.*, 2004). During development, the chick telencephalon, like that of the mouse, is exposed to an anterior source of FGF8 (from the anterior neural ridge which later becomes the commissural plate) and a dorsomedial source of BMP (from the hem) which regulate morphological and gene expression patterning (Crossley *et al.*, 1996, Golden *et al.*, 1999, Ohkubo *et al.*, 2002, Shimogori *et al.*, 2004). The avian cortical hem has also been shown to express specific markers of the region including *Wnt8b* and *Wnt7b* (Garda *et al.*, 2002). Transient *Plxdc2* expression was first evident in the dorsal midline of the telecephalon at HH stage 17 (Figure 3.2). At HH stage 18, *Plxdc2* expression was no longer evident at the cortical hem and by HH stage 20, the region was distinctly lacking in expression of the gene (Figure 3.2). By HH stage 21, widespread expression of *Plxdc2* in the hem and the surrounding mesoderm was evident. *Plxdc2* expression was also noted in a band of mesoderm at the mesencephalon-diencephalon boundary, a region of expression not documented in the mouse (Figure 3.3).

The expression pattern of *Plxdc2* in the developing chick brain was, on the whole, very similar to that documented in the mouse. Although expression in the cortical hem of the chick was more dynamic than that observed in the mouse, *Plxdc2* expression was evident

within this important patterning centre of the telencephalon. The documentation of *Plxdc2* expression in the dorsal midline of the chick brain highlighted additional similarities between *Plxdc2*, *Wnt1* and *Wnt3a* expression. As was mentioned previously, the existance of an antibody to Plxdc2 would have added greatly to Plxdc2 expression analyses, providing expression data at the protein level in addition to the RNA level. Nonetheless, similarities in the expression pattern of *Plxdc2* in the mouse and chick at the level of Plxdc2 transcript were robust. In addition, the Plxdc2 protein was also found to be highly conserved between species (Appendix 5.5) and functional analyses of *Plxdc2* were therefore proceeded with in the chick.

3.7.2. Thickening of the neural tube following Plxdc2 misexpression

Misexpression of *Plxdc2* in the neural tube of the HH stage 10-11 chick resulted in significant thickening of the experimental side, 24 hours following electroporation (Figures 3.7 and 3.8). Quantitative analysis of the phenotype was achieved in a non-biased manner by the comparison of mean neural tube thickness on either side of the midline, and the calculation of a maximum thickening ratio for each specimen (Section 3.4.4). Statistical analysis of thickening ratios highlighted a significant increase in neural tube thickness following misexpression of *Plxdc2* (independent T-test, $p \leq 0.0001$).

The neural tube thickening phenotype was also evident when a secreted form of murine Plxdc2 was expressed in the chick (Figure 3.11). This result indicates that Plxdc2 functions in a cell non-autonomous manner, most likely acting as a ligand. Reproduction of the neural tube thickening phenotype, using a second Plxdc2-encoding plasmid, validates initial results using chPlxdc2-Myc and confirms that the initial phenotype was not caused by expression of the molecular tag, Myc. Reproduction of the neural tube thickening phenotype, using msPlxdc2 also suggests that the biochemical function of the protein is conserved between species: in the chick, msPlxdc2 can bind a particular protein and activate the same pathways as the endogenous chick Plxdc2 protein.

Plxdc2-induced neural tube thickening was not confined to any one region of the developing brain, but was rather, correlated with expression of the chPlxdc2-Myc plasmid (Figure 3.9). Thickening of the neural tube was evident in regions spanning from the *Zona*

Limitans Intrathalamica (ZLI) to rhombomere 2 and more posteriorly into the spinal cord. Neural tube thickening was observed most commonly in the region surrrounding the MHB and its occurence decreased gradually as one moved through the neural tube in an anterior or posterior direction (Figure 3.9). This could be owing to the placement of electrodes during *in ovo* electroporation and therefore, to efficiency of electroporation of the chPlxdc2-Myc plasmid into cells of the neural tube. However, of five specimens exhibiting chPlxdc2-Myc expression in the region of rhombomere 2 and more posteriorly, only two exhibited clear thickening in this area (Figure 3.9, c and d). This could be indicative of a regional specification of the phenotype owing to differential expression of interacting proteins, but may also be owing to electroporation efficiency. Further experimentation altering the targetted site of electroporation is needed in order to define occurence of the thickening phenotype in this region of the neural tube.

3.7.3. Increased proliferation and differentiation following misexpression of Plxdc2

Examination of BrdU-positive cells in the neural tubes of chicks, 24 hours following electroporation, highlighted an increase in the number of proliferating cells on the experimental side (Figure 3.11). Statistical analysis of cell counts on either side of the neural tube confirmed an increase in BrdU-positive cells following ectopic expression of *Plxdc2* (Paired T-Test, $p \leq 0.0001$). The increase in BrdU-positive cells was not, however, directly correlated with the degree of thickening of the neural tube. Expression of chPlxdc2-Myc was driven by the CMV promoter in the pcDNA 3.1 myc-His (B) Plasmid. The use of such a promoter routinely drives expression of ectopic protein for 72 hours *in ovo* (Nakamura *et al.*, 2004). Cell proliferation in the neural tube was not examined at other time points, but embryos dissected at much later stages of development did not illustrate the gross morphological effects one might expect if cells were maintained in a proliferative state for a prolonged period of development (Figure 3.17). The effect of *Plxdc2* expression on proliferation is therefore most likely a transient one.

Misexpression of *Wnt1* in the neural tube of the HH stage 10 chick causes an increase in cell proliferation 48 hours after electroporation , but by 72 hours, a proliferation effect is no longer evident (Matsunaga *et al.*, 2002). Nonetheless, this transient increase in cell proliferation results in enlarged tectum and additional cerebellar folds by E14.5. In this case, increased proliferation is accompanied by repression of the proneural gene, *Cash1*. *Cash1* expression in *Plxdc2* misexpressing embryos was examined by *in situ* hybridisation,

24 hours after electroporation. In a study of seven embryos, chPlxdc2-Myc misexpression in the mesencephalon and posterior diencephalon of four specimens caused an increase in *Cash1* expression (figure 3.15). In the remaining three embryos, no effect on Cash1 expression was discerned.

The method of Plxdc2-induced increase in *Cash1* expression can only be speculated upon and requires investigation, in full, in subsequent experiments. The *Plxdc2*-induced increase in *Cash1* expression could occur in a number of ways. Firstly, *Plxdc2* could block activation of *Notch* signalling, resulting in prolonged transcriptional repression of *Hes1* and *Hes5* by the DNA binding protein RBP-J. This seems quite plausible, as the onset of proneural gene expression in subsets of progenitor cells coincides with a decrease in *Hes1* expression (Bai *et al.*, 2008, Kageyama *et al.*, 2005). Notch, and its ligands are transmembrane proteins expressed on neighbouring cells. Could expression of Plxdc2 interfere with Notch signalling, preventing activation of the pathway, by Delta and Jagged and thus inhibit Hes1 expression? As was introduced previously, disruption of Hes1 expression in Hes1 mutant mice leads to increased expression of proneural genes including Mash1 (Hatakeyama *et al.*, 2004, Ishibashi *et al.*, 1995). At the transcriptional level, *Hes1* repression of *Cash1* expression may also be interrupted by Plxdc2. Plxdc2 expression may induce the activation of a not yet specified pathway, a member of which could inhibit the binding of Hes1 to the promoter, allowing *Cash1* to be expressed in the cell. Alternatively, a member of this pathway may interrupt Hes1 repression at the level of protein-protein interaction, by preventing the formation of a non-functioning heterodimer with E47, thus allowing formation of the Cash1-E47 functional heterodimer.

The discrete co-expression of *Plxdc2* and members of the Wnt family in regions of the developing brain cannot be ignored. As was discussed previously, Wnt proteins have been implicated in both the control of cell proliferation and neural differentiation, and their effect on both of these processes seems to vary greatly, depending on the stage of embryonic development examined. Considering their co-expression in the cortical hem, floor plate, dorsal midline and midbrain-hindbrain boundary, it seems plausible that Plxdc2 may interact with a common Wnt pathway, canonical or otherwise. In a manner similar to the Wnt7a-induced activation of *Ngn1* in cortical neural progenitor cells (Hirabayashi *et al.*, 2004), could Plxdc2 misexpression result in activation of the canonical pathway, leading to direct regulation of the *Cash1* promoter by the β-catenin-TCF complex?

Plxdc2 misexpression caused a transient increase in proliferation in the neural tube at the same time as the increase in *Cash1* expression. In a similar fashion, members of the Wnt family do not always affect proliferation at the expense of differentiation and vice versa. Both *Wnt3a* and *Wnt5a* increase cell proliferation in tandem with neuronal differentiation *in vitro* (Yu *et al.*, 2006). Wnt3a expression results in increased neuronal differentiation through activation of the canonical pathway. However, the effect of *Wnt5a* on neuronal differentiation occurs through activation of the Wnt/Ca^{2+} pathway, which involves activation of *PLC* and *PKC* (Yu *et al.*, 2006). This pathway must also be considered a possible mediator of the Plxdc2 effect on *Cash1* expression.

3.7.4. Older chick brains lack gross morphological defects

Embryos dissected at much later stages of development do not illustrate the gross morphological effects one might expect following Plxdc2-induced neural tube thickening. The lack of morphological defects in the midbrains of older embryos suggests that increases in proliferation and *Cash1* expression do not have a dramatic effect on progenitor or neuronal cell number. This may be owing to management of increased progenitor or differentiated neural cell populations by regulatory apoptopic pathways later in development. Alternatively, a transient increase in proliferation may compensate for increased *Cash1* expression, and presumably neuronal differentiation, in Plxdc2 misexpressing embryos allowing for the normal differentation of later born cells. A lack of dramatic morphological effect in the older chick brain may also be owing to transient expression of the exogenous Plxdc2 protein. For long-term misexpression, RCAS provirus vector should be considered (Havens *et al.*, 2008, Mina *et al.*, 2007, Wu *et al.*, 2008). Misexpression is restricted to the descendents of the transfected cells and detailed cell lineages can be traced (Bell and Brickell, 1997, Krull, 2004, Nakamura *et al.*, 2004, Sugiyama and Nakamura, 2003). It is, however, important to note that slow onset of expression has been noted when retroviral vectors are used and a window of effectiveness of Plxdc2 misexpression may exist (Bron *et al.*, 2004, Harpavat and Cepko, 2006). Therefore, the use of retroviral vectors to drive Plxdc2 misexpression may not necessarily result in neural tube thickening.

3.7.5. Plxdc2 expression is upregulated in NSCs and neurons derived from ESCs in culture

Approximately a nine fold increase in relative *Plxdc2* expression was evident upon derivation of NSCs and neurons from ESCs in culture (Figure 3.17). The dramatic increase in *Plxdc2* expression is particularly relevant considering the increase in *Cash1* expression observed following *Plxdc2* misexpression in the chick. However, it is important to note that several alternative protocols for neural differentiation exist and may result in differing relative *Plxdc2* expression levels. As was discussed previously, progenitor cell populations become heterogeneous during neural tube development, including progenitors which do not express proneural genes and those which do (Bertrand *et al.*, 2002). Considering the experimental methods used (Conti *et al.*, 2005), it is not clear whether NSCs derived from ESCs in culture would express proneural genes such as *Mash1*. Progenitor cells initiate the expression of proneural genes in response to regional specific neurogenic signals (Guillemot, 2007, Lillien, 1998). In culture, an increase in *Plxdc2* expression could pre-empt expression of proneural genes, and progression to a neural state. On the other hand, an increase in *Plxdc2* expression could occur along side proneural gene expression. The expression of several murine proneural genes needs to be investigated in NSCs derived in this manner in order to fully characterise these neural progenitor cells in culture. This system may then provide an ideal model for perturbation of *Plxdc2* expression *in vitro*, and further analysis of Plxdc2-induced proliferation and differentiation.

3.7.6. Knockdown of endogenous Plxdc2

Successful knockdown of endogenous Plxdc2 expression was not confirmed by immunohistochemistry owing to the lack of a functioning antibody against the protein. Two antibodies against Plxdc2 failed to detect the endogenous protein *in vivo*. The production of an efficient antibody against Plxdc2 would greatly aid further investigation into knockdown of endogenous gene expression. Knockdown of chPlxdc2-Myc transcript *in vitro* was not examined and attempts to illustrate endogenous gene silencing by *in situ* hybridisation with a *Plxdc2* probe *in vivo* illustrated an apparent increase in transcript levels at the site of shRNA expression. ShRNA expression at early stages of embryonic development (prior to HH stage 7) has recently been shown to cause morphological phenotypes, misregulation of non targeted genes and activation of the p53 pathway (Mende *et al.*, 2008). Targetted knockdown of *Eya2 in vivo* led to an apparent increase in

transcript levels when examined by *in situ* hybridisation using a 3'UTR probe. This effect was not evident when a full length probe was used (Mende *et al.*, 2008). Non-specific binding of the probes to the vector sequences was ruled out and one possible explanation for the phenomenon is that introduction of shRNA vectors results in the production of short transcripts to which the shorter 3'UTR *Eya2* probe, but not the full length *Eya2* probe can bind (Mende *et al.*, 2008). The 1.1kb *Plxdc2* antisense probe used in *in situ* hybridisation experiments was made by reverse transcription of ChEST853h24 (Geneservice), which includes the latter half of the *Plxdc2* coding sequence and 320 bps of 3'UTR. It is possible that the production of a new full length *Plxdc2* probe may resolve problems in the detection of endogenous *Plxdc2* knockdown by *in situ* hybridisation. Morpholinos can now be routinely used in the chick and their use may be preferable over shRNAs, as they specifically reduce gene expression, but do not cause non-specific effects (Mende *et al.*, 2008). In future experiments, morpholinos could be used to investigate whether knockdown of endogenous Plxdc2 leads to defects in neural tube morphology.

3.8 Materials and Methods

3.8.1. Chicken husbandry

Fertilised chicken eggs (Ross 500 strain) were obtained from Cobbs Hatchery, Kildare and incubated at 37.5°C with controlled humidity in a Solway 24 incubator (Solway Feeders Ltd.). Chick embryos were staged according to Hamburger and Hamilton (1951) morphological criteria.

3.8.2. In situ hybridisation

DIG-labelled RNA probes for chick *Plxdc2* were produced using ChEST853h24 (Geneservice) as a template. In order to make antisense probe, 1µg ChEST853h24 was digested with *Not*I (New England Biolabs) and reverse transcribed using T3 RNA Polymerase in combination with DIG RNA labelling mix (both Roche, as per protocol). For the sense control, 1µg ChEST853h24 was digested with *Eco*RI (New England Biolabs) and reverse transcribed with T7 RNA Polymerase (Promega) following the same protocol. Cash1 probes have previously been described (Jasoni *et al.*, 1994) and were a kind gift of T.A.Reh (University of Washington, USA).

Wholemount *in situ* hybridisation was carried out as outlined in section 2.8.4 and sense controls were routinely used. Representative images of *in situ* hybridisation using Plxdc2 sense probe are shown in Appendix 5.11. For *Cash1* book preparations, neural tubes were dissected out and cut along the ventral/ dorsal axis prior to mounting on slides in 20% glycerol/ PBS. HH stage 36 brains were dissected out of chicks in DEPC treated PBS and were fixed in 4% PFA, overnight at 4°C. Brains were then embedded in 4% low melting point agarose (Sigma) and 100µm free floating sections collected using a vibrating microtome (Leica, model VT1000S). *In situ* hybridisation was carried out according to Riddle (1993) with minor adjustments. Brain sections were incubated in probe overnight at 65°C in a sealed humidifed chamber.

3.8.3. Extraction of RNA from chick embryos and reverse transcription

HH stage 21 chick embryos were dissected in RNAse free conditions, using instruments treated with Rnase Away (Invitrogen), and washed in diethylpyrocarbonate(DEPC)-treated PBS. RNA was extracted from stage 21 chick embryos using TRI Reagent (Sigma, as per

protocol). Extracted RNA was resuspended in 25µl DEPC-treated water and treated with DNAse (Promega, as per protocol). Samples were subsequently stored at -70°C. Analysis by gel electrophoresis on a 0.8% agarose gel in Tris-Acetate-EDTA (TAE) buffer was carried out, and the optical density of the samples measured at wavelengths of 260nm and 280nm. Reverse transcription of RNA was carried out using Superscript II reverse transcriptase (Invitrogen) and Oligo d(T) primer (New England Biolabs, as per protocol). Negative controls were routinely employed.RNA extraction and cDNA preparation was carried out by Deirdre Collins (undergraduate student).

3.8.4. PCR amplification of the Chick Plxdc2 transcript

A single forward primer and reverse primer were designed to the predicted chick *Plxdc2* cDNA sequence (Appendix 5.4). The target sequence of the ChPlxdc2forward primer was located in the 5' UTR, prior to the start codon of the *Plxdc2* gene. The target sequence of the ChPlxdc2reverse 1 primer was located upstream to the stop codon of the gene (Appendix, Figure 5.4). When inserted into the pcDNA3.1 myc-His (B) plasmid, the pcr product produced using this primer pair allowed translation of a myc tag. To allow insertion of pcr products in to the pcDNA3.1 myc-His (B) plasmid, the forward primer was designed to include the site for *Eco*RI cleavage and reverse primers were designed to include the sequence for *Xho*I cleavage.

PCR was carried out using Phusion High-Fidelity DNA Polymerase (Finnzymes, as per protocol). PCR products were run on a 0.8% TAE gel and bands of the correct size were cut from the gel and purified using the Nucleospin Extract II kit (Macherey-Nagel, as per protocol).

Primer	Primer Sequence	Product Size
ChPlxdc2forward	5'-CGGAATTCCGGAGAGTTGTCTCGGCA-3'	
ChPlxdc2reverse	5'-CGCTCGAGTGCTCTGATACAATGAAGCC-3'	1611 bp

Table 3.2 Primers used for the amplification of the *Plxdc2* transcript and the predicted size of the PCR product. The *Eco*RI (GAATTC) and *Xho*I (CTCGAG) cleavage sites were included in primer design for ease of ligation (red font).

PCR program	
Initial denaturation: 98°C for 30 sec	
35 cycles of:	
Denaturation:	98°C for 10 sec
Annealing:	60°C for 30 sec
Extension:	72°C for 45 sec
Final Extention:	72°C for 10 min

Table 3.3 PCR program used for the amplification of the full length *Plxdc2* transcript. PCR was carried out using Phusion High-Fidelity DNA Polymerase (Finnzymes).

1µg of pcr product was digested with *Eco*RI and *Xho*I (New England Biolabs, as per protocol). Digested transcript was subsequently run on a 0.8% TAE gel and bands of the correct size were cut from the gel and purified using the Nucleospin Extract II kit (Macherey-Nagel, as per protocol).

3.8.5. Ligation of the chick Plxdc2 transcript into pcDNA3.1 myc-His (B)

1µg of the pcDNA3.1 myc-His (B) plasmid was digested with *Eco*RI and *Xho*I (New England Biolabs, as per protocol) and treated with Bacterial Alkaline Phosphatase (Invitrogen) in order to dephosphorylate the plasmid prior to insert ligation. Ligation of the *ChPlxdc2* transcript into the pcDNA3.1 myc-His (B) plasmid was carried out using T4 DNA Ligase (Roche) in a 10µl total volume. A negative control ligation reaction of digested plasmid with no insert was also included. Following incubation overnight at 16°C, 5µl of the ligation product was transformed into 50µl of Top 10F' competent cells (Invitrogen) and plated on LB Agar plates containing ampicillin (100µg/ml). Plates were cultured overnight at 37°C.

Single colonies were cultured in LB/AMP broth overnight at 37°C with agitation. Small scale preparation of plasmid DNA was carried out using the QiaPREP Spin Miniprep Kit (Qiagen, as per protocol). Purified plasmid DNA was digested with *Eco*RI and *Xho*I (New England Biolabs, as per protocol) in order to check insert size. Insert orientation was checked by digestion with *Xba*I and BglII. The digestion of plasmid DNA containing the insertion in the correct orientation would result in three products of 1.2, 1.34 and 4.6 kb.

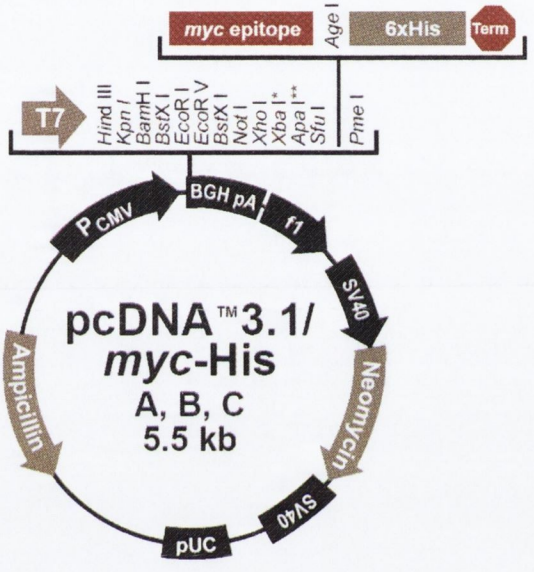

Figure 3.25 The pcDNA 3.1 myc-His (B) Plasmid (Invitrogen). The PCR amplified *Plxdc2* transcript was ligated into the pcDNA 3.1 myc-His (B) Plasmid using the *Eco*RI and *Xho*I restriction sites contained within the plasmid. Following successful ligation of transcript in the correct orientation, the CMV promoter would drive translation of full length Plxdc2, tagged with myc.

3.8.6. Design of shRNA constructs

ShRNA design was carried out according to Bron *et al.*, 2004, with modifications advised by the author. A recently designed pCA-β-EGFPm5-U6 construct (gift of author) allowed single step ligation of shRNA oligonucleotides into plasmid DNA using *Apa*I and *Eco*RV restriction enzyme sites (Figure 3.26).

Four, 21bp target sites for shRNA design were chosen using the SFOLD algorithm (http://sfold.wadsworth.org/index.pl; Table 3.3). Only those with a SFOLD score of 12 or higher were considered, and target sites were located throughout the 1.611kb coding sequence of *chPlxdc2* (Table 3.4).

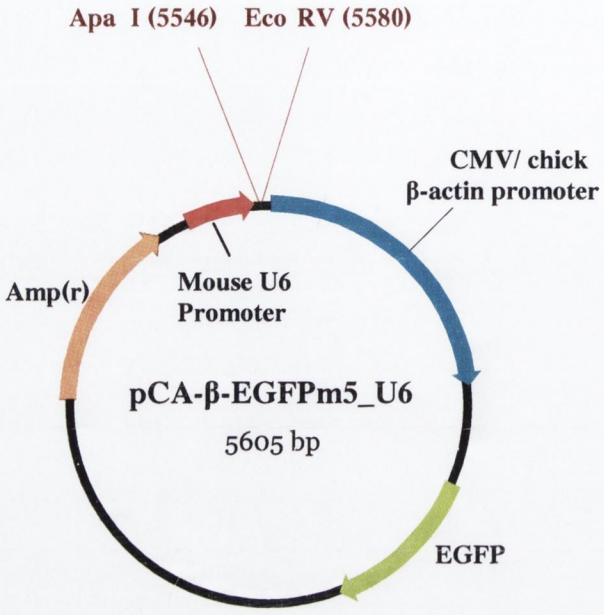

Figure 3.26 The pCA-β-EGFPm5-U6 plasmid. Annealed shRNA oligonucleotides were ligated into the plasmid using the *Apa*I and *Eco*RV restriction enzyme sites. Completed vector coexpresses green fluorescent protein (GFP; from the CMV/chick β-actin promoter) and short double-stranded hairpin RNA (from the mouse U6 promoter) specifically targeted to chick *Plxdc2*.

ID	Target Sequence	Target bp	SFOLD Score
shRNA1	CATGAGAATGCTACCCAGATT	297-318	17
shRNA2	AAGAAATTCAACAGTCAGATA	629-650	12
shRNA3	TCCAACTTGTCTCCAGTTTAA	971-992	17
shRNA4	ACCCACAGAAGATGATACCAA	1262-1283	17

Table 3.4 ShRNA sequences targetted to *Plxdc2*, location of the target sites and corresponding SFOLD scores.

ShRNA oligonucleotide design included a hairpin region 'TTCAAGAGA' which was modified to 'CTCAAGAGA' in shRNA1 (Table 3.5). Annealed oligonucleotides would have one blunt end and one *Apa*1 'sticky' end for ease of ligation into the pCA-β-EGFP-U6 plasmid (Table 3.5). Single strand oligonucleotides were ordered from Sigma-Genosys, denatured at 90°C for 3mins and annealed at 37°C for one hour (50µl reaction; 1x Sigma Taq Buffer, 2 µg sense oligonucleotide, 2µg antisense oligonucleotide).

ID	Annealed shRNA Oligonucleotides
shRNA1	5′- TGAGAATGCTACCCAGATT CTCAAGAGA AATCTGGGTAGCATTCTCATG TTTTTT-3′ 3′-CCGG ACTCTTACGATGGGTCTAA GAGTTCTCT TTAGACCCATCGTAAGAGTAC AAAAAA-5′
shRNA2	5′- GAAATTCAACAGTCAGATA TTCAAGAGA TATCTGACTGTTGAATTTCTT TTTT-3′ 3′-CCGG CTTTAAGTTGTCAGTCTAT AAGTTCTCT ATAGACTGACAACTTAAAGAA AAAA-5′
shRNA3	5′- CAACTTGTCTCCAGTTTAA TTCAAGAGA TTAAACTGGAGACAAGTTGGA TTTTTT-3′ 3′-CCGG GTTGAACAGAGGTCAAATT AAGTTCTCT AATTTGACCTCTGTTCAACCT AAAAAA-5′
shRNA4	5′- CCACAGAAGATGATACCAA TTCAAGAGA TTGGTATCATCTTCTGTGGGT TTTTTT-3′ 3′-CCGG GGTGTCTTCTACTCTGGTT AAGTTCTCT AACCATAGTAGAAGACACCCA AAAAAA-5′

Table 3.5 Design of shRNA template oligonucleotides. Red font, *Apa*I 'sticky' end; Blue font, hairpin sequence.

3.8.7. Ligation of annealed oligonucleotides in the pCA-β-EGFPm5-U6 plasmid

10µg pCA-β-EGFPm5-U6 plasmid was digested sequentially with *Apa*I and *Eco*RV restriction enzymes (New England Biolabs, as per protocol). Digested plasmid was run on a 0.8% TAE gel, purified using the Nucleospin Extract II kit (Macherey-Nagel, as per protocol) . Ligation of annealed oligonucleotides into the pCA-β-EGFPm5-U6 plasmid was carried out using T4 DNA Ligase (Roche, as per protocol) in a 10µl total volume. Ligation products were cleaned by phenol-chloroform extraction, precipitated in ethanol, and transformed into 50µl of Top 10F' competent cells (Invitrogen). The complete transformation mixture was plated on LB Agar plates containing ampicillin (100µg/ml). Plates were cultured overnight at 37°C. Single colonies were cultured in LB/AMP broth overnight at 37°C with agitation. Small scale preparation of plasmid DNA was carried out using the QiaPREP Spin Miniprep Kit (Qiagen, as per protocol). Purified plasmid DNA was digested with *Hind*III (New England Biolabs, as per protocol) in order to check for successful insertion of annealed oligonucleotides. *Hind*III digestion would linearise the

plasmid, giving a band of approximately 5.7 kb, when annealed oligonucleotides were present and would cut twice in the religated empty vector. Purified plasmid DNA from several colonies that linearised with *Hind*III to give a 5.7 kb fragment were sent for sequencing (MWG Biotech).

3.8.8. HEK 293T Cell culture

HEK 293T cells were seeded on Poly-l-lysine coated coverslips ($3.5x10^5$ cells per 35mm dish) in DMEM high glucose growth medium (10% FBS, 25mM HEPES, 1x glutamine, 1x penstrep). When approximately 60% competent, 1µg of chPlxdc2-myc and 1µg shRNA plasmid (in total) were co-transfected into cells using Fugene HD Transfection Reagent (Roche, as per protocol). Cells were cultured for a further 18 hours before processed for immuncocytochemistry.

3.8.9. Immunocytochemistry

Medium was removed from coverslips and cells were fixed in 4% PFA for 15mins at 4°C. Coverslips were washed twice (PBS/0.25% Triton-X100) and cells blocked in 10% Normal Goat Serum (Millipore; in PBS) for one hour at room temperature in a humidified chamber. Incubation in primary antibody was carried out for two hours at room temperature. Following several washes in PBS, cells were incubated in secondary antibody for 45 mins at room temperature (a complete list of antibodies used is included in Appendix 5.8). Further washes in PBS were carried out and coverslips were mounted on slides using Aqua Polymount (Polysciences Inc.).

3.8.10. Collection of protein and Western Blot Analysis

HEK293T cells were cultured in 35mm dishes and transfected with constructs as outlined in section 3.8.8. Eighteen hours post transfection, medium was removed and cells were lysed in 400µl RIPA buffer (50mM Tris-HCl, pH7.4; 150mM NaCl; 1% NP40; 1mM EDTA; 1x Complete Mini Proteinase Inhibitor, Roche) by constant agitation for 1hour at 4°C. Cells were scraped off wells, transferred into 1.5ml tubes and centrifuged at 15,000 x g, for 10 mins at 4°C. Supernatant was stored at -20°C. Protein concentration was calculated using the BCA Protein Assay (Pierce, as per protocol).

20μg protein was added to sample loading buffer (Bromophenol Blue, 200mM Tris HCl pH6.8, 10% glycerol) and boiled for 5min at 95°C prior to loading on a 10% denaturing polyacrylamide gel (see Appendix 5.9). Protein was run on the gel at 125V for approximately 1.5 hours. Protein was transferred to a nitrocellulose membrane (Protran, Whatman) at 100V for 1 hour. Membranes were blocked in 5% Marvel in TBST (TBS, 0.05% Tween 20) for 1 hour at room temperature, and incubated in primary antibody overnight at 4°C. β-actin was employed as a marker of equal protein loading across lanes. Following several washes in TBST, membranes were incubated in secondary antibody and exposed digitally using West Dura Chemoilluminescent detection (Pierce, as per protocol) and the LAS-3000 Image Reader (Fujifilm). The antibodies used in Western blot analysis are detailed in Appendix 5.8.

3.8.11. In ovo electroporation

In ovo electroporation was carried out according to Funahashi *et al.* (1999) with minor adjustments. Embryos were visualise with a drop of Fast Green (0.05% in sterile PBS, Sigma). HH stage 10-11 embryos were injected with plasmids at the concentrations detailed in Table 3.6. Controls were routinely employed using empty plasmids at the same concentration. The pCA-β-EGFPm5-U6 plasmid was routinely co-electroporated with chPlxdc2-Myc and Plxdc2-AP(CT), allowing visually assessment of transfection efficiency using the EGFP marker. Following injection into the lumen of the neural tube at the level of the myelencephalon, embryos were electroporated with four 50ms pulses of 21V, at an interval of 100ms. Parallel electrodes were configured with a space of 4.5mm. Specimens were dissected out, 24 hours post electroporation and fixed in 4% PFA for two hours (DEPC treated solutions were routinely used for *in situ* hybridisation experiments). For older specimens, embryos were left for 5/10 days post electroporation and were fixed in 4% PFA, overnight at 4°C.

3.8.12. Immunohistochemistry

Initially, immunohistochemistry was carried out on free floating vibratome sections (Figure 3.7). Embryos were embedded in 4% agar/PBS and 50μm free floating sections collected using a vibrating microtome (Leica, model VT1000S). Following several washes (PBS/0.4% Triton X-100), sections were blocked in 5% normal goat serum (NGS, in PBS/0.4% Triton X-100) for one hour at room temperature, with gentle agitation.

Incubation in primary antibody was carried out in PBS, overnight at 4°C (a complete list of antibodies used is available in Appendix 5.8). Sections were washed as before and incubated in secondary antibody for one hour at room temperature, in the dark. Sections were briefly air-dried onto glass slides and mounted in Aqua Polymount (Polysciences Inc.).

	Misexpression of chPlxdc2	Expression of secreted Plxdc2-AP(CT)	Knockdown of chPlxdc2 at MHB	chPlxdc2-Myc & shRNAs1&3
chPlxdc2-Myc	1μg/μl	----	----	0.8μg/μl
pCA-β-EGFPm5-U6	0.4μg/μl	0.4μg/μl	----	----
msPlxdc2-AP	----	1μg/μl	----	----
shRNA1	----	----	0.75μg/μl	0.4μg/μl
shRNA3	----	----	0.75μg/μl	0.4μg/μl

Table 3.6 Concentration of plasmids used in *in ovo* electroporation experiments. Controls were routinely employed using empty plasmids at the same concentration.

For cryostat sectioning, embryos were embedded in 1.5% Agarose/5% sucrose (Both from Sigma). Embedded embryos were then equilibrated in 30% sucrose solution overnight and frozen gradually on a metal tray cooled by contact with dry ice. Frozen specimens were stored at -20°C prior. 20μm sections were collected using a cryostat (Bright) and briefly air dried onto slides. Immunohistochemistry was carried out as outlined above, with minor alterations. Washes were carried out in PBS with 0.5% Triton X-100 and 0.1% Tween 20 and sections were mounted in ProLong Gold antifade reagent with DAPI (4',6-diamidino 2-phenylindole) (Invitrogen).

Wholemount embryos for immunohistochemistry were washed twice in TBST (0.025M Tris pH7.5, 0.15M NaCl, 2mM KCl, 0.1% Tween 20) at room temperature. Prior to incubation in primary antibody, embryos were blocked in 10% normal goat serum (NGS, with 0.1% NaN_3 in TBST) overnight at 4°C. Specimens were incubated in primary antibody in blocking solution for 6 days at 4°C. Following six washes in TBST at room temperature, a final wash in TBST was carried out overnight at 4°C, with gentle agitation. Embryos were incubated in secondary antibody in blocking solution overnight at 4°C. Final washes were carried out in TBST. Whole embryos were then processed for OPT as outlined in section 2.8.6.

3.8.13. Incorporation of BrdU

BrdU (Sigma, 10mM in sterile PBS) was injected into the yolk vein 24 hours after electroporation. Thirty minutes after BrdU injection, embryos were dissected out, fixed in 4% PFA and processed for immunohistochemistry.

3.8.14. Statistical Analysis

Statistical analyses of measurements and counts was carried out using Datadesk 6.1 software and appropriate tests. Individual data sets for each condition were checked for normality by the plotting of histograms and in all situations were found to be normal. Means and standard deviation were plotted on bar graphs. In the majority of cases, independent T-tests were employed in order to test for significant difference between the means of the data sets being investigated. For BrdU-positive cell counts, paired T-tests were used.

3.8.15. Real time PCR

RNA for real time PCR analysis was prepared by Julie Skotte, in the lab of Kristian Helin (University of Copenhagen). Neural stem cells were differentiated from mouse embryonic stem cells ('E14' cell line, Hooper *et al.*, 1987) according to the protocol of Conti *et al.* (2005). Neural cells were differentiated from mouse ES cells following the protocol of Bibel *et al.* (2004).

Real time PCR was carried out on reverse transcribed RNA as described in Section 2.8.7 using the primers detailed in Table 3.7. Primers for detection of *Plxdc2* transcript had previously been used on RNA extracted from mouse tissue to confirm *Plxdc2* knockdown in the Plxdc2GFP mouse line (Section 2.5.2). Primers for ESC, NSC and neuronal markers were designed, and routinely used, in the lab of Kristian Helin.

Gene	Primer Type	Primer Sequence (5'-3')
Plxdc2	Forward	CCAGTGAAAGTCGGGTTGTCTG
Plxdc2	Reverse	TGGGTATTTGCTGGATCCTGTG
RPO	Forward	TTCATTGTGGGAGCAGAC
RPO	Reverse	CAGCAGTTTCTCCAGAGC
Nestin	Forward	GCCTATAGTTCAACGCCCCC
Nestin	Reverse	AGACAGGCAGGGCTAGCAAG
Nanog	Forward	CCTCCAGCAGATGCAAGAACTC
Nanog	Reverse	CTTCAACCACTGGTTTTTCTGCC
β3-Tubulin	Forward	ACTTGGAACCTGGAACCATGG
β3-Tubulin	Reverse	GGCCTGAATAGGTGTCCAAAGG

Table 3.7 Primers used in real time PCR experiments

4. Conclusions and future directions

Plxdc2 encodes a transmembrane protein with an architecture and embryonic expression pattern indicative of a role in early development of the nervous system. The protein is highly conserved across species and expression in the developing nervous system of the chick and mouse is very similar. In particular, Plxdc2 is expressed in the cortical hem, midbrain-hindbrain boundary, floor plate and dorsal midline. Expression in these regions is highly indicative of a potential role in early brain development; in proliferation, apoptosis, differentiation or the patterning of neuronal cell fate.

Misexpression of Plxdc2 in the midbrain/hindbrain of the HH stage 10-11 chick results in neural tube thickening, 24 hours following electroporation. Neural tube thickening is significant, robust and reproducible. A similar thickening effect is observed when a secreted form of murine Plxdc2 is expressed in the neural tube of the chick. Plxdc2 therefore causes this effect in a cell non-autonomous manner, most likely acting as a ligand. The biochemical function of the protein also appears to be conserved between species: in the chick, the extracellular portion of the mouse Plxdc2 protein can bind a receptor and activate the same pathways as the endogenous chick Plxdc2 protein. Additional experimentation *in vivo* and in cell culture will be necessary in order to further elucidate endogenous Plxdc2 function.

4.1 A potential role for *Plxdc2* in proliferation

Plxdc2-induced neural tube thickening is accompanied by an increase in proliferation, 24 hours after electroporation. However, at this time point a simple relationship between the scale of increase in BrdU-positive cells and the degree of neural tube thickening does not exist. The relationship of the two findings should be clarified by examination of BrdU incorporation and neural tube thickening at earlier time points following Plxdc2 misexpression. The Plxdc2-induced effect on proliferation could also be examined in culture, following misexpression of Plxdc2 in embryonic or neural stem cells. BrdU incorporation and accurate counts of neurosphere formation have been successfully used to analyse proliferation in neural stem cells in culture (Yu *et al.*, 2006). There is also a wide range of commercially available kits for the analysis of cellular proliferation. However, it

is important to stress that *in vitro* methods should not substitute for further in depth analysis of the effect of Plxdc2 misexpression on proliferation *in vivo*.

4.2 *Plxdc2* in apoptosis?

To date, a potential role of Plxdc2 in programmed cell death has not been investigated. Decrease in progenitor cell apoptosis leads to neural tube overgrowth phenotypes in a number of mouse and chick models (Ahlgren *et al.*, 2003, Cecconi *et al.*, 1998, Hakem *et al.*, 1998, Inglis-Broadgate *et al.*, 2005, Kuida *et al.*, 1998, Yoshida *et al.*, 1998). However, overgrowth phenotypes are not always purely owing to decreased apoptosis. Effects on apoptosis and proliferation in a cell population are not mutually exclusive events and the intricate balance of apoptopic and proliferative events may be involved. For example, overexpression of FGFr3 in the mouse leads to doubling of the ventricular zone by E14.5, due to a mild increase in proliferation and a profound decrease in apoptosis (Inglis-Broadgate *et al.*, 2005). It is therefore, of upmost importance to examine apoptosis in the chick neural tube following misexpression of Plxdc2, as reduced apoptosis may be partly responsible for the Plxdc2-induced thickening effect. Apoptosis is routinely examined in *vivo* by terminal deoxynucleotidyl transferase dUTP nick end labelling (TUNEL).

4.3 A potential role for *Plxdc2* in neural differentiation and determination of cell fate

Plxdc2-induced neural tube thickening is accompanied by an increase in expression of the proneural gene, *Cash1*, 24 hours after electroporation. A significant increase in *Plxdc2* expression is observed when neural progenitor cells and neurons are derived from embryonic stem cells in culture. The relationship between *Plxdc2* expression and the onset of neural differentiation in progenitor cells should be investigated in detail in future experiments. Manipulation of *Plxdc2* expression in neural stem cells in culture and the characterisation of accompanying proneural gene expression by realtime PCR may shed some light on the potential position of *Plxdc2* in neuronal differentiation cascades and the determination of cell fate. These experiments could be carried out using the E14 embryonic stem cell line (Hooper *et al.*, 1987) and appropriate differentiation protocols (Bibel *et al.*, 2007, Bibel *et al.*, 2004, Conti *et al.*, 2005) or by using neural progenitor cells cultured from the embryonic mouse brain (Tate *et al.*, 2004, Hirabayashi *et al.*, 2004). If

cell culture experiments are found to mimic the *in vivo* Plxdc2-induced increase in proneural gene expression, investigation of potential activation pathways for proneural gene upregulation could also be investigated as outlined below.

Members of the Wnt family have been shown to upregulate expression of proneural genes and induce differentiation through activation of the canonical and Wnt/Ca^{2+} pathways. (Hirabayashi *et al.*, 2004, Yu *et al.*, 2006). Involvement of Wnt pathways in Plxdc2-induced increase in proneural gene expression could be investigated by the detection of Wnt pathway activity and by the inhibition of Wnt pathways in Plxdc2 expressing cells. Activation of the canonical Wnt pathway can be readily assayed in culture by examination of β-catenin levels (Hirabayashi *et al.*, 2004, Korinek *et al.*, 1997, Yu *et al.*, 2006). β-catenin may be assayed at the protein level by western blot analysis. Activity of the canonical pathway may also be demonstrated by the nuclear localisation of β-catenin. Additionally, reporter constructs can be used to detect target gene activity. For example, a luciferase reporter gene construct under the control of TCF-responsive elements (TOP-FLASH) (Korinek *et al.*, 1997) could be co-transfected with Plxdc2 constructs in culture in order to determine whether *Plxdc2* expression is correlated with activity of target genes. If activation of the canonical pathway following Plxdc2 expression is observed in embryonic/neural stem cells, stabilised β-catenin (Morin *et al.*, 1997) may lead to *Mash1* expression. Activation of the Wnt/Ca^{2+} pathway involves specific activation of PLC and PKC (Yu *et al.*, 2006). In culture, transfection of Plxdc2 and addition of specific β-catenin, PLC and PKC inhibitors (Yu *et al.*, 2006) could also be used to determine the activity of canonical versus Wnt/Ca^{2+} pathways.

Another pathway that might be involved in Plxdc2-induced increase in *Cash1* expression is the Notch signalling pathway. Notch signalling leads to activation of Hes expression and the repression of proneural gene expression (Honjo, 1996, Kageyama *et al.*, 2005, Ohtsuka *et al.*, 1999, Sasai *et al.*, 1992, Selkoe and Kopan, 2003). In culture, a potential Plxdc2-induced increase in proneural gene expression might occur by interference in Notch activation, resulting in prolonged repression of *Hes1 and Hes5* expression. This possibility could initially be investigated by the examination of *Hes* gene expression in neural stem cells following manipulation of Plxdc2 expression. However, Plxdc2 interference in the Notch signalling pathway may not occur at the level of Hes gene expression. The activation of a not yet specified pathway may interfere with Hes repression of proneural

gene expression at the transcriptional level and must also be considered. If a putative pathway mediating Plxdc2-induced increase in proneural gene expression is indentified in culture, constituents of the indicated pathway must be investigated further *in vivo.*

It is important to establish whether Plxdc2 misexpression causes a direct increase in neuronal differentiation and if so, does it occur at the expense of glial differentiation? Both these questions can be examined in neural stem cell culture. Protocols for the differentiation of neurons from embryonic and neural stem cells are described (Bibel *et al.*, 2007, Bibel *et al.*, 2004, Yu *et al.*, 2006). Manipulation of Plxdc2 expression in differentiating cells and subsequent analysis of neuronal cell number using appropriate markers such as βIII-tubulin (TuJI) could be used to investigate a potential Plxdc2-induced effect on neuronal differentiation. In parallel with this, glial populations in a mixed population of differentiated cells should be examined by the analysis of astrocytic and oligodendrocytic marker expression. Examination of the proportion of differentiated neuronal and glial cells following Plxdc2 misexpression may highlight a role for the protein in cell fate determination. Possible Plxdc2-induced effects on neuronal differentiation and cell fate determination which are observed in cell culture should then be investigated further *in vivo*.

4.4 Knockdown of endogenous *Plxdc2* expression and analysis of endogenous gene function

Successful knockdown of endogenous Plxdc2 protein in the chick has not been confirmed. Co-electroporation of shRNAs designed against chick *Plxdc2* with the full length *Plxdc2* plasmid resulted in the apparent rescue of the Plxdc2-induced neural tube thickening phenotype. However, proper controls were not used in these experiments and results must be viewed tentatively. Additional experiments must be carried out using the proper non-targetting shRNA controls and knockdown of *Plxdc2* should also be characterised at the transcript level. ShRNAs targetted to the gene may, however, be useful tools in future cell culture experiments involving the manipulation of exogenous chick Plxdc2 expression and the examination of potential roles of the gene in differentiation, proliferation and apoptosis.

The lack of an obvious morphological phenotype in Plxdc2GFP homozygote mice at embryonic stages suggests that the key to establishing endogenous Plxdc2 function is in

ectopic/overexpression of the gene and not in endogenous gene silencing. Plxdc2 may have a redundant function in the mouse or alternatively, loss of Plxdc2 expression may be compensated for by another protein. The Plxdc2GFP mouse line was made available late in the timespan of this project and preliminary analyses of the effect of loss of Plxdc2 were carried out. Tracts of neurons which normally express *Plxdc2* were examined for cell-autonomous axon guidance and morphological defects at E15.5. Plxdc2GFP homozygote analysis should be revisited in light of results in the chick highlighting the cell non-autonomous manner of the Plxdc2-induced effect on neural tube thickness. Phenotypic analyses should not purely focus on regions and neuronal tracts which normally express Plxdc2, but should also encompass neighbouring brain regions and structures during development. In addition, many genes involved in early patterning of the brain have been shown to have later functions in axon guidance (reviewed in section 1.2) and this may also be the case for *Plxdc2*. Homozygous Plxdc2GFP mutants should therefore be examined for axon guidance defects at later stages of development.

The Plxdc2 receptor is unknown and should be isolated. The chPlxdc2-Myc plasmid encodes full length chick Plxdc2 with additional Myc and His tags. This construct may therefore prove a useful tool in the analysis of potential Plxdc2 binding partners through immunoprecipitation or expression screening techniques. *In vivo*, widespread binding of the extracellular mouse Plxdc2 protein (tagged with AP) is evident and in this case, putative receptor protein expression may be masked by binding of Plxdc2-AP to nidogen. Previous attempts to isolate a binding partner for Plxdc2 using similar protein constructs have resulted in the isolation of cortactin, an intracellular protein which could not be the receptor of Plxdc2 (Nanda *et al.*, 2004). Wnt genes have been implicated in the control of proliferation and differentiation, and in axon guidance events at later stages of development (Reviewed in chapter 1). Considering the co-expression of *Plxdc2* in many Wnt rich regions, including the cortical hem, dorsal midline and midbrain-hindbrain boundary, it seems pertinent to examine the possible direct interaction of Plxdc2 with members of the Wnt family.

4.5 Final conclusion

Plxdc2 encodes a novel transmembrane protein which controls proliferation and differention in the developing neural tube of the chick. Plxdc2 is expressed in important signalling centres of the developing brain, including the cortical hem, midbrain-hindbrain

boundary and floor plate. The elucidation of its roles in proliferation and differentiation should thus greatly contribute to a deeper understanding of the control of these processes within the signalling centres of early brain development. In addition, Plxdc2 expression in discrete neuronal subsets at later stages of development alludes to possible roles in cell fate determination and axon guidance. Detailed analysis of endogenous gene function and identification of interacting proteins should further illuminate the multiple potential roles of this novel protein in neural development.

5. Appendix

5.1 Alignment of the murine Plxdc2 and Plxdc1 proteins

```
MsPlxdc2        MARFRRADLAAAGVMLLCHFLTDRFQFAHGEPGHHTNDWIYEVTNAFPWNEEGVEVDSQA 60
MsPlxdc1        ----MRAQLWLLQLLLLRG--AARALSPATPAGHNE-------GQDSAWT---AKRTRQG 44
                **:*    ::**    : *   .   .**:         :  .*.   .:   *.

MsPlxdc2        YNHRWKRNVDPFKAVDTNRASMGQASPESKGFTDLLLDDGQDNNTQIEEDTDHNYYISRI 120
MsPlxdc1        WSRRPRE--SPAQVLKPGKTQLSQD----LGGGSLAIDTLPDNRTRVVEDN-HNYYVSRV 97
                :.:* :.  .* :.:...::.:.*      *  .* :*   **.*:: **. ****:**:

MsPlxdc2        YGPADSASRDLWVNIDQMEKDKVKIHGILSNTHRQAARVNLSFDFPFYGHFLNEVTVATG 180
MsPlxdc1        YGPGEKQSQDLWVDLAVANRSHVKIHRILSSSHRQASRVVLSFDFPFYGHPLRQITIATG 157
                ***.:. *:****::   ::.:**** ***.:****:** ********** *.::*:***

MsPlxdc2        GFIYTGEVVHRMLTATQYIAPLMANFDPSVSRNSTVRYFDNGTALVVQWDHVHLQDNYNL 240
MsPlxdc1        GFIFMGDMLHRMLTATQYVAPLMANFNPGYSDNSTVAYFDNGTVFVVQWDHVYLQDREDR 217
                ***: *:::*********:*******:*. * **** ******.:*******:***. :

MsPlxdc2        GSFTFQATLLMDGRIIFGYKEIPVLVTQISSTNHPVKVGLSDAFVVVHRIQQIPNVRRRT 300
MsPlxdc1        GSFTFQAALHRDGRIVFGYKEIPMAVLDISSAQHPVKAGLSDAFMILNSSPEVPASQRRT 277
                *******:*  ****:*******: * :***::****.******::::   ::*  :***

MsPlxdc2        IYEYHRVELQMSKITNISAVEMTPLPTCLQFNGCGPCVSSQIGFNCSWCSKLQRCSSGFD 360
MsPlxdc1        IFEYHRVELDSSKITTTSAVEFTPLPTCLQHQSCDTCVSSNLTFNCSWCHVLQRCSSGFD 337
                *:*******: ****. ****:********.:.*..****:: ******  *********

MsPlxdc2        RHRQDWVDSGCPEEVQSKEKMCEKTEPGETSQTTTTSHTTTMQFRVLTTTRRAVTSQMPT 420
MsPlxdc1        RYRQEWLTYGCAQEAEG--KTCEDFQ--DDSHYSASPDSSFSPFNGDSTTS---SSLFID 390
                *:**:*:  **.:*.:.  * **. :  : *: ::::..::   *.  :**    :* :

MsPlxdc2        SLPTEDDTKIALHLKDSGASTDDSAAEKKGGTLHAGLIVGILILVLIIAAAILVTVYMYH 480
MsPlxdc1        SLTTEDDTKLNPYAEGDGLP-DHSSPKSKGPPVHLGTIVGIVLAVLLVAAIILAGIYISG 449
                **.******:  : :..* . *.*:.:.** .:* * ****:: **::** **. :*:

MsPlxdc2        HPTSAASIFFIERRPSRWPAMKFRRGSGHPAYAEVEPVG-EKEGFIVSEQC 530
MsPlxdc1        HPNSNAALFFIERRPHHWPAMKFHNHPNHSTYTEVEPSGHEKEGFVEAEQC 500
                **.* *::******* :******:. ..*.:*:**** * *****: :***
```

Figure 5.1 Alignment of the murine Plxdc2 and Plxdc1 proteins (ENSMUSP00000028081 and ENSMUSP00000017561 respectively, Ensembl Release 50). Protein architecture is conserved between the two members of the family and overall, proteins were 47% identical. Underlined green font, Signal peptide;Underlined blue font, domain of Nidogen homology; Underlined red font, PSI domain; underlined bold black font, transmembrane domain.

5.2 Alignment of Plxdc2 protein across species

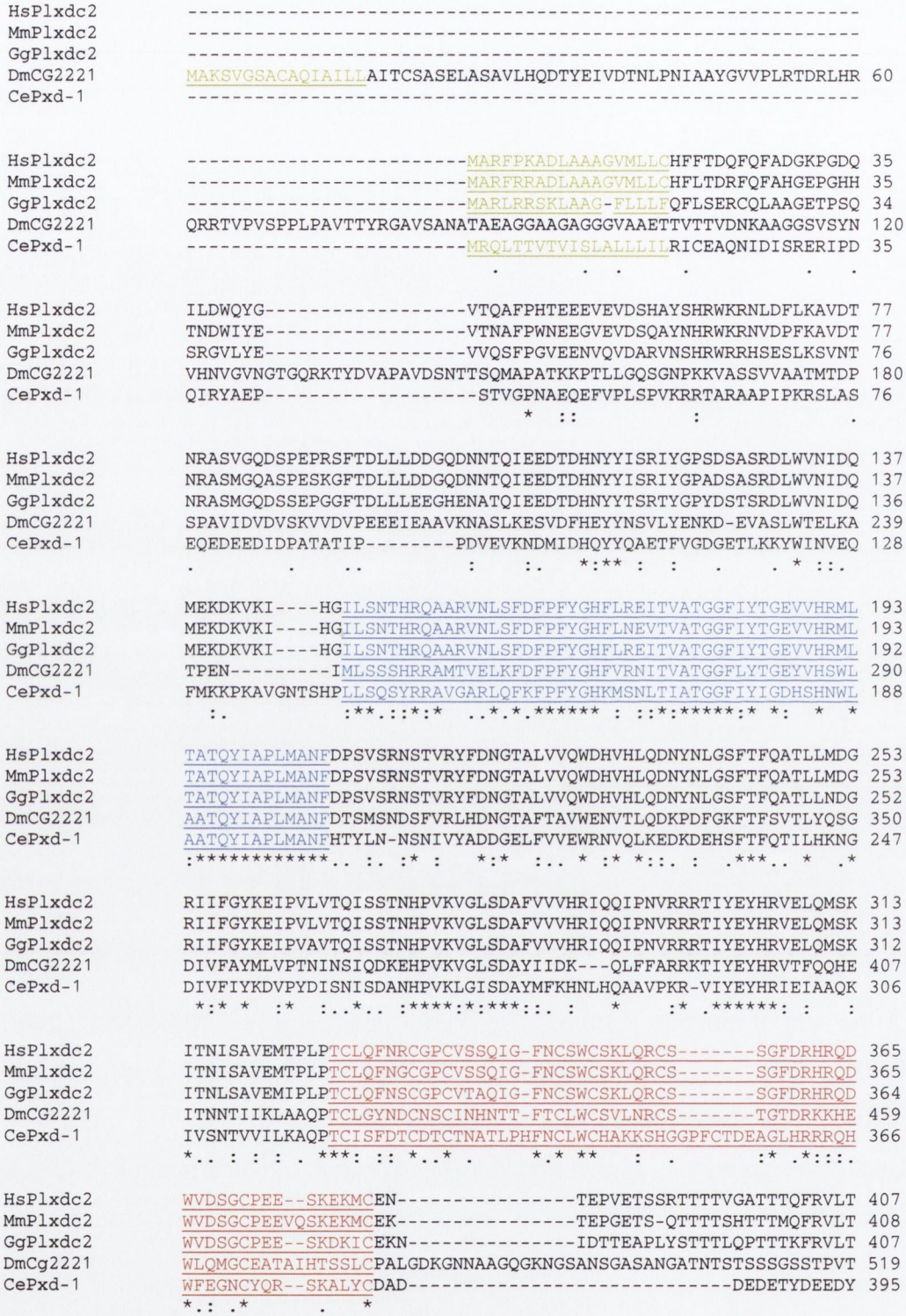

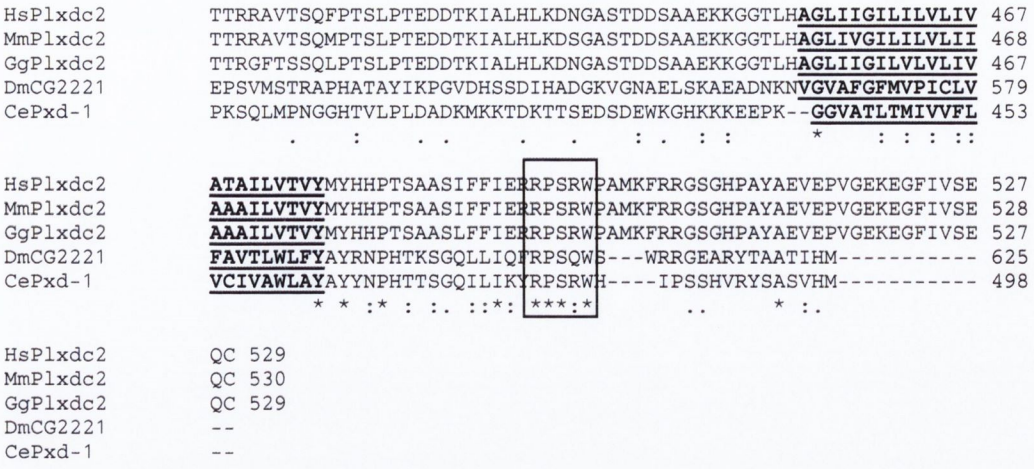

Figure 5.2 Plxdc2 is highly conserved in the human, mouse, chicken, fly and worm. Hs, *Homo sapiens*; Mm, *Mus musculus*; Gg, *Gallus gallus*; Dm, *Drosophila melanogaster*; Ce, *Caenorhabditis elegans*. Underlined green font, Signal peptide; Underlined blue font, Nidogen homology; Underlined red font, PSI domain; underlined bold black font, transmembrane domain; Black rectangle, conserved region of cytoplasmic tail.

5.3 Plxdc2GFP mouse line design

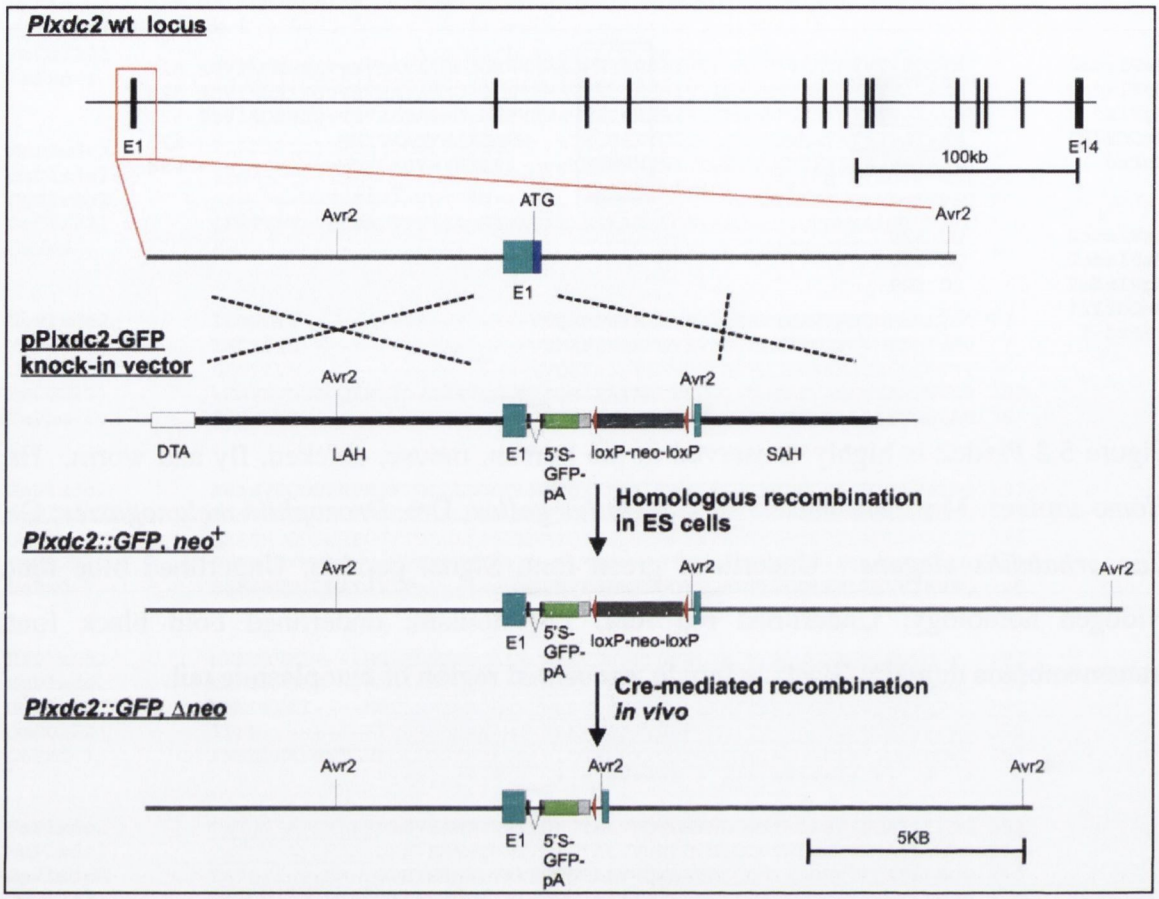

Figure 5.3 Cartoon of design strategy for the creation of the Plxdc2GFP mouse line. The *Plxdc2* start codon & leader peptide is replaced by a 5S-EGFP-pA cassette by homologous recombination in ES cells. The Plxdc2GFP mouse line was developed in the lab of T. Jessell, Colombia University, USA and was used with his permission.

5.4 Predicted *Plxdc2* Full Length Transcript showing sites of primer design

GCGGCTCGAGGCGGCTCGAGCGAGGAGCGGCGCGTACCCCGCATCCCGGAGAGTTGTCTCGGCAGCTCCGTGCT**ATG**GCGAGGCTGCGGAG
AAGCAAACTAGCCGCTGGATTTCTATTACTTTTCCAGTTCCTGAGCGAGCGCTGCCAGCTCGCCGCCGGAGAGACGCCGAGCCAGAGCCGC
GGTGTGCTTTATGAAGTTGTTCAGAGCTTCCCTGGAGTGGAGGAAAATGTGCAAGTGGATGCACGTGTAAATAGCCACAGGTGGAGAAGGC
ACTCAGAGTCTCTTAAATCAGTCAACACTAACAGAGCCAGTATGGGGCAGGATTCCTCTGAGCCAGGTGGTTTCACAGATCTGTTGCTTGA
AGAGGGACATGAGAATGCTACCCAGATTGAGGAGGACACAGATCATAATTATTATACTTCAAGGACATATGGCCCATATGATTCTACCAGC
CGGGATTTATGGGTCAATATAGACCAAATGGAGAAAGATAAAGTAAAGATTCATGGGATCCTCTCCAATACCCATCGACAAGCAGCAAGAG
TGAATCTGTCCTTTGATTTTCCATTTTATGGCCATTTTCTACGAGAAATTACAGTGGCAACTGGGGGTTTCATATATACTGGAGAAGTTGT
GCATCGAATGCTAACAGCTACACAATATATTGCACCCTTAATGGCAAATTTTGATCCCAGTGTATCAAGAAATTCAACAGTCAGATACTTT
GATAATGGCACAGCACTAGTTGTCCAGTGGGACCATGTTCACCTGCAGGATAATTACAACCTGGGCAGTTTCACTTTTCAGGCCACCCTTC
TCAATGATGGGCGTATCATTTTCGGCTACAAAGAAATTCCTGTCGCTGTGACACAGATAAGCTCAACCAACCACCCAGTGAAAGTTGGACT
ATCAGATGCATTTGTGGTTGTGCACAGGATCCAGCAAATTCCCAATGTCCGCAGAAGAACAATTTACGAATACCACAGGGTGGAGCTGCAG
ATGTCAAAGATTACAAATCTGTCAGCTGTTGAAATGATACCTCTTCCAACTTGTCTCCAGTTTAACAGCTGTGGCCCCTGTGTCACTGCCC
AGATTGGCTTCAACTGCAGCTGGTGCAGTAAACTCCAAAGATGCTCCAGCGGATTTGACCGTCACCGACAAGATTGGGTAGACAGTGGCTG
CCCTGAACAGTCAAAAGATAAGATTTGTGAGAAGAATATAGACACAACTGAAGCACCACTGTACTCTACCACCACTCTTCAACCAACCACC
ACAAAGTTCAGAGTTTTAACAACCACCAGAGGATTCACCAGCTCCCAGCTGCCAACCAGCCTACCCACAGAAGATGATACCAAGATAGCGC
TGCACCTAAAAGATAATGGAGCTTCCACAGATGACAGCGCTGCAGAGAAAAAAGGCGGAACACTTCATGCTGGTTTAATCATCGGCATTCT
AGTCCTGGTCCTCATCGTGGCTGCAGCCATCCTCGTGACTGTCTACATGTACCATCATCCAACATCAGCAGCCAGTCTCTTCTTCATAGAG
CGGCGTCCGAGCAGATGGCCAGCAATGAAATTCAGAAGAGGATCTGGACATCCTGCATATGCTGAAGTGGAACCAGTTGGAGAAAAAGAAG
GCTTCATTGTATCAGAGCAATGC**TAA**AATTCTTAGGACAGAACACCAGTACTGGCCTACAGGTGTAAGACATTTACTTTGCATCTCTATA

Figure 5.4 The chick *Plxdc2* transcript was predicted by the combination of two ESTs from the BBSRC chick EST database, ChEST 636b10 (black font) and ChEST 853h24 (blue font). Red font, region of overlap of ESTs; Grey font, UTR sequence; Bold black font, start and stop codons; Underlined font, forward and reverse primers used for PCR amplification.

5.5 Alignment of the EST predicted chick Plxdc2 protein against mouse Plxdc2

```
ChPlxdc2        MARLRRSKLAAG-FLLLFQFLSERCQLAAGETPSQSRGVLYEVVQSFPGVEENVQVDARV 59
MsPlxdc2        MARFRRADLAAAGVMLLCHFLTDRFQFAHGEPGHHTNDWIYEVTNAFPWNEEGVEVDSQA 60
                ***:**:.***. .:** :**::* *:* **.  ::.. :***.::**  **.*:**::.

ChPlxdc2        NSHRWRRHSESLKSVNTNRASMGQDSSEPGGFTDLLLEEGHENATQIEEDTDHNYYTSRT 119
MsPlxdc2        YNHRWKRNVDPFKAVDTNRASMGQASPESKGFTDLLLDDGQDNNTQIEEDTDHNYYISRI 120
                .***:*: :.:*:*:******** *.*. ********::*::* ************ **

ChPlxdc2        YGPYDSTSRDLWVNIDQMEKDKVKIHGILSNTHRQAARVNLSFDFPFYGHFLREITVATG 179
MsPlxdc2        YGPADSASRDLWVNIDQMEKDKVKIHGILSNTHRQAARVNLSFDFPFYGHFLNEVTVATG 180
                *** **:*********************************************.*:*****

ChPlxdc2        GFIYTGEVVHRMLTATQYIAPLMANFDPSVSRNSTVRYFDNGTALVVQWDHVHLQDNYNL 239
MsPlxdc2        GFIYTGEVVHRMLTATQYIAPLMANFDPSVSRNSTVRYFDNGTALVVQWDHVHLQDNYNL 240
                ************************************************************

ChPlxdc2        GSFTFQATLLNDGRIIFGYKEIPVAVTQISSTNHPVKVGLSDAFVVVHRIQQIPNVRRRT 299
MsPlxdc2        GSFTFQATLLMDGRIIFGYKEIPVLVTQISSTNHPVKVGLSDAFVVVHRIQQIPNVRRRT 300
                ********** ************* ***********************************

ChPlxdc2        IYEYHRVELQMSKITNLSAVEMIPLPTCLQFNSCGPCVTAQIGFNCSWCSKLQRCSSGFD 359
MsPlxdc2        IYEYHRVELQMSKITNISAVEMTPLPTCLQFNGCGPCVSSQIGFNCSWCSKLQRCSSGFD 360
                ****************:***** *********.*****::********************

ChPlxdc2        RHRQDWVDSGCPE--QSKDKICEKNIDTTEAPLYSTTTLQPTTTKFRVLTTTRGFTSSQL 417
MsPlxdc2        RHRQDWVDSGCPEEVQSKEKMCEKTEPGETS--QTTTTSHTTTMQFRVLTTTRRAVTSQM 418
                *************  ***:*:***.     :   :*** :.** :******** .:**:

ChPlxdc2        PTSLPTEDDTKIALHLKDNGASTDDSAAEKKGGTLHAGLIIGILVLVLIVAAAILVTVYM 477
MsPlxdc2        PTSLPTEDDTKIALHLKDSGASTDDSAAEKKGGTLHAGLIVGILILVLIIAAAILVTVYM 478
                ******************.*********************:***:****:**********

ChPlxdc2        YHHPTSAASLFFIERRPSRWPAMKFRRGSGHPAYAEVEPVGEKEGFIVSEQC- 529
MsPlxdc2        YHHPTSAASIFFIERRPSRWPAMKFRRGSGHPAYAEVEPVGEKEGFIVSEQC- 530
                *********:******************************************
```

Figure 5.5 Alignment of the predicted chick Plxdc2 protein sequence against mouse Plxdc2 (ENSMUSP00000028081, Ensembl Release 50). Alignment against the mouse Plxdc2 protein supported the validity of the predicted chick transcript. Protein architecture was conserved between species in the region of Nidogen homology (underlined blue font), the PSI domain (underlined red font) and the transmembrane domain (underlined, bold black font), and overall, proteins were 81% identical. Signal peptide, underlined green font.

5.6 Alignment of the PCR amplified *Plxdc2* transcript (clone 7) against the EST predicted transcript

```
chPlxdc2        ATGGCGAGGCTGCGGAGAAGCAAACTAGCCGCTGGATTTCTATTACTTTTCCAGTTCCTG 60
clone7          ATGGCGAGGCTGCGGAGAAGCAAACTAGCCGCTGGATTTCTATTACTTTTCCAGTTCCTG 60
                ************************************************************

chPlxdc2        AGCGAGCGCTGCCAGCTCGCCGCCGGAGAGACGCCGAGCCAGAGCCGCGGTGTGCTTTAT 120
clone7          AGCGAGCGCTGCCAGCTCGCCGCCGGAGAGACGCCGAGCCAGAGCCGCGGTGTGCTTTAT 120
                ************************************************************

chPlxdc2        GAAGTTGTTCAGAGCTTCCCTGGAGTGGAGGAAAATGTGCAAGTGGATGCACGTGTAAAT 180
clone7          GAAGTTGTTCAGAGCTTCCCTGGAGTGGAGGAAAATGTGCAAGTGGATGCACGTGTAAAT 180
                ************************************************************

chPlxdc2        AGCCACAGGTGGAGAAGGCACTCAGAGTCTCTTAAATCAGTCAACACTAACAGAGCCAGT 240
clone7          AGCCACAGGTGGAGAAGGCACTCAGAGTCTCTTAAATCAGTCAACACTAACAGAGCCAGT 240
                ************************************************************

chPlxdc2        ATGGGGCAGGATTCCTCTGAGCCAGGTGGTTTCACAGATCTGTTGCTTGAAGAGGGACAT 300
clone7          ATGGGGCAGGATTCCTCTGAGCCAGGTGGTTTCACAGATCTGTTGCTTGAAGAGGGACAT 300
                ************************************************************

chPlxdc2        GAGAATGCTACCCAGATTGAGGAGGACACAGATCATAATTATTATACTTCAAGGACATAT 360
clone7          GAGAATGCTACCCAGATTGAGGAGGACACAGATCATAATTATTATACTTCAAGGACATAT 360
                ************************************************************

chPlxdc2        GGCCCATATGATTCTACCAGCCGGGATTTATGGGTCAATATAGACCAAATGGAGAAAGAT 420
clone7          GGCCCATATGATTCTACCAGCCGGGATTTATGGGTCAATATAGACCAAATGGAGAAAGAT 420
                ************************************************************

chPlxdc2        AAAGTAAAGATTCATGGGATCCTCTCCAATACCCATCGACAAGCAGCAAGAGTGAATCTG 480
clone7          AAAGTAAAGATTCATGGGATCCTCTCCAATACCCATCGACAAGCAGCAAGAGTGAATCTG 480
                ************************************************************

chPlxdc2        TCCTTTGATTTTCCATTTTATGGCCATTTTCTACGAGAAATTACAGTGGCAACTGGGGGT 540
clone7          TCCTTTGATTTTCCATTTTATGGCCATTTTCTACGAGAAATTACAGTGGCAACTGGGGGT 540
                ************************************************************

chPlxdc2        TTCATATATACTGGAGAAGTTGTGCATCGAATGCTAACAGCTACACAATATATTGCACCC 600
clone7          TTCATATATACTGGAGAAGTTGTGCATCGAATGCTAACAGCTACACAATATATTGCACCC 600
                ************************************************************

chPlxdc2        TTAATGGCAAATTTTGATCCCAGTGTATCAAGAAATTCAACAGTCAGATACTTTGATAAT 660
clone7          TTAATGGCAAATTTTGATCCCAGTGTATCAAGAAATTCAACAGTCAGATACTTTGATAAT 660
                ************************************************************

chPlxdc2        GGCACAGCACTAGTTGTCCAGTGGGACCATGTTCACCTGCAGGATAATTACAACCTGGGC 720
clone7          GGCACAGCACTAGTTGTCCAGTGGGACCATGTTCACCTGCAGGATAATTACAACCTGGGC 720
                ************************************************************

chPlxdc2        AGTTTCACTTTTCAGGCCACCCTTCTCAATGATGGGCGTATCATTTTCGGCTACAAAGAA 780
clone7          AGTTTCACTTTTCAGGCCACCCTTCTCAATGATGGGCGTATCATTTTCGGCTACAAAGAA 780
                ************************************************************

chPlxdc2        ATTCCTGTCGCTGTGACACAGATAAGCTCAACCAACCACCCAGTGAAAGTTGGACTATCA 840
clone7          ATTCCTGTCGCTGTGACACAGATAAGCTCAACCAACCACCCAGTGAAAGTTGGACTATCA 840
                ************************************************************

chPlxdc2        GATGCATTTGTGGTTGTGCACAGGATCCAGCAAATTCCCAATGTCCGCAGAAGAACAATT 900
clone7          GATGCATTTGTGGTTGTGCACAGGATCCAGCAAATTCCCAATGTCCGCAGAAGAACAATT 900
                ************************************************************

chPlxdc2        TACGAATACCACAGGGTGGAGCTGCAGATGTCAAAGATTACAAATCTGTCAGCTGTTGAA 960
clone7          TACGAATACCACAGGGTGGAGCTGCAGATGTCAAAGATTACAAATCTGTCAGCTGTTGAA 960
                ************************************************************


chPlxdc2        ATGATACCTCTTCCAACTTGTCTCCAGTTTAACAGCTGTGGCCCCTGTGTCACTGCCCAG 1020
clone7          ATGATACCTCTTCCAACTTGTCTCCAGTTTAACAGCTGTGGCCCCTGTGTCACTGCCCAG 1020
                ************************************************************

chPlxdc2        ATTGGCTTCAACTGCAGCTGGTGCAGTAAACTCCAAAGATGCTCCAGCGGATTTGACCGT 1080
clone7          ATTGGCTTCAACTGCAGCTGGTGCAGTAAACTCCAAAGATGCTCCAGCGGATTTGACCGT 1080
                ************************************************************
```

```
chPlxdc2        CACCGACAAGATTGGGTAGACAGTGGCTGCCCTGAACAGTCAAAAGATAAGATTTGTGAG 1140
clone7          CACCGACAAGATTGGGTAGACAGTGGCTGCCCTGAAGAGTCAAAAGATAAGATTTGTGAG 1140
                ********************************** ************************

chPlxdc2        AAGAATATAGACACAACTGAAGCACCACTGTACTCTACCACCACTCTTCAACCAACCACC 1200
clone7          AAGAATATAGACACAACTGAAGCACCGCTGTACTCTACCACCACTCTTCAACCAACCACC 1200
                ************************** ********************************

chPlxdc2        ACAAAGTTCAGAGTTTTAACAACCACCAGAGGATTCACCAGCTCCCAGCTGCCAACCAGC 1260
clone7          ACAAAGTTCAGAGTTTTAACAACCACCAGAGGATTCACCAGCTCCCAGCTGCCAACCAGC 1260
                ************************************************************

chPlxdc2        CTACCCACAGAAGATGATACCAAGATAGCGCTGCACCTAAAAGATAATGGAGCTTCCACA 1320
clone7          CTACCCACAGAAGATGATACCAAGATAGCGCTGCACCTAAAAGATAATGGAGCTTCCACA 1320
                ************************************************************

chPlxdc2        GATGACAGCGCTGCAGAGAAAAAAGGCGGAACACTTCATGCTGGTTTAATCATCGGCATT 1380
clone7          GATGACAGCGCTGCAGAGAAAAAAGGCGGAACACTTCATGCTGGTTTAATCATCGGCATT 1380
                ************************************************************

chPlxdc2        CTAGTCCTGGTCCTCATCGTGGCTGCAGCCATCCTCGTGACTGTCTACATGTACCATCAT 1440
clone7          CTAGTCCTGGTCCTCATCGTGGCTGCAGCCATCCTCGTGACTGTCTACATGTACCATCAT 1440
                ************************************************************

chPlxdc2        CCAACATCAGCAGCCAGTCTCTTCTTCATAGAGCGGCGTCCGAGCAGATGGCCAGCAATG 1500
clone7          CCAACATCAGCAGCCAGTCTCTTCTTCATAGAGCGGCGTCCGAGCAGATGGCCAGCAATG 1500
                ************************************************************

chPlxdc2        AAATTCAGAAGAGGATCTGGACATCCTGCATATGCTGAAGTGGAACCAGTTGGAGAAAAA 1560
clone7          AAATTCAGAAGAGGATCTGGACATCCTGCATATGCTGAAGTGGAACCAGTTGGAGAAAAA 1560
                ************************************************************

chPlxdc2        GAAGGCTTCATTGTATCAGAGCAATGCTAA 1590
clone7          GAAGGCTTCATTGTATCAGAGCA------- 1583
                ***********************
```

Figure 5.6 Alignment of the PCR amplified chPlxdc2 transcript (Clone 7) against the EST predicted transcript. The *Plxdc2* insert in clone 7 differed to the predicted transcript at two points only, a C/G base change at 1117bp and an A/G base change at 1167bp (highlighted in yellow).

5.7 Alignment of translated *Plxdc2* cDNA against the EST predicted Plxdc2 protein sequence

```
Clone 7         MARLRRSKLAAGFLLLFQFLSERCQLAAGETPSQSRGVLYEVVQSFPGVEENVQVDARVN 60
ChPlxdc2        MARLRRSKLAAGFLLLFQFLSERCQLAAGETPSQSRGVLYEVVQSFPGVEENVQVDARVN 60
                ************************************************************

Clone 7         SHRWRRHSESLKSVNTNRASMGQDSSEPGGFTDLLLEEGHENATQIEEDTDHNYYTSRTY 120
ChPlxdc2        SHRWRRHSESLKSVNTNRASMGQDSSEPGGFTDLLLEEGHENATQIEEDTDHNYYTSRTY 120
                ************************************************************

Clone 7         GPYDSTSRDLWVNIDQMEKDKVKIHGILSNTHRQAARVNLSFDFPFYGHFLREITVATGG 180
ChPlxdc2        GPYDSTSRDLWVNIDQMEKDKVKIHGILSNTHRQAARVNLSFDFPFYGHFLREITVATGG 180
                ************************************************************

Clone 7         FIYTGEVVHRMLTATQYIAPLMANFDPSVSRNSTVRYFDNGTALVVQWDHVHLQDNYNLG 240
ChPlxdc2        FIYTGEVVHRMLTATQYIAPLMANFDPSVSRNSTVRYFDNGTALVVQWDHVHLQDNYNLG 240
                ************************************************************

Clone 7         SFTFQATLLNDGRIIFGYKEIPVAVTQISSTNHPVKVGLSDAFVVVHRIQQIPNVRRRTI 300
ChPlxdc2        SFTFQATLLNDGRIIFGYKEIPVAVTQISSTNHPVKVGLSDAFVVVHRIQQIPNVRRRTI 300
                ************************************************************

Clone 7         YEYHRVELQMSKITNLSAVEMIPLPTCLQFNSCGPCVTAQIGFNCSWCSKLQRCSSGFDR 360
ChPlxdc2        YEYHRVELQMSKITNLSAVEMIPLPTCLQFNSCGPCVTAQIGFNCSWCSKLQRCSSGFDR 360
                ************************************************************

Clone 7         HRQDWVDSGCPEESKDKICEKNIDTTEAPLYSTTTLQPTTTKFRVLTTTRGFTSSQLPTS 420
ChPlxdc2        HRQDWVDSGCPEQSKDKICEKNIDTTEAPLYSTTTLQPTTTKFRVLTTTRGFTSSQLPTS 420
                ***********:************************************************

Clone 7         LPTEDDTKIALHLKDNGASTDDSAAEKKGGTLHAGLIIGILVLVLIVAAAILVTVYMYHH 480
ChPlxdc2        LPTEDDTKIALHLKDNGASTDDSAAEKKGGTLHAGLIIGILVLVLIVAAAILVTVYMYHH 480
                ************************************************************

Clone 7         PTSAASLFFIERRPSRWPAMKFRRGSGHPAYAEVEPVGEKEGFIVSE-- 527
ChPlxdc2        PTSAASLFFIERRPSRWPAMKFRRGSGHPAYAEVEPVGEKEGFIVSEQC 529
                *********************************************
```

Figure 5.7 Alignment of the translated Plxdc2 cDNA clone (Clone 7) against the EST predicted protein sequence. A single amino acid difference in the translated protein at amino acid 373 corresponds to the annotation of glutamic acid at this location in the Ensembl and NCBI predicted *Plxdc2* proteins. Underlined green font, signal peptide; blue font, region of Nidogen homology; underlined red font, PSI domain; underlined, bold black font, transmembrane domain.

5.8 Antibodies

Primary Antibody	Dilution.	Secondary Antibody	Dilution
Mouse Anti-Neurofilament (DSHB)	1:100 (IHC)	Goat anti-Mouse Cy3 (Jackson Laboratories)	1:500 (ICC, IHC)
Rabbit anti-GFP (A11122, Invitrogen)	1:1000 (ICC, IHC)	Donkey anti-Rabbit Alexa 488 (A21206, Invitrogen)	1:500 (ICC, IHC)
mouse anti-myc 9E10 (DSHB)	1:200 (ICC, IHC) 1:2000 (WB)	Goat anti-Mouse Cy3 (Jackson Laboratories)	1:500 (ICC, IHC)
Mouse anti-FLAG M2 (F1804, Sigma-Aldrich)	1:1000 (ICC)	Goat anti-Mouse Cy3 (Jackson Laboratories)	1:500 (ICC)
Mouse anti-βactin (A2228, Sigma)	1:2000 (WB)	Goat Anti-Mouse HRP (Jackson Laboratories)	1:10,000 (WB)
Mouse anti-BrdU (DSHB)	1:1000 (IHC)	Goat anti-Mouse Cy3 (Jackson Laboratories)	1:500 (IHC)

Table 5.1 List of primary and secondary antibodies used in immunocytochemistry (ICC), immunohistochemistry (IHC) and western blot (WB) analysis

5.9 Western Blot Analysis

Denaturing Separating Gel (10%)

Protogel (National Diagnostics)	3.30ml
1.5M Tris-HCl pH 8.8	2.50ml
10% APS	0.10ml
10% SDS	0.10ml
H_20	4.00ml
TEMED	0.04ml

Denaturing Stacking Gel (5%)

Protogel (National Diagnostics)	3.40ml
1M Tris-HCl pH 6.8	0.63ml
10% APS	0.05ml
10% SDS	0.05ml
H_20	3.40ml
TEMED	0.005ml

Gel Running Buffer (1x)

Tris	3.02g
Glycine	18.8g
10% SDS	10.0ml
H_20 to 1L	

Transfer Buffer

Tris	3.03g
Glycine	14.44g
Methanol	200ml

H_20 to 1L

TBS

0.5M Tris pH 7.5

1.5M NaCl

5.10 Summary Data

Experiment	Number of Specimens	Specimen ID	HH Stage	Analysis	Thickening Ratio	Max. thickening Ratio
chPlxdc2-Myc	7	A	15	OPT	1.20	1.29
				OPT	1.21	
				OPT	1.04	
				OPT	1.25	
				OPT	1.29	
		B	16	OPT	1.49	1.49
		C	16	OPT	1.30	1.42
				OPT	1.42	
				OPT	1.15	
		D	16	OPT	1.01	1.25
				OPT	1.25	
		E	17	OPT	1.23	1.23
				OPT	1.16	
		F	17	OPT	1.24	
				OPT	1.25	1.25
				OPT	1.23	
				OPT	1.12	
		G	17	OPT	1.17	1.30
				OPT	1.30	
Plxdc2-AP	5	A	17	cryostat	1.18	1.27
				cryostat	1.27	
				cryostat	1.22	
				cryostat	1.14	
		B	17	cryostat	1.60	1.60
				cryostat	1.53	
				cryostat	1.37	

		C	16	cryostat	1.34	1.34
				cryostat	1.33	
				cryostat	1.24	
				cryostat	1.24	
		D	17	cryostat	1.25	1.56
				cryostat	1.14	
				cryostat	1.48	
				cryostat	1.56	
		E	18	cryostat	1.30	1.35
				cryostat	1.11	
				cryostat	1.18	
				cryostat	1.11	
				cryostat	1.20	
				cryostat	1.35	
				cryostat	1.09	
shRNA1&3	6	A	18	OPT	1.12	1.12
(MHB)		B	18	OPT	0.93	0.93
		C	18	OPT	0.97	0.97
		D	18	OPT	0.99	0.99
		E	17	OPT	1.19	1.19
		F	15	OPT	1.03	1.03
chPlxdc2-Myc &	6	A	17	cryostat	1.03	1.26
shRNA1&3				cryostat	1.12	
				cryostat	1.12	
				cryostat	0.97	
				cryostat	1.26	
				cryostat	0.97	
				cryostat	1.20	
		B	18	cryostat	1.18	1.18
				cryostat	0.98	

				cryostat	1.09	
				cryostat	0.92	
				cryostat	0.90	
				cryostat	0.91	
		C	18	cryostat	0.92	0.99
				cryostat	0.91	
				cryostat	0.99	
				cryostat	0.96	
		D	17	cryostat	1.07	1.15
				cryostat	0.99	
				cryostat	1.15	
				cryostat	0.92	
				cryostat	1.08	
				cryostat	1.14	
				cryostat	1.14	
				cryostat	1.03	
				cryostat	1.07	
		E	18	cryostat	0.90	0.99
				cryostat	0.93	
				cryostat	0.84	
				cryostat	0.95	
				cryostat	0.92	
				cryostat	0.86	
				cryostat	0.84	
				cryostat	0.99	
				cryostat	0.98	
				cryostat	0.88	
				cryostat	0.90	
				cryostat	0.96	
				cryostat	0.82	

				cryostat	0.87	
				cryostat	0.98	
				cryostat	0.94	
		F	16	cryostat	1.19	1.24
				cryostat	1.21	
				cryostat	1.24	
				cryostat	1.24	
				cryostat	1.20	
				cryostat	1.12	
				cryostat	1.00	
				cryostat	1.09	
CONTROLS:	10					
pcDNA3.1myc-	6	A	17	OPT	0.96	1.07
His (B)				OPT	1.07	
		B	18	vibratome	1.03	1.03
		C	16	vibratome	1.04	1.04
		D	16	cryostat	0.91	1.08
				cryostat	0.93	
				cryostat	0.97	
				cryostat	1.00	
				cryostat	1.08	
				cryostat	1.06	
		E	18	cryostat	1.10	1.11
				cryostat	1.08	
				cryostat	1.04	
				cryostat	1.11	
		F	18	cryostat	0.96	1.08
				cryostat	0.92	
				cryostat	1.08	
pAPtag5	2	G	16	cryostat	0.96	1.04

				cryostat	1.04	
				cryostat	0.98	
				cryostat	0.96	
				cryostat	0.96	
				cryostat	0.98	
				cryostat	1.03	
				cryostat	1.01	
		H	17	cryostat	0.98	1.15
				cryostat	1.07	
				cryostat	1.01	
				cryostat	1.05	
				cryostat	0.94	
				cryostat	0.97	
				cryostat	1.04	
				cryostat	0.93	
				cryostat	1.00	
				cryostat	1.15	
pCA-β-	2	I	16	OPT	0.98	0.98
EGFPm5-U6				OPT	0.92	
		J	16	OPT	0.99	1.01
				OPT	1.01	

5.11 Control Images

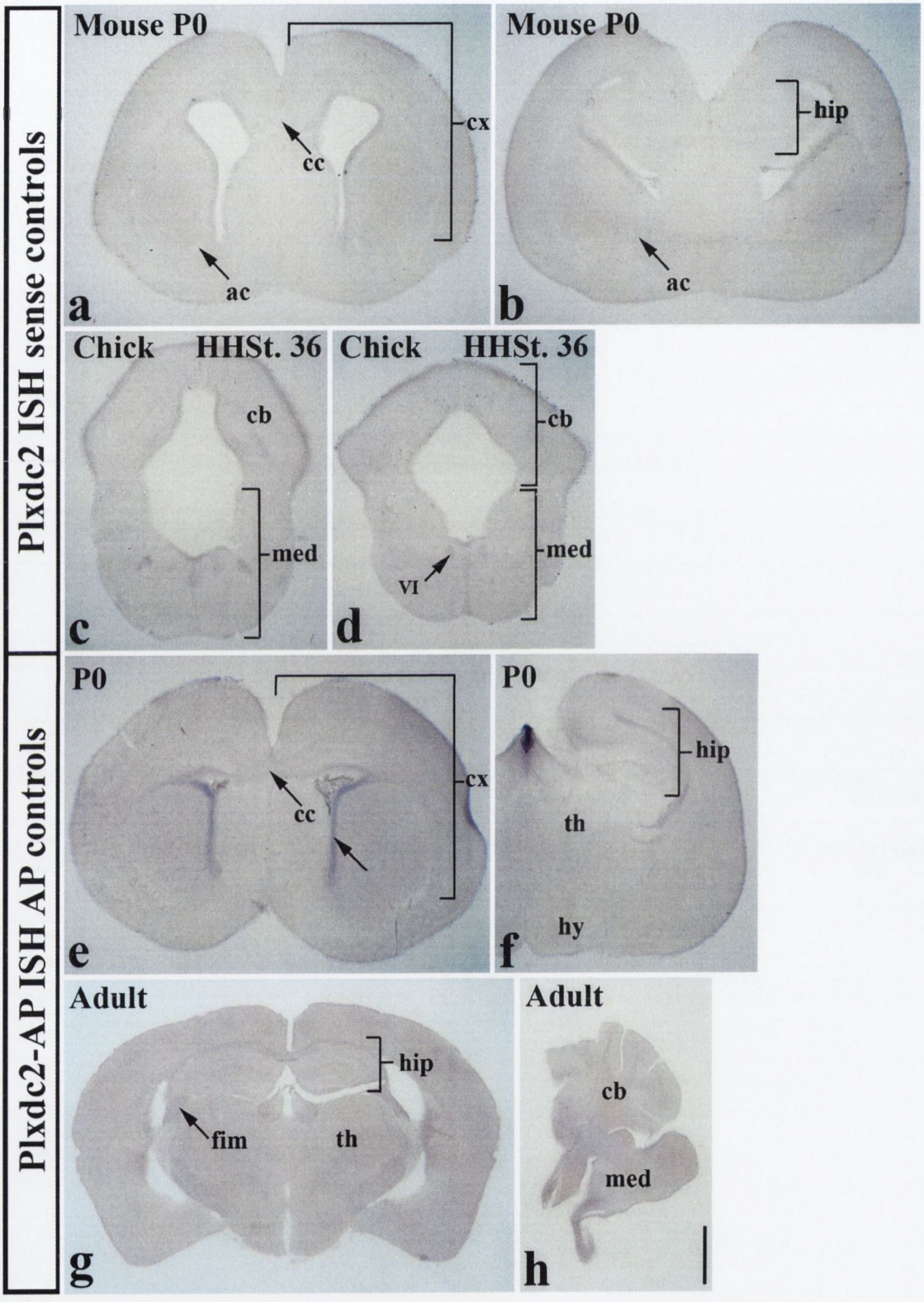

Figure 5.8 Representative images of controls for *in situ* hybridisation experiments. Sense controls were routinely used in *in situ* hybridisation experiments and were consistently clear of specific staining. a and b, *In situ* hybridisation of coronal sections through the brain of a P0 wildtype mouse using the sense probe for mouse *Plxdc2*. c and d, *In situ* hybridisation of coronal sections through the hindbrain of a HH stage 36 chick using the sense probe for chick *Plxdc2* described in section 3.3.1. AP produced by the pAPtag-5 plasmid (Genhunter) was routinely used as a negative control in AP *in situ* hybridisation experiments. e and f, AP *in situ* hybridisation of coronal sections through the brain of a P0 wildtype mouse using AP as a probe. arrow in e, background staining in the epithelium of the lateral ventricle. g and h, AP *in situ* hybridisation of coronal and sagittal section through the brain of an adult mouse respectively using AP as a probe. ac, anterior commissure; cb, cerebellum; cc, corpus callosum; cx, cortex; fim, fimbria; hip, hippocampus; hy, hypothalamus; med, medulla oblongata; th, thalamus; VI, abducens nucleus. Scale bar: a, b, e and f, 450μm; c and d, 500μm; g and h, 1mm.

6. References

ABRAMOFF, M.D., MAGELHAES, P.J., RAM, S.J. (2004) Image Processing with ImageJ. *Biophotonics International*, 11:7, 36-42.

ACAMPORA, D., MAZAN, S., LALLEMAND, Y., AVANTAGGIATO, V., MAURY, M., SIMEONE, A. & BRULET, P. (1995) Forebrain and Midbrain Regions Are Deleted in Otx2(-/-) Mutants Due to a Defective Anterior Neuroectoderm Specification During Gastrulation. *Development,* 121, 3279-3290.

AHLGREN, S., VOGT, P. & BRONNER-FRASER, M. (2003) Excess FoxG1 causes overgrowth of the neural tube. *Journal of Neurobiology,* 57, 337-349.

ALEXANDRE, D., CLARKE, J. D. W., OXTOBY, E., YAN, Y. L., JOWETT, T. & HOLDER, N. (1996) Ectopic expression of Hoxa-1 in the zebrafish alters the fate of the mandibular arch neural crest and phenocopies a retinoic acid-induced phenotype. *Development,* 122, 735-746.

ALNEMRI, E. S., LIVINGSTON, D. J., NICHOLSON, D. W., SALVESEN, G., THORNBERRY, N. A., WONG, W. W. & YUAN, J. (1996) Human ICE/CED-3 protease nomenclature. *Cell,* 87, 171.

ANDERSON, S. A., QIU, M. S., BULFONE, A., EISENSTAT, D. D., MENESES, J., PEDERSEN, R. & RUBENSTEIN, J. L. R. (1997) Mutations of the homeobox genes Dlx-1 and Dlx-2 disrupt the striatal subventricular zone and differentiation of late born striatal neurons. *Neuron,* 19, 27-37.

ANG, S. L., JIN, O., RHINN, M., DAIGLE, N., STEVENSON, L. & ROSSANT, J. (1996) A targeted mouse Otx2 mutation leads to severe defects in gastrulation and formation of axial mesoderm and to deletion of rostral brain. *Development,* 122, 243-252.

ASAYESH, A., SHARPE, J., WATSON, R. P., HECKSHER-SORENSEN, J., HASTIE, N. D., HILL, R. E. & AHLGREN, U. (2006) Spleen versus pancreas: strict control of organ interrelationship revealed by analyses of Bapx1(-/-) mice. *Genes & Development,* 20, 2208-2213.

AUGSBURGER, A., SCHUCHARDT, A., HOSKINS, S., DODD, J. & BUTLER, S. (1999) BMPs as mediators of roof plate repulsion of commissural neurons. *Neuron,* 24, 127-141.

BAGLIONI, C. & NILSEN, T. W. (1983) Mechanisms of antiviral action of interferon. *Interferon,* 5, 23-42.

BAI, S., KOPAN, R., ZOU, W., HILTON, M. J., ONG, C. T., LONG, F. X., ROSS, F. P. & TEITELBAUM, S. L. (2008) NOTCH1 regulates osteoclastogenesis directly in osteoclast precursors and indirectly via osteoblast lineage cells. *Journal of Biological Chemistry,* 283, 6509-6518.

BASILE, J. R., CASTILHO, R. M., WILLIAMS, V. P. & GUTKIND, J. S. (2006) Semaphorin 4D provides a link between axon guidance processes and tumor-induced angiogenesis. *Proc Natl Acad Sci U S A,* 103, 9017-22.

BEATY, R. M., EDWARDS, J. B., BOON, K., SIU, I. M., CONWAY, J. E. & RIGGINS, G. J. (2007) PLXDC1 (TEM7) is identified in a genome-wide expression screen of glioblastoma endothelium. *Journal of Neuro-Oncology,* 81, 241-248.

BECKER, E. B. E. & BONNI, A. (2005) Beyond proliferation - cell cycle control of neuronal survival and differentiation in the developing mammalian brain. *Seminars in Cell & Developmental Biology,* 16, 439-448.

BECKER, E. B. E., HOWELL, J., KODAMA, Y., BARKER, P. A. & BONNI, A. (2004) Characterization of the c-Jun N-terminal kinase-Bim(EL) signaling pathway in neuronal apoptosis. *Journal of Neuroscience,* 24, 8762-8770.

BELL, E., ENSINI, M., GULISANO, M. & LUMSDEN, A. (2001) Dynamic domains of gene expression in the early avian forebrain. *Developmental Biology,* 236, 76-88.

BELL, E., WINGATE, R. J. T. & LUMSDEN, A. (1999) Homeotic transformation of rhombomere identity after localized Hoxb1 misexpression. *Science,* 284, 2168-2171.

BELL, E. J. D. & BRICKELL, P. M. (1997) Replication-competent retroviral vectors for expressing genes in avian cells in vitro and in vivo. *Molecular Biotechnology,* 7, 289-298.

BERTRAND, N., CASTRO, D. S. & GUILLEMOT, F. (2002) Proneural genes and the specification of neural cell types. *Nature Reviews Neuroscience,* 3, 517-530.

BIBEL, M., RICHTER, J., LACROIX, E. & BARDE, Y. A. (2007) Generation of a defined and uniform population of CNS progenitors and neurons from mouse embryonic stem cells. *Nature Protocols,* 2, 1034-1043.

BIBEL, M., RICHTER, J., SCHRENK, K., TUCKER, K. L., STAIGER, V., KORTE, M., GOETZ, M. & BARDE, Y. A. (2004) Differentiation of mouse embryonic stem cells into a defined neuronal lineage. *Nature Neuroscience,* 7, 1003-1009.

BIELENBERG, D. R. & KLAGSBRUN, M. (2007) Targeting endothelial and tumor cells with semaphorins. *Cancer and Metastasis Reviews,* 26, 421-431.

BORK, P., DOERKS, T., SPRINGER, T. A. & SNEL, B. (1999) Domains in plexins: links to integrins and transcription factors. *Trends Biochem Sci,* 24, 261-3.

BOURIKAS, D., PEKARIK, V., BAERISWYL, T., GRUNDITZ, A., SADHU, R., NARDO, M. & STOECKLI, E. T. (2005) Sonic hedgehog guides commissural axons along the longitudinal axis of the spinal cord. *Nature Neuroscience,* 8, 297-304.

BOUWMEESTER, T., KIM, S. H., SASAI, Y., LU, B. & DEROBERTIS, E. M. (1996) Cerberus is a head-inducing secreted factor expressed in the anterior endoderm of Spemann's organizer. *Nature,* 382, 595-601.

BRAND, M., HEISENBERG, C. P., JIANG, Y. J., BEUCHLE, D., LUN, K., FURUTANISEIKI, M., GRANATO, M., HAFFTER, P., HAMMERSCHMIDT, M., KANE, D. A., KELSH, R. N., MULLINS, M. C., ODENTHAL, J., VANEEDEN, F. J. M. & NUSSLEINVOLHARD, C. (1996) Mutations in zebrafish genes affecting the formation of the boundary between midbrain and hindbrain. *Development,* 123, 179-190.

BRISCOE, J. & ERICSON, J. (1999) The specification of neuronal identity by graded sonic hedgehog signalling. *Seminars in Cell & Developmental Biology,* 10, 353-362.

BROCCOLI, V., BONCINELLI, E. & WURST, W. (1999) The caudal limit of Otx2 expression positions the isthmic organizer. *Nature,* 401, 164-168.

BRODSKI, C., WEISENHORN, D. M. V., SIGNORE, M., SILLABER, I., OESTERHELD, M., BROCCOLI, V., ACAMPORA, D., SIMEONE, A. & WURST, W. (2003) Location and size of dopaminergic and serotonergic cell populations are controlled by the position of the midbrain hindbrain organizer. *Journal of Neuroscience,* 23, 4199-4207.

BRON, R., EICKHOLT, B. J., VERMEREN, M., FRAGALE, N. & COHEN, J. (2004) Functional knockdown of neuropilin-1 in the developing chick nervous system by siRNA hairpins phenocopies genetic ablation in the mouse. *Developmental Dynamics,* 230, 299-308.

BRUMMELKAMP, T. R., BERNARDS, R. & AGAMI, R. (2002) A system for stable expression of short interfering RNAs in mammalian cells. *Science,* 296, 550-553.

BUNCH, T. A., HELSTEN, T. L., KENDALL, T. L., SHIRAHATTI, N., MAHADEVAN, D., SHATTIL, S. J. & BROWER, D. L. (2006) Amino acid changes in Drosophila alphaPS2betaPS integrins that affect ligand affinity. *J Biol Chem,* 281, 5050-7.

BUTLER, S. J. & DODD, J. (2003) A role for BMP heterodimers in roof plate-mediated repulsion of commissural axons. *Neuron,* 38, 389-401.

BYLUND, M., ANDERSSON, E., NOVITCH, B. G. & MUHR, J. (2003) Vertebrate neurogenesis is counteracted by Sox1-3 activity. *Nature Neuroscience,* 6, 1162-1168.

CAMPBELL, D. H., SUTHERLAND, R. L. & DALY, R. J. (1999) Signaling pathways and structural domains required for phosphorylation of EMS1/cortactin. *Cancer Research,* 59, 5376-5385.

CAMPOS, L. S., DUARTE, A. J., BRANCO, T. & HENRIQUE, D. (2001) mDll1 and mDll3 expression in the developing mouse brain: Role in the establishment of the early cortex. *Journal of Neuroscience Research,* 64, 590-598.

CANNING, C. A., LEE, L., IRVING, C., MASON, I. & JONES, C. M. (2007) Sustained interactive Wnt and FGF signaling is required to maintain isthmic identity. *Dev Biol,* 305, 276-86.

CARMELIET, P. & TESSIER-LAVIGNE, M. (2005) Common mechanisms of nerve and blood vessel wiring. *Nature,* 436, 193-200.

CARSON-WALTER, E. B., WATKINS, D. N., NANDA, A., VOGELSTEIN, B., KINZLER, K. W. & CROIX, B. S. (2001) Cell surface tumor endothelial markers are conserved in mice and humans. *Cancer Research,* 61, 6649-6655.

CECCONI, F., ALVAREZ-BOLADO, G., MEYER, B. I., ROTH, K. A. & GRUSS, P. (1998) Apaf1 (CED-4 homolog) regulates programmed cell death in mammalian development. *Cell,* 94, 727-737.

CHAPMAN, S. C., BROWN, R., LEES, L., SCHOENWOLF, G. C. & LUMSDEN, A. (2004) Expression analysis of chick Wnt and frizzled genes and selected inhibitors in early chick patterning. *Dev Dyn,* 229, 668-76.

CHARRON, F., STEIN, E., JEONG, J., MCMAHON, A. P. & TESSIER-LAVIGNE, M. (2003) The morphogen Sonic hedgehog is an axonal chemoattractant that collaborates with Netrin-1 in midline axon guidance. *Cell,* 113, 11-23.

CHARRON, F. & TESSIER-LAVIGNE, M. (2005) Novel brain wiring functions for classical morphogens: a role as graded positional cues in axon guidance. *Development,* 132, 2251-2262.

CHEN, H., THIAGALINGAM, A., CHOPRA, H., BORGES, M. W., FEDER, J. N., NELKIN, B. D., BAYLIN, S. B. & BALL, D. W. (1997) Conservation of the Drosophila lateral inhibition pathway in human lung cancer: A hairy-related protein (HES-1) directly represses achaete-scute homolog-1 expression. *Proceedings of the National Academy of Sciences of the United States of America,* 94, 5355-5360.

CHENN, A. & WALSH, C. A. (2002) Regulation of cerebral cortical size by control of cell cycle exit in neural precursors. *Science,* 297, 365-369.

CHESNUTT, C., BURRUS, L. W., BROWN, A. M. C. & NISWANDER, L. (2004) Coordinate regulation of neural tube patterning and proliferation by TGF beta and WNT activity. *Developmental Biology,* 274, 334-347.

CHESNUTT, C. & NISWANDER, L. (2004) Plasmid-based short-hairpin RNA interference in the chicken embryo. *Genesis,* 39, 73-78.

CHEUNG, A. F., POLLEN, A. A., TAVARE, A., DEPROTO, J. & MOLNAR, Z. (2007) Comparative aspects of cortical neurogenesis in vertebrates. *J Anat,* 211, 164-76.

CHI, C. L., MARTINEZ, S., WURST, W. & MARTIN, G. R. (2003) The isthmic organizer signal FGF8 is required for cell survival in the prospective midbrain and cerebellum. *Development,* 130, 2633-2644.

CHIANG, C., YING, L. T. T., LEE, E., YOUNG, K. E., CORDEN, J. L., WESTPHAL, H. & BEACHY, P. A. (1996) Cyclopia and defective axial patterning in mice lacking Sonic hedgehog gene function. *Nature,* 383, 407-413.

CONTI, L., POLLARD, S. M., GORBA, T., REITANO, E., TOSELLI, M., BIELLA, G., SUN, Y., SANZONE, S., YING, Q. L., CATTANEO, E. & SMITH, A. (2005) Niche-independent symmetrical self-renewal of a mammalian tissue stem cell. *PLoS Biol,* 3, e283.

CROSSLEY, P. H., MARTINEZ, S. & MARTIN, G. R. (1996) Midbrain development induced by FGF8 in the chick embryo. *Nature,* 380, 66-68.

DAS, R. M., VAN HATEREN, N. J., HOWELL, G. R., FARRELL, E. R., BANGS, F. K., PORTEOUS, V. C., MANNING, E. M., MCGREW, M. J., OHYAMA, K., SACCO, M. A., HALLEY, P. A., SANG, H. M., STOREY, K. G., PLACZEK, M., TICKLE, C., NAIR, V. K. & WILSON, S. A. (2006) A robust system for RNA interference in the chicken using a modified microRNA operon. *Developmental Biology,* 294, 554-563.

DICKINSON, M. E., KRUMLAUF, R. & MCMAHON, A. P. (1994) Evidence for a Mitogenic Effect of Wnt-1 in the Developing Mammalian Central-Nervous-System. *Development,* 120, 1453-1471.

DICKSON, B. J. (2002) Molecular mechanisms of axon guidance. *Science,* 298, 1959-1964.

DOLAN, J., WALSHE, K., ALSBURY, S., HOKAMP, K., O'KEEFFE, S., OKAFUJI, T., MILLER, S. F., TEAR, G. & MITCHELL, K. J. (2007) The extracellular leucine-rich repeat superfamily; a comparative survey and analysis of evolutionary relationships and expression patterns. *BMC Genomics,* 8, 320.

DONOVAN, N., BECKER, E. B. E., KONISHI, Y. & BONNI, A. (2002) JNK phosphorylation and activation of BAD couples the stress-activated signaling pathway to the cell death machinery. *Journal of Biological Chemistry,* 277, 40944-40949.

DOUARIN, N. L. (1973) Biological Cell Labeling Technique and Its Use in Experimental Embryology. *Developmental Biology,* 30, 217-222.

ECHEVARRIA, D., VIEIRA, C., GIMENO, L. & MARTINEZ, S. (2003) Neuroepithelial secondary organizers and cell fate specification in the developing brain. *Brain Research Reviews,* 43, 179-191.

ENGELMANN, M., LANDGRAF, R. & WOTJAK, C., T. (2004) The hypothalamic-neurohypophysial system regulates the hypothalamic-pituitary-adrenal axis under stress: An old concept revisited. *Frontiers in Neuroendocrinology* 25, 132-149.

ERICKSON, A. C. & COUCHMAN, J. R. (2000) Still more complexity in mammalian basement membranes. *J Histochem Cytochem,* 48, 1291-306.

ERICSON, J., MUHR, J., PLACZEK, M., LINTS, T., JESSELL, T. M. & EDLUND, T. (1995) Sonic Hedgehog Induces the Differentiation of Ventral Forebrain Neurons - a Common Signal for Ventral Patterning within the Neural-Tube. *Cell,* 81, 747-756.

FIRE, A., XU, S. Q., MONTGOMERY, M. K., KOSTAS, S. A., DRIVER, S. E. & MELLO, C. C. (1998) Potent and specific genetic interference by double-stranded RNA in Caenorhabditis elegans. *Nature,* 391, 806-811.

FISHER, M. E., CLELLAND, A. K., BAIN, A., BALDOCK, R. A., MURPHY, P., DOWNIE, H., TICKLE, C., DAVIDSON, D. R. & BUCKLAND, R. A. (2008) Integrating technologies for comparing 3D gene expression domains in the developing chick limb. *Developmental Biology,* 317, 13-23.

FREITAS, C., LARRIVEE, B. & EICHMANN, A. (2008) Netrins and UNC5 receptors in angiogenesis. *Angiogenesis,* 11, 23-29.

FRIEDEL, R. H., PLUMP, A., LU, X. W., SPILKER, K., JOLICOEUR, C., WONG, K., VENKATESH, T. R., YARON, A., HYNES, M., CHEN, B., OKADA, A., MCCONNELL, S. K., RAYBURN, H. & TESSIER-LAVIGNE, M. (2005) Gene targeting using a promoterless gene trap vector ("targeted trapping") is an efficient method to mutate a large fraction of genes. *Proceedings of the National Academy of Sciences of the United States of America,* 102, 13188-13193.

FUCHS, B., MAHLUM, E., HALDER, C., MARAN, A., YASZEMSKI, M., BODE, B., BOLANDER, M. & SARKAR, G. (2007) High expression of tumor endothelial marker 7 is associated with metastasis and poor survival of patients with osteogenic sarcoma. *Gene,* 399, 137-143.

FUNAHASHI, J., OKAFUJI, T., OHUCHI, H., NOJI, S., TANAKA, H. & NAKAMURA, H. (1999) Role of Pax-5 in the regulation of a mid-hindbrain organizer's activity. *Development Growth & Differentiation,* 41, 59-72.

FURUTA, Y., PISTON, D. W. & HOGAN, B. L. (1997) Bone morphogenetic proteins (BMPs) as regulators of dorsal forebrain development. *Development,* 124, 2203-12.

FUTAMURA, M., KAMINO, H., MIYAMOTO, Y., KITAMURA, N., NAKAMURA, Y., OHNISHI, S., MASUDA, Y. & ARAKAWA, H. (2007) Possible role of semaphorin 3F, a candidate tumor suppressor gene at 3p2l1.3, in p53-regulated tumor angiogenesis suppression. *Cancer Research,* 67, 1451-1460.

GALCERAN, J., MIYASHITA-LIN, E. M., DEVANEY, E., RUBENSTEIN, J. L. & GROSSCHEDL, R. (2000) Hippocampus development and generation of dentate gyrus granule cells is regulated by LEF1. *Development,* 127, 469-82.

GARDA, A. L., PUELLES, L., RUBENSTEIN, J. L. R. & MEDINA, L. (2002) Expression patterns of Wnt8b and Wnt7b in the chicken embryonic brain suggest a correlation with forebrain patterning centers and morphogenesis. *Neuroscience,* 113, 689-698.

GARDNER, C. A. & BARALD, K. F. (1991) The Cellular Environment Controls the Expression of Engrailed-Like Protein in the Cranial Neuroepithelium of Quail Chick Chimeric Embryos. *Development,* 113, 1037-1048.

GLINKA, A., WU, W., DELIUS, H., MONAGHAN, A. P., BLUMENSTOCK, C. & NIEHRS, C. (1998) Dickkopf-1 is a member of a new family of secreted proteins and functions in head induction. *Nature,* 391, 357-362.

GLINKA, A., WU, W., ONICHTCHOUK, D., BLUMENSTOCK, C. & NIEHRS, C. (1997) Head induction by simultaneous repression of Bmp and Wnt signalling in Xenopus. *Nature,* 389, 517-519.

GOLDEN, J. A., BRACILOVIC, A., MCFADDEN, K. A., BEESLEY, J. S., RUBENSTEIN, J. L. & GRINSPAN, J. B. (1999) Ectopic bone morphogenetic proteins 5 and 4 in the chicken forebrain lead to cyclopia and holoprosencephaly. *Proc Natl Acad Sci U S A,* 96, 2439-44.

GROVE, E. A., TOLE, S., LIMON, J., YIP, L. W. & RAGSDALE, C. W. (1998) The hem of the embryonic cerebral cortex is defined by the expression of multiple Wnt genes and is compromised in Gli3-deficient mice. *Development,* 125, 2315-2325.

GUILLEMOT, F. (2007) Spatial and temporal specification of neural fates by transcription factor codes. *Development,* 134, 3771-3780.

HAKEM, R., HAKEM, A., DUNCAN, G. S., HENDERSON, J. T., WOO, M., SOENGAS, M. S., ELIA, A., DE LA POMPA, J. L., KAGI, D., KHOO, W., POTTER, J., YOSHIDA, R., KAUFMAN, S. A., LOWE, S. W., PENNINGER, J. M. & MAK, T. W. (1998) Differential requirement for Caspase 9 in apoptotic pathways in vivo. *Cell,* 94, 339-352.

HAM, J., EILERS, A., WHITFIELD, J., NEAME, S. J. & SHAH, B. (2000) c-Jun and the transcriptional control of neuronal apoptosis. *Biochemical Pharmacology,* 60, 1015-1021.

HAMBURGER, V. & HAMILTON, H., L. (1951) A series of normal stages in the development of the chick embryo. *Journal of Morphology*, 88:1, 49-92.

HARPAVAT, S. & CEPKO, C. L. (2006) RCAS-RNAi: A loss-of-function method for the developing chick retina. *Bmc Developmental Biology,* 6.

HARPER, S. J. & LOGRASSO, P. (2001) Signalling for survival and death in neurones - The role of stress-activated kinases, JNK and p38. *Cellular Signalling,* 13, 299-310.

HASHIMOTO-TORII, K., MOTOYAMA, J., HUI, C. C., KUROIWA, A., NAKAFUKU, M. & SHIMAMURA, K. (2003) Differential activities of Sonic hedgehog mediated by Gli transcription factors define distinct neuronal subtypes in the dorsal thalamus. *Mechanisms of Development,* 120, 1097-1111.

HATAKEYAMA, J., BESSHO, Y., KATOH, K., OOKAWARA, S., FUJIOKA, M., GUILLEMOT, F. & KAGEYAMA, R. (2004) Hes genes regulate size, shape and histogenesis of the nervous system by control of the timing of neural stem cell differentiation. *Development,* 131, 5539-5550.

HAVENS, B. A., VELONIS, D., KRONENBERG, M. S., LICHTLER, A. C., OLIVER, B. & MINA, M. (2008) Roles of FGFR3 during morphogenesis of Meckel's cartilage and mandibular bones. *Developmental Biology,* 316, 336-349.

HEBERT, J. M., MISHINA, Y. & MCCONNELL, S. K. (2002) BMP signaling is required locally to pattern the dorsal telencephalic midline. *Neuron,* 35, 1029-41.

HIRABAYASHI, Y., ITOH, Y., MASUYAMA, N. & GOTOH, Y. (2004) The Wnt-beta-catenin pathway directs neuronal differentiation of cortical neural precursor cells. *Cell Structure and Function,* 29, 83-83.

HOLLYDAY, M., MCMAHON, J. A. & MCMAHON, A. P. (1995) Wnt expression patterns in chick embryo nervous system. *Mech Dev,* 52, 9-25.

HOLMBERG, J., HANSSON, E., MALEWICZ, M., SANDBERG, M., PERLMANN, T., LENDAHL, U. & MUHR, J. (2008) SoxB1 transcription factors and Notch signaling use distinct mechanisms to regulate proneural gene function and neural progenitor differentiation. *Development,* 135, 1843-1851.

HONJO, T. (1996) The shortest path from the surface to the nucleus: RBP-J kappa/Su(H) transcription factor. *Genes to Cells,* 1, 1-9.

HOOPER, M., HARDY, K., HANDYSIDE, A., HUNTER, S. & MONK, M. (1987) HPRT-deficient (Lesch-Nyhan) mouse embryos derived from germline colonization by cultured cells. *Nature,* 326, 292-5.

HOUART, C., CANEPARO, L., HEISENBERG, C. P., BARTH, K. A., TAKE-UCHI, M. & WILSON, S. W. (2002) Establishment of the telencephalon during gastrulation by local antagonism of Wnt signaling. *Neuron,* 35, 255-265.

HOUART, C., WESTERFIELD, M. & WILSON, S. W. (1998) A small population of anterior cells patterns for forebrain during zebrafish gastrulation. *Nature,* 391, 788-792.

HUANG, C., LIU, J. L., HAUDENSCHILD, C. C. & ZHAN, X. (1998) The role of tyrosine phosphorylation of cortactin in the locomotion of endothelial cells. *Journal of Biological Chemistry,* 273, 25770-25776.

HUANG, X., LITINGTUNG, Y. & CHIANG, C. (2007) Ectopic sonic hedgehog signaling impairs telencephalic dorsal midline development: implication for human holoprosencephaly. *Hum Mol Genet,* 16, 1454-68.

IJPENBERG, A., PEREZ-POMARES, J. M., GUADIX, J. A., CARMONA, R., PORTILLO-SANCHEZ, V., MACIAS, D., HOHENSTEIN, P., MILES, C. M., HASTIE, N. D. & MUNOZ-CHAPULI, R. (2007) Wt1 and retinoic acid signaling are essential for stellate cell development and liver morphogenesis. *Dev Biol,* 312, 157-70.

IKEYA, M., LEE, S. M., JOHNSON, J. E., MCMAHON, A. P. & TAKADA, S. (1997) Wnt signalling required for expansion of neural crest and CNS progenitors. *Nature,* 389, 966-70.

INGLIS-BROADGATE, S. L., THOMSON, R. E., PELLICANO, F., TARTAGLIA, M. A., PONTIKIS, C. C., COOPER, J. D. & IWATA, T. (2005) FGFR3 regulates brain size by controlling progenitor cell proliferation and apoptosis during embryonic development. *Developmental Biology,* 279, 73-85.

IRVING, C. & MASON, I. (1999) Regeneration of isthmic tissue is the result of a specific and direct interaction between rhombomere 1 and midbrain. *Development,* 126, 3981-3989.

ISHIBASHI, M., ANG, S. L., SHIOTA, K., NAKANISHI, S., KAGEYAMA, R. & GUILLEMOT, F. (1995) Targeted disruption of mammalian hairy and Enhancer of split homolog-1 (HES-1) leads to up-regulation of neural helix-loop-helix factors, premature neurogenesis, and severe neural tube defects. *Genes & Development,* 9, 3136-3148.

ISHIBASHI, M. & MCMAHON, A. P. (2002) A sonic hedgehog-dependent signaling relay regulates growth of diencephalic and mesencephalic primordia in the early mouse embryo. *Development,* 129, 4807-4819.

ISHIBASHI, M., SAITSU, H., KOMADA, M. & SHIOTA, K. (2005) Signaling cascade coordinating growth of dorsal and ventral tissues of the vertebrate brain, with special reference to the involvement of Sonic Hedgehog signaling. *Anat Sci Int,* 80, 30-6.

ISHIKAWA, T., TAMAI, Y., ZORN, A. M., YOSHIDA, H., SELDIN, M. F., NISHIKAWA, S. & TAKETO, M. M. (2001) Mouse Wnt receptor gene Fzd5 is essential for yolk sac and placental angiogenesis. *Development,* 128, 25-33.

JARRIAULT, S., BROU, C., LOGEAT, F., SCHROETER, E. H., KOPAN, R. & ISRAEL, A. (1995) Signaling Downstream of Activated Mammalian Notch. *Nature,* 377, 355-358.

JASONI, C. L., WALKER, M. B., MORRIS, M. D. & REH, T. A. (1994) A chicken achaete-scute homolog (CASH-1) is expressed in a temporally and spatially discrete manner in the developing nervous system. *Development,* 120, 769-83.

KAGEYAMA, R., OHTSUKA, T., HATAKEYAMA, J. & OHSAWA, R. (2005) Roles of bHLH genes in neural stem cell differentiation. *Experimental Cell Research,* 306, 343-348.

KATAHIRA, T. & NAKAMURA, H. (2003) Gene silencing in chick embryos with a vector-based small interfering RNA system. *Development Growth & Differentiation,* 45, 361-367.

KEEBLE, T. R., HALFORD, M. M., SEAMAN, C., KEE, N., MACHEDA, M., ANDERSON, R. B., STACKER, S. A. & COOPER, H. M. (2006) The Wnt receptor Ryk is required for Wnt5a-mediated axon guidance on the contralateral side of the corpus callosum. *Journal of Neuroscience,* 26, 5840-5848.

KIECKER, C. & LUMSDEN, A. (2005) Compartments and their boundaries in vertebrate brain development. *Nature Reviews Neuroscience,* 6, 553-564.

KORINEK, V., BARKER, N., MORIN, P. J., VANWICHEN, D., DEWEGER, R., KINZLER, K. W., VOGELSTEIN, B. & CLEVERS, H. (1997) Constitutive transcriptional activation by a beta-catenin-Tcf complex in APC(-/-) colon carcinoma. *Science,* 275, 1784-1787.

KOS, R., REEDY, M. V., JOHNSON, R. L. & ERICKSON, C. A. (2001) The winged-helix transcription factor FoxD3 is important for establishing the neural crest lineage and repressing melanogenesis in avian embryos. *Development,* 128, 1467-1479.

KOS, R., TUCKER, R. P., HALL, R., DUONG, T. D. & ERICKSON, C. A. (2003) Methods for introducing morpholinos into the chicken embryo. *Developmental Dynamics,* 226, 470-477.

KRULL, C. E. (2004) A primer on using *in ovo* electroporation to analyze gene function. *Developmental Dynamics,* 229, 433-439.

KRUMLAUF, R. (1994) Hox Genes in Vertebrate Development. *Cell,* 78, 191-201.

KUAN, C. Y., YANG, D. D., ROY, D. R. S., DAVIS, R. J., RAKIC, P. & FLAVELL, R. A. (1999) The Jnk1 and Jnk2 protein kinases are required for regional specific apoptosis during early brain development. *Neuron,* 22, 667-676.

KUIDA, K., HAYDAR, T. F., KUAN, C. Y., GU, Y., TAYA, C., KARASUYAMA, H., SU, M. S. S., RAKIC, P. & FLAVELL, R. A. (1998) Reduced apoptosis and cytochrome c-mediated caspase activation in mice lacking Caspase 9. *Cell,* 94, 325-337.

KUIDA, K., ZHENG, T. S., NA, S. Q., KUAN, C. Y., YANG, D., KARASUYAMA, H., RAKIC, P. & FLAVELL, R. A. (1996) Decreased apoptosis in the brain and premature lethality in CPP32-deficient mice. *Nature,* 384, 368-372.

KUSY, S., NASARRE, P., CHAN, D., POTIRON, V., MEYRONET, D., GEMMILL, R. M., CONSTANTIN, B., DRABKIN, H. A. & ROCHE, J. (2005) Selective suppression of in vivo tumorigenicity by semaphorin SEMA3F in lung cancer cells. *Neoplasia,* 7, 457-465.

LARSEN, C. W., ZELTSER, L. M. & LUMSDEN, A. (2001) Boundary formation and compartition in the avian diencephalon. *Journal of Neuroscience,* 21, 4699-4711.

LE DOUARIN, N. M. (2004) The avian embryo as a model to study the development of the neural crest: a long and still ongoing story. *Mechanisms of Development,* 121, 1089-1102.

LECUYER, E., YOSHIDA, H., PARTHASARATHY, N., ALM, C., BABAK, T., CEROVINA, T., HUGHES, T. R., TOMANCAK, P. & KRAUSE, H. M. (2007) Global analysis of mRNA localization reveals a prominent role in organizing cellular architecture and function. *Cell,* 131, 174-87.

LEE, H. K., BAE, H. R., PARK, H. K., SEO, I. A., LEE, E. Y., SUH, D. J. & PARK, H. T. (2005) Cloning, characterization and neuronal expression profiles of tumor endothelial marker 7 in the rat brain. *Molecular Brain Research,* 136, 189-198.

LEE, H. K., KANG, D. S., SEO, I. A., CHOI, E. J., PARK, H. T. & PARK, J. I. (2006a) Expression of tumor endothelial marker 7 mRNA and protein in the dorsal root ganglion neurons of the rat. *Neurosci Lett,* 402, 71-5.

LEE, H. K., SEO, I. A., PARK, H. K. & PARK, H. T. (2006b) Identification of the basement membrane protein nidogen as a candidate ligand for tumor endothelial marker 7 in vitro and in vivo. *Febs Letters,* 580, 2253-2257.

LEE, H. K., SEO, I. A., PARK, H. K., PARK, Y. M., AHN, K. J., YOO, Y. H. & PARK, H. T. (2007) Nidogen is a prosurvival and promigratory factor for adult Schwann cells. *Journal of Neurochemistry,* 102, 686-698.

LEE, K. J. & JESSELL, T. M. (1999) The specification of dorsal cell fates in the vertebrate central nervous system. *Annual Review of Neuroscience,* 22, 261-294.

LEE, S. K. & PFAFF, S. L. (2003) Synchronization of neurogenesis and motor neuron specification by direct coupling of bHLH and homeodomain transcription factors. *Neuron,* 38, 731-745.

LEE, S. M. K., DANIELIAN, P. S., FRITZSCH, B. & MCMAHON, A. P. (1997) Evidence that FGF8 signalling from the midbrain-hindbrain junction regulates growth and polarity in the developing midbrain. *Development,* 124, 959-969.

LEE, S. M. K., TOLE, S., GROVE, E. & MCMAHON, A. P. (2000) A local Wnt-3a signal is required for development of the mammalian hippocampus. *Development,* 127, 457-467.

LEIGHTON, P. A., MITCHELL, K. J., GOODRICH, L. V., LU, X., PINSON, K., SCHERZ, P., SKARNES, W. C. & TESSIER-LAVIGNE, M. (2001a) Defining brain wiring patterns and mechanisms through gene trapping in mice. *Nature,* 410, 174-9.

LEYNS, L., BOUWMEESTER, T., KIM, S. H., PICCOLO, S. & DEROBERTIS, E. M. (1997) Frzb-1 is a secreted antagonist of Wnt signaling expressed in the Spemann organizer. *Cell,* 88, 747-756.

LILLIEN, L. (1998) Progenitor cells: What do they know and when do they know it? *Current Biology,* 8, R872-R874.

LIN, J. C. & CEPKO, C. L. (1998) Granule cell raphes and parasagittal domains of Purkinje cells: complementary patterns in the developing chick cerebellum. *Journal of Neuroscience*, 18, 9342-9353.

LITINGTUNG, Y. & CHIANG, C. (2000) Control of Shh activity and signaling in the neural tube. *Dev Dyn,* 219, 143-54.

LIU, A. M. & JOYNER, A. L. (2001) EN and GBX2 play essential roles downstream of FGF8 in patterning the mouse mid/hindbrain region. *Development,* 128, 181-191.

LIU, A. M., LOSOS, K. & JOYNER, A. L. (1999) FGF8 can activate Gbx2 and transform regions of the rostral mouse brain into a hindbrain. *Development,* 126, 4827-4838.

LIU, J., WILSON, S. & REH, T. (2003) BMP receptor 1b is required for axon guidance and cell survival in the developing retina. *Developmental Biology,* 256, 34-47.

LU, X. W., LE NOBLE, F., YUAN, L., JIANG, Q. J., DE LAFARGE, B., SUGIYAMA, D., BREANT, C., CLAES, F., DE SMET, F., THOMAS, J. L., AUTIERO, M., CARMELIET, P., TESSIER-LAVIGNE, M. & EICHMANN, A. (2004) The netrin receptor UNC5B mediates guidance events controlling morphogenesis of the vascular system. *Nature,* 432, 179-186.

LUMSDEN, A. & KRUMLAUF, R. (1996) Patterning the vertebrate neuraxis. *Science,* 274, 1109-1115.

LYUKSYUTOVA, A. I., LU, C. C., MILANESIO, N., KING, L. A., GUO, N. N., WANG, Y. S., NATHANS, J., TESSIER-LAVIGNE, M. & ZOU, Y. M. (2003) Anterior-posterior guidance of commissural Axons by Wnt-frizzled signaling. *Science,* 302, 1984-1988.

MAINE, E. M. (2008) Studying gene function in Caenorhabditis elegans using RNA-mediated interference. *Brief Funct Genomic Proteomic,* 7, 184-94.

MALPIGHI, M. (1672) De formatione pulli *in ovo*. Royal Society, London.

MALPIGHI, M. (1675) Repetitas auctasque de ovo incubato observationes continens. Johannis Martyn, London.

MARIN, F. & PUELLES, L. (1995) Morphological Fate of Rhombomeres in Quail-Chick Chimeras - a Segmental Analysis of Hindbrain Nuclei. *European Journal of Neuroscience,* 7, 1714-1738.

MARTINEZ, S., ALVARADOMALLART, R. M., MARTINEZDELATORRE, M. & PUELLES, L. (1991) Retinal and Tectal Connections of Embryonic Nucleus Superficialis Magnocellularis and Its Mature Derivatives in the Chick. *Anatomy and Embryology,* 183, 235-243.

MARTINEZ, S., CROSSLEY, P. H., COBOS, I., RUBENSTEIN, J. L. R. & MARTIN, G. R. (1999) FGF8 induces formation of an ectopic isthmic organizer and isthmocerebellar development via a repressive effect on Otx2 expression. *Development,* 126, 1189-1200.

MASCKAUCHAN, T. H. N. & KITAJEWSKI, J. (2006) Wnt/Frizzled signaling in the vasculature: New angiogenic factors in sight. *Physiology,* 21, 181-188.

MASCKAUCHAN, T. N. H., AGALLIU, D., VORONTCHIKHINA, M., AHN, A., PARMALEE, N. L., LI, C. M., KHOO, A., TYCKO, B., BROWN, A. M. C. & KITAJEWSKI, J. (2006) Wnt5a signaling induces proliferation and survival of endothelial cells in vitro and expression of MMP-1 and Tie-2. *Molecular Biology of the Cell,* 17, 5163-5172.

MATSUNAGA, E., KATAHIRA, T. & NAKAMURA, H. (2002) Role of Lmx1b and Wnt1 in mesencephalon and metencephalon development. *Development,* 129, 5269-5277.

MCMAHON, A. P. & BRADLEY, A. (1990) The Wnt-1 (Int-1) Protooncogene Is Required for Development of a Large Region of the Mouse-Brain. *Cell,* 62, 1073-1085.

MEGASON, S. G. & MCMAHON, A. P. (2002) A mitogen gradient of dorsal midline Wnts organizes growth in the CNS. *Development,* 129, 2087-2098.

MENA-SEGOVIA, J., BOLAM, P. & MAGILL, P. J. (2004) Pedunculopontine nucleus and basal ganglia: distant relatives or part of the same family? *Trends in Neurosciences* 27 (10), 585-588.

MENDE, M., NICOLAS, A., D., STREIT, A. (2008) Specific and effective gene knock-down in early chick embryos using morpholinos but not pRFPRNAi vectors. *Mechanisms of Development*, Epub ahead of print.

MEYERS, E. N., LEWANDOSKI, M. & MARTIN, G. R. (1998) An Fgf8 mutant allelic series generated by Cre- and Flp-mediated recombination. *Nature Genetics,* 18, 136-141.

MIELKE, K., DAMM, A., YANG, D. D. & HERDEGEN, T. (2000) Selective expression of JNK isoforms and stress-specific JNK activity in different neural cell lines. *Molecular Brain Research,* 75, 128-137.

MILLER, S. F., SUMMERHURST, K., RUNKER, A. E., KERJAN, G., FRIEDEL, R. H., CHEDOTAL, A., MURPHY, P. & MITCHELL, K. J. (2007) Expression of Plxdc2/TEM7R in the developing nervous system of the mouse. *Gene Expr Patterns,* 7, 635-44.

MILLET, S., CAMPBELL, K., EPSTEIN, D. J., LOSOS, K., HARRIS, E. & JOYNER, A. L. (1999) A role for Gbx2 in repression of Otx2 and positioning the mid/hindbrain organizer. *Nature,* 401, 161-4.

MINA, M., HAVENS, B. & VELONIS, D. A. (2007) FGF signaling in mandibular skeletogenesis. *Orthod Craniofac Res,* 10, 59-66.

MITCHELL, K. J., PINSON, K. I., KELLY, O. G., BRENNAN, J., ZUPICICH, L., SCHERZ, P., LEIGHTON, P. A., GOODRICH, L. V., LU, X. W., AVERY, B. J., TATE, P., DILL, K., PANGILINAN, E., WAKENIGHT, P., TESSIER-LAVIGNE, M. & SKARNES, W. C. (2001) Functional analysis of secreted and transmembrane proteins critical to mouse development. *Nature Genetics,* 28, 241-249.

MONKLEY, S. J., DELANEY, S. J., PENNISI, D. J., CHRISTIANSEN, J. H. & WAINWRIGHT, B. J. (1996) Targeted disruption of the Wnt2 gene results in placentation defects. *Development,* 122, 3343-3353.

MORIN, P. J., SPARKS, A. B., KORINEK, V., BARKER, N., CLEVERS, H., VOGELSTEIN, B. & KINZLER, K. W. (1997) Activation of beta-catenin-Tcf signaling in colon cancer by mutations in beta-catenin or APC. *Science,* 275, 1787-1790.

MOULD, A. P., TRAVIS, M. A., BARTON, S. J., HAMILTON, J. A., ASKARI, J. A., CRAIG, S. E., MACDONALD, P. R., KAMMERER, R. A., BUCKLEY, P. A. & HUMPHRIES, M. J. (2005) Evidence that monoclonal antibodies directed against the integrin beta subunit plexin/semaphorin/integrin domain stimulate function by inducing receptor extension. *Journal of Biological Chemistry,* 280, 4238-4246.

MRAVEC, B. & KISS, A. (2004) The brain catecholamines: brief anatomy and participation in the stress reaction and regulation of cardiovascular function. *Cesk Fysiol* 53(3), 102-16.

MUKHOPADHYAY, M., SHTROM, S., RODRIGUEZ-ESTEBAN, C., CHEN, L., TSUKUI, T., GOMER, L., DORWARD, D. W., GLINKA, A., GRINBERG, A., HUANG, S. P., NIEHRS, C., BELMONTE, J. C. I. & WESTPHAL, H. (2001) Dickkopf1 is required for embryonic head induction and limb morphogenesis in the mouse. *Developmental Cell,* 1, 423-434.

MURAMATSU, T., MIZUTANI, Y., OHMORI, Y. & OKUMURA, J. (1997) Comparison of three nonviral transfection methods for foreign gene expression in early chicken embryos *in ovo*. *Biochemical and Biophysical Research Communications,* 230, 376-380.

MUROYAMA, Y., KONDOH, H. & TAKADA, S. (2004) Wnt proteins promote neuronal differentiation in neural stem cell culture. *Biochemical and Biophysical Research Communications,* 313, 915-921.

MURPHY, P., DAVIDSON, D. R. & HILL, R. E. (1989) Segment-specific expression of a homoeobox-containing gene in the mouse hindbrain. *Nature,* 341, 156-9.

NAKAMURA, H., KATAHIRA, T., SATO, T., WATANABE, Y. & FUNAHASHI, J. (2004) Gain- and loss-of-function in chick embryos by electroporation. *Mechanisms of Development,* 121, 1137-1143.

NAKAMURA, H., WATANABE, Y. & FUNAHASHI, J. (2000) Misexpression of genes in brain vesicles by *in ovo* electroporation. *Development Growth & Differentiation,* 42, 199-201.

NANDA, A., BUCKHAULTS, P., SEAMAN, S., AGRAWAL, N., BOUTIN, P., SHANKARA, S., NACHT, M., TEICHER, B., STAMPFL, J., SINGH, S., VOGELSTEIN, B., KINZLER, K. W. & CROIX, B. S. (2004) Identification of a binding partner for the endothelial cell surface proteins TEM7 and TEM7R. *Cancer Research,* 64, 8507-8511.

NEEDHAM, J. (1934) A history of embryology. Cambridge University Press, Cambridge.

NEUFELD, G. & KESSLER, O. (2008) The semaphorins: versatile regulators of tumour progression and tumour angiogenesis. *Nature Reviews Cancer,* 8, 632-645.

NICHOLSON, D. W. & THORNBERRY, N. A. (1997) Caspases: killer proteases. *Trends in Biochemical Sciences,* 22, 299-306.

NIETO, M., SCHUURMANS, C., BRITZ, O. & GUILLEMOT, F. (2001) Neural bHLH genes control the neuronal versus glial fate decision in cortical progenitors. *Neuron,* 29, 401-413.

O'LEARY, D. D., CHOU, S. J. & SAHARA, S. (2007) Area patterning of the mammalian cortex. *Neuron,* 56, 252-69.

OHKUBO, Y., CHIANG, C. & RUBENSTEIN, J. L. (2002) Coordinate regulation and synergistic actions of BMP4, SHH and FGF8 in the rostral prosencephalon regulate morphogenesis of the telencephalic and optic vesicles. *Neuroscience,* 111, 1-17.

OHTSUKA, T., ISHIBASHI, M., GRADWOHL, G., NAKANISHI, S., GUILLEMOT, F. & KAGEYAMA, R. (1999) Hes1 and Hes5 as Notch effectors in mammalian neuronal differentiation. *Embo Journal,* 18, 2196-2207.

OKAFUJI, T., FUNAHASHI, J. & NAKAMURA, H. (1999) Roles of Pax-2 in initiation of the chick tectal development. *Developmental Brain Research,* 116, 41-49.

OKAMOTO, M., TOMONARI, S., NAITO, Y., SAIGO, K., NOJI, S., UI-TEI, K. & OHUCHI, H. (2008) Introduction of silencing-inducing transgene against Fgf19 does not affect expression of Tbx5 and beta 3-tubulin in the developing chicken retina. *Development Growth & Differentiation,* 50, 159-168.

OPPENHEIM, R. W. (1991) Cell-Death During Development of the Nervous-System. *Annual Review of Neuroscience,* 14, 453-501.

PADDISON, P. J., CAUDY, A. A., BERNSTEIN, E., HANNON, G. J. & CONKLIN, D. S. (2002) Short hairpin RNAs (shRNAs) induce sequence-specific silencing in mammalian cells. *Genes & Development,* 16, 948-958.

PANCHISION, D. M., PICKEL, J. M., STUDER, L., LEE, S. H., TURNER, P. A., HAZEL, T. G. & MCKAY, R. D. (2001) Sequential actions of BMP receptors control neural precursor cell production and fate. *Genes Dev,* 15, 2094-110.

PANHUYSEN, M., WEISENHORN, D. M. V., BLANQUET, V., BRODSKI, C., HEINZMANN, U., BEISKER, W. & WURST, W. (2004) Effects of Wnt1 signaling on proliferation in the developing mid-/hindbrain region. *Molecular and Cellular Neuroscience,* 26, 101-111.

PAUL, C. P., GOOD, P. D., WINER, I. & ENGELKE, D. R. (2002) Effective expression of small interfering RNA in human cells. *Nature Biotechnology,* 20, 505-508.

PERA, E. M. & KESSEL, M. (1997) Patterning of the chick forebrain anlage by the prechordal plate. *Development,* 124, 4153-4162.

PICCOLO, S., AGIUS, E., LEYNS, L., BHATTACHARYYA, S., GRUNZ, H., BOUWMEESTER, T. & DE ROBERTIS, E. M. (1999) The head inducer Cerberus is a multifunctional antagonist of Nodal, BMP and Wnt signals. *Nature,* 397, 707-710.

PLACZEK, M. & BRISCOE, J. (2005) The floor plate: multiple cells, multiple signals. *Nat Rev Neurosci,* 6, 230-40.

POITRAS, L., GHANEM, N., HATCH, G. & EKKER, M. (2007) The proneural determinant MASH1 regulates forebrain Dlx1/2 expression through the I12b intergenic enhancer. *Development,* 134, 1755-1765.

POSCHL, E., SCHLOTZER-SCHREHARDT, U., BRACHVOGEL, B., SAITO, K., NINOMIYA, Y. & MAYER, U. (2004) Collagen IV is essential for basement membrane stability but dispensable for initiation of its assembly during early development. *Development,* 131, 1619-1628.

PRICE, M., LAZZARO, D., POHL, T., MATTEI, M. G., RUTHER, U., OLIVO, J. C., DUBOULE, D. & DILAURO, R. (1992) Regional Expression of the Homeobox Gene Nkx-2.2 in the Developing Mammalian Forebrain. *Neuron,* 8, 241-255.

PU, H. F. & YOUNG, A. P. (1990) Glucocorticoid-Inducible Expression of a Glutamine Synthetase-Cat-Encoding Fusion Plasmid after Transfection of Intact Chicken Retinal Explant Cultures. *Gene,* 89, 259-263.

PUELLES, L. & MARTINEZ, S. (1996) Boundaries in the forebrain. *International Journal of Developmental Neuroscience,* 14, 65.

PUELLES, L. & RUBENSTEIN, J. L. R. (2003) Forebrain gene expression domains and the evolving prosomeric model. *Trends in Neurosciences,* 26, 469-476.

PUTCHA, G. V., LE, S. Y., FRANK, S., BESIRLI, C. G., CLARK, K., CHU, B. Y., ALIX, S., YOULE, R. J., LAMARCHE, A., MARONEY, A. C. & JOHNSON, E. M. (2003) JNK-mediated BIM phosphorylation potentiates BAX-dependent apoptosis. *Neuron,* 38, 899-914.

RAIBLE, F. & BRAND, M. (2004) Divide et Impera - the midbrain-hindbrain boundary and its organizer. *Trends in Neurosciences,* 27, 727-734.

REICHERT, H. (2002) Conserved genetic mechanisms for embryonic brain patterning. *International Journal of Developmental Biology,* 46, 81-87.

REIFERS, F., BOHLI, H., WALSH, E. C., CROSSLEY, P. H., STAINIER, D. Y. R. & BRAND, M. (1998) Fgf8 is mutated in zebrafish acerebellar (ace) mutants and is required for maintenance of midbrain-hindbrain boundary development and somitogenesis. *Development,* 125, 2381-2395.

RIDDLE, R. D., JOHNSON, R. L., LAUFER, E. & TABIN, C. (1993) Sonic hedgehog mediates the polarizing activity of the ZPA. *Cell,* 75, 1401-16.

RUBENSTEIN, J. L. R., MARTINEZ, S., SHIMAMURA, K. & PUELLES, L. (1994) The Embryonic Vertebrate Forebrain - the Prosomeric Model. *Science,* 266, 578-580.

SAITSU, H., KOMADA, M., SUZUKI, M., NAKAYAMA, R., MOTOYAMA, J., SHIOTA, K. & ISHIBASHI, M. (2005) Expression of the mouse fgf15 gene is directly initiated by Sonic hedgehog signaling in the diencephalon and midbrain. *Developmental Dynamics,* 232, 282-292.

SANDBERG, M., KALLSTROM, M. & MUHR, J. (2005) Sox21 promotes the progression of vertebrate neurogenesis. *Nature Neuroscience,* 8, 995-1001.

SASAI, Y., KAGEYAMA, R., TAGAWA, Y., SHIGEMOTO, R. & NAKANISHI, S. (1992) 2 Mammalian Helix Loop Helix Factors Structurally Related to Drosophila Hairy and Enhancer of Split. *Genes & Development,* 6, 2620-2634.

SAUNDERS, J. W. (1948) The Proximo-Distal Sequence of Origin of the Parts of the Chick Wing and the Role of the Ectoderm. *Journal of Experimental Zoology,* 108, 363-403.

SCARDIGLI, R., BAUMER, N., GRUSS, P., GUILLEMOT, F. & LE ROUX, I. (2003) Direct and concentration-dependent regulation of the proneural gene Neurogenin2 by Pax6. *Development,* 130, 3269-3281.

SCHOLPP, S., FOUCHER, I., STAUDT, N., PEUKERT, D., LUMSDEN, A. & HOUART, C. (2007) Otx1l, Otx2 and Irx1b establish and position the ZLI in the diencephalon. *Development,* 134, 3167-3176.

SCHOLPP, S., WOLF, O., BRAND, M. & LUMSDEN, A. (2006) Hedgehog signalling from the zona limitans intrathalamica orchestrates patterning of the zebrafish diencephalon. *Development,* 133, 855-864.

SELKOE, D. & KOPAN, R. (2003) Notch and presenilin: Regulated intramembrane proteolysis links development and degeneration. *Annual Review of Neuroscience,* 26, 565-597.

SHARPE, J., AHLGREN, U., PERRY, P., HILL, B., ROSS, A., HECKSHER-SORENSEN, J., BALDOCK, R. & DAVIDSON, D. (2002) Optical projection tomography as a tool for 3D microscopy and gene expression studies. *Science,* 296, 541-545.

SHAWLOT, W. & BEHRINGER, R. R. (1995) Requirement for Lim1 in Head-Organizer Function. *Nature,* 374, 425-430.

SHIMAMURA, K., HARTIGAN, D. J., MARTINEZ, S., PUELLES, L. & RUBENSTEIN, J. L. R. (1995) Longitudinal organization of the anterior neural plate and neural tube. *Development,* 121, 3923-3933.

SHIMOGORI, T., BANUCHI, V., NG, H. Y., STRAUSS, J. B. & GROVE, E. A. (2004) Embryonic signaling centers expressing BMP, WNT and FGF proteins interact to pattern the cerebral cortex. *Development,* 131, 5639-5647.

SHU, W. G., JIANG, Y. Q., LU, M. M. & MORRISEY, E. E. (2002) Wnt7b regulates mesehchymal proliferation and vascular development in the lung. *Development,* 129, 4831-4842.

SIMEONE, A., ACAMPORA, D., GULISANO, M., STORNAIUOLO, A. & BONCINELLI, E. (1992) Nested Expression Domains of 4 Homeobox Genes in Developing Rostral Brain. *Nature,* 358, 687-690.

ST CROIX, B., RAGO, C., VELCULESCU, V., TRAVERSO, G., ROMANS, K. E., MONTGOMERY, E., LAL, A., RIGGINS, G. J., LENGAUER, C., VOGELSTEIN, B. & KINZLER, K. W. (2000) Genes expressed in human tumor endothelium. *Science,* 289, 1197-1202.

STERN, C. D. (2004) The chick embryo - past, present and future as a model system in developmental biology - Preface. *Mechanisms of Development,* 121, 1011-1013.

STERN, C. D. (2005) The chick: A great model system becomes even greater. *Developmental Cell,* 8, 9-17.

STORM, E. E., GAREL, S., BORELLO, U., HEBERT, J. M., MARTINEZ, S., MCCONNELL, S. K., MARTIN, G. R. & RUBENSTEIN, J. L. (2006) Dose-dependent functions of Fgf8 in regulating telencephalic patterning centers. *Development,* 133, 1831-44.

STUDER, M., LUMSDEN, A., ARIZAMCNAUGHTON, L., BRADLEY, A. & KRUMLAUF, R. (1996) Altered segmental identity and abnormal migration of motor neurons in mice lacking Hoxb-1. *Nature,* 384, 630-634.

SUGIYAMA, S. & NAKAMURA, H. (2003) The role of Grg4 in tectal laminar formation. *Development,* 130, 451-462.

SUI, G. C., SOOHOO, C., AFFAR, E., GAY, F., SHI, Y. J., FORRESTER, W. C. & SHI, Y. (2002) A DNA vector-based RNAi technology to suppress gene expression in mammalian cells. *Proceedings of the National Academy of Sciences of the United States of America,* 99, 5515-5520.

SUMMERHURST, K., STARK, M., SHARPE, J., DAVIDSON, D. & MURPHY, P. (2008) 3D representation of Wnt and Frizzled gene expression patterns in the mouse embryo at embryonic day 11.5 (Ts19). *Gene Expression Patterns,* 8, 331-348.

SVOBODA, P., STEIN, P. & SCHULTZ, R. M. (2001) RNAi in mouse oocytes and preimplantation embryos: Effectiveness of hairpin dsRNA. *Biochemical and Biophysical Research Communications,* 287, 1099-1104.

TAO, W. & LAI, E. (1992) Telencephalon-Restricted Expression of Bf-1, a New Member of the Hnf-3 Fork Head Gene Family, in the Developing Rat-Brain. *Neuron,* 8, 957-966.

TATE, M. C., GARCIA, A. J., KESELOWSKY, B. G., SCHUMM, M. A., ARCHER, D. R. & LAPLACA, M. C. (2004) Specific beta(1) integrins mediate adhesion, migration, and differentiation of neural progenitors derived from the embryonic striatum. *Molecular and Cellular Neuroscience,* 27, 22-31.

TESSIERLAVIGNE, M. & GOODMAN, C. S. (1996) The molecular biology of axon guidance. *Science,* 274, 1123-1133.

THOMAS, K. R. & CAPECCHI, M. R. (1990) Targeted Disruption of the Murine Int-1 Protooncogene Resulting in Severe Abnormalities in Midbrain and Cerebellar Development. *Nature,* 346, 847-850.

TICKLE, C. (2004) The contribution of chicken embryology to the understanding of vertebrate limb development. *Mechanisms of Development,* 121, 1019-1029.

TOLE, S., RAGSDALE, C. W. & GROVE, E. A. (2000) Dorsoventral patterning of the telencephalon is disrupted in the mouse mutant extra-toes(J). *Dev Biol,* 217, 254-65.

TOMITA, K., MORIYOSHI, K., NAKANISHI, S., GUILLEMOT, F. & KAGEYAMA, R. (2000) Mammalian achaete-scute and atonal homologs regulate neuronal versus glial fate determination in the central nervous system. *Embo Journal,* 19, 5460-5472.

TOMIZAWA, Y., SEKIDO, Y., KONDO, M., GAO, B. N., YOKOTA, J., ROCHE, J., DRABKIN, H., LERMAN, M. I., GAZDAR, A. F. & MINNA, J. D. (2001) Inhibition of lung cancer cell growth and induction of apoptosis after reexpression of 3p21.3 candidate tumor suppressor gene SEMA3B. *Proceedings of the National Academy of Sciences of the United States of America,* 98, 13954-13959.

TORRES, M. A., GOMEZPARDO, E. & GRUSS, P. (1996) Pax2 contributes to inner ear patterning and optic nerve trajectory. *Development,* 122, 3381-3391.

TROUSSE, F., MARTI, E., GRUSS, P., TORRES, M. & BOVOLENTA, P. (2001) Control of retinal ganglion cell axon growth: a new role for Sonic hedgehog. *Development,* 128, 3927-3936.

TSE, C., XIANG, R. H., BRACHT, T. & NAYLOR, S. L. (2002) Human Semaphorin 3B (SEMA3B) located at chromosome 3p21.3 suppresses tumor formation in an adenocarcinoma cell line. *Cancer Research,* 62, 542-546.

VASILIAUSKAS, D. & STERN, C. D. (2001) Patterning the embryonic axis: FGF signaling and how vertebrate embryos measure time. *Cell,* 106, 133-136.

VENKATARAMAN, S., STEVENSON, P., YANG, Y., RICHARDSON, L., BURTON, N., PERRY, T. P., SMITH, P., BALDOCK, R. A., DAVIDSON, D. R. & CHRISTIANSEN, J. H. (2008) EMAGE--Edinburgh Mouse Atlas of Gene Expression: 2008 update. *Nucleic Acids Res,* 36, D860-5.

VITI, J., GULACSI, A. & LILLIEN, L. (2003) Wnt regulation of progenitor maturation in the cortex depends on Shh or fibroblast growth factor 2. *Journal of Neuroscience,* 23, 5919-5927.

WALLS, J. R., COULTAS, L., ROSSANT, J. & HENKELMAN, R. M. (2008) Three-dimensional analysis of vascular development in the mouse embryo. *PLoS ONE,* 3, e2853.

WANG, S. W., KRINKS, M., LIN, K. M., LUYTEN, F. P. & MOOS, M. (1997) Frzb, a secreted protein expressed in the Spemann organizer, binds and inhibits Wnt-8. *Cell,* 88, 757-766.

WANG, X. Q., SHEIBANI, N. & WATSON, J. C. (2005) Modulation of tumor endothelial cell marker 7 expression during endothelial cell capillary morphogenesis. *Microvascular Research,* 70, 189-197.

WADDINGTON, C. (1940) Organisers and genes. Cambridge University Press, Cambridge.

WATERS, S. T. & LEWANDOSKI, M. (2006) A threshold requirement for Gbx2 levels in hindbrain development. *Development,* 133, 1991-2000.

WILKINSON, D. G. (1992) *In situ hybridisation: A Practical Approach,* Oxford, IRL Press.

WILKINSON, D. G., BHATT, S., COOK, M., BONCINELLI, E. & KRUMLAUF, R. (1989) Segmental Expression of Hox-2 Homeobox-Containing Genes in the Developing Mouse Hindbrain. *Nature,* 341, 405-409.

WILLIAMS, B. R. G. (1999) PKR; a sentinel kinase for cellular stress. *Oncogene,* 18, 6112-6120.

WOLPERT, L. (2004) Much more from the chicken's egg than breakfast - a wonderful model system. *Mechanisms of Development,* 121, 1015-1017.

WU, Q. Q., WANG, M. N., ZUSCIK, M. J., CHEN, D., O'KEEFE, R. J. & ROSIER, R. N. (2008) Regulation of embryonic endochondral ossification by Smurf2. *Journal of Orthopaedic Research,* 26, 704-712.

XIANG, R. H., DAVALOS, A. R., HENSEL, C. H., ZHOU, X. J., TSE, C. & NAYLOR, S. L. (2002) Semaphorin 3F gene from human 3p21.3 suppresses tumor formation in nude mice. *Cancer Research,* 62, 2637-2643.

YAMADA, T., PLACZEK, M., TANAKA, H., DODD, J. & JESSELL, T. M. (1991) Control of Cell Pattern in the Developing Nervous-System - Polarizing Activity of the Floor Plate and Notochord. *Cell,* 64, 635-647.

YAMAGUCHI, T. P., BRADLEY, A., MCMAHON, A. P. & JONES, S. (1999) A Wnt5a pathway underlies outgrowth of multiple structures in the vertebrate embryo. *Development,* 126, 1211-1223.

YANG, X. L., KHOSRAVIFAR, R., CHANG, H. Y. & BALTIMORE, D. (1997) Daxx, a novel Fas-binding protein that activates JNK and apoptosis. *Cell,* 89, 1067-1076.

YOSHIDA, H., KONG, Y. Y., YOSHIDA, R., ELIA, A. J., HAKEM, A., HAKEM, R., PENNINGER, J. M. & MAK, T. W. (1998) Apaf1 is required for mitochondrial pathways of apoptosis and brain development. *Cell,* 94, 739-750.

YOSHIKAWA, S., MCKINNON, R. D., KOKEL, M. & THOMAS, J. B. (2003) Wnt-mediated axon guidance via the Drosophila derailed receptor. *Nature,* 422, 583-588.

YU, J. M., KIM, J. H., SONG, G. S. & JUNG, J. S. (2006) Increase in proliferation and differentiation of neural progenitor cells isolated from postnatal and adult mice brain by Wnt-3a and Wnt-5a. *Molecular and Cellular Biochemistry,* 288, 17-28.

YU, J. Y., DERUITER, S. L. & TURNER, D. L. (2002) RNA interference by expression of short-interfering RNAs and hairpin RNAs in mammalian cells. *Proceedings of the National Academy of Sciences of the United States of America,* 99, 6047-6052.

YU, T. W. & BARGMANN, C. I. (2001) Dynamic regulation of axon guidance. *Nature Neuroscience,* 4, 1169-1176.

YUN, K., FISCHMAN, S., JOHNSON, J., DE ANGELIS, M. H., WEINMASTER, G. & RUBENSTEIN, J. L. R. (2002) Modulation of the notch signaling by Mash1 and Dlx1/2 regulates sequential specification and differentiation of progenitor cell types in the subcortical telencephalon. *Development,* 129, 5029-5040.

ZANG, Q. & SPRINGER, T. A. (2001) Amino acid residues in the PSI domain and cysteine-rich repeats of the integrin beta(2) subunit that restrain activation of the integrin alpha(x)beta(2). *Journal of Biological Chemistry,* 276, 6922-6929.

ZERLIN, M., JULIUS, M. A. & KITAJEWSKI, J. (2008) Wnt/Frizzled signaling in angiogenesis. *Angiogenesis,* 11, 63-69.

ZHANG, M. B., KIM, H. J., MARSHALL, H., GENDRONMAGUIRE, M., LUCAS, D. A., BARON, A., GUDAS, L. J., GRIDLEY, T., KRUMLAUF, R. & GRIPPO, J. F. (1994) Ectopic Hoxa-1 Induces Rhombomere Transformation in Mouse Hindbrain. *Development,* 120, 2431-2442.

ZHOU, Q. & ANDERSON, D. J. (2002) The bHLH transcription factors OLIG2 and OLIG1 couple neuronal and glial subtype specification. *Cell,* 109, 61-73.

ZHU, L., MARVIN, M. J., GARDINER, A., LASSAR, A. B., MERCOLA, M., STERN, C. D. & LEVIN, M. (1999) Cerberus regulates left-right asymmetry of the embryonic head and heart. *Current Biology,* 9, 931-938.

ZWILLING, E. & HANSBOROUGH, L. A. (1956) Interaction between Limb Bud Ectoderm and Mesoderm in the Chick Embryo .3. Experiments with Polydactylous Limbs. *Journal of Experimental Zoology,* 132, 219-237.